Application of the Wigner Distribution to Monitoring Cutting Tool Condition

Zheng, Kougen

Center for Micro-Engineering and Metrology,

Department of Engineering,

University of Warwick

This thesis is submitted for the degree of Doctor of Philosophy

31 May 1992

Acknowledgements

While I am indebted to many people for their help throughout the course of my research, I would like to thank, in particular, the following:

My supervisor, Prof. D.J. Whitehouse, for his continuous encouragement and constructive criticism, and originally suggesting the possible use of the ambiguity function, the Wigner distribution, and the Hough transform.

Prof. D.K. Bowen for his supervision while Prof. D.J. Whitehouse was on temporary sickleave.

Dr. D.G. Chetwynd, Dr. J.H. Rakels, Dr. S.T. Smith, and Mr. T.R. Judge, Mr. R. D. Dale-Jones, for proof reading this thesis and many useful discussions.

Mr. R.A. Bridgeland for his assistance with the use of Talyrond 200. Mr. P.R. Bellwood and Mr. D.J. Robinson for their help in building the instrument for vibration measurement.

Finally, but not least, I am very grateful to my family and particularly my wife. Without their support, this thesis would not have been completed.

Zheng, Kougen

Declaration

This thesis is presented in accordance with the regulations for the degree of Doctor of Philosophy. It has been composed by myself and has not been submitted in any previous application for any degree. The work described in this thesis has been done by myself except where stated otherwise.

Zheng, Kougen

To my mum!

Summary

This thesis is about the application of the Wigner distribution to cutting tool monitoring and control. After reviewing traditional methods, a new method is proposed. This is to regard the surface texture and geometric error of form of a machined workpiece as the fingerprint of a cutting process, to analyse it, and to extract cutting tool vibration information from it, which can then be used for cutting tool monitoring.

In order to analyse the surface texture effectively, three analysing tools, i.e. the Fourier transform, the ambiguity function, the Wigner distribution (WD), are examined and compared with each other, and it is concluded that the WD is best able to analyse both stationary and nonstationary signals. Furthermore, computer simulation of both chirp signals and frequency modulated signals is then carried out, and it is shown that the WD can be used to extract useful parameters successively.

In order to demonstrate the suitability of the WD for machine tool condition monitoring, first cutting tool vibration are measured directly by two linear variable differential transformers mounted on the cutting tool, and then these measured data about vibration are used to verify those parameters extracted from the surface of the machined workpiece by the WD. It is found that

- the extracted frequencies in both horizontal and vertical direction are within 10% of those measured,
- the extracted amplitudes in both horizontal and vertical direction are highly correlated with those measured.

This result confirms the feasibility of this technique. In spite of being an off-line process, this technique is simple, reliable, and can reveal the direct effect of cutting processes.

Nomenclature

Except where stated explicitly, the signal and its transform are regarded as being continuous.

$A_f(\varpi, \chi)$ The ambiguity function for $f(x)$.

$A_{f_a}(\varpi, \chi)$ The ambiguity function for $f_a(x)$.

$A_f(\varpi, \eta)$ The discrete ambiguity function for $f[n]$.

$A_{f_a}(\varpi, \eta)$ The discrete ambiguity function for $f_a[n]$.

$f(x)$ A real-valued or complex-valued signal.

$f_a(x)$ An analytical signal for a real-valued signal $f(x)$.

$F(\omega)$ The Fourier transform for $f(x)$.

$F_a(\omega)$ The Fourier transform for $f_a(x)$.

$f[n]$ A discrete, real-valued or complex-valued signal.

$f_a[n]$ An analytical signal for a discrete, real-valued signal $f[n]$.

$F(\theta)$ The discrete Fourier transform for $f[n]$.

$F_a(\theta)$ The discrete Fourier transform for $f_a[n]$.

$m_f(x)$ The second-order local moment in frequency ω for $W_f(x, \omega)$.

$M_f(\omega)$ The second-order local moment in space x for $W_f(x, \omega)$.

$m_f[n]$ The second-order local moment in frequency θ for $W_f(n, \theta)$.

$M_f(\theta)$ The second-order local moment in space n for $W_f(n, \theta)$.

$p_f(x)$ The zeroth-order local moment in frequency ω for $W_f(x,\omega)$.

$P_f(\omega)$ The zeroth-order local moment in space x for $W_f(x,\omega)$.

$p_f(n)$ The zeroth-order local moment in frequency θ for $W_f(n,\theta)$.

$P_f(\theta)$ The zeroth-order local moment in space n for $W_f(n,\theta)$.

$W_f(x,\omega)$ The Wigner distribution for $f(x)$.

$W_{f_a}(x,\omega)$ The Wigner distribution for $f_a(x)$.

$W_f(n,\theta)$ The discrete Wigner distribution for $f[n]$.

$W_{f_a}(n,\theta)$ The discrete Wigner distribution for $f_a[n]$.

$\Omega_f(x)$ The first-order local moment in frequency ω for $W_f(x,\omega)$.

$\Theta_f(n)$ The first-order local moment in frequency ω for $W_f(n,\theta)$.

Contents

Chapter 1

Review of Cutting Tool Monitoring and Control

1.1 Introduction

The remarkable progress in every facet of computer science during the past 50 years has brought about rapid changes in every field. Manufacturing industry is no exception. The first contribution of computer technology was *computer numerical control* (CNC), then came *computer aided design* (CAD) and *computer aided manufacturing* (CAM). Today, *flexible manufacturing system* (FMS) and *computer-integrated manufacturing* (CIM) are emerging and promise to change manufacturing industry beyond recognition.

One crucial part of FMS and CIM is to be able to successfully and automatically monitor and control the machining process. This includes

1. monitoring the machine, in particular, spindle bearings, guideways, feed drives.
2. monitoring the cutting tool, such as tool wear and breakage, tool vibration.
3. checking the workpiece for its dimensions, shape and surface texture.

In this thesis, it is the monitoring of the cutting tool in turning that is investigated. This is because it is widely used, and the cutting tool has an important

influence on productivity as well as performance of workpieces (Whitehouse and Zheng 1992).

1.2 Cutting tool failure and its monitoring

There are many kinds of tool failure, the most common causes being

1. temperature failure, where the tool temperature becomes high enough to cause plastic deformation at the cutting edge,
2. fracturing, either a complete tool failure or small chipping of the cutting edge, caused by fatigue or excessive forces,
3. gradual wear, including both crater wear and flank wear,
4. tool vibration etc.

For both crater wear and flank wear, see Figure 1.1 and Figure 1.2

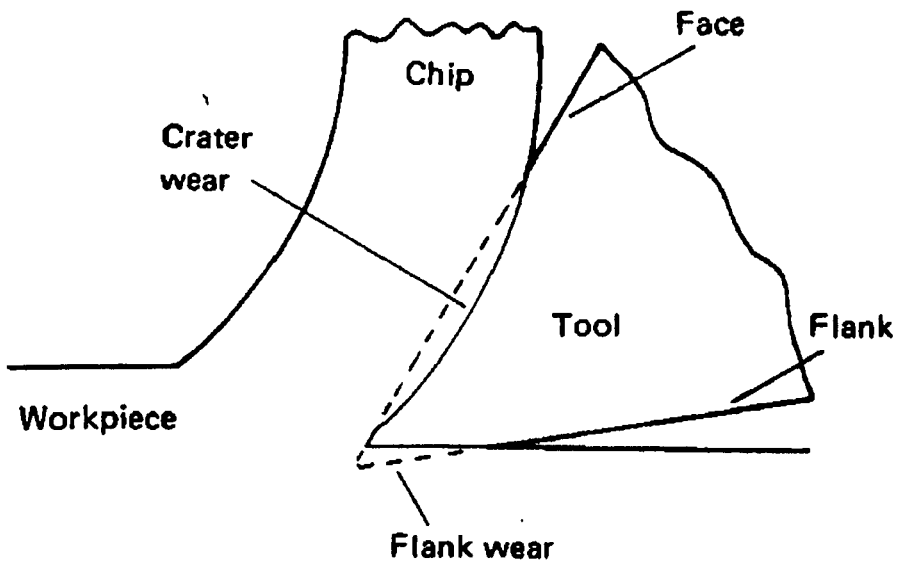

Figure 1.1: Regions of tool wear (from Boothroyd 1975, p 109).

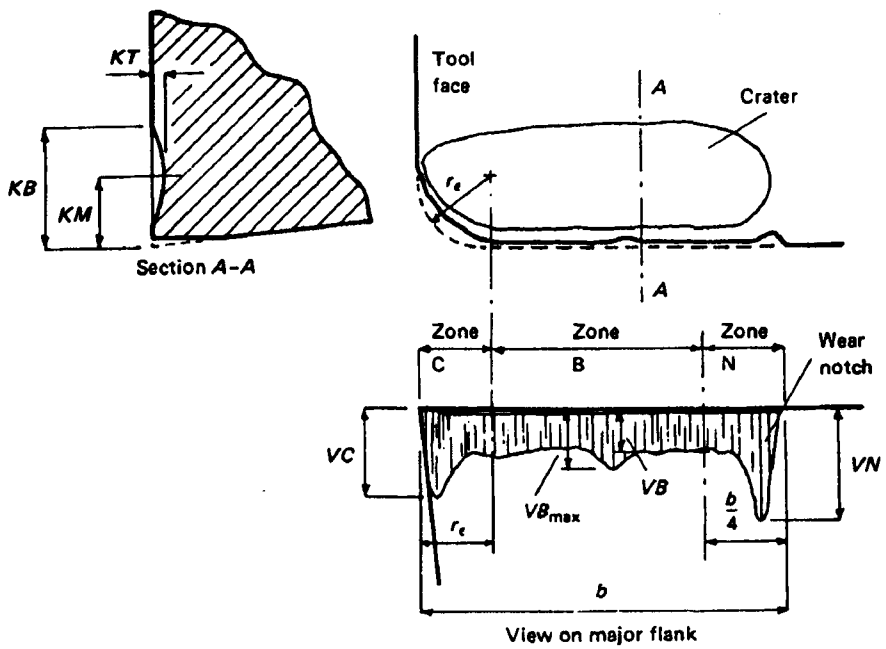

Figure 1.2: Features of single-point-tool wear (from Boothroyd 1975, p 112). KT is the crater depth measured at the deepest point of the crater, VB is the average wear land width in the central portion of the active cutting edge, VC is the width of the flank wear land at the tool corner, VN is the width of the wear land at the wear notch.

With regard to monitoring the cutting tool in turning, there are three types of methods (Cook 1980; Jones 1989; Kegg 1984; Li and Mathew 1990; Micheletti, Koenig and Vitor 1976; Tlusty and Andrews 1983; Tönshoff *et al* 1988):

1. direct methods, involving measurement of the actual tool wear and fracture from a cutting tool (such as optical techniques and radioactive methods).

2. indirect methods, involving measurement of parameters correlated with cutting processes (such as cutting forces, vibration, sound, power input, acoustic emission, cutting temperature)

3. surface analysis, based on the fact that the surface texture of a machined workpiece is the fingerprint of a cutting process.

In this chapter, the above methods will be examined. After this, a novel method of machine tool monitoring based on the Wigner distribution will be introduced briefly.

1.3 Direct methods

1.3.1 Optical methods

The lapping-comparator technique has been employed for investigating tool wear (Tsao et al 1986). First, a transparent thermoplastic mould of a tool crater was made, then lapped to show contour lines on an optical comparator. These contours were seen as clear, sharp lines of high contrast. The depth of the crater can be easily and accurately measured by reading the height of the mould on the optical comparator screen.

A fiber optic sensor for in-process measurement of tool flank wear has been developed (Giusti 1979). This was capable of giving information about tool flank wear conditions, and could scan different zones of the wear-land. It was simple and easy to implement. Another method for measurement of flank wear has been presented by Jeon and Kim (1988). This method was based on real time

vision technology in which the tool was illuminated by the beam of a laser and the wear zone was viewed by means of a Vidicon camera. The image was then converted into digital form and processed to detect the wear land width. It was reported that this method was capable of detecting tool wear to an accuracy of 0.1 mm within 1.7 second processing time. Pedersen (1990) has also developed a prototype experimental computer vision system for flank wear measurement. The wear measured conformed with the traditional three-stage wear pattern normally observed for cutting tools (initial, steady-state, and terminal wear.) The measurement program took about 7 seconds to execute.

The morphology of the cutting tool has been examined by a TV camera (Matsushima, Kawabata, and Sata 1979), and the wear pattern was extracted by an image processing technique and classified into five predetermined categories. When an undesirable morphology was found, the tool material or the tool geometry was changed according to a decision table which was constructed in advance by a learning algorithm. In the experiments, the system was able to fulfill the intended functions.

The optical method has been applied to a NC lathe (Giusti, Santochi and Tantussi 1984) . The tool wear was sensed by a TV camera and then processed by a computer to extract the actual value of wear, which was then used to control the lathe.

Optical sensing can only be used between cutting cycles when the tool is removed from the workpiece, and as such is not strictly an *in-process* technique. However, it appears to be accurate and reliable, especially when machine vision is used. It has its share of problems though, in that there can be instances when it is difficult to detect tool wear if a built-up edge or metal deposit exists.

1.3.2 Radioactive techniques

A simple and safe method has been developed in order to provide information prior to tool replacement (Cook and Subramanian 1978). This method involved attaching a small quantity of radioactive material (less than 10^{-8} Curie) to the

flank of the tool. At the end of each cutting cycle, the tool was quickly tested to determine whether the spot was still there, and so whether the tool had reached some predefined state of wear and whether the tool had to be replaced. This is in effect a "Go, No-go" gauge.

In practice, some measures must be taken to minimize the effects of radiation on the shop floor. Moreover it is inevitable that operators are somewhat prejudiced against using methods involving radioactivity no matter how small the level is.

1.4 Indirect methods

There are many theoretical models for indirect methods, for example (Bhattacharyya and Ham 1969; Koren 1978; Kramer and Suh 1980; Lenz, Katz and Ber 1976; Ramalingam, Peng and Watson 1978; Ramalingam and Watson 1978; Tlusty and Masood 1978; Usui and Hirota 1978; Wu 1964). These are interesting and useful, however there are more practical methods which have found significant use in industry. These methods will be explained below.

1.4.1 Cutting forces

Among the many parameters which can be used to characterise tool wear, one is the cutting force. This has the advantage that it is relatively easy to measure. It can be used to monitor the cutting processes because it changes as the tool wears. It usually get greater because of the increase in the coefficient of friction between tool and workpiece. Force sensing methods have been reported that are very sensitive, in fact in some cases more sensitive than vibration and power measurements (Martin *et al* 1986).

An early work (Micheletti, De Filippi and Ippolito 1968) has claimed that it is difficult to derive accurate information on tool wear based on measurements of cutting forces in turning. It was shown that significant increases in force occurs only at the moment of tool failure. Therefore this technique was said to be

limited to the detection of tool failure only and not wear in its many forms. In spite of this, cutting forces have been widely employed by many research workers for monitoring cutting processes.

Some theoretical models based on force measurements for on-line tool wear and breakage sensing have been presented and verified by experiments (Akgerman and Frisch 1971; Danai and Ulsoy 1987; Koren and Lenz 1970; Shiliam 1971; Usui and Hirota 1978). One (Koren 1986) is based on the fact that as a tool wears, the tool face force decreases with increasing crater wear while the tool clearance force increases with increasing wearland. From measuring these two forces, tool wear can be estimated.

It has been experimentally shown that the relationship between the feed force and the feed per revolution is strongly influenced by the tool wear. Based on this, tool wear can be detected by the cutting force measurement (Uehara, Kiyosawa and Takeshita 1979). A special NC program consisting of a flank wear detection procedure and crater wear detection element was inserted at the beginning of the NC tape for every workpiece. In the tests, both VB and KT (see Figure 1.2) were determined quantitatively. The limit of the method was 0.15 mm for VB and 20 μm for KT. The method was also effective in detecting chipping of cutting tools.

With a large rake angle, the feed force at steady levels was negative, but achieved relatively high positive levels for short periods of time at both the beginning and the end of the cut (Colwell 1971). The level and duration of these positive excursions increased rapidly with even small amounts of tool wear, even though it was also influenced by the cutting conditions. A phase shift between the main cutting force and feed force with a zero rake angle cutting tool was considered to be due to the rubbing effect of the initial cut. Both phenomena offered the possibility of monitoring tool wear in initial rough cuts.

Cutting forces have been sensed during turning cuts carried out on an NC lathe (Colwell 1975). It was found that the influence of the tool was much more evident during the dwell and set-up periods than in steady state cutting. During the dwell period, the main cutting force F_c and the feed force F_n dropped to equal

each other with a sharp tool while the value of F_c dropped to a level greater or less than F_n according to the flank wear. Therefore the feed force, or even better, the ratio of the feed component to the cutting component was a sensitive means for monitoring tool wear.

A method of wear estimation for carbide tools, using a function of the cutting forces, was presented by Mackinnon, Wilson and Wilkinson in 1986. In this, a wear index was proposed to categorize the state of wear on a tool as a percentage. For perfect tools the value was defined as 0% while for extremely badly damaged tools it was given a value of 100%. Tests demonstrated that the strategy was reliable. Although the system could not prevent breakage, by anticipating it, time-wasting due to the continuation of machining following breakage was avoided. Moreover, the strategy could halt cutting when a tool became severely affected by plastic deformation since this also resulted in a large increase in the value of the force ratio.

It should be stated in conclusion that although the cutting force method is one of the most commonly used techniques for the detection of tool failure, it can not be generalised because tool wear and failure have a complex relationship with cutting forces and results can be different for sensing tool wear in similar studies.

1.4.2 Drive motor current

During the cutting process, the current consumed by the spindle motor or feed motor is related to the output torque of the motor and therefore the tool load. Hence this current can be used for monitoring machine tool just like cutting forces.

The current from the spindle motor of an NC lathe has been measured (Matsushima, Bertok and Sata 1982) by a current transformer, then rectified, amplified, and further low pass filtered. The resulting signal was found to drop instantaneously and soon to recover to a certain level when tool breakage occurred. With the aid of the statistical quality control concept, a lower limit was

generated from the normal process data. The breakage of a cutting tool was detected when a data point intersected the lower limit threshold. Furthermore, it was found that under the constant spindle speed cutting conditions, the percentage increase of the current from the beginning until the end of a tool's useful life was approximately constant if the same material was used. This result was employed to develop a method by which to judge whether a tool reached its service life expectancy. A disadvantage was the small bandwidth of its frequency response.

Meter'kov and Liberman (1989) have proposed a method to use the current from a spindle motor — by isolating the frequency part related to tool breakage by means of band pass filters. Third order filters were suggested as an ideal choice.

A model based on the current from a feed motor has been presented and verified experimentally on a lathe (Stein *et al* 1984).

The current measurement system is relatively simpler and cheaper, more durable and flexible than a dynamometer. It has been found to be reliable in monitoring tool breakage at medium and heavy cuts (Novak and Ossbahr 1986). However, it is less sensitive for tool wear sensing when compared to force sensing and vibration measurement (Martin *et al* 1986).

1.4.3 Temperature

During the metal cutting, heat is generated in the region of tool cutting edge (Figure 1.3), therefore temperatures are high. These temperatures have a significant influence on the tool wear. As a result, the cutting temperature can be used to monitor tool failure.

However, in a study by Boothroyd, Eagle, and Chisholm (1967), it is suggested that for a variety of reasons, reliability of the cutting temperature for monitoring tool wear is doubtful:

1. the thermal voltage (from the thermocouple used for measurement of the

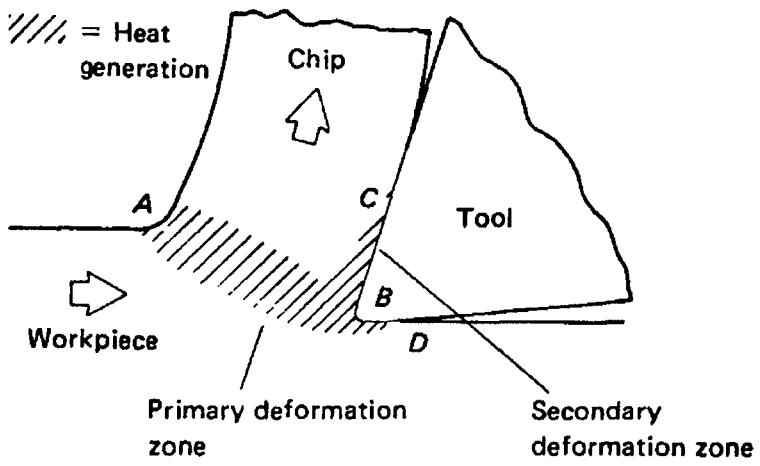

Figure 1.3: Heat generation in metal cutting (Boothroyd 1975, p93)

cutting temperature), and hence the cutting temperature, were sensitive to the cutting conditions.

2. the thermal voltage, and hence the cutting temperature, tended to stabilize after an initial increase.

3. the noise signal was about 60 percent of the signal's level due to tool wear, which complicated the task of obtaining the trend data from the signal.

4. the increase in the signal due to tool wear in either absolute terms or as a percentage of the initial signal level, did not bear a consistent relation with the cutting variables.

Zakaria and El Gomayel (1975) have also doubted the reliability.

In spite of the doubt, many methods based on temperature have been developed.

The temperature at a position on the cutting tool remote from the cutting edge has been measured by a thermocouple (Groover, Karpovich and Levy 1977). It was found that the temperature measured had a strong correlation with tool wear. Thus,

$$TW = W_0 + WR(T - T_0) \tag{1.1}$$

where TW (mm^2) is tool wear, W_0 (mm^2) is the initial interface area between tool and chip before wear begins, T, T_0 (^0C) are the temperature measured during cutting and at the beginning of cutting, WR ($mm^2/^0C$) is the wear rate. Under various conditions, the correlation coefficient was between 0.837 and 0.978. At the initial cutting, the error was the largest. This method is limited because the work-tool thermocouple method gives no indication of the distribution of temperature along the rake face.

Another method is to employ the tool-work thermocouple technique. In this technique, the emf between the tool and workpiece is taken as a measure of the mean temperature of chip-tool interface. Using this method, the tool and workpiece should be electrically isolated from the machine tool structure. Akgerman and Frisch (1971) have used this method for tracking tool failure and controlling the cutting process.

The temperature at the cutting edge of a tool in machining glass fiber reinforced plastic (GFRP) has been measured by a special thermocouple method (Sakuma and Seto 1981). In this method, two insulated wires were set in a hole drilled in the workpiece, and fixed by bonding. When these wires were cut together with the workpiece, the hot junction of the thermocouple was established, the temperature at the cutting edge could be measured and used to estimate the flank wear. However, the widespread use of this method is unlikely.

1.4.4 Vibration

As metal is being cut, the workpiece and the chips rub against the worn tool and produce vibration which can be measured. This information may then be used in various ways for tool failure control.

According to the investigation by Martin, Mutel and Drapier (1974), the vertical tool vibrations in the course of stable machining were almost sinusoidal, with frequency equal to the natural frequency of the tool. In the experiments conducted, the power of the acceleration signal obtained by spectral analysis was a linear function of the cutting speed and of the tool wear, and varied in the ratio

of 1:10 between a new tool and a worn tool. These experiments correlated with theory.

The inter-relationship between tool wear and the power spectrum of the flexural vibrations of the tool during cutting has been investigated (Del Taglia, Portuna and Toni 1976). It was discovered that

1. In the frequency range up to 2.5 kHz, a very small percentage of the total power of the acceleration signal varied in a typical way with wear. It increased up to seven times, while tool wear increased from a very small value to about 1.3-1.5 mm. A further increase of wear beyond this point caused the power contained in this frequency range to fall rapidly to the values found for small amounts of wear.

2. The cross power spectra, obtained from each recording and the previous recording in the range of 0-2.5 kHz, showed a trend similar to that of the power spectra with increasing of wear.

3. The mean coherence of a recording and the previous one in the same range lessened in a fairly predictable manner with wear up to a certain degree of wear and then increased again.

The sensitivity found in the fixed frequency range of 0-2.5 kHz was fairly satisfactory, at least for a certain class of machine tools.

The Data Dependent System (DDS) has been developed (Pandit 1977, 1978; Pandit and Kashou 1982) to measure tool wear by using the signal from an accelerometer mounted on the tool holder at a safe distance away from the cutting process. The DDS picked the mode of vibration most sensitive to tool wear and gave its power contribution, which decreased with increasing wear at the beginning, reached a minimum when the critical point of tool wear was reached, and increased again, much the same way as a rate of wear curve. The trend remained unchanged under different cutting conditions. Therefore the minimum actual power contribution or minimum tool acceleration could be used on-line to monitor tool wear.

By comparison of relative vibration spectra of the machine tool (an experimental spectrum and a specified basic spectrum), the state of a machine tool can be assessed (Selezneva 1987). This can be used to find and eliminate vibration sources.

In summary, vibration signals vary with tool failure in certain frequency ranges and are widely employed in tool condition monitoring. With the growing sophistication of transducers and instrumentation used in vibration measurement and analysis, this technique will become more practical and cost-effective.

1.4.5 Sound

Sound produced during the metal-cutting process contains all sorts of information, some components of which have been used to monitor the condition of the cutting edge.

As early as 1968, Weller, Schrier and Weichbrodt had built an electronic-mechanical system which utilized sonic signals to detect the degree of cutting edge wear in cutting and automatically trigger a cutting edge change.

Machining noise has been found to exhibit a characteristic frequency at around 4–6 kHz for a large variety of workpiece-material combinations and operating conditions(Lee 1986). At the characteristic frequency, the SPL (sound pressure level) appeared to be distinctively higher than free running and showed a good correlation with tool wear. The drop of SPL before a rapid increase in the maximum flank wear showed that the tertiary wear zone has been reached. This could be used to predict the onset of tool failure. However due to the high ambient noise level in factory environments (typically around 90 dB), this method is perhaps impractical.

Tool flank wear has been detected by measuring the emitted low frequency noise from the rubbing action of the tool and workpiece (Sadat and Raman 1987). A significant increase in the noise level in the frequency range 2.75–3.50 kHz was observed from comparisons of the noise spectra of a sharp tool with a worn tool, and this increase was high during the initial stages of tool wear and then

tended to saturate. However, this noise spectrum was influenced by other cutting conditions.

1.4.6 Acoustic emission

This method is based on acoustic emission from the cutting process. During the cutting process, deformation and fracture will occur which causes the strain energies stored in the solid material to be released. This results in acoustic emission (AE).

A quantitative model relating the peak value of the RMS AE signals, to both the fractured area and the resultant cutting force at tool fracture, has been developed (Diei 1987). With certain approximations, it can be written as

$$V_p = CF(\Delta A)^{1.5}$$

where V_p is the peak AE RMS voltage at tool fracture, F is the resultant cutting force, ΔA is the area of the fracture surface, C is a constant related to the the material and the geometry. It was pointed out that the theoretical prediction agreed with the experimental results.

Acoustic emission has been detected at the end of tool shank and processed in a number of different ways (Iwata and Moriwaki 1976). The frequency spectrum increased as the tool wear increased, but tended to saturate after further increase of tool wear. The total count of acoustic emission over certain time period was also taken, and had good correlation with tool wear, which could be used for in-process sensing of tool wear.

Significant bursts of AE were generated at the moment of tool breakage (Lan and Dornfeld 1984). Furthermore, it was found that the amplitude of the RMS energy of burst AE events was larger if the tool fracture area was larger.

A technique based on spectral analysis and pattern recognition of AE signals has been developed (Emel and Kannatey-Asibu 1988), and applied to sample sets of data obtained under fixed cutting conditions. It was found that the reliable

frequency range was between 100 kHz and 1 MHz. Progressive tool wear was found to be associated with increasing power within the 400 to 700 kHz band, while catastrophic tool failure had a power spectrum spanning a much wider frequency range. The reliability of detecting tool failure was between 84% to 94%.

Dalpiaz and Remondi (1988) have investigated the relationship between the AE signal on one hand and both tool deterioration phenomena and cutting conditions on the other, by performing turning tests under practical conditions. Many parameters for characterizing AE were considered. It was found that the AE burst frequency matched the chip breaking frequency, thus confirming that chip breakage is the source of the signal bursts.

In conclusion, AE sensing techniques appear to have a quick response time and consistency. It seems to be more sensitive to tool fracture than cutting force measurements and tool vibration analysis, although no convincing experimental evidence of the relative sensitivity has yet been demonstrated.

1.4.7 Workpiece size changes

A device for sensing the change of the workpiece diameter during turning operations has been developed in order to measure tool wear (El Gomayel and Bregger 1986). The change of the workpiece diameter was sensed by electromagnetic sensors which gave a voltage directly related to the gap between the sensor and the workpiece. Two sensors operating in differential modes were used so as to compensate for deflections and vibrations. Small amounts of wear could be detected with this device. For example, using a K21 carbide insert at a cutting speed of 1.79 m/s (350 feet/minute), a feed of 0.528 mm (0.0208 inch), a depth of cut 2.54 mm (0.100 inch), a change in flank wear from 0.206 to 0.241 mm (0.0081 to 0.0095 inch) was measured. At the same time the nose wear remained constant at 15.4 μm (0.0006 inch). The diameter increase was found to be 7.62 μm (0.0003 inch).

During straight turning, tool wear can also be detected by measuring the

change in distance between a tool holder and work surface using a stylus which is mounted on the tool holder (Suzuki and Weinmann 1985). The motion of the stylus was sensed by a displacement transducer, such as an eddy current type. The result of the experiments was found satisfactory. This tool wear sensor is inexpensive because of its simplicity. The drawbacks are that inaccurate slideway motion, changes in the feed force, and the large distance between tool tip and stylus can introduce errors, and that it cannot be readily applied to contour cutting.

Pneumatic gauges have been used for in-process correction of tool wear by monitoring the distance between the tool post or tool and workpiece surface (Bath and Sharp 1968; Stoferle and Bellmann 1975).

Although these measuring systems can detect tool wear by diameter increases, they are not able to diagnose tool failure modes. For example, it is not possible to distinguish between nose wear and flank wear using this technique. Moreover, errors can also be introduced by thermo-expansion of the workpiece and by inaccurate movements of the machine tool.

1.5 Surface analysis

As pointed out by Whitehouse (1978), the surface and its measurement provide a link between the manufacturing workpiece and its function.

As Figure 1.4 shows, the surface can be used to predict how well the parts will function. However, the question arises of how it can also be used to monitor the manufacturing process. The surface texture is, in fact, the fingerprint of the whole machining process, therefore it contains much information about the process, particularly tool wear and vibration. So through analysing the surface, it is possible to estimate the severity of vibration, which enables control of the process. For this method, there are two approaches: one is based on probability and stochastic theory, and the other is deterministic.

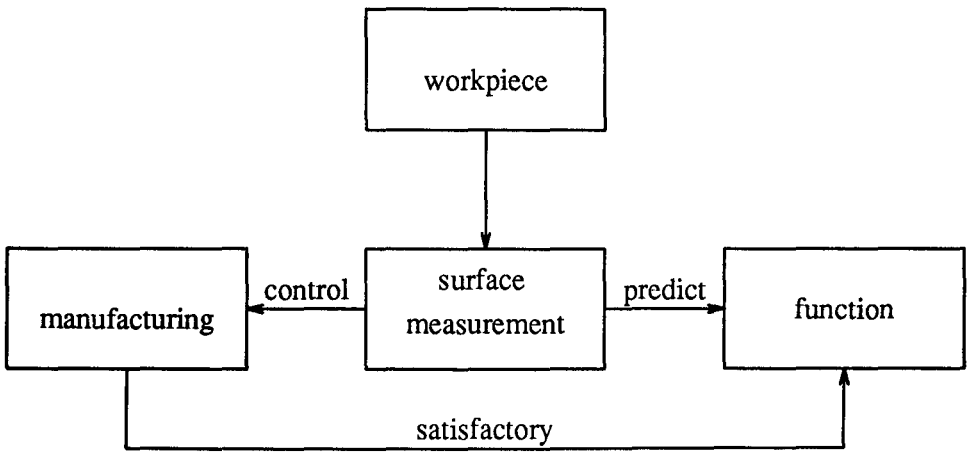

Figure 1.4: Surface: the link between manufacture and function

1.5.1 Statistical approach

Parameters for characterising the surface

In order to measure the surface, there are quite a few quantities to choose from. Here R_a, R_q, $\triangle_q$, and λ_q are used. Their definitions are given as

$$R_a = \frac{1}{l}\int_0^l |y(x)|dx \tag{1.2}$$

$$R_q = \sqrt{\frac{1}{l}\int_0^l y^2(x)dx} \tag{1.3}$$

$$\triangle_q = \sqrt{\frac{1}{l}\int_0^l \left(\frac{dy(x)}{dx}\right)^2 dx} \tag{1.4}$$

$$\lambda_q = 2\pi\frac{R_q}{\triangle_q} \tag{1.5}$$

where $y(x)$ is the profile with respect to the reference line (the reference line is chosen to represent the form of the profile usually such that the areas enclosed above and below the line are equal), x is the distance along a profile, and l is the evaluation length.

To measure these parameters, there are many instruments: optical and non-optical. For non-optical, there are the stylus instrument, electron microscope, scanning tunnelling microscope, and so on. Among them, the stylus instrument,

such as Talysurf VI, is most widely used and it provides all national standard parameters despite the fact that it is slow, not in-process, only provides information for a profile section of surface not an area of surface, and may cause undesirable permanent damage to the surface.

For optical instruments, they can be further divided into those which can record the topographic structure of surface, such as the Foucault knife probe, or interference microscopy, and those which gives parametric values such as R_q.

Monitoring

Since R_q, Δ_q, and λ_q are determined by the cutting tool and cutting condition, we can use them for evaluating the tool wear and monitoring cutting processes.

An optical fibre transducer has been used for in-process indication of surface roughness during a finish turning process (Spurgeon 1974). The transducer was used to trace the same path as the cutting tool, the reflectivity of light from a newly turned surface varied inversely as the roughness of that surface. With the surface having $1\mu m < R_a < 3\mu m$ (R_a is the arithmetical mean deviation), such an optical transducer gave a good indication of surface roughness and thus, indirectly tool wear (for tool nose radius wear has a direct correlation with surface roughness).

Based on diffraction, Rakels and Hingle (1986) have developed an optical instrument capable of in situ measurement of information about the surface roughness and therefore the behaviour of the machine tool which produced the component.

Rau and Huebner (1986) has constructed an optoelectronic device for evaluating the distribution of the scattered light reflected from the surface. A characteristic can be derived from the optical signal in such a way that the results correspond to the frequency analysis of the testing machine. It was claimed that economic 100% control of the shafts with regard to chatter marks was possible if this method applied.

1.5.2 Deterministic approach

Besides the approach on statistics, the deterministic approach can be used. This has been tried by many researchers.

Raja and Whitehouse (1983) have applied complex demodulation technique to surface analysis. It was shown that this technique enabled small changes in the manufacturing process to be identified quickly and positively via the surface profiles. It was predicted that this type of technique would become necessary in future for the control of the manufacturing and also for monitoring the condition of the machine and tool. Further work (Raja and Whitehouse 1984) has confirmed that it is a real possibility to use surface profiles for machine tool surveillance.

Hingle (1986) has studied tool wear monitoring by Fourier analysis of the surface of a component turned by an NC lathe. A computer simulation was performed and verified by experiments. It was found that the maximum value of the power spectral density reached a minimum value at the useful limit of tool life. Comparison of the time to reach the minimum value with tool life time showed good correlation.

The above methods all used Fourier analysis in one way or another to analyze the surface texture of a workpiece. This is not surprising, it is well known that Fourier analysis can be used to analyse stationary signals effectively. However, Fourier analysis is not satisfactory for nonstationary signals. (Fourier analysis will be studied in detail in Chapter 2.) This means that it cannot reveal all the information contained in a nonstationary signal because the surface texture is a very complicated spatial signal and contains nonstationary as well as stationary signals. As a result, the practical application of the above methods are limited.

1.6 Comparative tables of traditional methods

The major advantages and disadvantages of the aforementioned techniques are outlined in Table 1.1

Table 1.1: Comparative tables of traditional methods

		Advantages and Disadvantages	General Remarks
Direct Methods	Optical methods	accurate, can be expensive, sometimes difficult to implement	straightforward, reliable, not in-process
	Radioactive technique	problem of radiation, safety issue, qualitative results only	
Indirect Methods	Cutting forces	commonly used, effective, sometimes difficult to measure at the tip	in-process, influenced by cutting conditions, complicated signal processing sometimes required
	Motor currents	simpler, less sensitive, can have significant time delay, small bandwidth	
	Temperature	sensitive, difficult to implement	
	Vibration	widely used, practical, cost-effective, complicated signal processing sometimes required	
	Sound	similar to vibration method, but less practical	
	Acoustic emission	quick, consistent, sensitive	
	Workpiece sizes	cheap, only for cylindrical workpieces, less sensitive	
Surface Analysis	Statistical approaches	simple, reliable, giving average results only, slow	not in-process, control of manufacturing, prediction of performance
	Deterministic approaches	accurate, reliable, limited if only the Fourier transform is used	

1.7 An approach by the Wigner distribution

Upon considering the comparative table in the previous section, it appears that the method of analysing surface texture by a deterministic approach seems more promising than others. This method is based on the fact:

1. that the surface texture is the fingerprint of the cutting process which generated the surface and contains all sorts of information about the process, and

2. that extracting this information enables us to control machining processes and predict the performance of the workpiece.

However, the wide use of this method has so far been limited. This is because the Fourier transform, which is only suitable for stationary signals, has been used.

In order to analyse all kinds of surface texture effectively, three mathematical analysing tools, i.e. the Fourier transform (FT), the ambiguity function (AF), the Wigner distribution (WD) will be examined in some detail, and their suitability for the task will be assessed. It emerges that the WD is most useful (Chapter 2-3) (Whitehouse and Zheng 1992.)

The rest of the thesis is devoted to validating the technique both by simulated and practical examples (Chapter 4, 5, and 6) (Zheng and Whitehouse 1992).

Chapter 2

The Fourier Transform and the Ambiguity Function

2.1 Introduction

In engineering, there are various types of signals. The type of signal to be analysed has a very important influence on both the type of analysis to be carried out and the choice of analysis parameters. Table 2.1 shows the basic types of signals.

Table 2.1: Signal classification

A signal $f(x)$ where x may be distance, time, or other variable			
stationary		non-stationary	
deterministic	random	deterministic	random

The most fundamental division is into stationary and nonstationary signals. The stationary signal $f(x)$ is interpreted as being those whose average properties does not vary with x and is thus independent of the particular sample record used to determine them. This applies to both deterministic and random signals. Stationary deterministic signals $f(x)$ are usually regarded as those whose Fourier spectrum do not vary with x while stationary random signals are treated as those whose statistics are independent of x. Nonstationary signals are of course

understood as those that are not stationary.

In order to analyse signals, the Fourier transform (FT) is usually employed in practice. Now the question is whether the FT is able to analyse both stationary and nonstationary signals. If not, is there any function which can do so? To answer these questions, the FT, the ambiguity function (AF), and the Wigner distribution (WD) will be examined and their suitability for analysis of signals will be assessed.

For the FT, most of its properties are well known. Therefore most of its proofs are omitted, which can be found in any standard textbook, for example, see (Papoulis 1962).

Because of its practical usage, the discrete Fourier transform is also discussed.

The AF and WD, in both continuous and discrete forms, are similarly examined (Whitehouse and Zheng 1992.)

In order to be systematic and emphasize the similar nature of the variables, the following symbols are chosen to represent distance and frequency variable in continuous and discrete cases signals.

continuous signals		discrete signals	
distance (continuous)	frequency	distance (discrete)	frequency
x	ϖ	n	ϑ
χ	ω	η	θ

2.2 A few notes on mathematics

In this chapter and this thesis as a whole, there is a good deal of mathematics. In order to be precise and clear, a few important points about the mathematics used need to be mentioned.

2.2.1 The Lebesgue integration

In engineering, the Riemann integral (Rudin 1976, Chapter 6) is usually used. The Riemann-integrable functions are subject to rather stringent continuity conditions. Moreover, many limit operations can not be carried out nicely. For example, limits of Riemann-integrable functions may fail to be Riemann-integrable. However, the Lebesgue integral (Rudin 1976, Chapter 11) does not have these problems. The set of Lebesgue-integrable functions is larger than the set of Riemann-integrable functions. In fact, every Riemann-integrable function is also Lebesgue-integrable. Besides this, in Lebesgue theory, many limiting operations can be handled very well. In a word, Lebesgue integration is complete while Riemann integration is not. This is analogous to the fact that the real number system is complete while the rational number system is not (because of irrational numbers). As a result, Lebesgue integration rather than Riemann integration is chosen here.

Summation is treated as a special case of Lebesgue integration. Therefore, many of the theorems about integration can be readily applied to summation (Rudin 1986).

2.2.2 The Fourier transform

In this thesis, the FT and the inverse FT are widely used. For a signal $f(x)$, its FT is not always defined. In order to be valid, $f(x)$ must belong to some set of functions. Here, $f(x)$ is assumed to be in L^2 where

$$L^2 = \{f(x) \mid \left(\int_{-\infty}^{\infty} |f(x)|^2 dx\right)^{\frac{1}{2}} < \infty\} \tag{2.1}$$

In engineering, this set is the set of functions which have finite energy.

If $f(x)$ is not in L^2, it is then extended to L^1

$$L^1 = \{f(x) \mid \int_{-\infty}^{\infty} |f(x)| dx < \infty\} \tag{2.2}$$

Usually, this is the set of absolutely integrable functions. Note that L^2 is a proper subset of L^1. For more, see (Rudin 1986).

If $f(x)$ does not even belong to L^1, then $f(x)$ is extented to the generalized function or distribution. For more, see (Rudin 1973).

If a signal $f(x)$ is in L^2, or L^1, or generalized functions, all the theorems about the FT will be valid (Rudin 1986, Chapter 9; Rudin 1973, Chapter 7).

2.3 The Fourier transform (FT)

The Fourier transform (mainly due to the French engineer J.B.J. Fourier) was developed about two hundred years ago. Since then, it has found wide applications in every area of science and technology (Brigham 1988; Oppenheim 1983).

2.3.1 Definition

Let $f(x)$ be a complex-valued signal of a real variable x, then its *Fourier transform* (FT) $F(\omega)$ is defined (Papoulis 1962) as

$$F(\omega) = \int_{-\infty}^{\infty} f(x)e^{-j\omega x}dx \tag{2.3}$$

where x is normally a time or spatial variable, and ω is its corresponding frequency variable.

From $F(\omega)$, its *inverse Fourier transform* (IFT) $f(x)$ can be constructed by

$$f(x) = \frac{1}{2\pi}\int_{-\infty}^{\infty} F(\omega)e^{j\omega x}d\omega \tag{2.4}$$

Eqn 2.4 is usually called the *inversion formula* or *inversion theorem.*

Since $f(x)$ and $F(\omega)$ are closely related, they are termed a *Fourier transform pair*, this relationship can be represented by the notation

$$f(x) \overset{\mathcal{F}}{\longleftrightarrow} F(\omega) \tag{2.5}$$

2.3.2 Simple properties

There are many useful properties about the Fourier transform, particularly those outlined below (Papoulis 1962; Rudin 1986). In order to avoid repetition, some Fourier transform pairs that will be used in this thesis are listed below:

$$f(x) \overset{\mathcal{F}}{\longleftrightarrow} F(\omega)$$
$$f_1(x) \overset{\mathcal{F}}{\longleftrightarrow} F_1(\omega)$$
$$f_2(x) \overset{\mathcal{F}}{\longleftrightarrow} F_2(\omega)$$
$$g(x) \overset{\mathcal{F}}{\longleftrightarrow} G(\omega)$$
$$h(x) \overset{\mathcal{F}}{\longleftrightarrow} H(\omega)$$
$$m(x) \overset{\mathcal{F}}{\longleftrightarrow} M(\omega)$$

Symmetry

$$F(x) \overset{\mathcal{F}}{\longleftrightarrow} 2\pi f(-\omega)$$

Sum formula

Let a_1 and a_2 be two arbitrary constants, then

$$a_1 f_1(x) + a_2 f_2(x) \overset{\mathcal{F}}{\longleftrightarrow} a_1 F_1(\omega) + a_2 F_2(\omega) \tag{2.6}$$

Spatial scaling

If $a \neq 0$ is a real constant, then

$$f(ax) \overset{\mathcal{F}}{\longleftrightarrow} \frac{1}{|a|} F\left(\frac{\omega}{a}\right) \tag{2.7}$$

Spatial shifting

If $f(x)$ is shifted by a constant x_0, then its FT remains the same, but a linear term $-x_0\omega$ is added to its phase angle, i.e.,

$$f(x - x_0) \overset{\mathcal{F}}{\longleftrightarrow} F(\omega)e^{-j\omega x_0} \tag{2.8}$$

Frequency shifting

If ω_0 is a real constant, then

$$f(x)e^{j\omega_0 x} \overset{\mathcal{F}}{\longleftrightarrow} F(\omega - \omega_0) \tag{2.9}$$

Spatial differentiation

$$\frac{d^n f(x)}{dx^n} \overset{\mathcal{F}}{\longleftrightarrow} F(\omega)(j\omega)^n \tag{2.10}$$

Frequency differentiation

$$f(x)(-jx)^n \overset{\mathcal{F}}{\longleftrightarrow} \frac{d^n F(\omega)}{d\omega^n} \tag{2.11}$$

Moment theorem

This means that

$$m_n = j^n \frac{d^n F(0)}{d\omega^n} \tag{2.12}$$

where m_n is called the nth *moment* of $f(x)$, defined by

$$m_n = \int_{-\infty}^{\infty} f(x)x^n dx$$

Proof: Because of

$$\begin{aligned} F(\omega) &= \int_{-\infty}^{\infty} f(x)e^{-j\omega x}dx \\ &= \int_{-\infty}^{\infty} f(x)\left(\sum_{n=0}^{\infty}\frac{(-j\omega x)^n}{n!}\right)dx \\ &= \sum_{n=0}^{\infty}\left(\int_{-\infty}^{\infty} f(x)x^n dx\right)(-j)^n\frac{\omega^n}{n!} \\ &= \sum_{n=0}^{\infty} m_n\,(-j)^n\frac{\omega^n}{n!} \end{aligned}$$

and

$$F(\omega) = \sum_{n=0}^{\infty}\frac{d^nF(0)}{d\omega^n}\frac{\omega^n}{n!}$$

The proof is obtained by equating coefficients of equal powers of ω in the two equations above.

Convolution

If $g(x)$ is the *convolution* of $f(x)$ and $h(x)$, i.e.

$$g(x) = f(x) * h(x) = \int_{-\infty}^{\infty} f(\chi\,)h(x-\chi\,)d\chi \tag{2.13}$$

then

$$G(\omega) = F(\omega)H(\omega) \tag{2.14}$$

Proof:

$$\begin{aligned} G(\omega) &= \int_{-\infty}^{\infty}\left(\int_{-\infty}^{\infty} f(\chi\,)h(x-\chi\,)d\chi\,\right)e^{-j\omega x}dx \\ &= \int_{-\infty}^{\infty} f(\chi\,)\left(\int_{-\infty}^{\infty} h(x-\chi\,)e^{-j\omega x}dx\right)d\chi \\ &= \int_{-\infty}^{\infty} f(\chi\,)H(\omega)e^{-j\omega\chi}\,d\chi \\ &= F(\omega)H(\omega) \end{aligned}$$

Modulation

If

$$g(x) = f(x)h(x) \tag{2.15}$$

then

$$G(\omega) = \frac{1}{2\pi}F(\omega) * H(\omega) = \frac{1}{2\pi}\int_{-\infty}^{\infty} F(\varpi)H(\omega - \varpi)d\varpi \tag{2.16}$$

Proof:

$$\begin{aligned} g(x) &= \frac{1}{2\pi}\int_{-\infty}^{\infty} G(\omega)e^{j\omega x}d\omega \\ &= \frac{1}{2\pi}\int_{-\infty}^{\infty} \left(\frac{1}{2\pi}\int_{-\infty}^{\infty} F(\varpi)H(\omega - \varpi)d\varpi\right) e^{j\omega x}d\omega \\ &= \frac{1}{2\pi}\int_{-\infty}^{\infty} F(\varpi)\left(\frac{1}{2\pi}\int_{-\infty}^{\infty} H(\omega - \varpi)e^{j\omega x}d\omega\right) d\varpi \\ &= \frac{1}{2\pi}\int_{-\infty}^{\infty} F(\varpi)h(x)e^{j\varpi x}d\varpi \\ &= f(x)h(x) \end{aligned}$$

Parseval's formula

For any $f(x)$,

$$\int_{-\infty}^{\infty}|f(x)|^2dx = \frac{1}{2\pi}\int_{-\infty}^{\infty}|F(\omega)|^2d\omega \tag{2.17}$$

Proof: From

$$\begin{aligned} f(x) &\overset{\mathcal{F}}{\longleftrightarrow} F(\omega) \\ f^*(x) &\overset{\mathcal{F}}{\longleftrightarrow} F^*(-\omega) \end{aligned}$$

and Eqn 2.16, it follows that

$$\int_{-\infty}^{\infty}|f(x)|^2e^{-j\omega x}dx = \frac{1}{2\pi}\int_{-\infty}^{\infty} F(\varpi)F^*(-(\omega - \varpi))d\varpi$$

Let $\omega = 0$, Eqn 2.17 is then obtained.

2.3.3 Application to signals

Periodic signals

For $f(x) = ae^{j\omega_o x}$ where a is a constant, then

$$F(\omega) = a \cdot 2\pi\delta(\omega - \omega_o)$$

which shows the spectrum of the signal very clearly.

Chirp signals

For a chirp signal $f(x) = ae^{j\frac{\alpha}{2}x^2}$ where a is a constant, then

$$F(\omega) = a \cdot \left(\sqrt{\frac{\pi}{4\alpha}}\left(\cos\frac{\omega^2}{2\alpha} + \sin\frac{\omega^2}{2\alpha}\right) + j\sqrt{\frac{\pi}{4\alpha}}\left(\cos\frac{\omega^2}{2\alpha} - \sin\frac{\omega^2}{2\alpha}\right)\right)$$

which is not helpful for revealing the varying spectrum of the chirp signal.

2.4 The discrete Fourier transform (DFT)

2.4.1 Definition

Let $f[n]$ be a complex-valued signal where $n = \cdots, -2, -1, 0, 1, 2, \cdots$, then its *discrete Fourier transform* (DFT) $F(\theta)$ is defined as (Oppenheim 1983).

$$F(\theta) = \sum_{n=-\infty}^{\infty} f(n)e^{-j\theta n} \tag{2.18}$$

From $F(\theta)$, $f(n)$ can be obtained via

$$f[n] = \frac{1}{2\pi}\int_{-\pi}^{\pi} F(\theta)e^{j\theta n}d\theta \tag{2.19}$$

The same notation as employed in the continuous case will be used to describe the relationship between $f(n)$ and $F(\theta)$.

$$f[n] \overset{\mathcal{F}}{\longleftrightarrow} F(\theta) \tag{2.20}$$

2.4.2 Properties

The properties are similar to those of the continuous FT, however there are some differences. For completeness and by virtue of the wide usage of the DFT, its properties are listed below. For more, see (Oppenheim 1983).

Periodicity

For any $f[n]$, its DFT $F(\theta)$ is periodic with period 2π.

$$F(\theta) = F(\theta + 2\pi) \tag{2.21}$$

Sum formula

Let a and b be any arbitrary constants, then

$$af_1[n] + bf_2[n] \overset{\mathcal{F}}{\longleftrightarrow} aF_1(\theta) + bF_2(\theta) \tag{2.22}$$

Spatial shifting

$$f[n - n_0] \overset{\mathcal{F}}{\longleftrightarrow} F(\theta)e^{-j\theta n_0} \tag{2.23}$$

Frequency shifting

$$f[n]e^{j\theta_0 n} \overset{\mathcal{F}}{\longleftrightarrow} F(\theta - \theta_0) \tag{2.24}$$

Scaling

For any positive integer k,

$$f_{(k)}[n] \overset{\mathcal{F}}{\longleftrightarrow} F(k\theta) \tag{2.25}$$

where

$$f_{(k)}[n] = \begin{cases} f[n/k], & \text{if } n \text{ is a multiple of k} \\ 0, & \text{if } n \text{ is not a multiple of k} \end{cases} \tag{2.26}$$

Proof:

$$\begin{aligned} & \sum_{n=-\infty}^{\infty} f_{(k)}[n]\, e^{-j\theta n} \\ &= \sum_{m=-\infty}^{\infty} f_{(k)}[mk]\, e^{-j\theta mk} \\ &= \sum_{m=-\infty}^{\infty} f[m]\, e^{-jk\theta m} \\ &= F(k\theta) \end{aligned}$$

Differentiation in frequency

$$nf[n] \overset{\mathcal{F}}{\longleftrightarrow} j\frac{dF(\theta)}{d\theta} \tag{2.27}$$

Parseval's relation

$$\sum_{n=-\infty}^{\infty} |f^2[n]| = \frac{1}{2\pi}\int_{-\pi}^{\pi} |F(\theta)|^2 d\theta \tag{2.28}$$

Proof:

$$\begin{aligned} & \sum_{n=-\infty}^{\infty} |f^2[n]| \\ &= \sum_{n=-\infty}^{\infty} f[n]f^*[n] \\ &= \sum_{n=-\infty}^{\infty} f[n]\left(\frac{1}{2\pi}\int_{-\pi}^{\pi} F^*(\theta)e^{-j\theta n}d\theta\right) \\ &= \frac{1}{2\pi}\int_{-\pi}^{\pi} F^*(\theta)\left(\sum_{n=-\infty}^{\infty} f[n]e^{-j\theta n}\right)d\theta \\ &= \frac{1}{2\pi}\int_{-\pi}^{\pi} |F(\theta)|^2 d\theta \end{aligned}$$

Convolution

Let $g[n]$ be the convolution of $f[n]$ and $h[n]$, i.e.

$$g[n] = f[n] * h[n] = \sum_{\eta=-\infty}^{\infty} f[\eta]h[n-\eta] \tag{2.29}$$

then

$$G(\theta) = F(\theta)H(\theta) \tag{2.30}$$

Proof:

$$\begin{aligned}
& G(\theta) \\
&= \sum_{n=-\infty}^{\infty}\sum_{\eta=-\infty}^{\infty} (f[\eta]h[n-\eta])e^{-j\theta n} \\
&= \sum_{\eta=-\infty}^{\infty} f[\eta](\sum_{n=-\infty}^{\infty} h[n-\eta]e^{-j\theta n}) \\
&= \sum_{\eta=-\infty}^{\infty} f[\eta](H(\theta)e^{-j\theta\eta}) \\
&= \sum_{\eta=-\infty}^{\infty} f[\eta]e^{-j\theta\eta}\, H(\theta) \\
&= F(\theta)H(\theta)
\end{aligned}$$

Modulation

If $g[n] = f[n]h[n]$, then

$$G(\theta) = \frac{1}{2\pi}F(\theta) * H(\theta) = \frac{1}{2\pi}\int_{\pi}^{\pi} F(\vartheta)H(\theta-\vartheta)d\vartheta \tag{2.31}$$

Proof:

$$\begin{aligned}
& G(\theta) \\
&= \sum_{n=-\infty}^{\infty} f[n]h[n]e^{-j\theta n} \\
&= \sum_{n=-\infty}^{\infty} h[n]\left(\frac{1}{2\pi}\int_{-\pi}^{\pi} F(\vartheta)e^{j\vartheta n}d\vartheta\right)e^{-j\theta n}
\end{aligned}$$

$$= \frac{1}{2\pi}\int_{-\pi}^{\pi} F(\vartheta)\left(\sum_{n=-\infty}^{\infty} h[n]e^{-j(\theta-\vartheta)n}\right)d\vartheta$$
$$= \frac{1}{2\pi}\int_{-\pi}^{\pi} F(\vartheta)H(\theta-\vartheta)d\vartheta$$

2.4.3 The fast Fourier transform

In theoretical work, the continuous FT is normally used. However, the DFT is used in practice because there is an efficient algorithm called *the fast Fourier transform* (FFT) which can compute the DFT very efficiently (Cooley and Tukey 1965).

Let $f[n]$ be restricted to $[0, N]$.

$$F(\theta) = \sum_{n=0}^{N-1} f(n)e^{-j\theta n} \tag{2.32}$$

When $\theta = \frac{2\pi k}{N}$

$$F[k] = F(\frac{2\pi k}{N}) = \sum_{n=0}^{N-1} f(n)e^{-j(2\pi/N)nk} \tag{2.33}$$

The complexity of this algorithm is $O(N^2)$. This algorithm is very slow for large N.

However, the complexity of the FFT is $O(N \log N)$. As a result, this algorithm is very efficient even for large N. As a result of this development, applications of the DFT has spread quickly. For the algorithm itself, see Appendix A.

2.4.4 Applications to signals

As a measure of its usefulness, the FT will be applied to a number of signals often found in manufacturing engineering. Some examples are given in Fig 2.1 to Fig 2.4.

In Figure 2.1, $f[n]$ is

$$f[n] = \begin{cases} e^{j\theta_0 n} & \text{when } 0 \le n \le N-1 \\ 0 & \text{otherwise} \end{cases} \tag{2.34}$$

where $\theta_0 = \frac{\pi}{4}$ and $N = 256$.

In Figure 2.2, $f[n]$ is the sum of three terms which are of the type:

$$f[n] = \begin{cases} \sum_{i=1}^{3} A_i e^{j\theta_i n} & \text{when } 0 \leq n \leq N-1 \\ 0 & \text{otherwise} \end{cases} \tag{2.35}$$

where $A_1 = 0.5, \theta_1 = \frac{\pi}{8}$; $A_2 = 1.0, \theta_2 = \frac{\pi}{4}$; and $A_3 = 0.25, \theta_3 = \frac{3\pi}{8}$ and $N = 256$.

It is clearly seen that the *Fourier transform can analyse stationary signals very effectively* from Figure 2.1 and Figure 2.2,

In Figure 2.3, $f[n]$ is where

$$f[n] = \begin{cases} e^{j(\alpha/2)n^2} & \text{when } 0 \leq n \leq N-1 \\ 0 & \text{otherwise} \end{cases} \tag{2.36}$$

where $\alpha = \frac{\pi}{2N}$ and $N = 256$. This $f[n]$ is normally called as a chirp signal, a typically nonstationary signal.

In Figure 2.4,

$$f[n] = \begin{cases} e^{j(\theta_0 n + b\sin(\theta_m n))} & \text{when } 0 \leq n \leq N-1 \\ 0 & \text{otherwise} \end{cases} \tag{2.37}$$

where $\theta_0 = \frac{\pi}{4}$, $\theta_m = \frac{\pi}{32}$, and $b = 3.0$. This is a frequency-modulated (FM) signal.

From Fig 2.3 and Fig 2.4, it can be seen that the Fourier transform can not reveal how the local spectrum varies with space or time. It can be concluded that *the Fourier transform is not very helpful for analysing nonstationary signals.*

To overcome this, other type of transform is evidently needed if the nonstationary properties are to be easily revealed. A transform which encompasses both space (or time) and frequency simultaneously seems an obvious solution. One such possibility is the ambiguity function, which is investigated next.

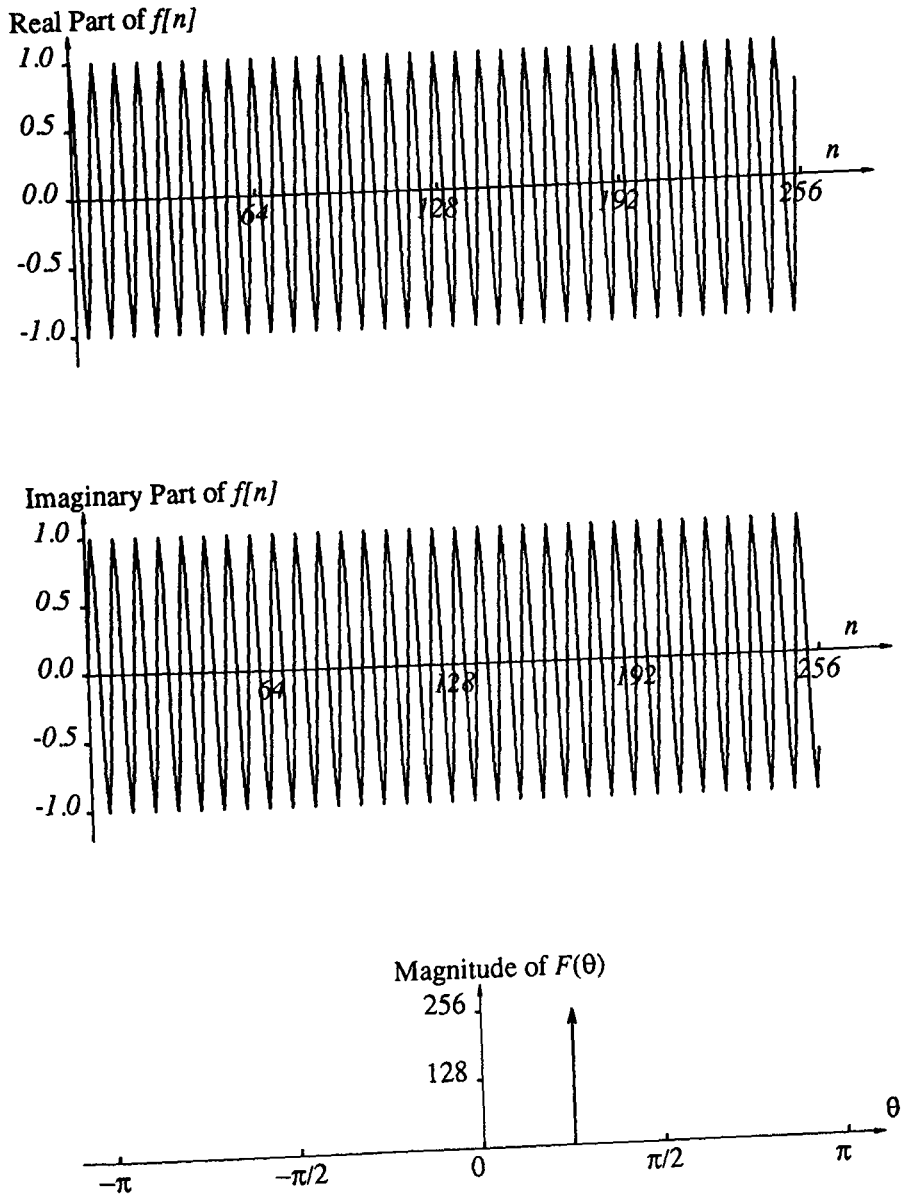

Figure 2.1: A stationary signal $f[n]$ and its DFT $|F(\theta)|$.

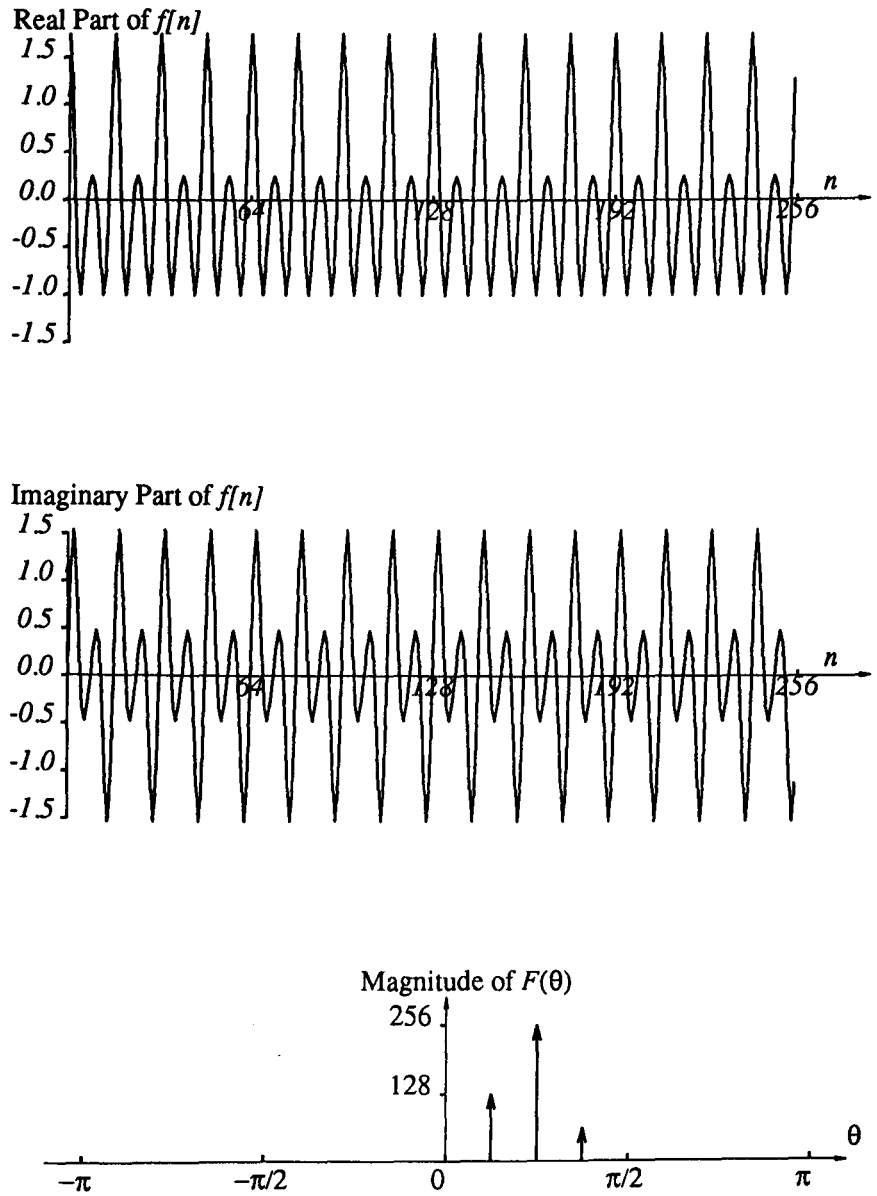

Figure 2.2: Another stationary signal $f[n]$ and its DFT $|F(\theta)|$.

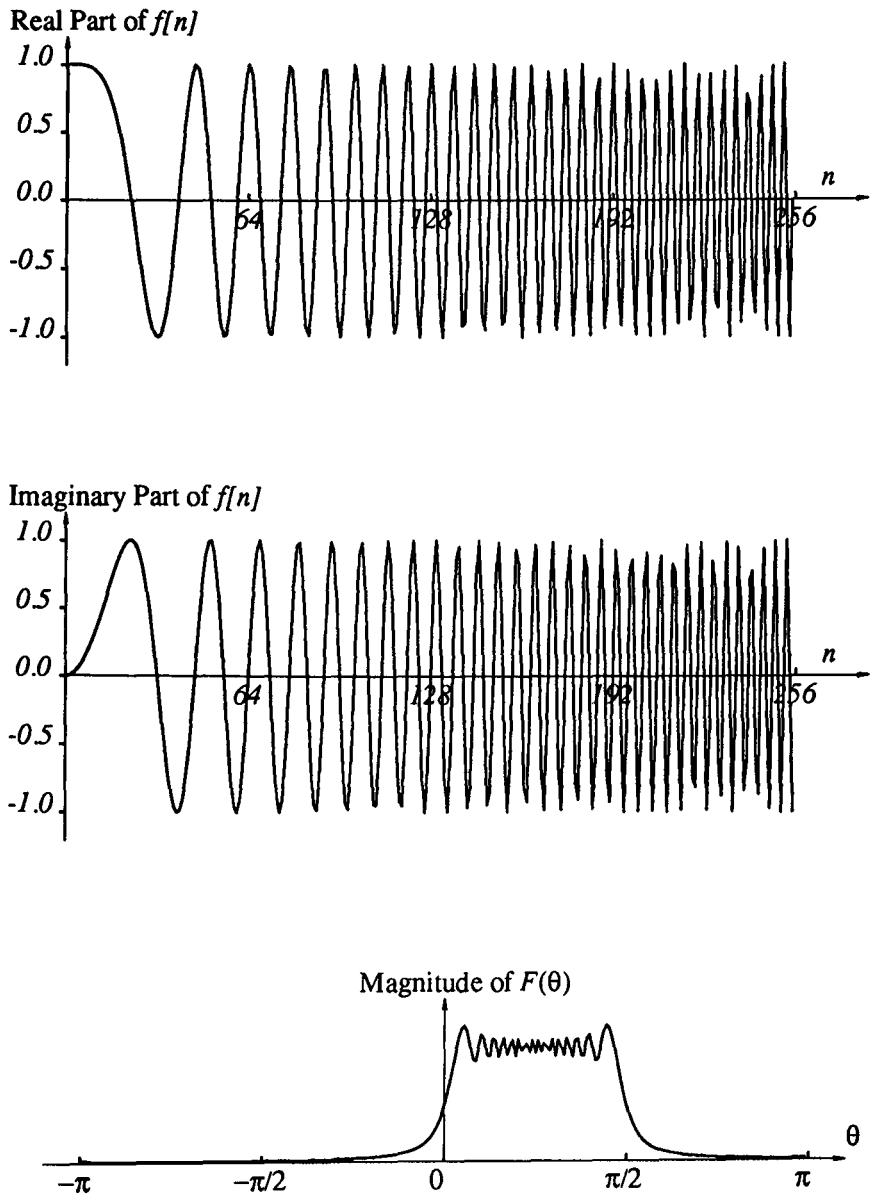

Figure 2.3: A chirp signal $f[n]$ and its DFT $|F(\theta)|$.

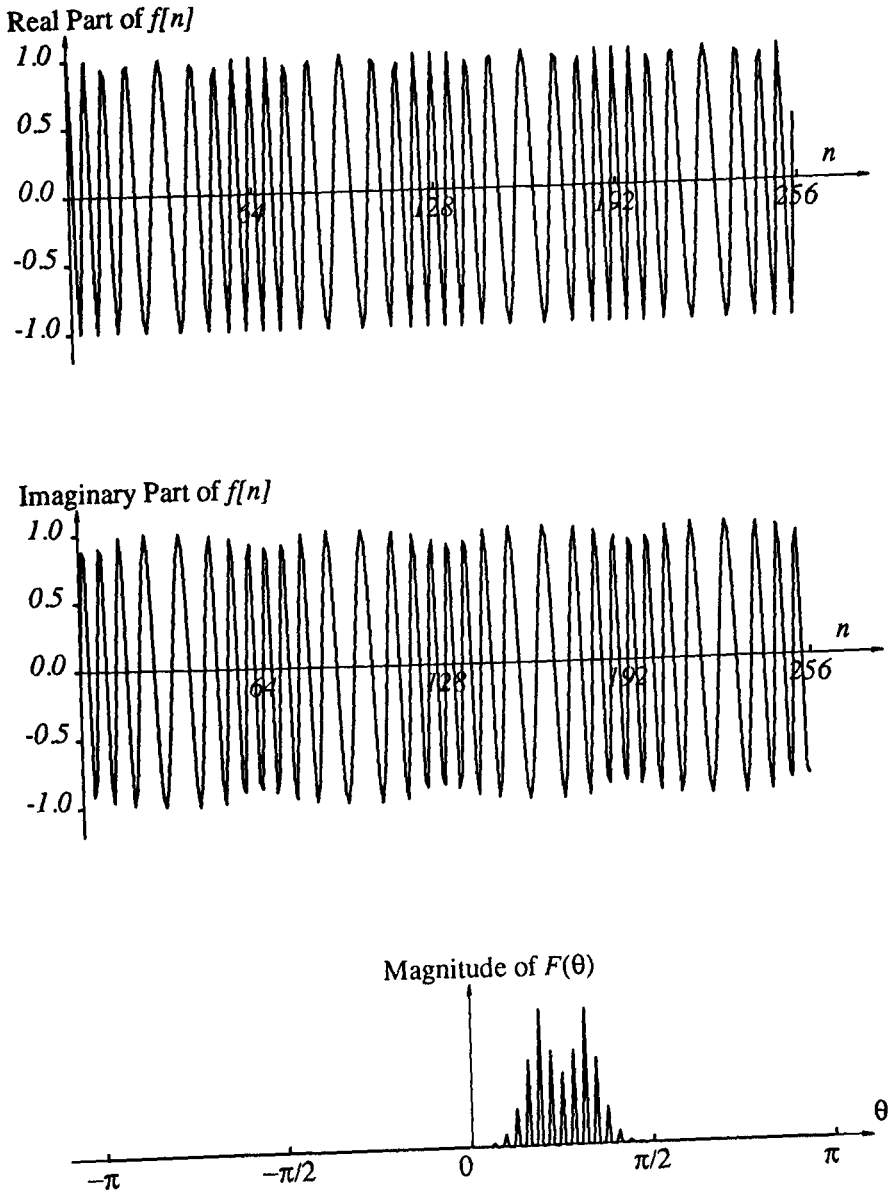

Figure 2.4: A frequency modulated signal $f[n]$ and its DFT $|F(\theta)|$.

2.5 The ambiguity function (AF)

The ambiguity function was originally introduced by Woodward (1953) into Radar for detection of the distance and velocity of aeroplanes. Since then it has been applied to optical signal processing (Bruck and Sodin 1979; Guigay 1978; Lee et al. 1980; Marks, Walkup, and Krile 1977; Marks and Hall 1979; Papoulis 1974; Said and Cooper 1973). As a tool for analysing signals, the ambiguity function has been studied in a great detail by many researchers (Papoulis 1974; Papoulis 1984; Reis 1962; Siebert 1958; Stutt 1959; Stutt 1964; Sussman 1962; Titlebaum and DeClaris 1966).

2.5.1 Definition

For any complex-valued signal $f(x)$ where x is an independent continuous variable, then its *ambiguity function* (AF), denoted as $A_f(\varpi, \chi)$, is defined[1] as

$$A_f(\varpi, \chi) = \int_{-\infty}^{\infty} f(x + \frac{\chi}{2}) f^*(x - \frac{\chi}{2}) e^{-j\varpi x} dx \tag{2.39}$$

The AF $A_f(\varpi, \chi)$ can aslo be definded as

$$A_f(\varpi, \chi) = \frac{1}{2\pi} \int_{-\infty}^{\infty} F(\omega + \frac{\varpi}{2}) F^*(\omega - \frac{\varpi}{2}) e^{j\omega\chi} d\omega \tag{2.40}$$

In fact, from the change-of-variables theorem (Rudin 1976, p 252; or Rudin 1986, p 153), it follows that

$$\begin{aligned} &\int_{-\infty}^{\infty}\int_{-\infty}^{\infty} f(x + \frac{\chi}{2}) f^*(x - \frac{\chi}{2})\, e^{-j\varpi x}\, e^{-j\omega\chi} dx d\chi \\ &= \int_{-\infty}^{\infty}\int_{-\infty}^{\infty} f(t) f^*(\tau) e^{-j\varpi(t+\tau)/2}\, e^{-j\omega(t-\tau)} \cdot dt d\tau \end{aligned}$$

[1] Besides the definition by Eqn 2.39, there is another definition which is also often used:

$$A_f(\varpi, \chi) = \int_{-\infty}^{\infty} f(x) f^*(x - \chi) e^{-j\varpi x} dx \tag{2.38}$$

$$
\begin{aligned}
&= \int_{-\infty}^{\infty}\int_{-\infty}^{\infty} f(t)f^*(\tau)e^{-j(\omega+\frac{\varpi}{2})t}\, e^{-j(\frac{\varpi}{2}-\omega)\tau}dtd\tau \\
&= F(\omega+\frac{\varpi}{2})F^*(-(\frac{\varpi}{2}-\omega)) \\
&= F(\omega+\frac{\varpi}{2})F^*(\omega-\frac{\varpi}{2})
\end{aligned}
$$

where x and χ are substituted by $\frac{t+\tau}{2}$ and $t-\tau$ respectively. Hence,

$$
\frac{1}{2\pi}\int_{-\infty}^{\infty} F(\omega+\frac{\varpi}{2})F^*(\omega-\frac{\varpi}{2})e^{j\omega\chi}d\omega = \int_{-\infty}^{\infty} f(x+\frac{\chi}{2})f^*(x-\frac{\chi}{2})e^{-j\varpi x}dx \quad (2.41)
$$

If the $A_f(\varpi,\chi)$ is known, then we can reconstruct the orginal signal $f(x)$ within a constant factor. In fact, it can be proved that (Papoulis 1984, p. 287)

$$
f(\chi)\cdot f^*(0) = \frac{1}{2\pi}\int_{-\infty}^{\infty} A_f(\varpi,\chi)e^{j\varpi\frac{\chi}{2}}d\varpi \quad (2.42)
$$

Proof: From Eqn 2.39,

$$
\frac{1}{2\pi}\int_{-\infty}^{\infty} A_f(\varpi,\chi)e^{j\varpi x}d\varpi = f(x+\frac{\chi}{2})f^*(x-\frac{\chi}{2}) \quad (2.43)
$$

Let $x=\frac{\chi}{2}$,

$$
f(\chi)f^*(0) = \frac{1}{2\pi}\int_{-\infty}^{\infty} A_f(\varpi,\chi)e^{j\varpi\frac{\chi}{2}}d\varpi \quad (2.44)
$$

Just like the Fourier transform pair, we will express $f(x)$ and $A_f(\varpi,\chi)$ together as

$$
f(x) \overset{\mathcal{A}}{\longleftrightarrow} A_f(\varpi,\chi)
$$

2.5.2 Simple properties

For more detail, see (Papoulis 1984).

Spatial shifting

$$
f(x-x_0) \overset{\mathcal{A}}{\longleftrightarrow} A_f(\varpi,\chi)e^{-j\varpi x_0} \quad (2.45)
$$

Frequency shifting

$$f(x)e^{j\omega_0 x} \overset{\mathcal{A}}{\longleftrightarrow} A_f(\varpi, \chi)e^{j\omega_0 \chi} \tag{2.46}$$

Spatial limited signals

If $f(x)$ is restricted to $[x_a, x_b]$, then $A_f(\varpi, \chi)$ is restricted to $[-(x_b - x_a), x_b - x_a]$ with respect to χ.

Frequency limited signals

If $f(x)$ is band-limited to $[\omega_a, \omega_b]$, then $A_f(\varpi, \chi)$ is limited to $[-(\omega_b - \omega_a), \omega_b - \omega_a]$ in terms of ϖ.

Concentration of energy

For any $f(x)$,

$$|A_f(\varpi, \chi)| \leq \int_{-\infty}^{\infty} |f(x)|^2 dx = A_f(0,0)$$

Proof: Because of

$$|A_f(\varpi, \chi)| \leq \int_{-\infty}^{\infty} |f(x + \tfrac{\chi}{2}) f^*(x - \tfrac{\chi}{2})| dx \tag{2.47}$$

and

$$\int_{-\infty}^{\infty} |f(x+\tfrac{\chi}{2}) f^*(x-\tfrac{\chi}{2})| dx \leq \left(\int_{-\infty}^{\infty} |f(x + \tfrac{\chi}{2})| dx\right)^{\frac{1}{2}} \cdot \left(\int_{-\infty}^{\infty} |f(x - \tfrac{\chi}{2})| dx\right)^{\frac{1}{2}} \tag{2.48}$$

from *the Schwarz inequality* (Rudin 1986, Theorem 3.5), it follows

$$\begin{aligned}
&|A_f(\varpi, \chi)| \\
&\leq \left(\int_{-\infty}^{\infty} |f(x + \tfrac{\chi}{2})| dx\right)^{\frac{1}{2}} \cdot \left(\int_{-\infty}^{\infty} |f(x - \tfrac{\chi}{2})| dx\right)^{\frac{1}{2}} \\
&= \int_{-\infty}^{\infty} |f(x)|^2 dx \\
&= \int_{-\infty}^{\infty} f(x) f^*(x) dx \\
&= A_f(0,0)
\end{aligned}$$

Total energy

$$\frac{1}{2\pi}\int_{-\infty}^{\infty}\int_{-\infty}^{\infty}|A_f(\varpi,\chi)|^2 d\varpi d\chi = \|f(x)\|^4$$

Proof: From Eqn 2.39 and Parseval's formula (Eqn 2.17)

$$\frac{1}{2\pi}\int_{-\infty}^{\infty}|A_f(\varpi,\chi)|^2 d\varpi = \int_{-\infty}^{\infty}|f(x+\tfrac{\chi}{2})f^*(x-\tfrac{\chi}{2})|^2 dx$$

Hence,

$$\frac{1}{2\pi}\int_{-\infty}^{\infty}\int_{-\infty}^{\infty}|A_f(\varpi,\chi)|^2 d\varpi d\chi = \int_{-\infty}^{\infty}\int_{-\infty}^{\infty}|f(x+\tfrac{\chi}{2})f^*(x-\tfrac{\chi}{2})|^2 dx d\chi$$

But from Theorem 10.9 (Rudin 1976),

$$\int_{-\infty}^{\infty}\int_{-\infty}^{\infty}|f(x+\tfrac{\chi}{2})f^*(x-\tfrac{\chi}{2})|^2 dx d\chi = \int_{-\infty}^{\infty}\int_{-\infty}^{\infty}|f(x_1)f^*(x_2)|^2 dx_1 dx_2$$

Combining the two equations above, we obtain the proof.

Convolution

If $g(x) = f(x) * h(x)$, then

$$A_g(\varpi,\chi) = \int_{-\infty}^{\infty} A_f(\varpi,x)A_h(\varpi,\chi - x)dx \tag{2.49}$$

Proof:

$$\begin{aligned}
&A_g(\varpi,\chi)\\
&= \frac{1}{2\pi}\int_{-\infty}^{\infty} G(\omega+\tfrac{\varpi}{2})G^*(\omega-\tfrac{\varpi}{2})e^{j\omega\chi}d\omega\\
&= \frac{1}{2\pi}\int_{-\infty}^{\infty} F(\omega+\tfrac{\varpi}{2})F^*(\omega-\tfrac{\varpi}{2})\cdot H(\omega+\tfrac{\varpi}{2})H^*(\omega-\tfrac{\varpi}{2})e^{j\omega\chi}d\omega\\
&= \int_{-\infty}^{\infty} A_f(\varpi,x)A_h(\varpi,\chi - x)dx
\end{aligned}$$

The last equation is obtained by regrarding χ and ω as variables, treating ϖ as a fixed parameter, and applying Eqn 2.13.

Modulation

If $g(x) = f(x)m(x)$, then

$$A_g(\varpi, \chi) = \frac{1}{2\pi}\int_{-\infty}^{\infty} A_f(\omega, \chi) A_h(\varpi - \omega, \chi) d\omega \tag{2.50}$$

Proof:

$$\begin{aligned} & A_g(\varpi, \chi) \\ &= \int_{-\infty}^{\infty} g(x + \tfrac{\chi}{2}) g^*(x - \tfrac{\chi}{2}) e^{-j\varpi x} dx \\ &= \int_{-\infty}^{\infty} f(x + \tfrac{\chi}{2}) f^*(x - \tfrac{\chi}{2}) \cdot h(x + \tfrac{\chi}{2}) h^*(x - \tfrac{\chi}{2}) e^{-j\varpi x} dx \\ &= \frac{1}{2\pi}\int_{-\infty}^{\infty} A_f(\omega, \chi) A_h(\varpi - \omega, \chi) d\omega \end{aligned}$$

The last equation is from Eqn 2.16.

2.5.3 Application to signals

Periodic signals

Let $f(x) = ae^{j\omega_0 x}$ where a is a constant,

$$a_f(\varpi, \chi) = |a|^2 \cdot e^{j\varpi_0 \chi} \cdot 2\pi\delta(\varpi) \tag{2.51}$$

Chirp signals

Let $f(\chi) = ae^{j\frac{1}{2}\alpha x^2}$ where a is a constant,

$$a_f(\varpi, \chi) = |a|^2 \cdot 2\pi\delta(\varpi - \alpha\chi) \tag{2.52}$$

2.6 The discrete ambiguity function (DAF)

Although the AF has been studied in great detail, the discrete ambiguity function has hardly been investigated. In fact, the literature about it is very limited. Here, the way it is defined as Eqn 2.53 is to make the comparison with the discrete Wigner distribution (see Section 3.3) easier.

2.6.1 Definition

For a complex-valued signal $f[n]$ where $n = \cdots, -2, -1, 0, 1, 2, \cdots$, its *discrete Ambiguity function* (DAF), denoted as $A_f(\vartheta, \eta)$, can be defined as

$$A_f(\vartheta, \eta) = \sum_{n=-\infty}^{\infty} 2f[n+\eta]f^*[n-\eta]e^{-j2\vartheta n} \tag{2.53}$$

The DAF can also be defined as

$$A_f(\vartheta, \eta) = \frac{1}{\pi}\int_{-\pi}^{\pi} F(\theta+\vartheta)F^*(\theta-\vartheta)e^{j2\theta\eta}d\theta \tag{2.54}$$

where $F(\vartheta)$ is the DFT of $f[n]$.
In fact,

$$\begin{aligned}
A_f(\vartheta, \eta) &= \sum_{n=-\infty}^{\infty} 2f[n+\eta]f^*[n-\eta]e^{-j2n\vartheta} \\
&= 2\sum_{n=-\infty}^{\infty} f[n+\eta]e^{-j2\vartheta n}\cdot f^*[-(\eta-n)] \\
&= \frac{1}{\pi}\int_{-\pi}^{\pi} F(\theta+2\vartheta)e^{j(\theta+2\vartheta)\eta}\cdot F^*(\theta)e^{j\theta\eta}d\theta \\
&= \frac{1}{\pi}\int_{-\pi}^{\pi} F(\theta+\vartheta+\vartheta)F^*(\theta+\vartheta-\vartheta)e^{j2(\theta+\vartheta)\eta}d\theta \\
&= \frac{1}{\pi}\int_{-\pi}^{\pi} F(\theta+\vartheta)F^*(\theta-\vartheta)e^{j2\theta\eta}d\theta
\end{aligned}$$

Just like the continuous AF, the following notation will be used

$$f[n] \overset{\mathcal{A}}{\longleftrightarrow} A_f(\vartheta, \eta) \tag{2.55}$$

to represent the relationship between $f[n]$ and $A_f(\vartheta, \eta)$.

2.6.2 Properties

Periodicity

$$A_f(\vartheta, \eta) = A_f(\vartheta + \pi, \eta) \tag{2.56}$$

Spatial shifting

$$f[n - n_0] \overset{\mathcal{A}}{\longleftrightarrow} A_f(\vartheta, \eta) \cdot e^{-j2\theta n_0} \tag{2.57}$$

Frequency shifting

$$f[n]e^{j\theta_0 n} \overset{\mathcal{A}}{\longleftrightarrow} A_f(\vartheta, \eta) \cdot e^{j2\theta_0 \eta} \tag{2.58}$$

Spatial-limited signals

If $f[n]$ is restricted to $[n_a, n_b]$, then $A_f(\vartheta, \eta)$ is restricted to $[-n_c, n_c]$ where n_c is the quotient of $n_b - n_a$ divided by 2.

Frequency-limited signals

If $F(\vartheta)$ (the DFT of $f[n]$) is restricted to $[\vartheta_a, \vartheta_b]$, then $A_f(\vartheta, \eta)$ is restricted to $[-(\vartheta_b - \vartheta_a), \vartheta_b - \vartheta_a]$.

Concentration of energy

$$|A_f(\vartheta, \eta)| \leq 2 \sum_{n=-\infty}^{\infty} |f[n]|^2 = A_f(0, 0) \tag{2.59}$$

Proof: From Eqn 2.53,

$$\begin{aligned} & |A_f(\vartheta, \eta)| \\ \leq & 2 \sum_{n=-\infty}^{\infty} |f[n + \eta] f^*[n - \eta]| \\ \leq & 2 \sum_{n=-\infty}^{\infty} |f[n]|^2 \qquad \text{(the Schwarz inequality)} \\ = & A_f(0, 0) \end{aligned}$$

2.6.3 Computation of the DAF

When $f[n]$ is restricted to $[0, N-1]$ where N is even[2], computation of the DAF is straightforward. This is achieved as follows

1. Compute $r[\eta, n] = 2f[n+\eta]f^*[n-\eta]$ for $n = 0, 1, \cdots, N-1$ and $\eta = -M, \cdots, 0, \cdots, M$ where $M = \frac{N}{2} - 1$.

2. By means of the FFT, compute $\sum_{n=0}^{N-1} r[\eta, n] e^{-j\frac{2\pi kn}{N}}$ for $\eta = -M, \cdots, 0, \cdots, M$

3. $A_f(\varpi, \eta)$ is then obtained for $\varpi = \frac{k\pi}{N}$ where $k = 0, 1, \cdots, N-1$ and $\eta = -M, \cdots, 0, \cdots, M$. Because of $A_f(\varpi, \eta)$ is restricted in η and periodic in ϖ, so $A_f[k, \eta] = A_f(\frac{k\pi}{N}, \eta)$ is obtained for $k, \eta = -\cdots, -2, -1, 0, 1, 2, \cdots$.

2.6.4 Application to signals useful in manufacturing

Figure 2.6.4, 2.6, 2.7 and 2.8 show four DAFs computed for the same signals as in Section 2.4.4.

In addition to three-dimensional (3D) plots, both density plots and contour plots are also added. In a density plot, the height of the function at each point is shown by shading: the higher the lighter; the lower the darker. In a contour plot, the contour lines are just like those in a standard topographical map, they join points on the same height. Because of its nature, when *Mathematica* makes a contour plot, it tries to include only the "interesting" parts of the plot. If a function increases very rapidly, or has singularities, the parts where it gets too large will be cut off while the parts with small values may be plot out. Therefore, it is necessary to concentrate on the main feature of a contour plot. For 3D plots and density plots, there is no such a problem for the plot range is chosen to be large enough to display the whole range.

[2]For odd N, it is similar provided that it can be represented by $N = N_1 \cdot N_2 \cdots N_k$

For the two stationary signals, the DAFs are mainly concentrated on the $\vartheta = 0$. In other words, the DAF can not distinguish the high frequency stationary signals from the low frequency ones. This means that the AF is not suitable for stationary signals. However, for two nonstationary signals, the DAFs do display changes of instantaneous frequencies.

It can be concluded that *although the DAF is good for analysing nonstationary signals, it is not so for stationary signals from these figures.*

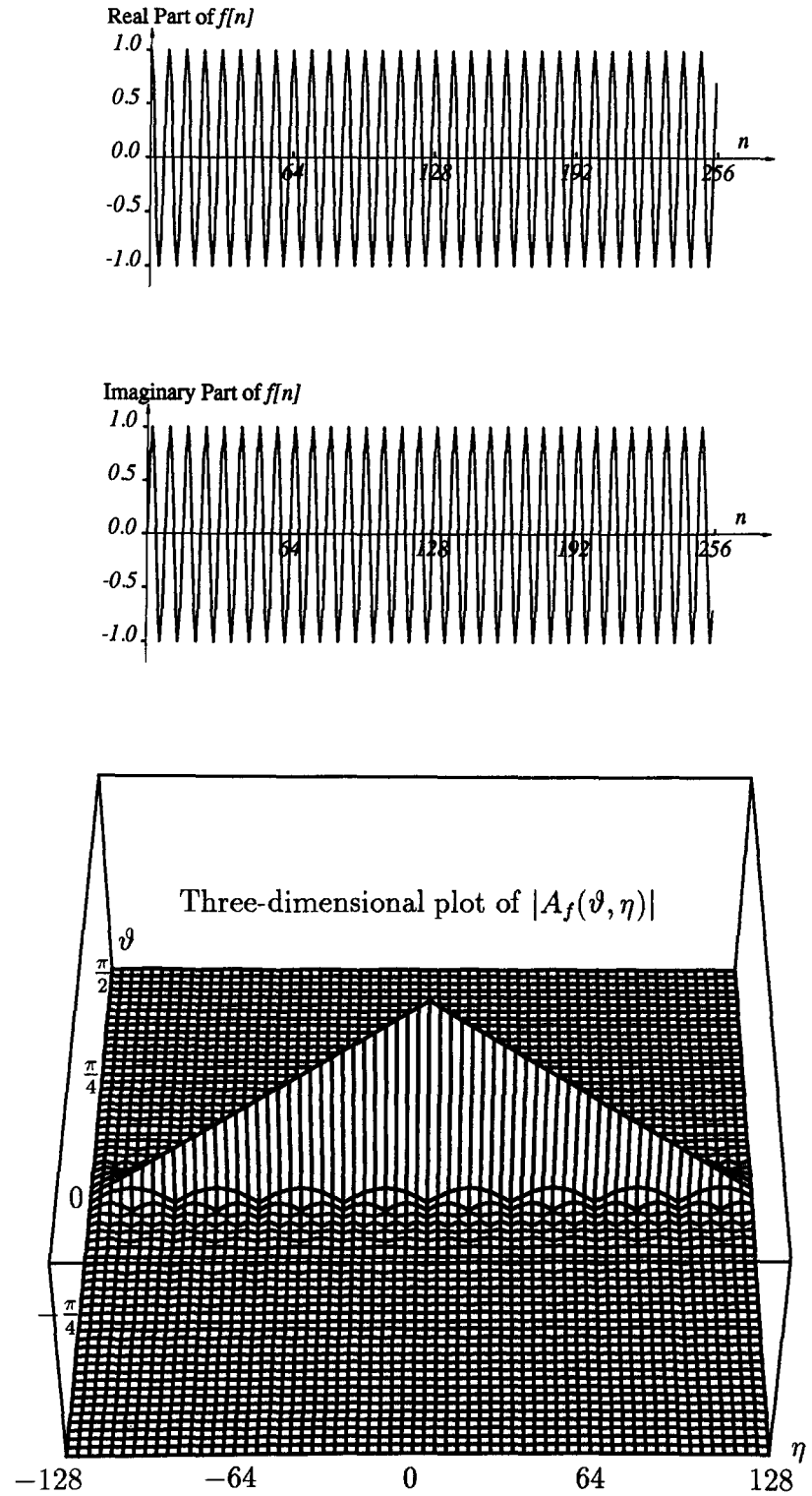

Figure 2.5: A stationary signal $f[n]$ and its DAF.

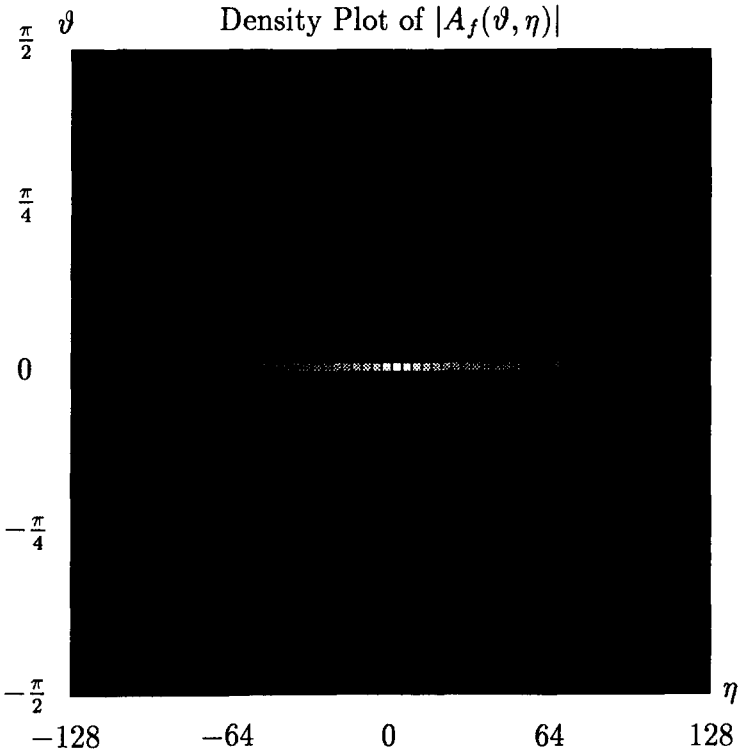

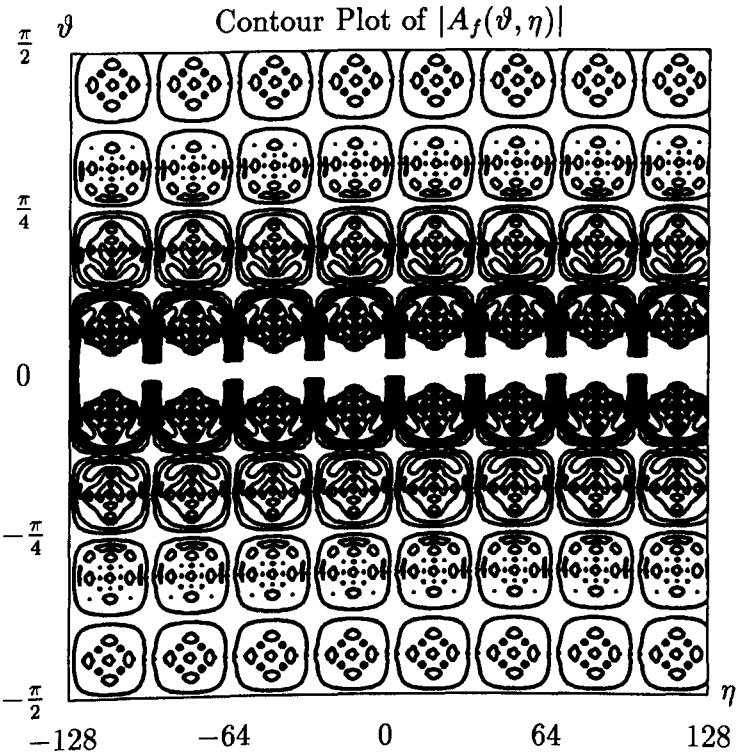

A stationary signal $f[n]$ and its DAF (continued).

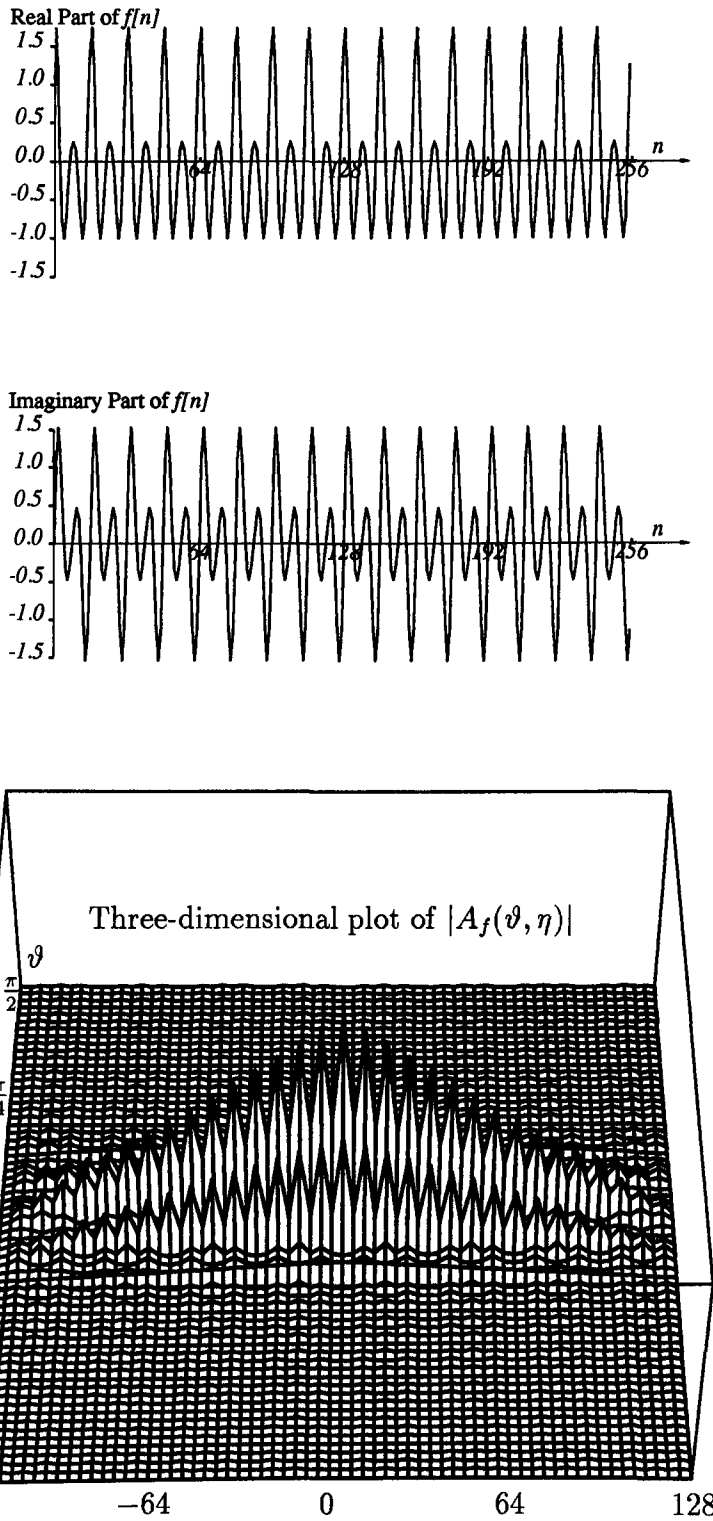

Figure 2.6: Another stationary signal $f[n]$ and its DAF.

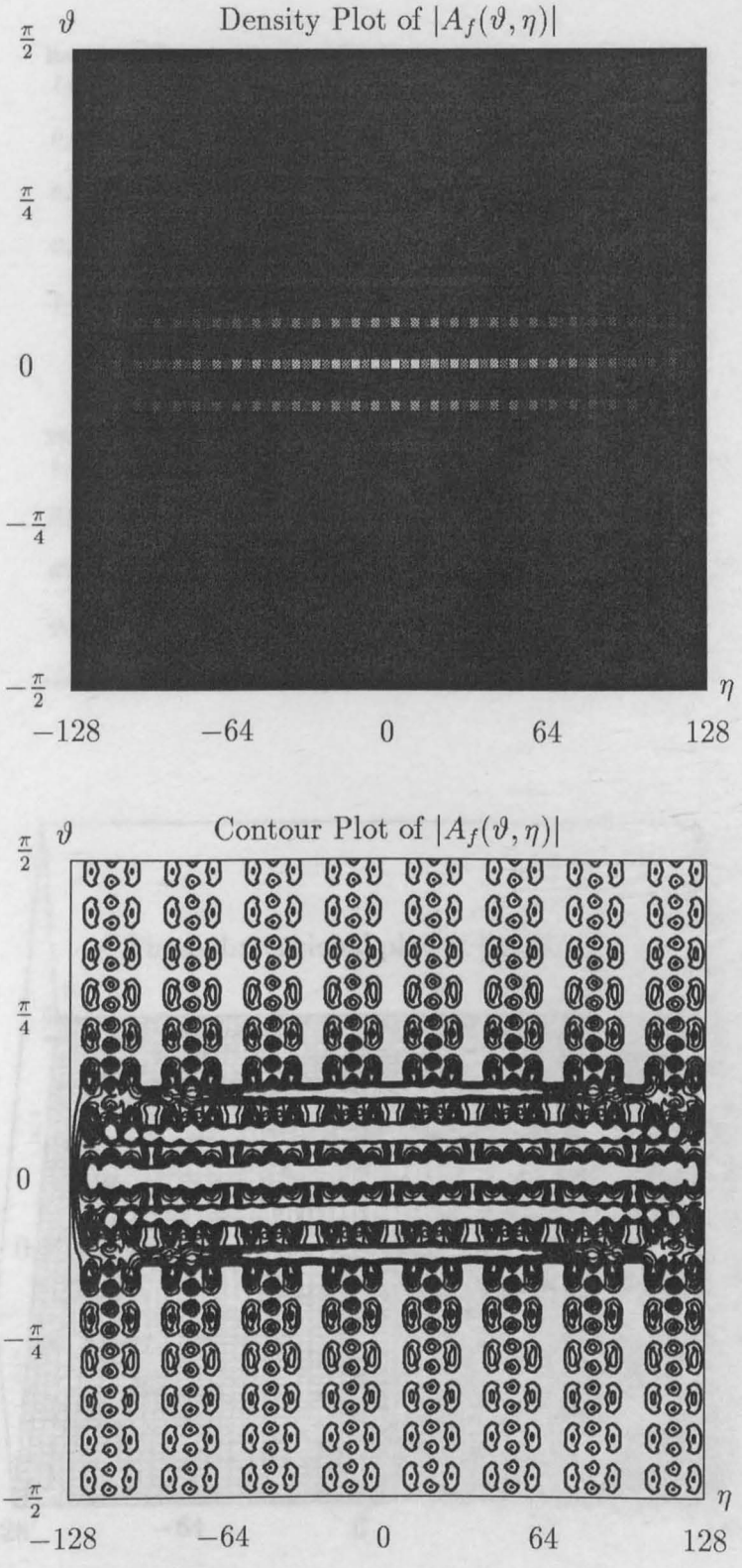

Another stationary signal $f[n]$ and its DAF (continued).

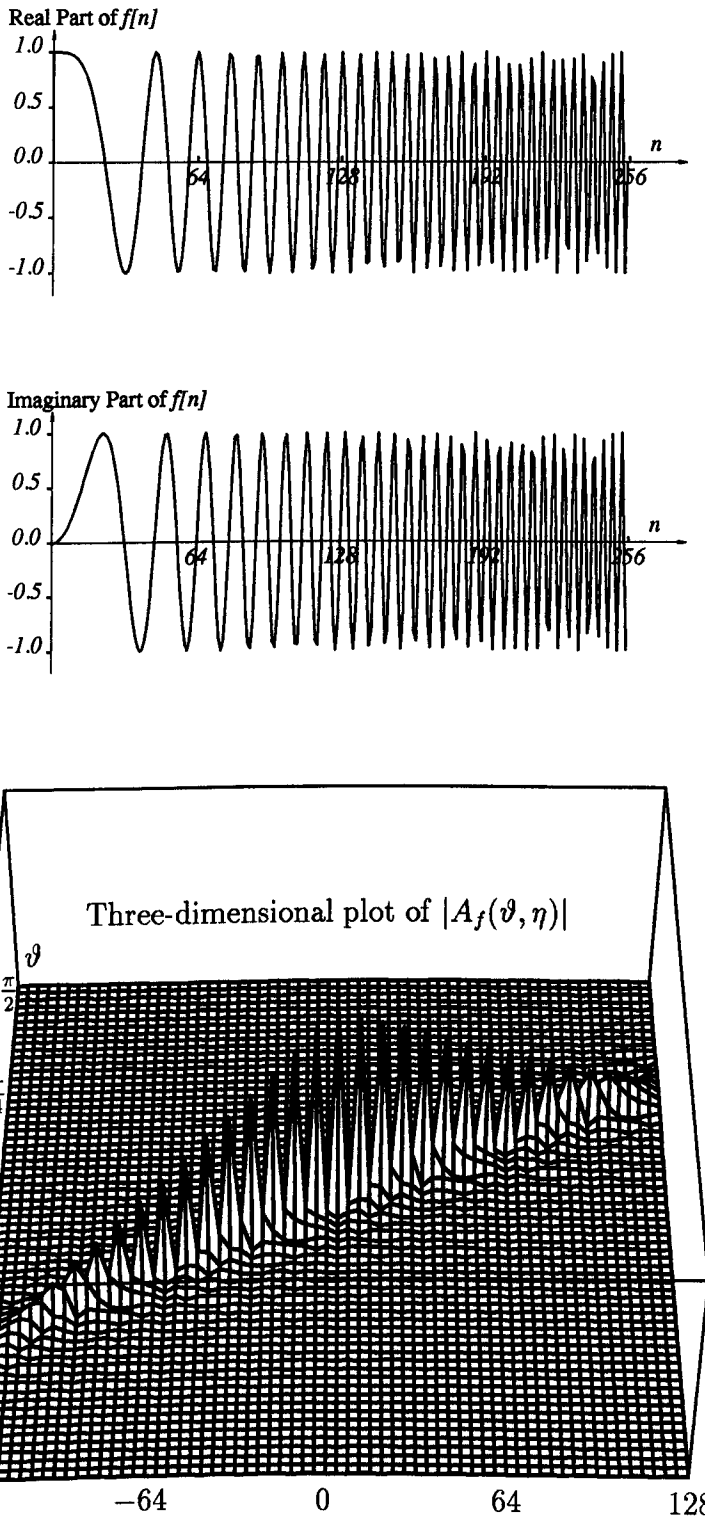

Figure 2.7: A chirp signal $f[n]$ and its DAF.

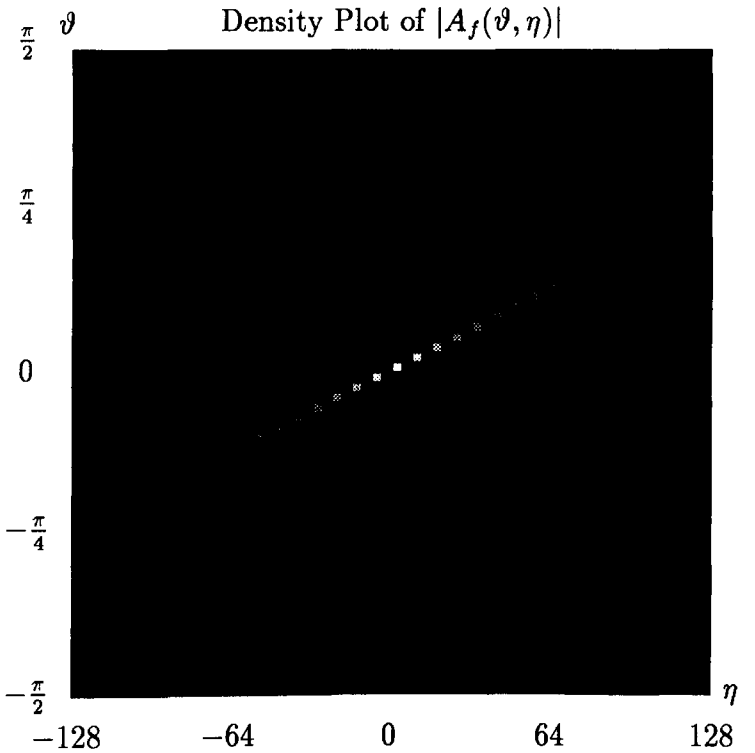

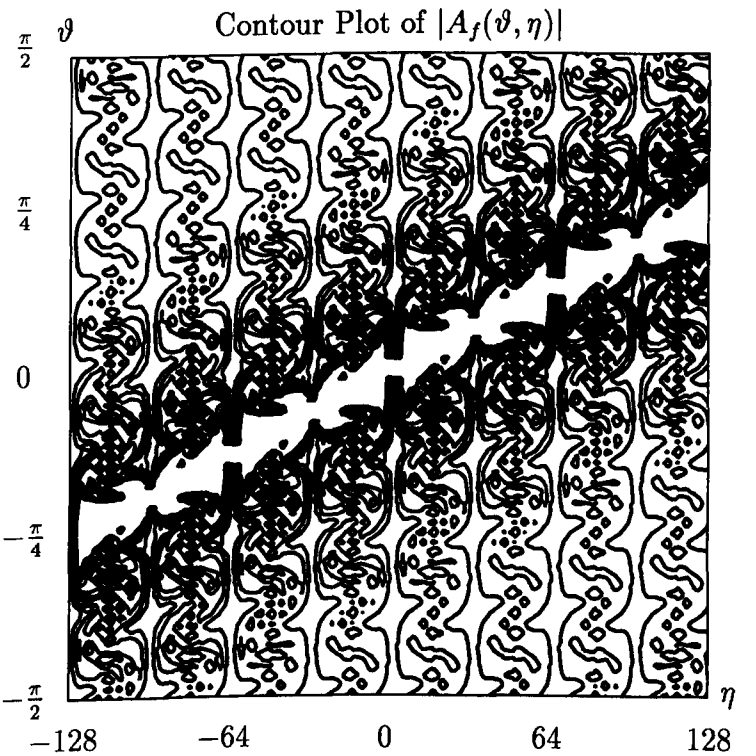

A chirp signal $f[n]$ and its DAF (continued).

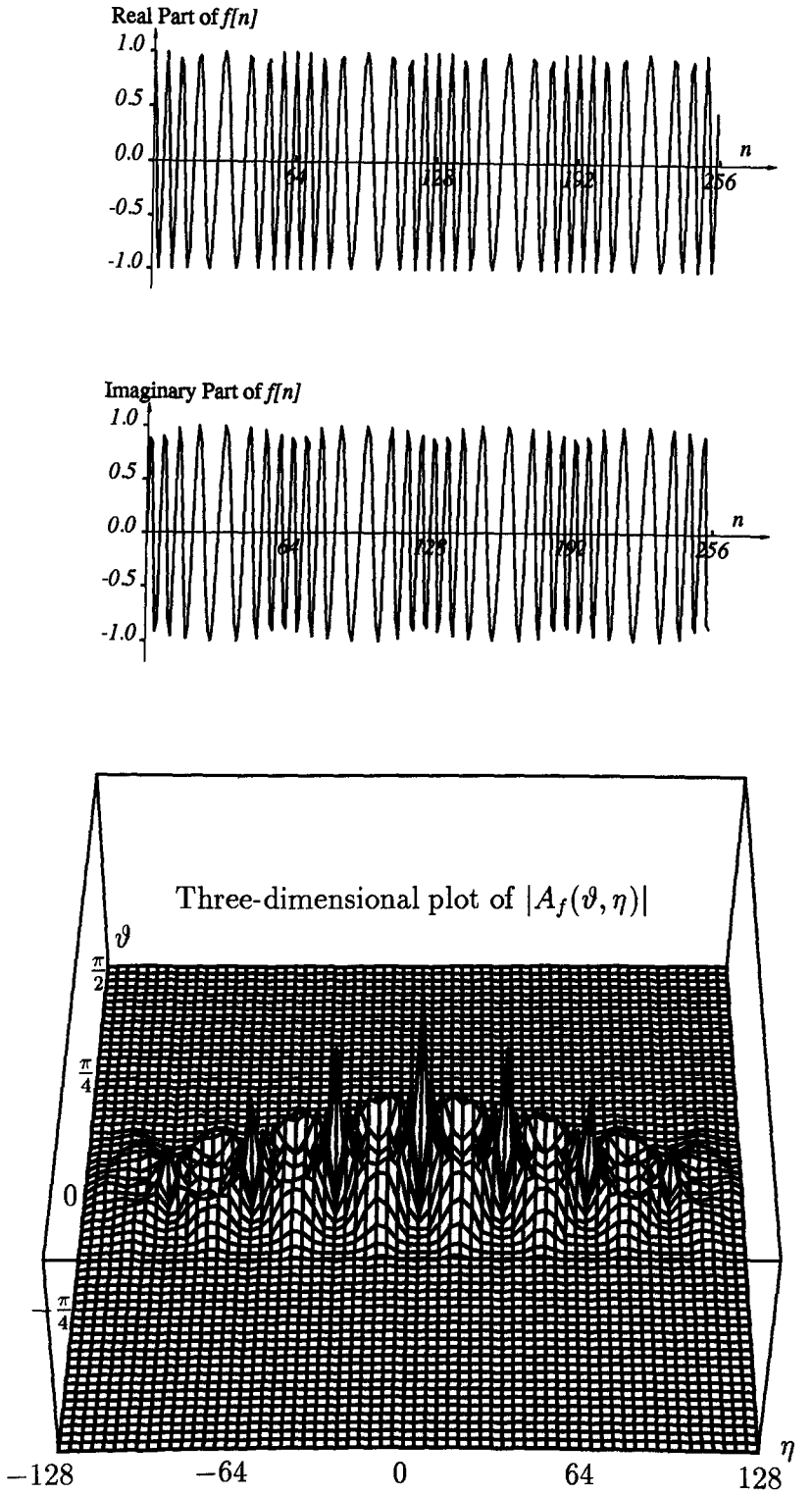

Figure 2.8: A frequency modulated signal $f[n]$ and its DAF.

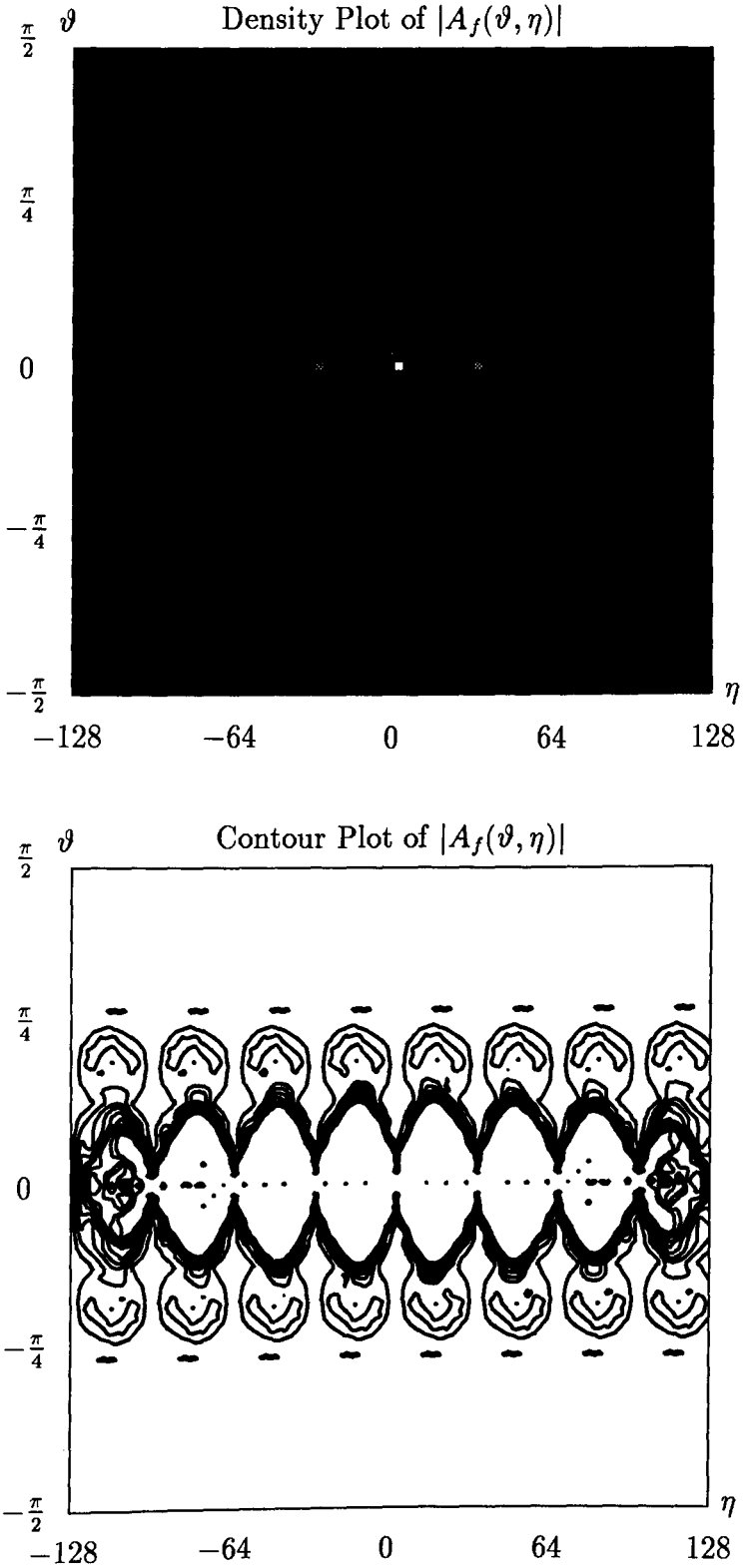

A frequency-modulated signal $f[n]$ and its DAF (continued).

2.6.5 Application to signals with noise

Figure 2.9, 2.10, 2.11 and 2.12 show four DAFs computed for the same signals as in Section 2.4.4, but with noise. The noise is of type

$$n(x) = n_1(x) + jn_2(x)$$

where $n_1(x)$ and $n_2(x)$ are random noise with the range as $[-0.1, 0.1]$, about 10% percent of the original signal, $j = \sqrt{-1}$.

From these figures, it can still be concluded that *although the DAF is good for analysing nonstationary signals, it is not so for stationary signals from these figures.*

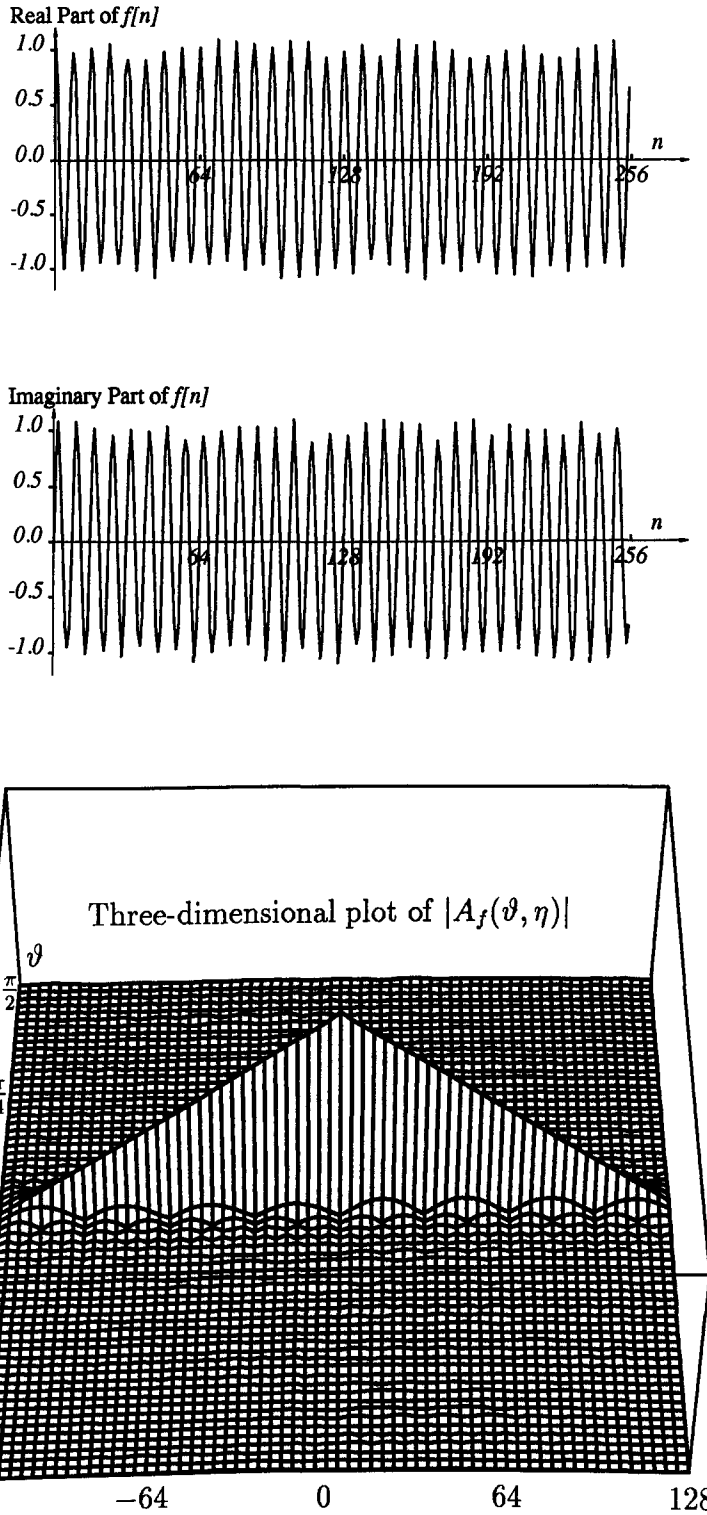

Figure 2.9: A stationary signal with noise and its DAF.

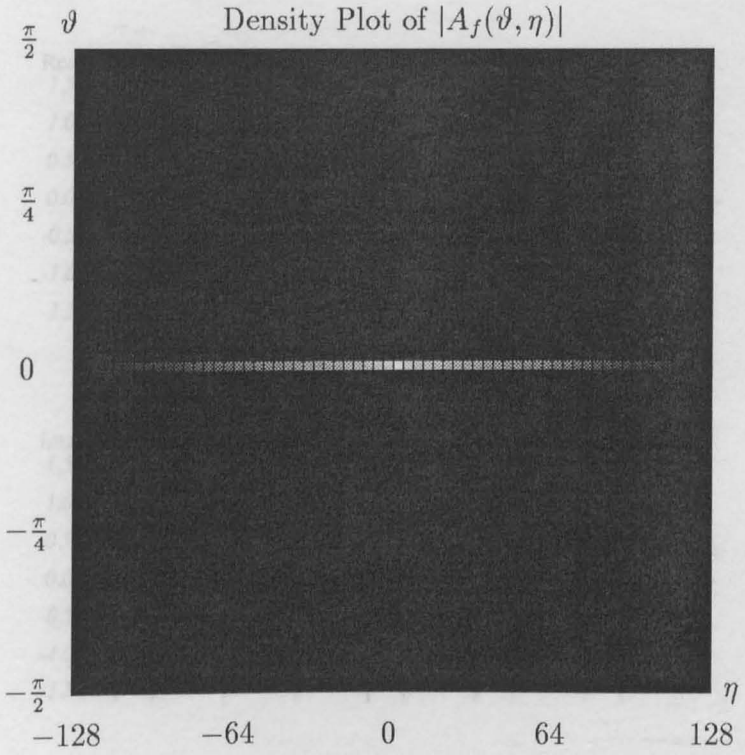

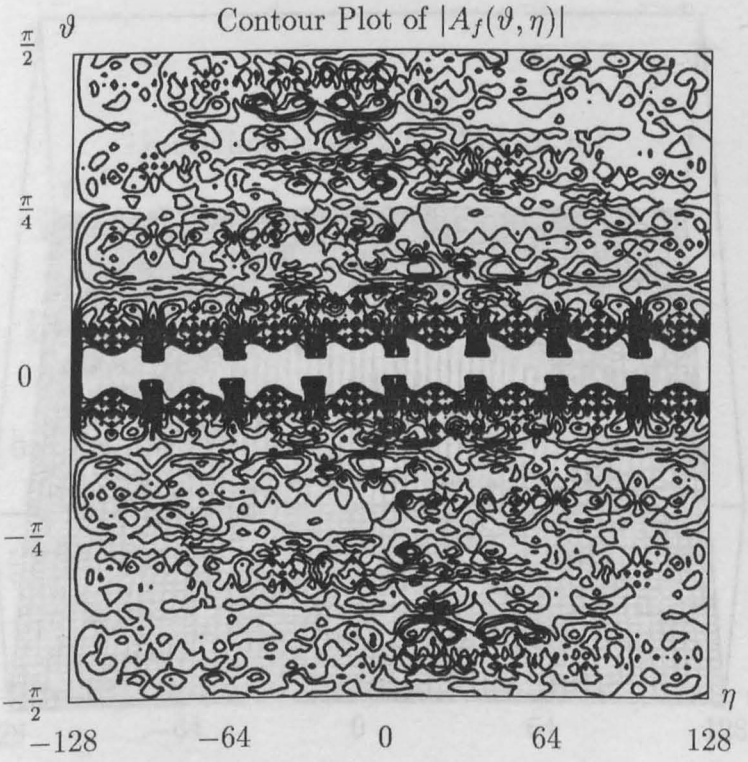

A stationary signal with noise and its DAF (continued).

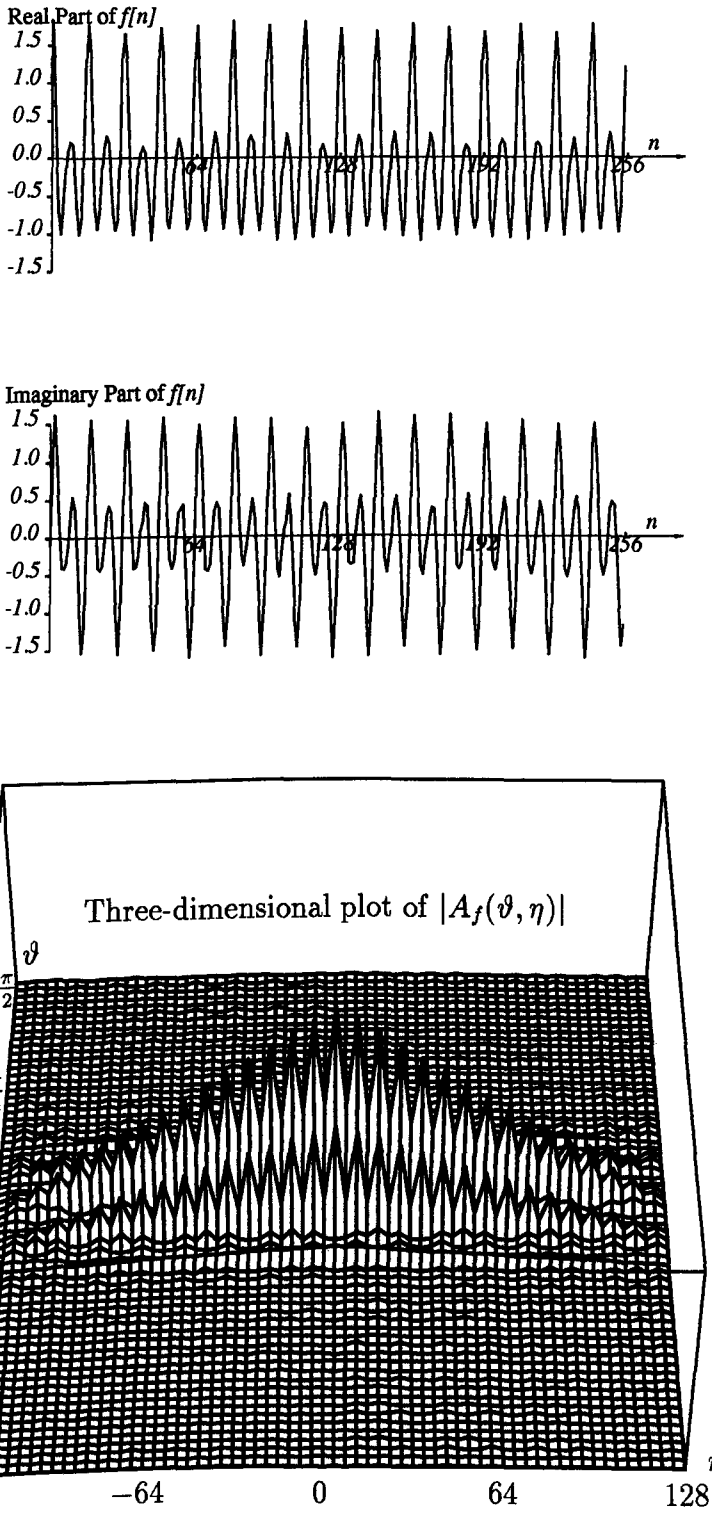

Figure 2.10: Another stationary signal with noise and its DAF.

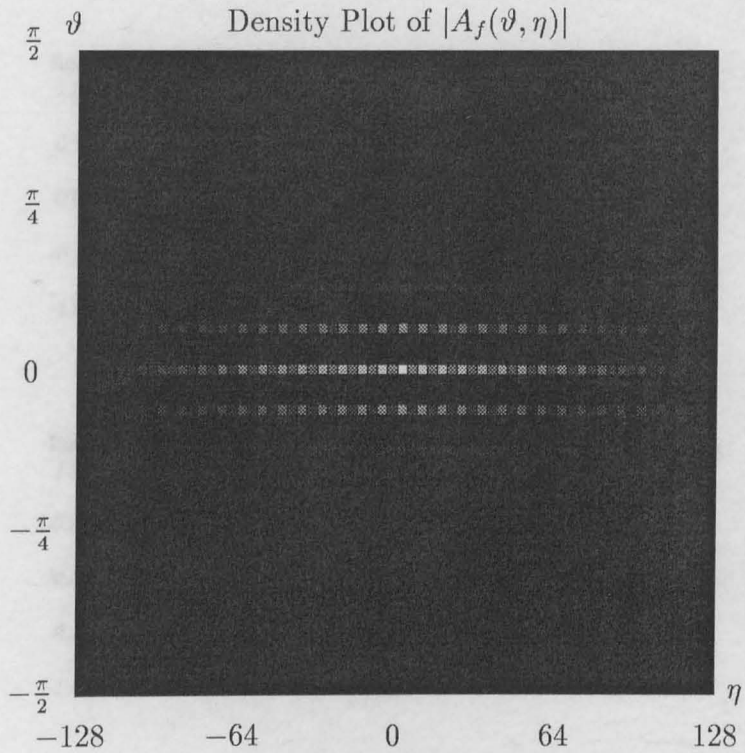

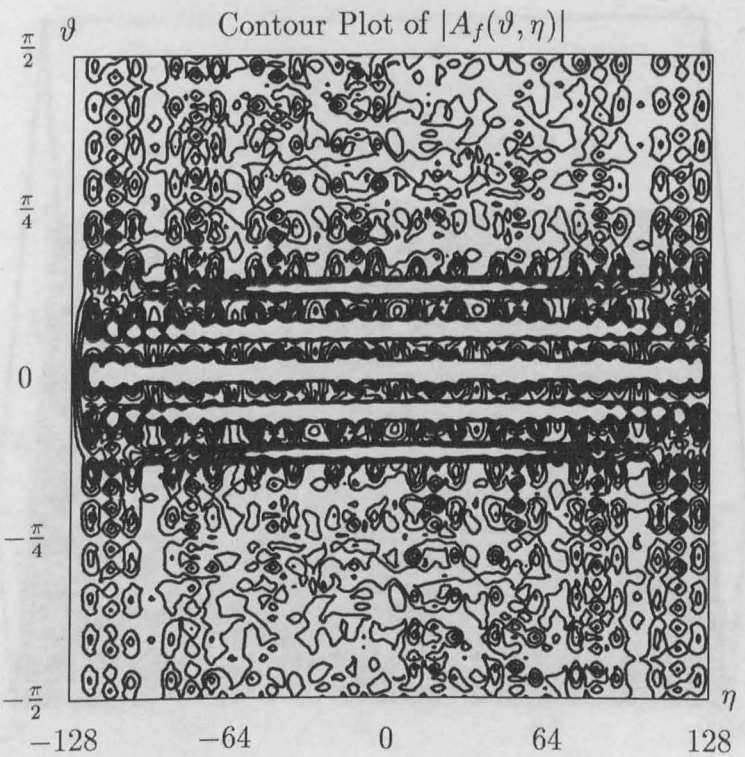

Another stationary signal with noise and its DAF (continued).

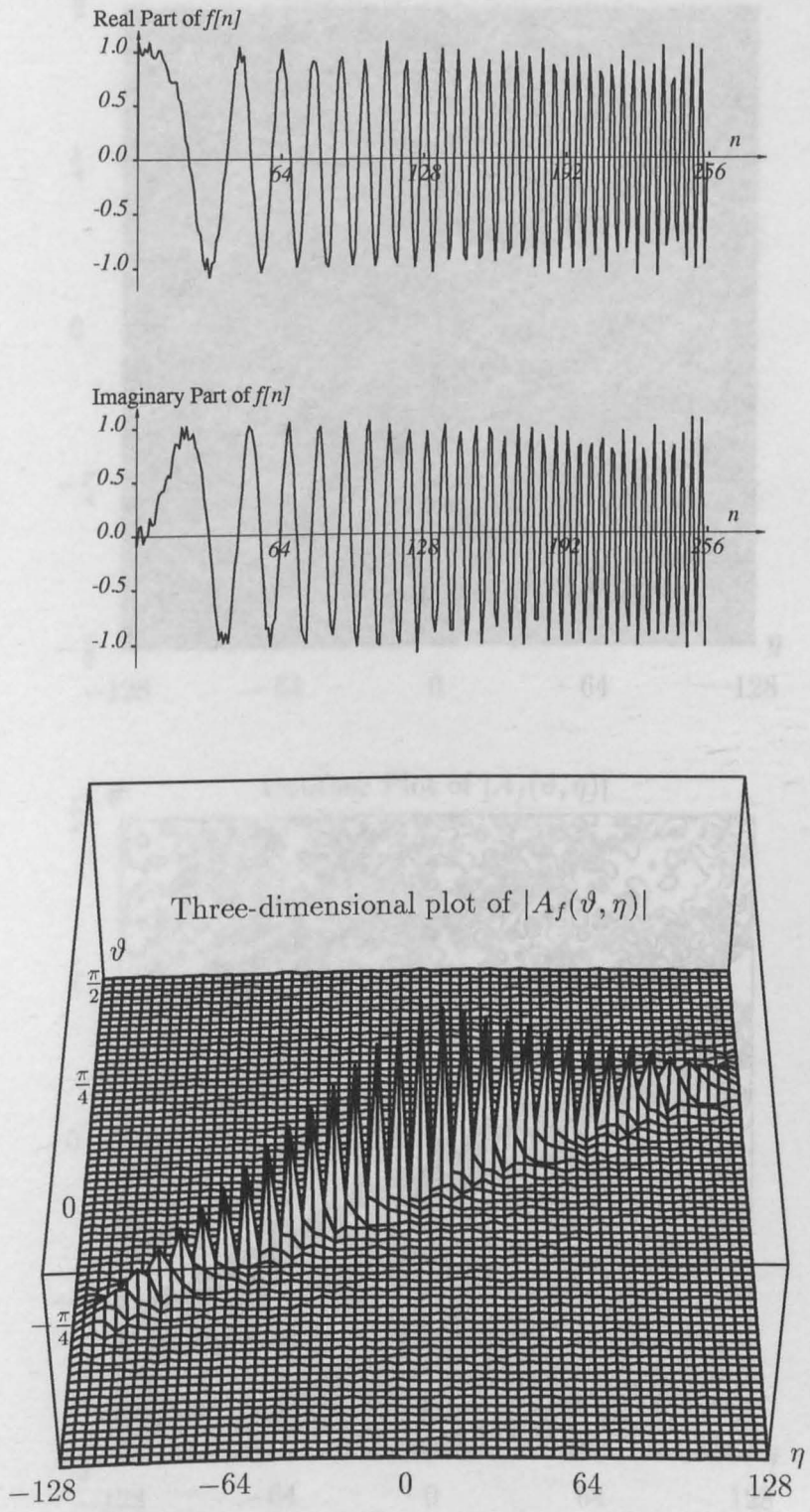

Figure 2.11: A chirp signal with noise and its DAF.

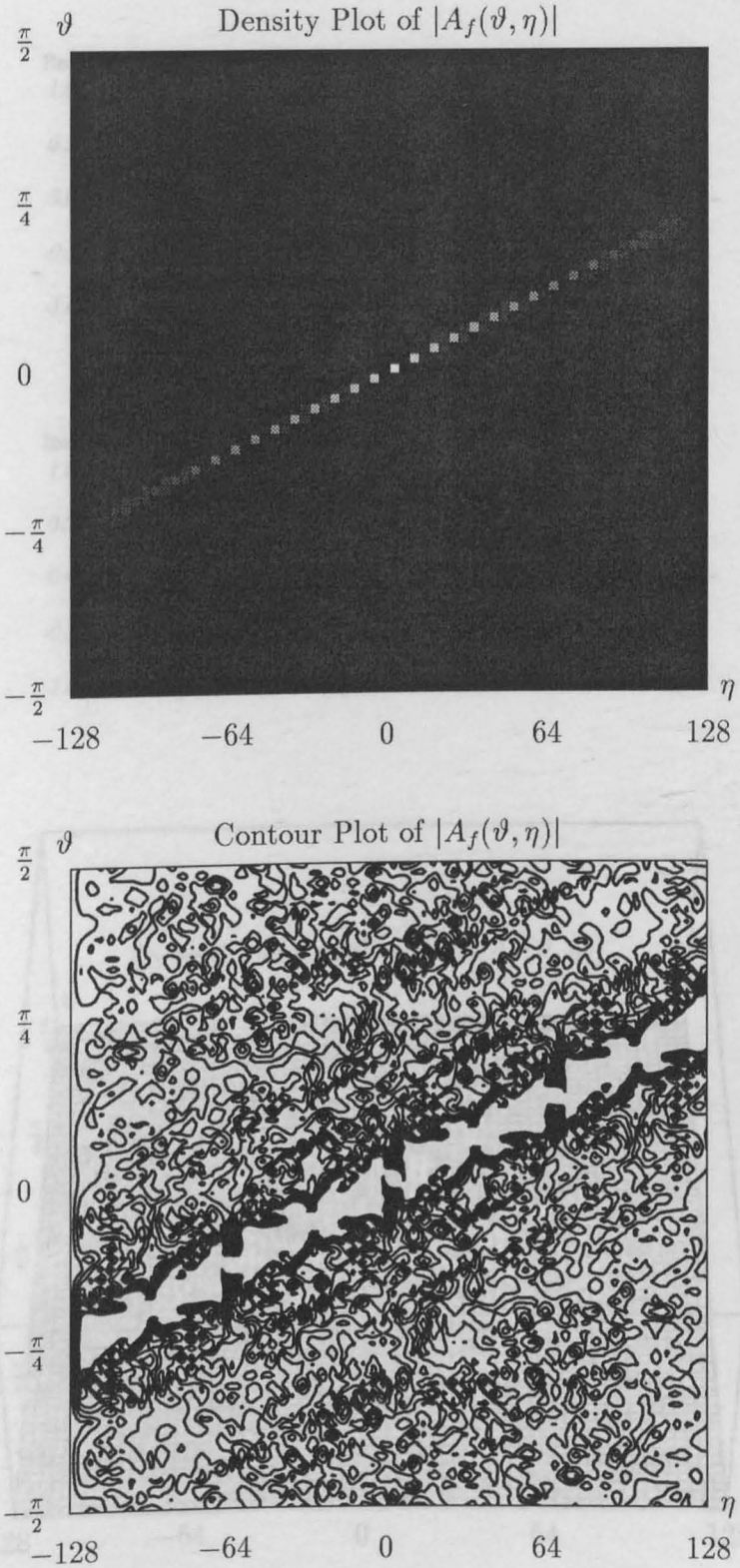

A chirp signal with noise and its DAF (continued).

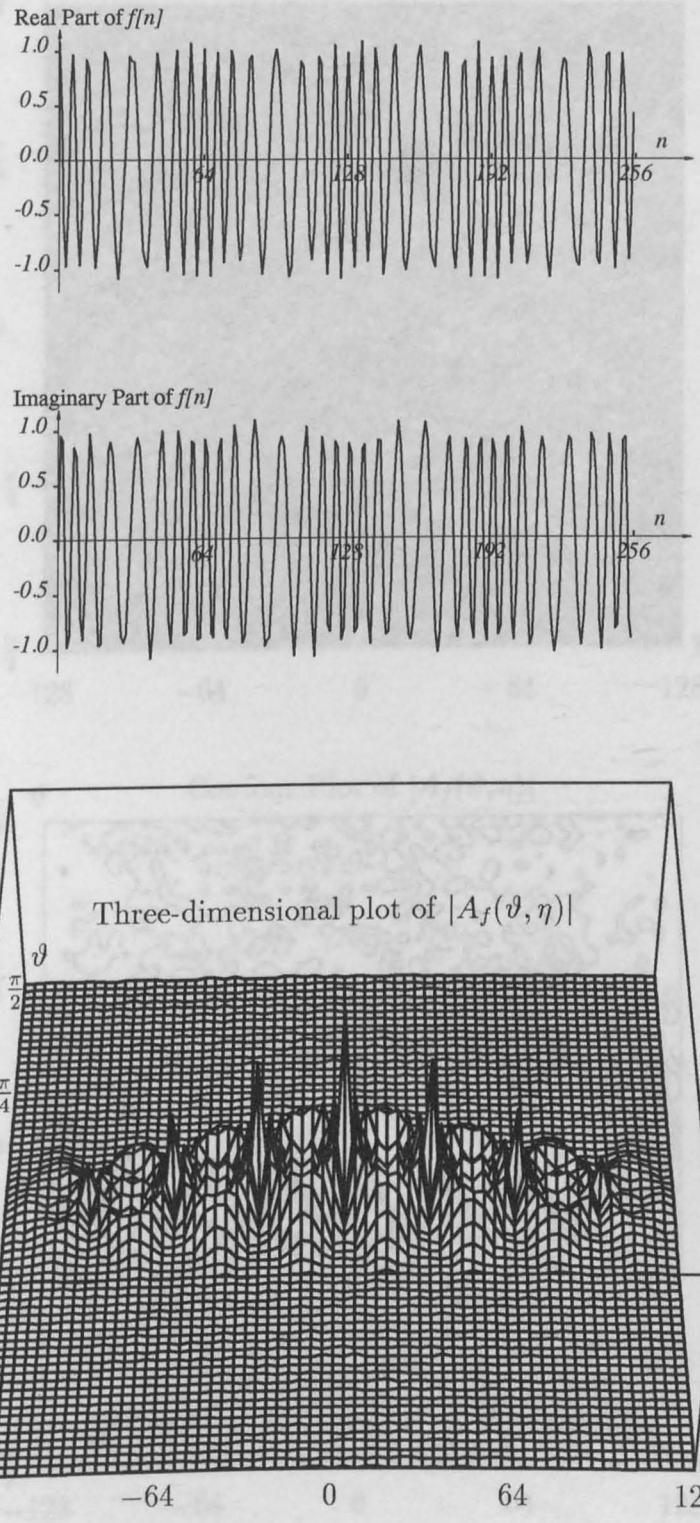

Figure 2.12: A frequency modulated signal with noise and its DAF.

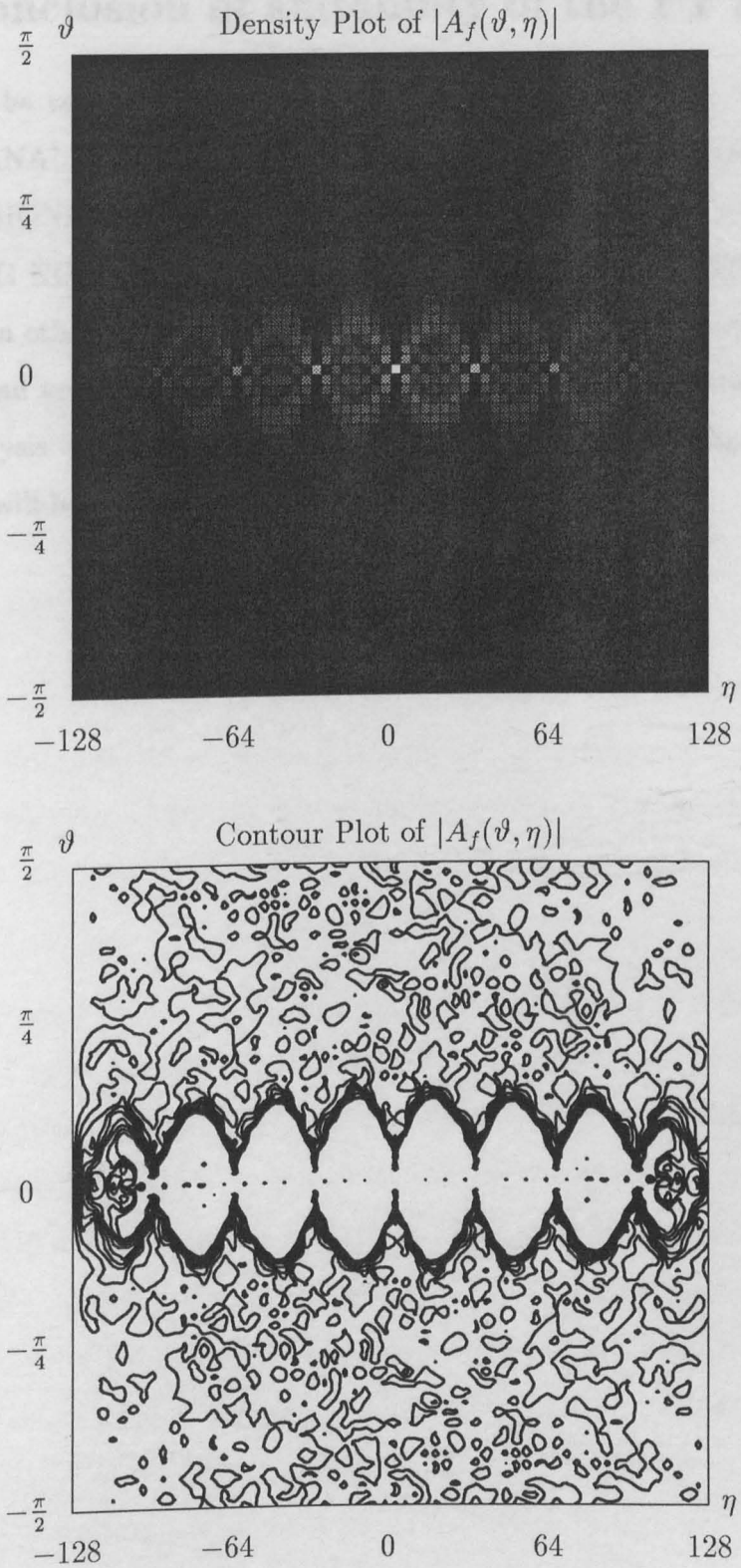

A frequency-modulated signal with noise and its DAF (continued).

2.7 Conclusion of suitability of the FT and AF

Now it can be concluded that ON ONE HAND THE FT IS A VERY USEFUL FOR ANALYSING STATIONARY SIGNALS, BUT NOT FOR NONSTATIONARY SIGNALS; ON THE OTHER HAND THE AF IS EFFECTIVE FOR ANALYSING NONSTATIONARY SINGALS, BUT NOT FOR STATIONARY SIGNALS. In other words, neither of the FT and AF is good for analysing both stationary and nonstationary signals. In order to overcome this problem, a new tool for analysis of signals is required. This can be met by the Wigner distribution, which will be discussed in the next chapter.

Chapter 3

The Wigner Distribution

3.1 Recapitulation of the problem

From the previous chapter, it is known that the Fourier transform (FT) is capable of analysing stationary signals, but becomes unsatisfactory for analysing nonstationary signals. Therefore, the usage of the FT is limited for there are many nonstationary signals in practice. One example is a piece of music (De Bruijn 1967).

> "..., if f represents a piece of music, then the composer does not produce f itself; he does not even define it. He may try to prescribe the exact frequency and the exact time interval of a note (although the uncertainty principle says that he can never be completely successful in this effort), but he does not try to prescribe the phase. The composer does not deal with f; it is only the gramophone company which produces and sells an f. On the other hand, the composer certainly does not want to describe the Fourier transform. This Fourier transform is very useful for solving mathematical and physical problems, but it gives an absolutely unreadable picture of the given piece of music.

> What the composer really does, or thinks he does, or should think he does, is something entirely different from describing either f or $\mathcal{F}$. Instead, he constructs a function of two variables. The variables are the time and the frequency, the function describes the intensity of the sound. He describes the function by a complicated set of dots on score paper. His way of describing time is slightly different from what a mathematician would do, but certainly vertical lines denote constant time, and horizontal lines denote constant frequency. ..."

In order to be able to analyse such nonstationary signals, short-time Fourier transforms are often used (Allen and Rabiner 1977). This is based on the assumption that some signals can be regarded as stationary signals on a short-time basis. Despite the wide usage of this technique, it has an important drawback, i.e. the length of the assumed short-time stationarity determines the frequency resolution which can be obtained. To increase the frequency resolution, a longer range has to be taken, which means that nonstationarities will be made vague in both time and frequency. Therefore, to overcome this problem, a mixed time-frequency representation of signals is required.

The ambiguity function is a kind of time-frequency representation of a signal as shown in the last chapter. It enables the analysis of nonstationary signals to be made but not stationary signals, which means that it is not an ideal tool for analysing general signals.

Unlike both the short-time Fourier transform and ambiguity function, the Wigner distribution can be used to analyse both stationary and nonstationary signals because it has some important properties which make it suitable for signal processing which will be explained in the rest of this chapter.

3.2 Introduction

The concept of the Wigner distribution was originally introduced in the context of quantum mechanics by Wigner (1932), while attempting to formulate mathemat-

ical tools for solving quantum problems which involved Heisenberg's Uncertainty Principle. Then in 1948, Ville reintroduced it for signal processing, although it did not receive wide attention at that time.

However, recently the Wigner distribution has become more and more popular because it is potentially an ideal tool for space-frequency (or time-frequency) representation of signals.

The Wigner distribution has been studied by many researchers (Bamler and Glunder 1983; Boudreaux-Bartels and Parks 1986; Boashash and Black 1987; Boashash 1988; Classen and Mecklenbrauker 1980, 1983; De Bruijn 1973; Kumar, Neuman, and Deros 1986; Peyrin and Prost 1986; Szu and Blodgett 1981; White and Boashash 1988; Yu and Cheng 1987) and applied to many areas (Bastiaans 1978, 1979, 1980; Frensley 1987 Kaluzynski 1989; Zhu, Peix and Babot 1990).

For the mathematical background of the Wigner distribution refer to (De Bruijn 1973); while for a more practical reference see (Classen and Mecklenbrauker 1980).

3.3 The Wigner distribution (WD)

3.3.1 Definition

For any complex-valued signal $f(x)$ where x is a continuous variable such as distance, time and etc., its *Wigner distribution* (WD) is defined as

$$W_f(x,\omega) = \int_{-\infty}^{\infty} f(x+\tfrac{\chi}{2}) f^*(x-\tfrac{\chi}{2}) e^{-j\omega\chi} d\chi \tag{3.1}$$

The WD can also be defined as

$$W_f(x,\omega) = \frac{1}{2\pi}\int_{-\infty}^{\infty} F(\omega+\tfrac{\varpi}{2}) F^*(\omega-\tfrac{\varpi}{2}) e^{j\varpi x} d\varpi \tag{3.2}$$

where $F(\varpi)$ is the Fourier transform of $f(x)$.

In fact, from

$$f(x) \overset{\mathcal{F}}{\longleftrightarrow} F(\varpi)$$

it follows that

$$f(x)f^*(\chi) \overset{\mathcal{F}}{\longleftrightarrow} F(\varpi)F^*(-\omega)$$

Hence,

$$f(x+\frac{\chi}{2})f^*(x-\frac{\chi}{2}) \overset{\mathcal{F}}{\longleftrightarrow} F(\omega+\frac{\varpi}{2})F^*(\omega-\frac{\varpi}{2})$$

Therefore, Eqn 3.2 is obtained by using the Fourier transform.

Just like the Fourier transform pair and the ambiguity function pair, we will express the Wigner distribution pair $f(x)$ and $W_f(x,\omega)$ as

$$f(x) \overset{\mathcal{W}}{\longleftrightarrow} W_f(x,\omega) \tag{3.3}$$

Compared with the definition of the ambiguity function

The definitions of the WD and AF are very similar. For the differences, see Table 3.1.

Table 3.1: The definitions of the WD and AF for signal $f(x)$

	space domain	frequency domain
$W_f(x,\omega)$	$\int_{-\infty}^{\infty} f(x+\frac{\chi}{2})f^*(x-\frac{\chi}{2})e^{-j\omega\chi}d\chi$	$\frac{1}{2\pi}\int_{-\infty}^{\infty} F(\omega+\frac{\varpi}{2})F^*(\omega-\frac{\varpi}{2})e^{j\varpi x}d\varpi$
$A_f(\varpi,\chi)$	$\int_{-\infty}^{\infty} f(x+\frac{\chi}{2})f^*(x-\frac{\chi}{2})e^{-j\varpi x}dx$	$\frac{1}{2\pi}\int_{-\infty}^{\infty} F(\omega+\frac{\varpi}{2})F^*(\omega-\frac{\varpi}{2})e^{j\omega\chi}d\omega$

The cross Wigner distribution for two signals

For two signals $f_1(x)$ and $f_2(x)$, their *cross Wigner distribution* can be defined as

$$W_{f_1,f_2}(x,\omega) = \int_{-\infty}^{\infty} f_1(x+\frac{\chi}{2}) f_2^*(x-\frac{\chi}{2}) e^{-j\omega\chi} d\chi \tag{3.4}$$

The WD for multidimensional signals

For a complex-valued signal $f(\mathbf{x})$ where $\mathbf{x} \in \mathcal{R}^n$, its WD is defined as

$$\int_{-\infty}^{\infty} f(\mathbf{x}+\frac{\chi}{2}) f^*(\mathbf{x}-\frac{\chi}{2}) e^{-j\omega\cdot\chi} d\chi = W_f(\chi,\omega) \tag{3.5}$$

where $\omega \in \mathcal{C}^n$

3.3.2 Simple properties

Symmetry

For any real-valued signal, the WD is an even function of the frequency:

$$W_f(x,\omega) = W_f(x,-\omega) \tag{3.6}$$

Realness

For any complex-valued signal, the WD is real-valued:

$$W_f(x,\omega) = (W_f(x,\omega))^* \tag{3.7}$$

Spatial-shifting

A spatial shift in $f(x)$ corresponds to a same shift in its WD, i.e.

$$f(x+x_0) \overset{W}{\longleftrightarrow} W_f(x+x_0,\omega) \tag{3.8}$$

Frequency-shifting

Just like spatial-shift, a frequency shift in $f(x)$ corresponds to a same shift in its WD:

$$f(x)e^{j\omega_0 x} \overset{W}{\longleftrightarrow} W_f(x,\omega-\omega_0) \tag{3.9}$$

Sum formula

For $f(x) = f_1(x) + f_2(x)$,

$$W_f(x,\omega) = W_{f_1}(x,\omega) + W_{f_2}(x,\omega) + 2\mathrm{Re}W_{f_1,f_2}(x,\omega) \tag{3.10}$$

Spatial-limited signals

If $f(x)$ is restricted to $[x_a, x_b]$, so is $W_f(x,\omega)$.

Frequency-limited signals

If $f(x)$ is band-limited to $[\omega_a,\omega_b]$, so is $W_f(x,\omega)$.

Spatial-energy

This is that the integral of the WD in ω at a fixed x is equal to the instantaneous energy at that x, i.e.

$$\frac{1}{2\pi}\int_{-\infty}^{\infty} W_f(x,\omega)d\omega = |f(x)|^2 \tag{3.11}$$

Frequency-energy

The integral of the WD over x at a certain ω gives the energy spectrum at that ω, i.e.

$$\int_{-\infty}^{\infty} W_f(x,\omega)dx = |F(\omega)|^2 \tag{3.12}$$

Total energy

$$\frac{1}{2\pi}\int_{-\infty}^{\infty}\int_{-\infty}^{\infty} W_f(x,\omega)dxd\omega = \|f(x)\|^2 \tag{3.13}$$

This means that the integral of the WD over the whole plane (x,ω) is equal to the total energy of $f(x)$.

Moyal's formula

$$\frac{1}{2\pi}\int_{-\infty}^{\infty}\int_{-\infty}^{\infty} W_f^2(x,\omega)dxd\omega = \|f(x)\|^4 \tag{3.14}$$

This means that the integral of the squared WD over the whole plane (x,ω) is equal to the square of the total energy of $f(x)$. This is similar to the Parseval's formula about the FT.

Convolution

Let $g(x)$ be the convolution of $f(x)$ and $h(x)$, i.e.

$$g(x) = f(x) * h(x) \tag{3.15}$$

then

$$W_g(x,\omega) = \int_{-\infty}^{\infty} W_f(\chi,\omega)W_h(x-\chi,\omega)d\chi \tag{3.16}$$

Proof:

$$\begin{aligned} W_g(x,\omega) &= \frac{1}{2\pi}\int_{-\pi}^{\pi} F(\omega+\frac{\varpi}{2})H(\omega+\frac{\varpi}{2})F^*(\omega-\frac{\varpi}{2})H^*(\omega-\frac{\varpi}{2})e^{j\varpi x}d\varpi \\ &= \frac{1}{2\pi}\int_{-\pi}^{\pi} F(\omega+\frac{\varpi}{2})F^*(\omega-\frac{\varpi}{2})H(\omega+\frac{\varpi}{2})H^*(\omega-\frac{\varpi}{2})e^{j\varpi x}d\varpi \\ &= \int_{-\infty}^{\infty} W_f(\chi,\omega)W_h(x-\chi,\omega)d\chi \end{aligned}$$

From Eqn 3.16, it follows that the WD of the convolution is the convolution of the WD provided that ω is regarded as a fixed parameter in the WD.

Modulation

If

$$g(x) = f(x)m(x)$$

then

$$W_g(x,\omega) = \frac{1}{2\pi}\int_{-\infty}^{\infty} W_f(x,\varpi)W_m(x,\omega-\varpi)d\varpi \tag{3.17}$$

Proof:

$$\begin{aligned} W_g(x,\omega) &= \int_{-\infty}^{\infty} f(x+\tfrac{\chi}{2})m(x+\tfrac{\chi}{2})\, f^*(x-\tfrac{\chi}{2})m^*(x-\tfrac{\chi}{2})e^{-j\omega\chi}d\chi \\ &= \int_{-\infty}^{\infty} f(x+\tfrac{\chi}{2})f^*(x-\tfrac{\chi}{2})\, m(x+\tfrac{\chi}{2})m^*(x-\tfrac{\chi}{2})e^{-j\omega\chi}d\chi \\ &= \frac{1}{2\pi}\int_{-\infty}^{\infty} W_f(x,\varpi)W_m(x,\omega-\varpi)d\varpi \end{aligned}$$

3.3.3 The WD for analytical signals

One point which needs to be highlighted before the WD can be applied widely, is that the WD should be applied to analytical signals, i.e. those which have no redundant spectrum.

This is achieved for any real-valued signal $f(x)$ by constructing its *analytical signal* $f_a(x)$ as

$$f_a(x) = f(x) + j\hat{f}(x) \tag{3.18}$$

where $\hat{f}(x)$ is the *Hilbert transform* of $f(x)$:

$$\hat{f}(x) = \frac{1}{\pi}\int_{-\infty}^{\infty} \frac{f(\chi)}{x-\chi}d\chi \tag{3.19}$$

If $F(\varpi)$ and $F_a(\varpi)$ are the FTs of $f(x)$ and $f_a(x)$, then

$$F_a(\varpi) = \begin{cases} 2F(\varpi) & \varpi > 0 \\ F(0) & \varpi = 0 \\ 0 & \varpi < 0 \end{cases} \tag{3.20}$$

which means that the analytical signal does not contain redundant spectrum which in turn means that neither does the WD.

$$W_{f_a}(x,\omega) = 0 \qquad \omega < 0 \tag{3.21}$$

This trick considerably reduces aliasing problems.

Furthermore,

$$W_{f_a}(x,\omega) = \begin{cases} \frac{4}{\pi}\int_{-\infty}^{\infty} W_f(x-\chi,\omega)\frac{\sin 2\omega\chi}{\chi}d\chi & \omega \geq 0 \\ 0 & \omega < 0 \end{cases} \tag{3.22}$$

Proof: For $\omega \geq 0$

$$\begin{aligned} W_{f_a}(x,\omega) &= \frac{1}{2\pi}\int_{-\infty}^{\infty} F_a(\omega+\frac{\varpi}{2})F_a^*(\omega-\frac{\varpi}{2})e^{j\varpi x}d\varpi \\ &= \frac{2}{\pi}\int_{-2\omega}^{2\omega} F(\omega+\frac{\varpi}{2})F^*(\omega-\frac{\varpi}{2})e^{j\varpi x}d\varpi \\ &= \frac{2}{\pi}\int_{-2\omega}^{2\omega}\left(\int_{-\infty}^{\infty} W_f(\chi,\omega)e^{-j\varpi\chi}d\chi\right)e^{j\varpi x}d\varpi \\ &= \frac{2}{\pi}\int_{-\infty}^{\infty} W_f(\chi,\omega)\left(\int_{-2\omega}^{2\omega} e^{-j\varpi(\chi-x)}d\varpi\right)d\chi \\ &= \frac{4}{\pi}\int_{-\infty}^{\infty} W_f(\chi,\omega)\frac{\sin(2\omega(\chi-x))}{\chi-x}d\chi \\ &= \frac{4}{\pi}\int_{-\infty}^{\infty} W_f(x-\chi,\omega)\frac{\sin 2\omega\chi}{\chi}d\chi \end{aligned}$$

3.3.4 Moments

From the properties of the WD, specially those related to the energy distribution, it can be seen that the WD could be interpreted as the energy distribution in the mixed space-frequency plane. Therefore, in order to get an idea of how the energy in a signal is distributed in space and frequency, it is only necessary to compute the WD of the signal. Moreover, moments can be introduced to characterise the distribution rather than using the values of the WD over the whole plane, thereby condensing the amount of information considerablely. There are two types of moments: local moments in frequency or space and global moments over the whole space-frequency plane. These moments can be used to specify averages and the spread of the WD and turn out to be very useful for characterising instantaneous properties of the signal.

Local moments in frequency

The *0th-order moment in frequency* $p_f(x)$ is defined as

$$p_f(x) = \frac{1}{2\pi}\int_{-\infty}^{\infty} W_f(x,\omega)d\omega \tag{3.23}$$

From Eqn 3.11,

$$p_f(x) = |f(x)|^2 \tag{3.24}$$

which means that $p_f(x)$ is the instantaneous power of $f(x)$, which is non-negative.

The *1st-order moment in frequency* $\Omega_f(x)$ is defined as

$$\Omega_f(x) = \frac{1}{2\pi}\int_{-\infty}^{\infty} \omega W_f(x,\omega)d\omega / p_f(x) \tag{3.25}$$

It can be proved that

$$\Omega_f(x) = \mathrm{Im}\frac{f'(x)}{f(x)} \tag{3.26}$$

Proof: From Eqn 3.1 and the inverse Fourier transform,

$$\frac{1}{2\pi}\int_{-\infty}^{\infty} W_f(x,\omega)e^{j\omega\chi}d\chi = f(x+\frac{\chi}{2})f^*(x-\frac{\chi}{2})$$

Differentiating with respect to χ,

$$\frac{1}{2\pi}\int_{-\infty}^{\infty} j\omega W_f(x,\omega)e^{j\omega\chi}d\omega = \frac{1}{2}\left(f'(x+\frac{\chi}{2})f^*(x-\frac{\chi}{2}) - f(x+\frac{\chi}{2})(f')^*(x-\frac{\chi}{2})\right) \tag{3.27}$$

i.e.

$$\frac{1}{2\pi}\int_{-\infty}^{\infty} \omega W_f(\omega,x)e^{-j\omega\chi}d\omega = \frac{1}{2j}\left(f'(x+\frac{\chi}{2})f^*(x-\frac{\chi}{2}) - f(x+\frac{\chi}{2})(f')^*(x-\frac{\chi}{2})\right)$$

When $\chi = 0$, it follows that

$$\frac{1}{2\pi}\int_{-\infty}^{\infty} \omega W_f(\omega,x)d\omega = \frac{1}{2j}\left(f'(x)f^*(x) - f(x)(f')^*(x)\right) = \mathrm{Im}f'(x)f^*(x)$$

Divided by $f(x)f^*(x)$, the result is obtained.

The *2nd-order moment in frequency* $m_f(x)$ is defined as

$$m_f(x) = \frac{1}{2\pi}\int_{-\infty}^{\infty} (\omega - \Omega_f(x))^2 W_f(x,\omega)d\omega/p_f(x) \tag{3.28}$$

For $m_f(x)$,

$$m_f(x) = -\frac{1}{2}\mathrm{Re}\frac{d}{dx}\frac{f'(x)}{f(x)} \tag{3.29}$$

Proof: Differentiating Eqn 3.27 with respect to χ,

$$\begin{aligned}
&\frac{1}{2\pi}\int_{-\infty}^{\infty} (-j\omega)^2 W_f(x,\omega)e^{j\omega\chi}d\omega \\
&= \frac{1}{4}f''(x+\frac{\chi}{2})f^*(x-\frac{\chi}{2}) - \frac{1}{2}f'(x+\frac{\chi}{2})(f')^*(x-\frac{\chi}{2}) \\
&\quad + \frac{1}{4}f(x+\frac{\chi}{2})(f'')^*(x-\frac{\chi}{2})
\end{aligned}$$

Let $\chi = 0$,

$$\frac{1}{2\pi}\int_{-\infty}^{\infty} \omega^2 W_f(x,\omega)d\omega = -\frac{1}{4}f''(x)f^*(x) + \frac{1}{2}f'(x)(f')^*(x) - \frac{1}{4}f(x)(f'')^*(x)$$

Combined with the 0th-order moment and the 1st-order moment,

$$\begin{aligned}
&\frac{1}{2\pi}\int_{-\infty}^{\infty} (\omega - \Omega_f(x))^2 W_f(x,\omega)d\omega \\
&= -\frac{1}{4}f''(x)f^*(x) + \frac{1}{2}f'(x)(f')^*(x) - \frac{1}{4}f(x)(f'')^*(x) \\
&\quad -\Omega_f^2(x)\cdot p_f(x) \\
&= -\frac{1}{4}f''(x)f^*(x) + \frac{1}{2}f'(x)(f')^*(x) - \frac{1}{4}f(x)(f'')^*(x) \\
&\quad + \frac{1}{4}\frac{(f'(x)f^*(x) - f(x)(f')^*(x))^2}{f(x)f^*(x)} \\
&= -\frac{1}{4}f''(x)f^*(x) - \frac{1}{4}f(x)(f'')^*(x) + \frac{1}{2}f'(x)(f')^*(x) \\
&\quad + \frac{1}{4}\frac{(f')^2(x)f^*(x)}{f(x)} + \frac{1}{4}\frac{f(x)((f')^2)^*(x)}{f^*(x)} - \frac{1}{2}f'(x)(f')^*(x) \\
&= -\frac{1}{4}f''(x)f^*(x) - \frac{1}{4}f(x)(f'')^*(x)
\end{aligned}$$

$$+\frac{1}{4}\frac{(f')^2(x)f^*(x)}{f(x)}+\frac{1}{4}\frac{f(x)((f')^2)^*(x)}{f^*(x)}$$

Divided by $f(x)f^*(x)$,

$$\begin{aligned}
&\frac{1}{2\pi}\int_{-\infty}^{\infty}(\omega-\Omega_f(x))^2W_f(x,\omega)d\omega/p_f(x)\\
&=-\frac{1}{4}\frac{f''(x)}{f(x)}-\frac{1}{4}\frac{(f'')^*(x)}{f^*(x)}\\
&\quad+\frac{1}{4}\frac{(f')^2(x)}{f^2(x)}+\frac{1}{4}\frac{((f^*)')^2(x)}{(f^*)^2(x)}\\
&=-\frac{1}{2}\mathrm{Re}\left(\frac{f''(x)}{f(x)}-\frac{(f')^2(x)}{f^2(x)}\right)
\end{aligned}$$

Hence, the proof is obtained.

For a signal $f(x)=A(x)e^{j\phi(x)}$, then its 0th-order, 1st-order, 2nd-order moment is

$$p_f(x)=|A(x)|^2 \tag{3.30}$$

$$\Omega_f(x)=\phi'(x) \tag{3.31}$$

$$m_f(x)=-\frac{1}{2}\frac{d}{dx}\frac{A'(x)}{A(x)} \tag{3.32}$$

From the above three equations, it can be seen that the 0th-order moment $p_f(x)$ is the instantaneous power of the signal, the 1st-order moment $\Omega_f(x)$ is the instantaneous frequency of the signal, and the 2nd-order moment $m_f(x)$ is dependent on the envelope of the signal. For a real-valued signal, a similar conclusion can be reached if its analytical signal is used.

Local moments in space

The *0th-order moment in space* $P_f(\omega)$ is defined as

$$P_f(\omega)=\int_{-\infty}^{\infty}W_f(x,\omega)dx \tag{3.33}$$

From Eqn 3.12,

$$P_f(\omega) = |F(\omega)|^2 \tag{3.34}$$

The *1st-order moment in space* $X_f(\omega)$ is defined as

$$X_f(\omega) = \int_{-\infty}^{\infty} xW_f(x,\omega)dx/P_f(\omega) \tag{3.35}$$

In fact,

$$X_f(\omega) = -\mathrm{Im}\frac{F'(\omega)}{F(\omega)} \tag{3.36}$$

The *2nd-order moment in space* $M_f(\omega)$ is defined as

$$M_f(\omega) = \int_{-\infty}^{\infty} (x - X_f(\omega))^2 W_f(x,\omega)dx/P_f(\omega) \tag{3.37}$$

It can be proved that

$$M_f(\omega) = -\frac{1}{2}\mathrm{Re}\frac{d}{d\omega}\frac{F'(\omega)}{F(\omega)} \tag{3.38}$$

For a signal $f(x)$ whose FT is $F(\omega) = A(\omega)e^{j\phi(\omega)}$, its moments in space are

$$P_f(\omega) = |A(\omega)|^2 \tag{3.39}$$

$$T_f(\omega) = -\phi'(\omega) \tag{3.40}$$

$$M_f(\omega) = -\frac{1}{2}\frac{d}{d\omega}\frac{A'(\omega)}{A(\omega)} \tag{3.41}$$

Global moments

Besides local moments, global moments can also be used. Some of them are listed here.

For the *0th-order global moment* of the WD,

$$\overline{P_f} = \frac{1}{2\pi}\int_{-\infty}^{\infty}\int_{-\infty}^{\infty} W_f(x,\omega)dxd\omega = \|f\|^2 \tag{3.42}$$

For the *1st-order global moment with respect to frequency* of the WD,

$$\overline{\Omega_f} = \frac{1}{2\pi}\int_{-\infty}^{\infty}\int_{-\infty}^{\infty}\omega W_f(x,\omega)dxd\omega/\overline{P_f} \tag{3.43}$$

For the *1st-order global moment with respect to space* of the WD,

$$\overline{X_f} = \frac{1}{2\pi}\int_{-\infty}^{\infty}\int_{-\infty}^{\infty}xW_f(x,\omega)dxd\omega/\overline{P_f} \tag{3.44}$$

3.3.5 Application to signals

For $f(x) = ae^{j\omega_0 x}$ where a is a constant, then

$$W_f(x,\omega) = |a|^2 \cdot 2\pi \cdot \delta(\omega - \omega_0) \tag{3.45}$$

Just like the FT, the WD is also concentrated at $\omega = \omega_0$ for $e^{j\omega_0 x}$.

For $f(x) = ae^{j\frac{\alpha}{2}x^2}$ where a is a constant,

$$W_f(x,\omega) = |a|^2 \cdot 2\pi \cdot \delta(\omega - \alpha x) \tag{3.46}$$

This means that the WD for a chirp signal is concentrated around the instantaneous frequency so that the chirp effect is clearly visible and measureable from its WD.

3.4 The discrete Wigner distribution (DWD)

3.4.1 Definition

Let $f[n]$ be a complex-valued signal where $n = \cdots, -2, -1, 0, 1, 2, \cdots$, then its *discrete Wigner distribution* (DWD) is defined as

$$W_f(n,\theta) = \sum_{\eta=-\infty}^{\infty} 2f[n+\eta]f^*[n-\eta]e^{-j2\theta\eta} \tag{3.47}$$

The DWD can also be defined as

$$W_f(n,\theta) = \frac{1}{\pi}\int_{-\pi}^{\pi} F(\theta+\vartheta)F^*(\theta-\vartheta)e^{j2\vartheta n}d\vartheta \tag{3.48}$$

where $F(\vartheta)$ is the DFT of $f[n]$.

In fact

$$\begin{aligned}
&\sum_{\eta=-\infty}^{\infty} 2f[n+\eta]f^*[n-\eta]e^{-j2\theta\eta} \\
&= \sum_{\eta=-\infty}^{\infty} 2f[n+\eta]e^{-j2\theta\eta}\cdot f^*[n-\eta] \\
&= \frac{1}{\pi}\int_{-\pi}^{\pi} F(\vartheta+2\theta)e^{j(\vartheta+2\theta)n}F^*(-\vartheta)e^{j\vartheta n}d\vartheta \\
&= \frac{1}{\pi}\int_{-\pi}^{\pi} F(\theta+\vartheta+\theta)F^*(\theta-(\vartheta+\theta))e^{2jn(\theta+\vartheta)}d\vartheta
\end{aligned}$$

3.4.2 Basic properties

Some useful properties are listed here[1].

Periodicity

$$W_f(n,\theta) = W_f(n,\theta+\pi) \tag{3.49}$$

[1]The proofs for Eqn 3.57, Eqn 3.62 and Eqn 3.64, as shown here, are given by myself.

Symmetry

For a real-valued $f[n]$,

$$W_f(n,\theta) = W_f(n,-\theta) \tag{3.50}$$

Realness

For any signal $f[n]$,

$$W_f(n,\theta) = W_f^*(n,\theta) \tag{3.51}$$

Spatial shifting

Let n_0 be a fixed integer,

$$f[n-n_0] \overset{W}{\longleftrightarrow} W_f(n-n_0,\theta) \tag{3.52}$$

Frequency shifting

Let θ_0 be a fixed constant,

$$f[n]e^{j\theta_0 n} \overset{W}{\longleftrightarrow} W_f(n,\theta-\theta_0) \tag{3.53}$$

Spatial-limited signals

If $f[n]$ is restricted to $[n_a,n_b]$, so is its DWD.

Band-limited signals

If $f(n)$ is band-limited to $[\theta_a,\theta_b]$, so is its DWD provided that $0 < \theta_b - \theta_a < \pi$.

Sum formula

For $f[n] = f_1[n] + f_2[n]$,

$$W_f(n,\theta) = W_{f_1}(n,\theta) + W_{f_2}(n,\theta) + 2\mathrm{Re}W_{f_1,f_2}(n,\theta) \tag{3.54}$$

where $W_{f_1,f_2}(n,\theta)$ is the cross Wigner distribution of f_1 and f_2:

$$W_{f_1,f_2}(n,\theta) = \sum_{\eta=-\infty}^{\infty} 2f_1[n+\eta]f_2^*[n-\eta]e^{-j2\theta\eta} \tag{3.55}$$

Spatial-energy

$$\sum_{n=-\infty}^{\infty} W_f(n,\theta) = \frac{1}{2}(|F(\theta)|^2 + |F(\theta+\pi)|^2) \tag{3.56}$$

Proof: From the definition of the DWD, it follows that

$$\begin{aligned}
&\sum_{n=-\infty}^{\infty} W_f(n,\theta)e^{-j2\vartheta n} \\
&= \sum_{n=-\infty}^{\infty} \left(\frac{1}{\pi}\int_{-\pi}^{\pi} F(\theta+\vartheta_1)F^*(\theta-\vartheta_1)e^{j2\vartheta_1 n}d\vartheta_1\right) e^{-j2\vartheta n} \\
&= \frac{1}{\pi}\int_{-\pi}^{\pi} F(\theta+\vartheta_1)F^*(\theta-\vartheta_1)\left(\sum_{n=-\infty}^{\infty} e^{-j2(\vartheta-\vartheta_1)n}\right)d\vartheta_1 \\
&= \frac{1}{\pi}\int_{-\pi}^{\pi} F(\theta+\vartheta_1)F^*(\theta-\vartheta_1)\left(\sum_{k=-\infty}^{\infty} 2\pi\delta(2\vartheta-2\vartheta_1-2\pi k)\right)d\vartheta_1 \\
&= \int_{-\pi}^{\pi} F(\theta+\vartheta_1)F^*(\theta-\vartheta_1)\left(\sum_{k=-\infty}^{\infty} \delta(\vartheta_1-\vartheta+\pi k)\right)d\vartheta_1
\end{aligned}$$

Therefore,

$$\sum_{n=-\infty}^{\infty} W_f(n,\theta)e^{-j2\vartheta n} = F(\theta+\vartheta)F^*(\theta-\vartheta) + F(\theta+\vartheta+\pi)F^*(\theta-\vartheta+\pi) \tag{3.57}$$

Eqn 3.57 is very useful for proving other theorems. Eqn 3.56 is then obtained by letting $\vartheta = 0$.

For any analytical signal f_a or *over-sampled* signal[2], Eqn 3.56 becomes

$$\sum_{n=-\infty}^{\infty} W_f(n,\theta) = F(\theta)F^*(\theta) = |F(\theta)|^2 \tag{3.58}$$

which is similar to its contnuous case.

[2]Let a signal $f(x)$ be band-limited to $[-\omega_c,\omega_c]$, the over-sampled signal $f_s[n]$ is obtained if the sampling frequency is larger then $4\omega_c$.

Frequency-energy

$$\frac{1}{2\pi}\int_{-\frac{\pi}{2}}^{\frac{\pi}{2}} W_f(n,\theta)d\theta = |f[n]|^2 \tag{3.59}$$

Total-energy

$$\frac{1}{2\pi}\int_{-\frac{\pi}{2}}^{\frac{\pi}{2}}\sum_{n=-\infty}^{\infty} W_f(n,\theta)d\theta = \frac{1}{2\pi}\int_{-\pi}^{\pi}|F(\theta)|^2 d\theta = \sum_{n=-\infty}^{\infty}|f[n]|^2 \tag{3.60}$$

Moyal's formula

For a analytical (or over-sampled) signal,

$$\frac{1}{2\pi}\int_{-\frac{\pi}{2}}^{\frac{\pi}{2}}\sum_{n=-\infty}^{\infty} W_f^2(n,\theta)d\theta = \|f[n]\|^4 \tag{3.61}$$

Convolution

Let

$$g[n] = f[n] * h[n]$$
$$g^o[n] = f[n] * \left(h[n]e^{j\pi n}\right)$$

then

$$W_g(n,\theta) + W_{g^o}(n,\theta) = \sum_{\eta=-\infty}^{\infty} W_f(\eta,\theta)W_h(n-\eta,\theta) \tag{3.62}$$

Proof: Eqn 3.62 is from the inverse Fourier transform, Eqn 3.57, and

$$\begin{aligned}
&F(\theta+\frac{\vartheta}{2})H(\theta+\frac{\vartheta}{2})F^*(\theta-\frac{\vartheta}{2})H^*(\theta-\frac{\vartheta}{2})\\
&+F(\theta+\frac{\vartheta}{2}+\pi)H(\theta+\frac{\vartheta}{2}+\pi)F^*(\theta-\frac{\vartheta}{2}+\pi)H^*(\theta-\frac{\vartheta}{2}+\pi)\\
&+F(\theta+\frac{\vartheta}{2})H(\theta+\frac{\vartheta}{2}+\pi)F^*(\theta-\frac{\vartheta}{2})H^*(\theta-\frac{\vartheta}{2}+\pi)\\
&+F(\theta+\frac{\vartheta}{2}+\pi)H(\theta+\frac{\vartheta}{2})F^*(\theta-\frac{\vartheta}{2}+\pi)H^*(\theta-\frac{\vartheta}{2})\\
&=\\
&\left(F(\theta+\frac{\vartheta}{2})F^*(\theta-\frac{\vartheta}{2})+F(\theta+\frac{\vartheta}{2}+\pi)F^*(\theta-\frac{\vartheta}{2}+\pi)\right)
\end{aligned}$$

$$\cdot \left(H(\theta + \frac{\vartheta}{2}) H^*(\theta - \frac{\vartheta}{2}) + H(\theta + \frac{\vartheta}{2} + \pi) H^*(\theta - \frac{\vartheta}{2} + \pi) \right)$$

If both f and h are both band-limited to $[-\frac{\pi}{2}, \frac{\pi}{2}]$, then g^o is zero, therefore

$$W_g(n,\theta) = \sum_{\eta=-\infty}^{\infty} W_f(\eta,\theta) W_h(n-\eta,\theta) \tag{3.63}$$

Modulation

If

$$g[n] = f[n]h[n]$$

then

$$g[n] \overset{W}{\longleftrightarrow} \frac{1}{2\pi} \int_{-\frac{\pi}{2}}^{\frac{\pi}{2}} W_f(n,\vartheta) W_h(n,\theta-\vartheta) d\vartheta \tag{3.64}$$

Proof:

$$\begin{aligned} W_g(n,\theta) &= \sum_{\eta=-\infty}^{\infty} 2f[n+\eta]h[n+\eta] \cdot f^*[n-\eta]h^*[n-\eta] e^{-j2\theta\eta} \\ &= \frac{1}{2} \cdot \sum_{\eta=-\infty}^{\infty} 2f[n+\eta]f^*[n-\eta] \cdot 2h[n+\eta]h^*[n-\eta] e^{-j2\theta\eta} \\ &= \frac{1}{4\pi} \int_{-\pi}^{\pi} W_f(n, \frac{\vartheta}{2}) W_h(n, \frac{\theta-\vartheta}{2}) d\vartheta \\ &= \frac{1}{2\pi} \int_{-\frac{\pi}{2}}^{\frac{\pi}{2}} W_f(n,\vartheta) W_h(n,\theta-\vartheta) d\vartheta \end{aligned}$$

3.4.3 The DWD for analytical signals

For a signal $f[n]$, its analytical signal $f_a[n]$ is of the form (Oppenheim and Schafer 1975)

$$f_a[n] = f[n] + j\hat{f}[n] \tag{3.65}$$

where $\hat{f}[n]$ is the discrete Hilbert transform of $f[n]$, defined by

$$\hat{f}[n] = (\mathcal{H}_d f)[n] = \sum_{\eta=-\infty}^{\infty} f[\eta] \frac{2}{\pi} \frac{\sin^2 \frac{\pi(n-\eta)}{2}}{(n-\eta)} \tag{3.66}$$

The DFT of f_a and f is related as

$$F_a(\vartheta) = \begin{cases} 2F(\vartheta) & 0 < \vartheta < \pi \\ F(0) & \vartheta = 0 \\ 0 & -\pi \leq \vartheta < 0 \end{cases} \tag{3.67}$$

Since f_a is band-limited to $[0, \pi)$, its DWD does not have the aliasing effect.

3.4.4 Moments

For any signal $f[n]$, both local moments and global moments can also be used to simplify the usage of the DWD. They are listed below.

Local moments in frequency

The *0th-order moment in frequency* $p_f[n]$ is defined as

$$p_f[n] = \frac{1}{2\pi} \int_{-\frac{\pi}{2}}^{\frac{\pi}{2}} W_f(n, \theta) d\theta \tag{3.68}$$

From Eqn 3.59,

$$p_f[n] = |f[n]|^2 \tag{3.69}$$

which means that the 0th-order moment in frequency is equal to the instantaneous power of the signal.

The *1st-order moment in frequency* $\Theta_f[n]$:

$$\Theta_f[n] = \frac{1}{2} \arg \left(\int_{-\frac{\pi}{2}}^{\frac{\pi}{2}} e^{j2\theta} W_f(n, \theta) d\theta \right) \tag{3.70}$$

then

$$\Theta_f[n] = \frac{1}{2} \arg(f[n+1] f^*[n-1]) \tag{3.71}$$

For $f[n] = v[n]e^{j\phi[n]}$, then

$$\Theta_f[n] = \frac{\phi[n+1] - \phi[n-1]}{2} \bmod \pi \tag{3.72}$$

which means that the 1st-order moment in frequency can be used to represent the instantaneous frequency.

The *2nd-order moment in frequency* $m_f[n]$:

$$m_f[n] = \frac{p_f[n] - \left|\frac{1}{2\pi}\int_{-\frac{\pi}{2}}^{\frac{\pi}{2}} e^{j2\theta} W_f(n,\theta)d\theta\right|}{p_f[n] + \left|\frac{1}{2\pi}\int_{-\frac{\pi}{2}}^{\frac{\pi}{2}} e^{j2\theta} W_f(n,\theta)d\theta\right|} \tag{3.73}$$

$m_f[n]$ can be expressed as

$$m_f[n] = \frac{|f[n]|^2 - |f[n+1]f^*[n-1]|}{|f[n]|^2 + |f[n+1]f^*[n-1]|} \tag{3.74}$$

Local moments in space

The *0th-order moment in space* $P_f(\theta)$:

$$P_f(\theta) = \sum_{n=-\infty}^{\infty} W_f(n,\theta) = |F(\theta)|^2 + |F(\theta+\pi)|^2 \tag{3.75}$$

The *1st-order moment in space* $X_f(\theta)$:

$$X_f(\theta) = \frac{\sum_{n=-\infty}^{\infty} W_f(n,\theta)n}{P_f(\theta)} \tag{3.76}$$

For over-sampled or analytical signals, X_f can be expressed by

$$X_f(\theta) = -\mathrm{Im}\frac{d\ln F(\theta)}{d\theta} \tag{3.77}$$

Proof: Differentiating Eqn 3.57 with respect to ϑ obtains

$$\sum_{n=-\infty}^{\infty} W_f(\theta,n)ne^{-j2\vartheta n}$$

$$= \frac{j}{2}F'(\theta+\vartheta)F^*(\theta-\vartheta) - \frac{j}{2}F(\theta+\vartheta)(F^*)'(\theta-\vartheta)$$
$$+\frac{j}{2}F'(\theta+\vartheta+\pi)F^*(\theta-\vartheta+\pi) - \frac{j}{2}F(\theta+\vartheta+\pi)(F^*)'(\theta-\vartheta+\pi)$$

then

$$\sum_{n=-\infty}^{\infty} W_f(\theta,n)n$$
$$= \frac{j}{2}F'(\theta)F^*(\theta) - \frac{j}{2}F(\theta)(F^*)'(\theta)$$
$$+\frac{j}{2}F'(\theta+\pi)F^*(\theta+\pi) - \frac{j}{2}F(\theta+\pi)(F^*)'(\theta+\pi)$$

Because of f is over-sampled or analytical,

$$\sum_{n=-\infty}^{\infty} W_f(\theta,n)n = \frac{j}{2}F'(\theta)F^*(\theta) - \frac{j}{2}F(\theta)(F^*)'(\theta)$$

Therefore

$$X_f(\theta) = \frac{\frac{j}{2}F'(\theta)F^*(\theta) - \frac{j}{2}F(\theta)(F^*)'(\theta)}{F(\theta)F^*(\theta)}$$
$$= \frac{j}{2}\left(\frac{F'(\theta)}{F(\theta)} - \left(\frac{F'(\theta)}{F(\theta)}\right)^*\right)$$
$$= -\mathrm{Im}\left(\frac{F'(\theta)}{F(\theta)}\right)$$

The *2nd-order moment in space* $M_f(\theta)$:

$$M_f(\theta) = \frac{\sum_{n=-\infty}^{\infty}[n - T_f(\theta)]^2 W_f(n,\theta)}{P_f(\theta)} \tag{3.78}$$

For over-sampled or analytical signals, M_f becomes

$$M_f(\theta) = -\frac{1}{2}\mathrm{Re}\frac{d}{d\theta}\frac{F'(\theta)}{F(\theta)} \tag{3.79}$$

Global moments

The *0th-order global moment* of the DWD:

$$\overline{P_f} = \frac{1}{2\pi}\int_{-\frac{\pi}{2}}^{\frac{\pi}{2}} \sum_{n=-\infty}^{\infty} W_f(n,\theta)d\theta = \|f\|^2 = \|F\|^2 \tag{3.80}$$

The *1st-order global moment with respect to frequency* of the DWD:

$$\overline{\Theta_f} = \frac{1}{2}\arg\left[\int_{-\frac{\pi}{2}}^{\frac{\pi}{2}} \sum_{n=-\infty}^{\infty} e^{j2\theta} W_f(n,\theta)d\theta\right] \tag{3.81}$$

The *1st-order global moment with respect to space* of the DWD:

$$\overline{X_f} = \sum_{n=-\infty}^{\infty} \frac{1}{2\pi}\int_{-\frac{\pi}{2}}^{\frac{\pi}{2}} nW_f(n,\theta)d\theta/\overline{P_f} \tag{3.82}$$

3.4.5 Application to signals

Figure 3.1, 3.2, 3.3, and 3.4 show four DWDs computed for the same signals as in Section 2.3.

For the two stationary signals, the DWDs are helpful. In fact, the power-spectrum can be obtained by simply integrating the DWD along n at a fixed θ provided that the original signal is over-sampled or analytical.

For the two nonstationary signals, the DWDs are mainly concentrated around at the instantaneous frequency and shows the trend of local spectrum.

It can be concluded that *the DWD is good for analysing both stationary and nonstationary signals* from these figures

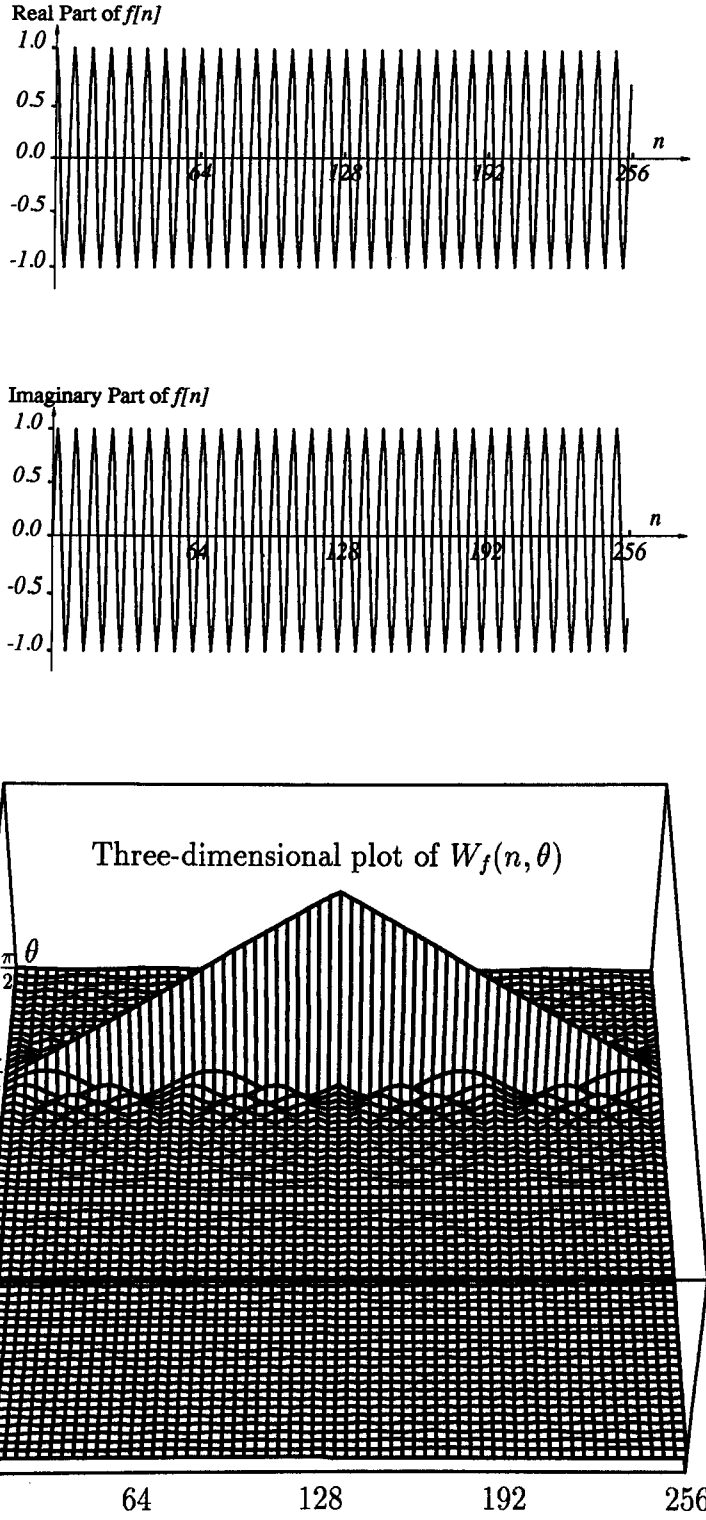

Figure 3.1: A stationary signal $f[n]$ and its DWD

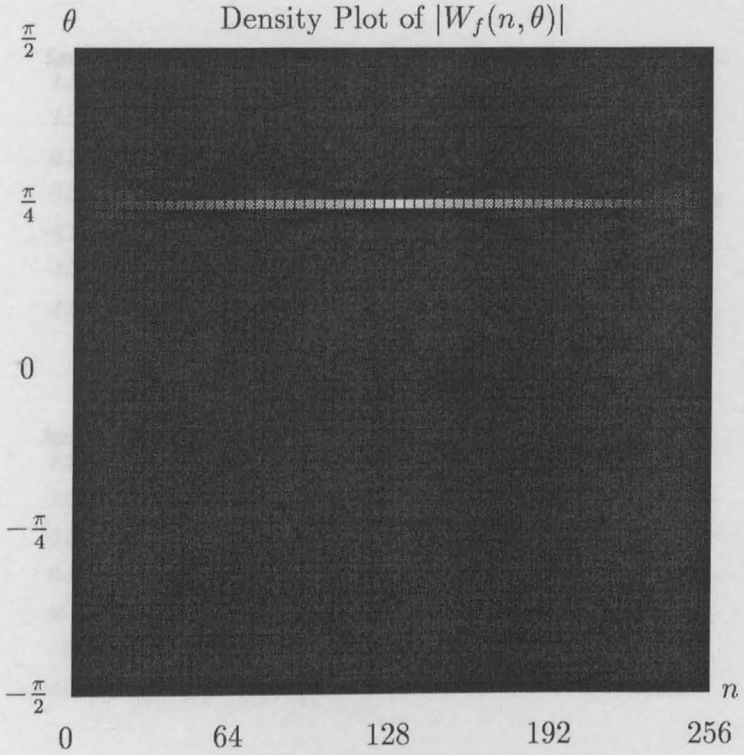

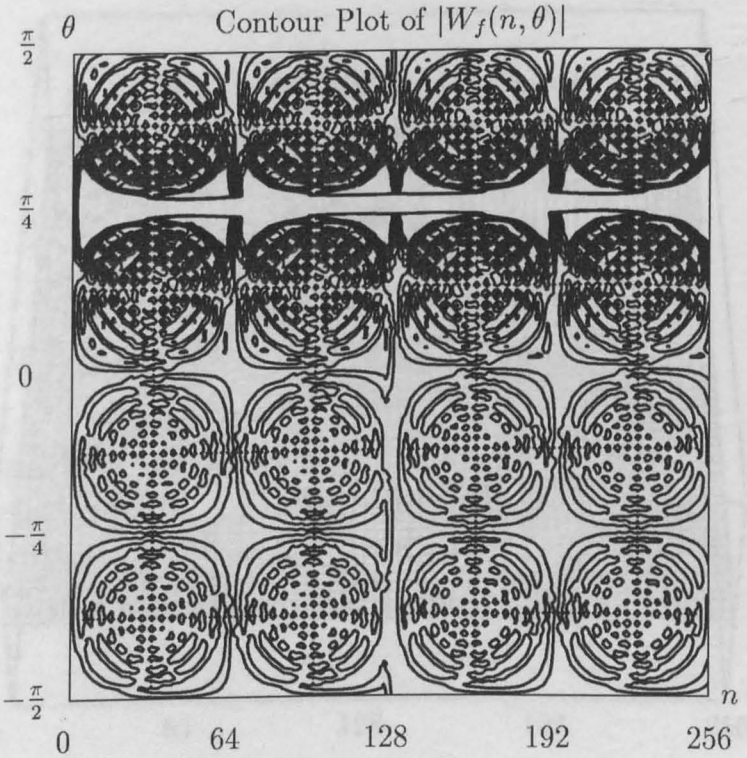

A stationary signal $f[n]$ and its DWD (continued)

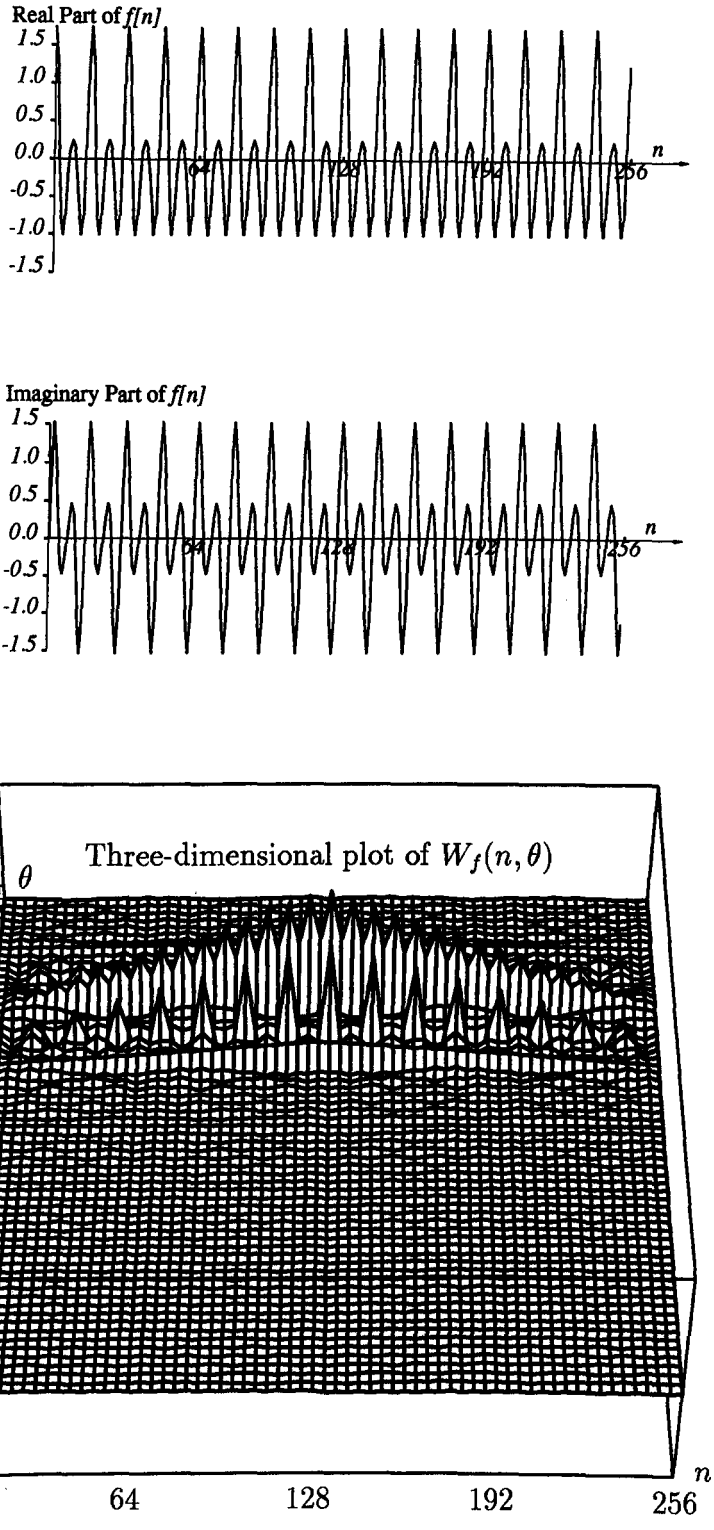

Figure 3.2: Another stationary signal $f[n]$ and its DWD

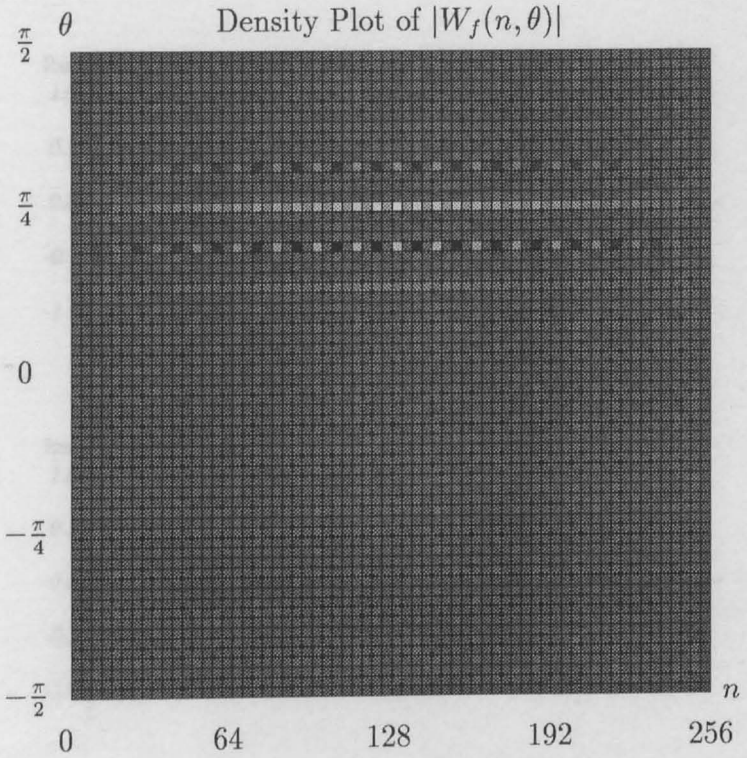

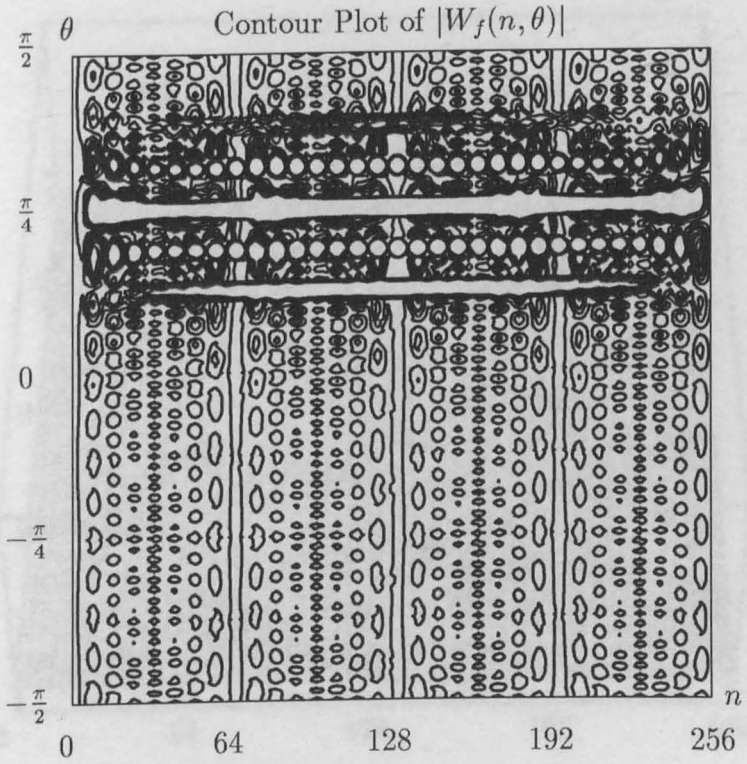

Another stationary signal $f[n]$ and its DWD (continued)

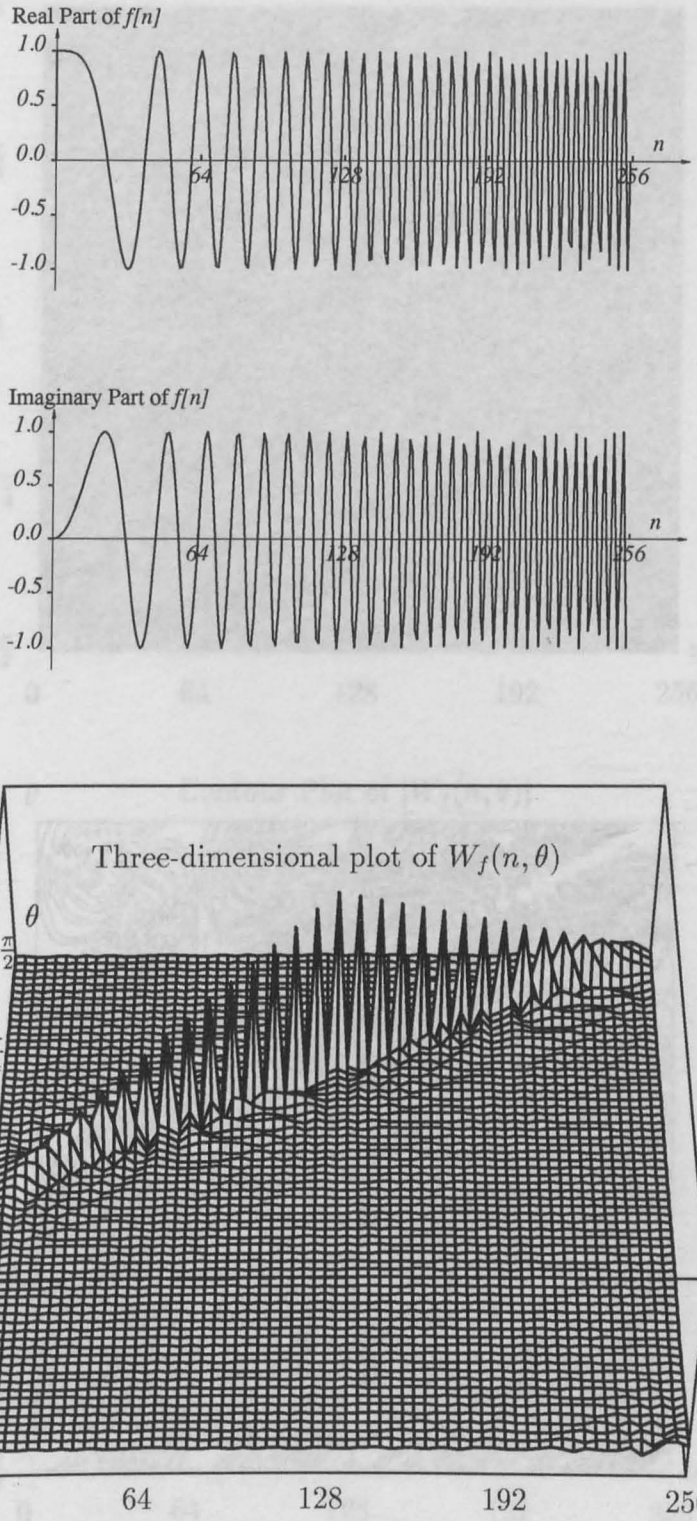

Figure 3.3: A chirp signal $f[n]$ and its DWD

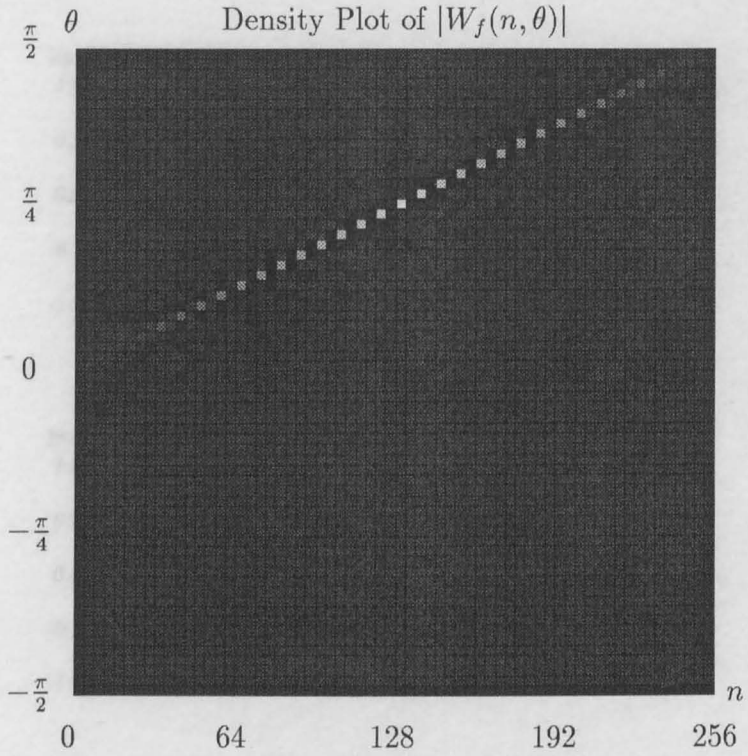

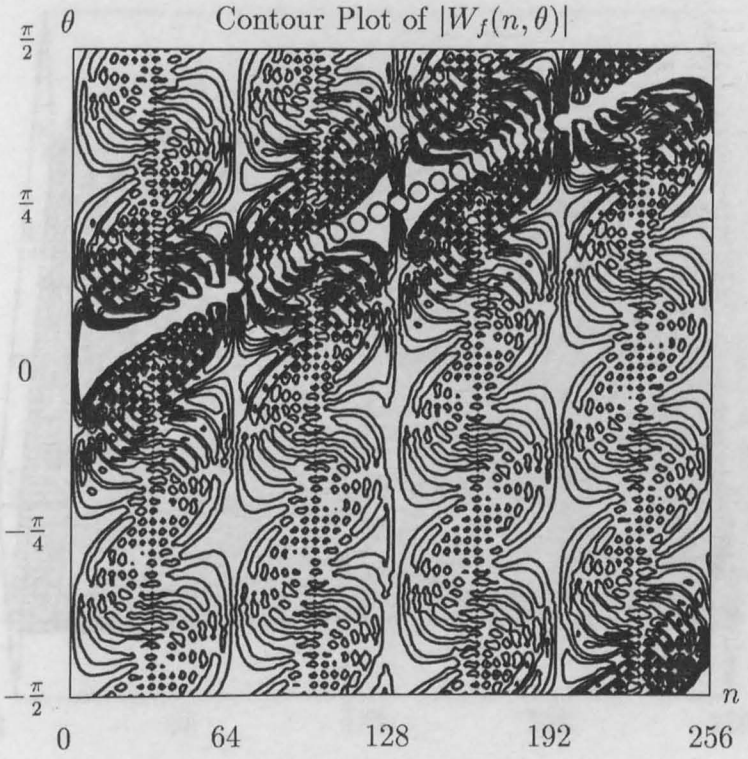

A chirp signal $f[n]$ and its DWD (continued)

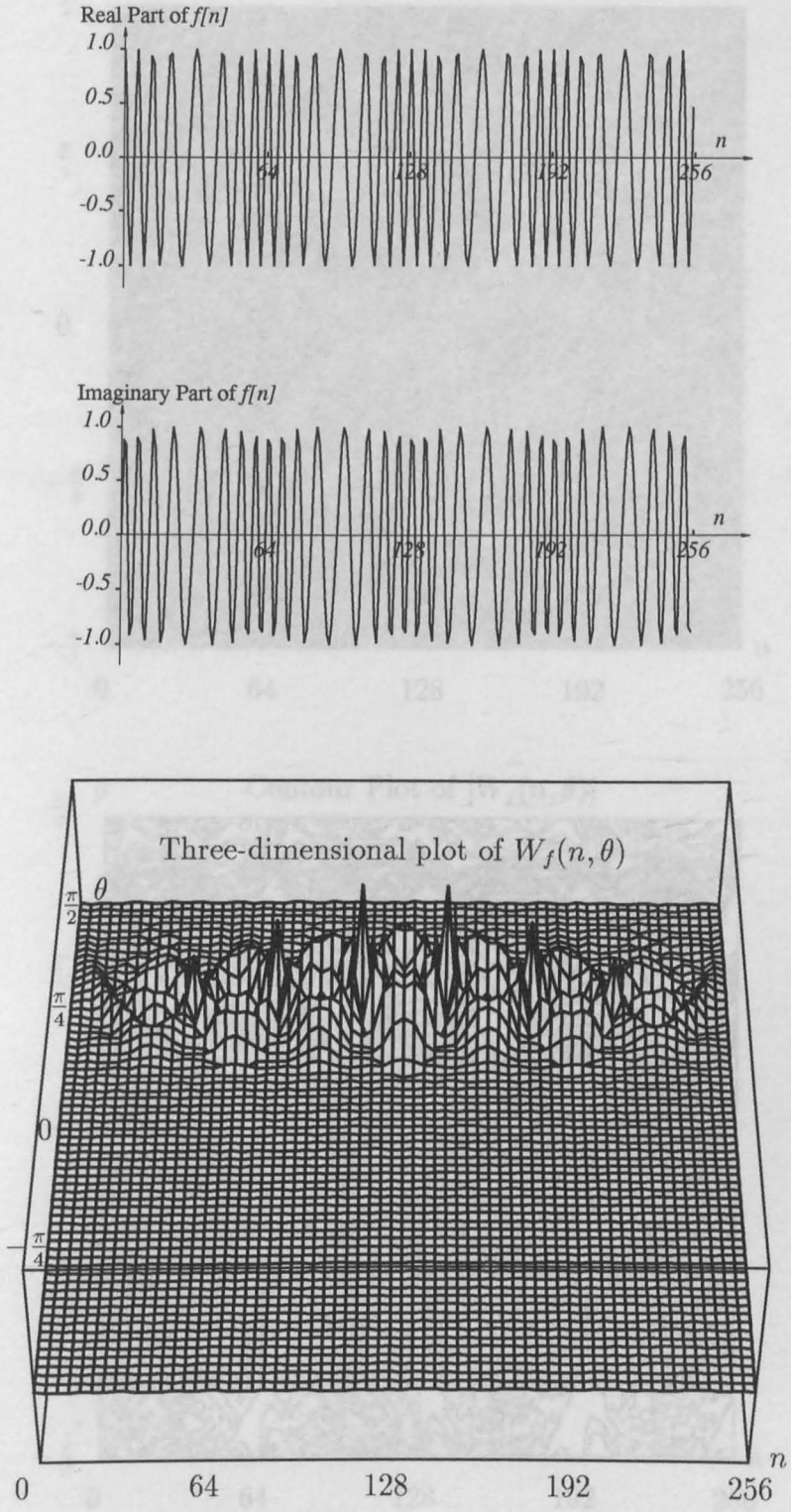

Figure 3.4: A frequency modulated signal $f[n]$ and its DWD

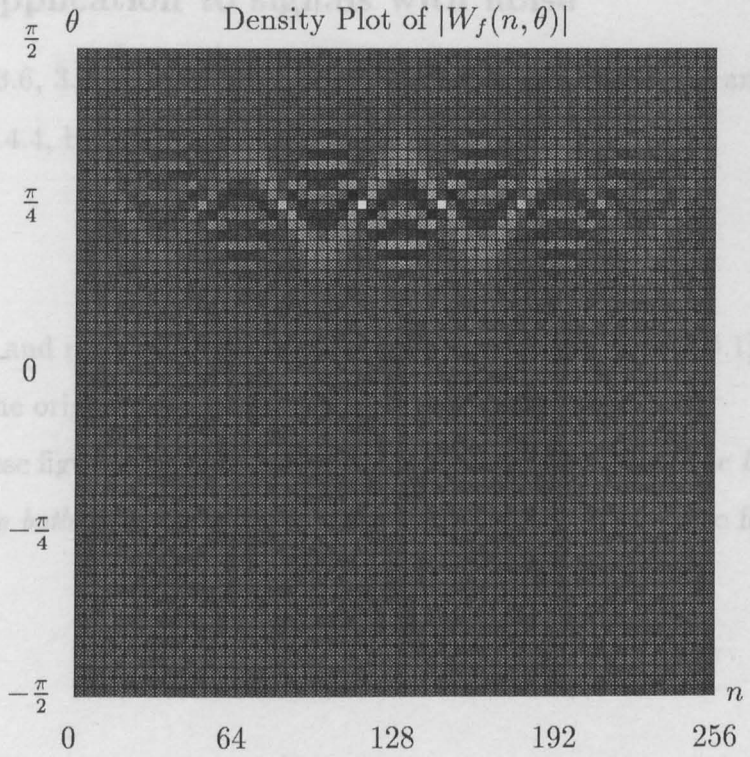

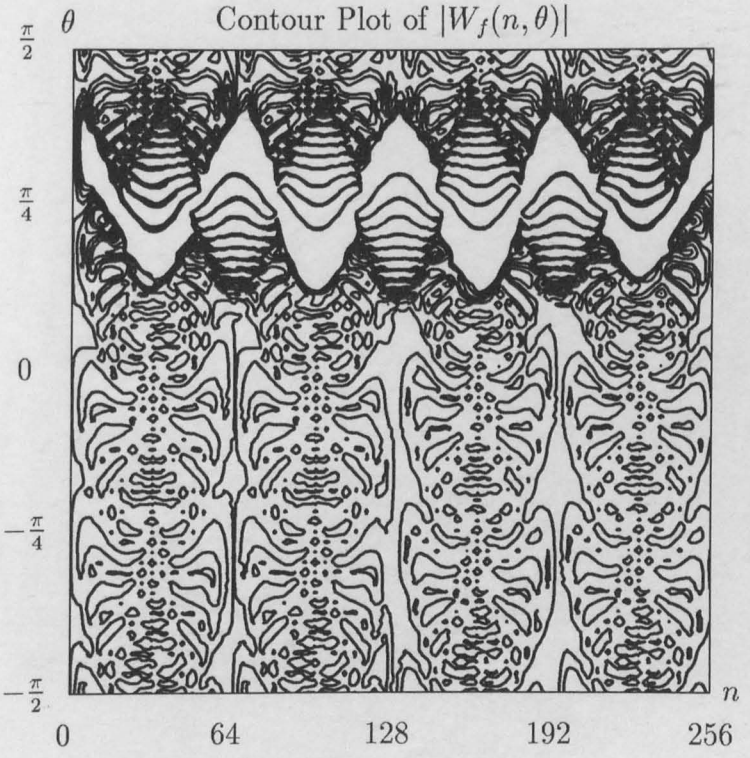

A frequency-modulated signal $f[n]$ and its DWD (continued)

3.4.6 Application to signals with noise

Figure 3.5, 3.6, 3.7, and 3.8 show four DWDs computed for the same signals as in Section 2.4.4, but with noise. The noise is of type

$$n(x) = n_1(x) + in_2(x)$$

where $n_1(x)$ and $n_2(x)$ are random noise with the range as $[-0.1, 0.1]$, about 10% percent of the original signal.

From these figures, the same conclusion can be reached that *the DWD is good for analysing both stationary and nonstationary signals* from these figures.

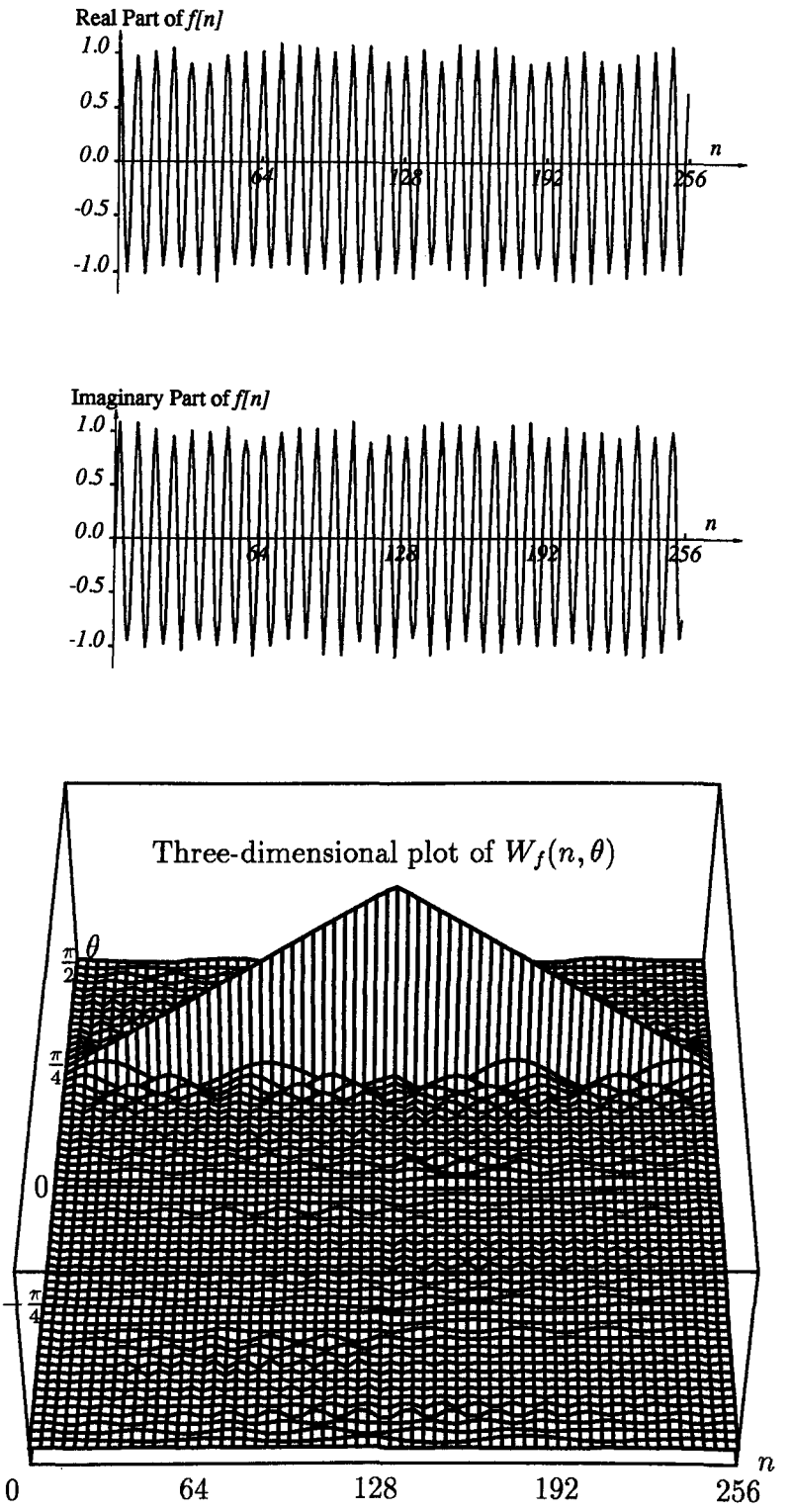

Figure 3.5: A stationary signal with noise and its DWD

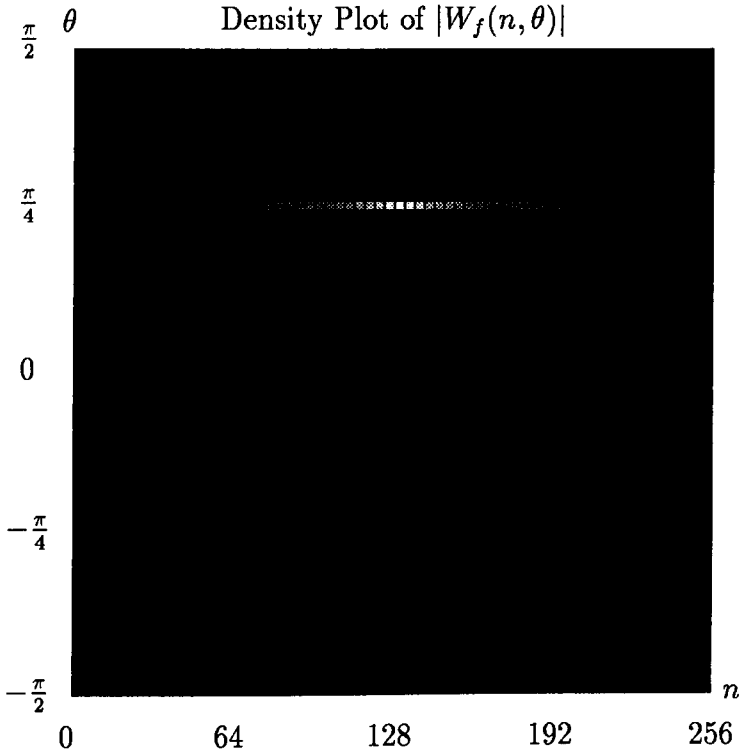

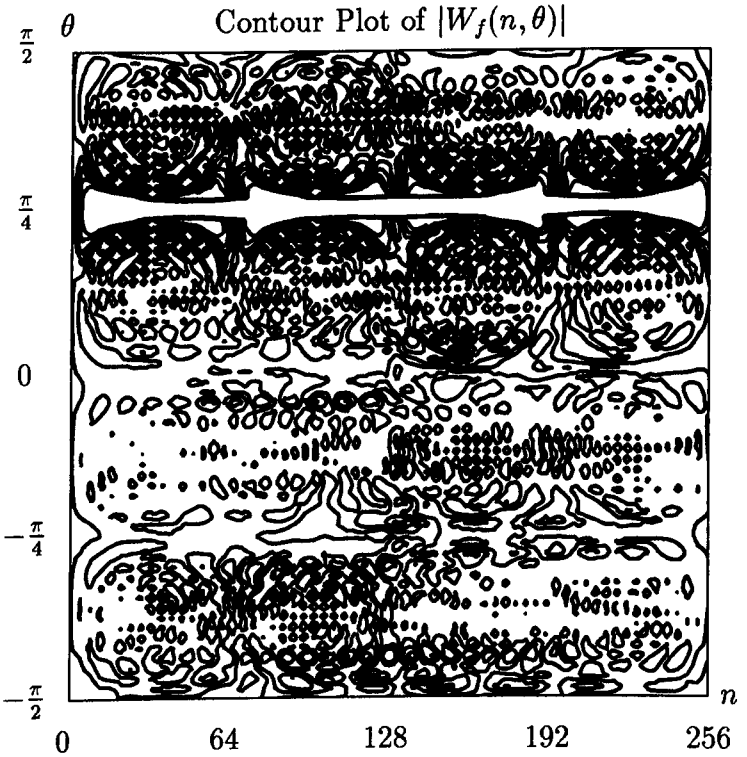

A stationary signal with noise and its DWD (continued)

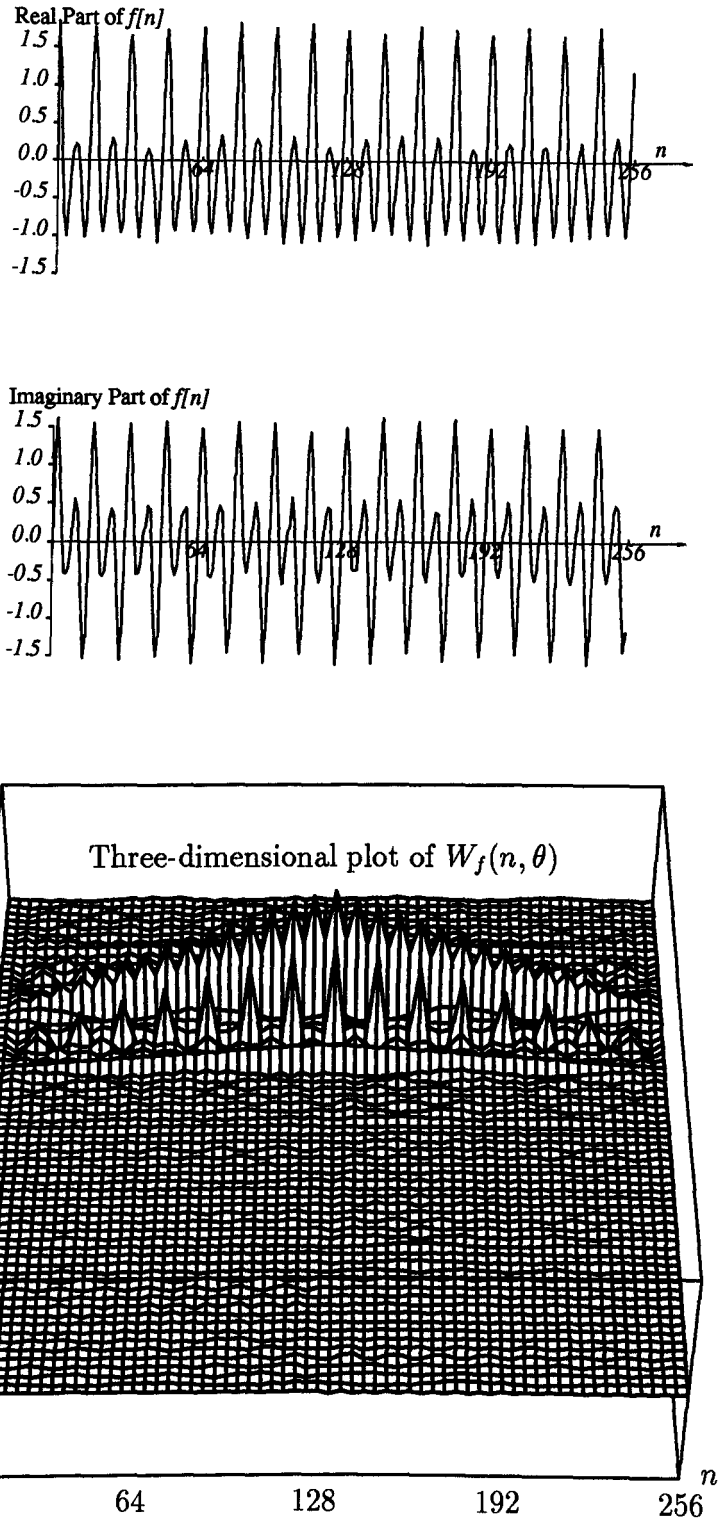

Figure 3.6: Another stationary signal with noise and its DWD

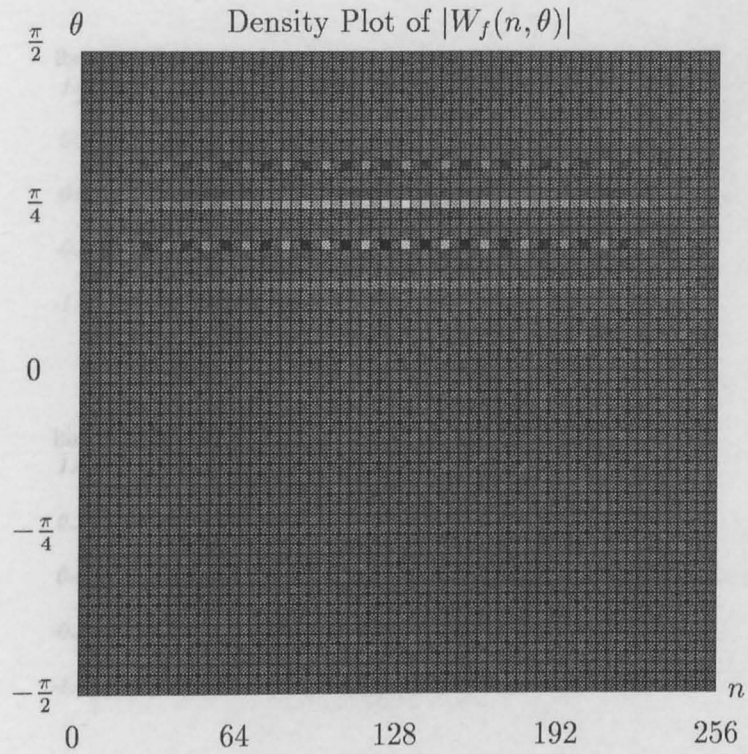

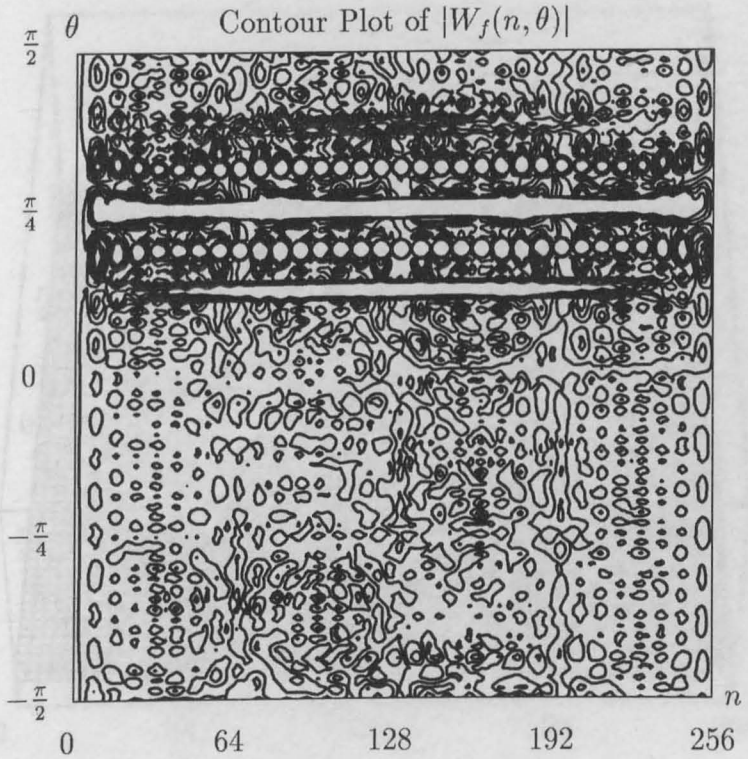

Another stationary signal with noise and its DWD (continued)

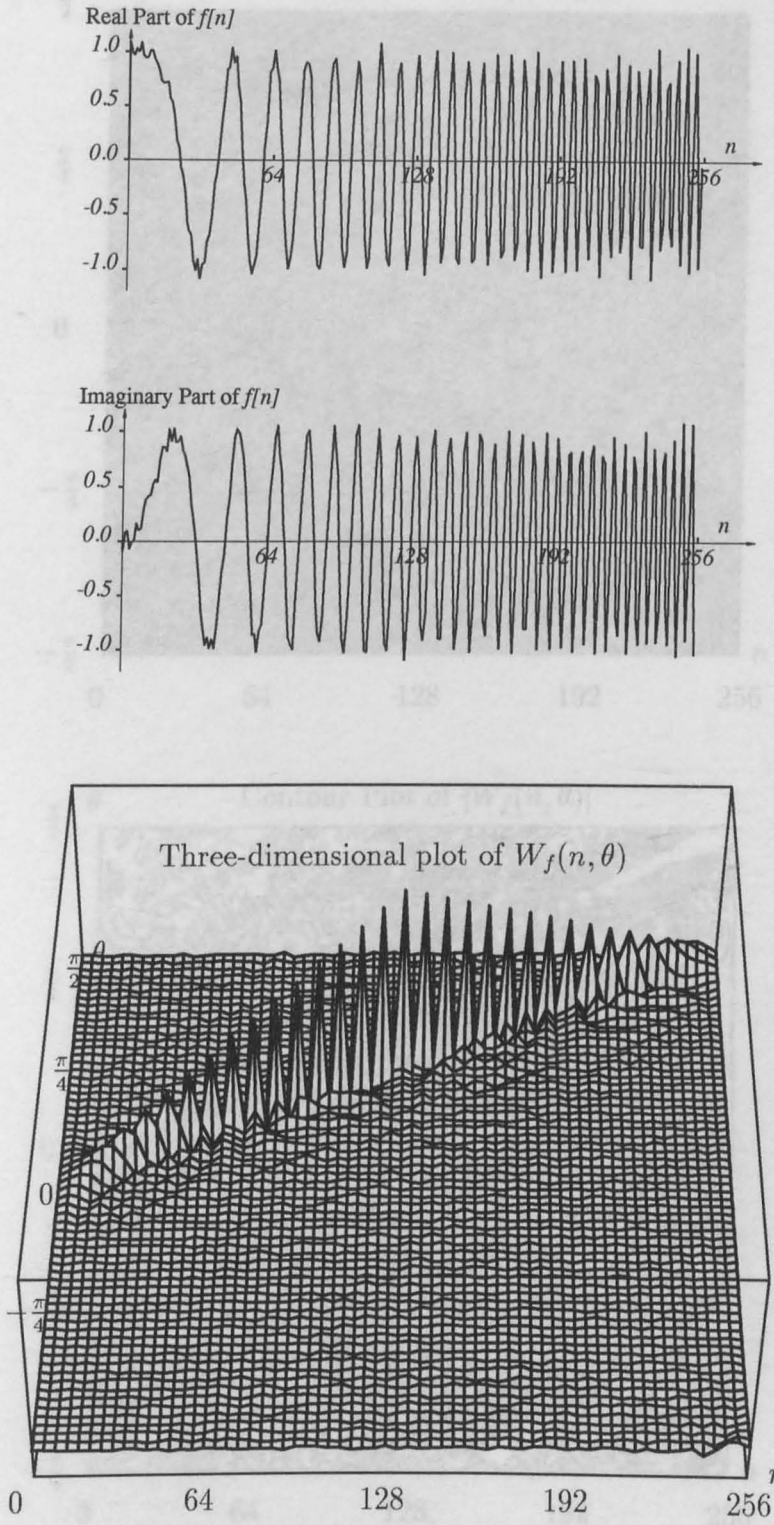

Figure 3.7: A chirp signal with noise and its DWD

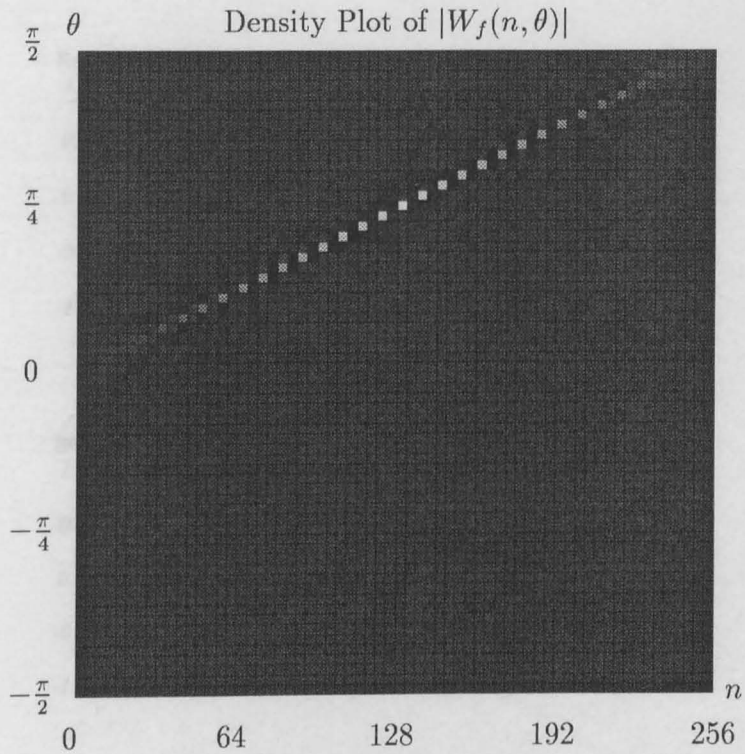

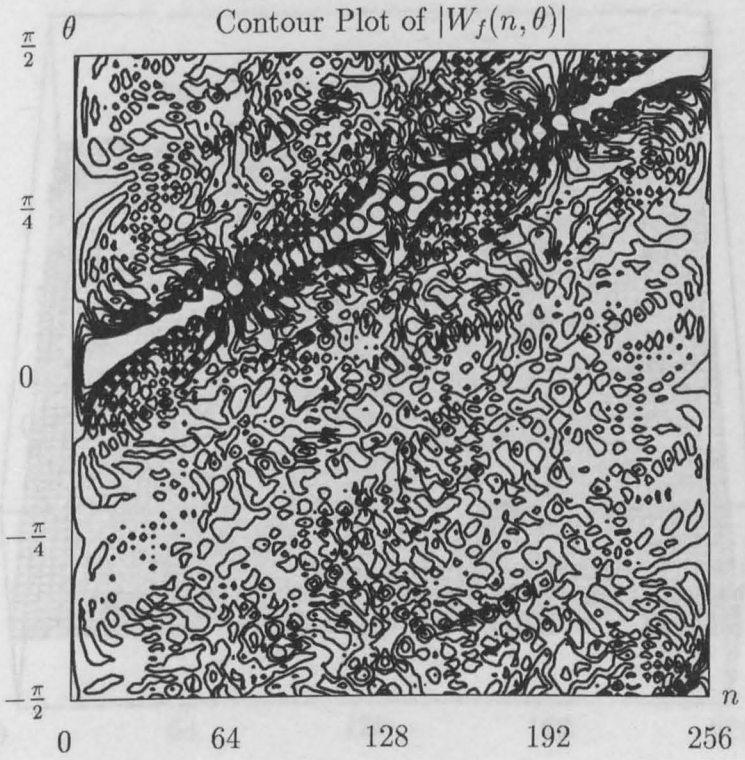

A chirp signal with noise and its DWD (continued)

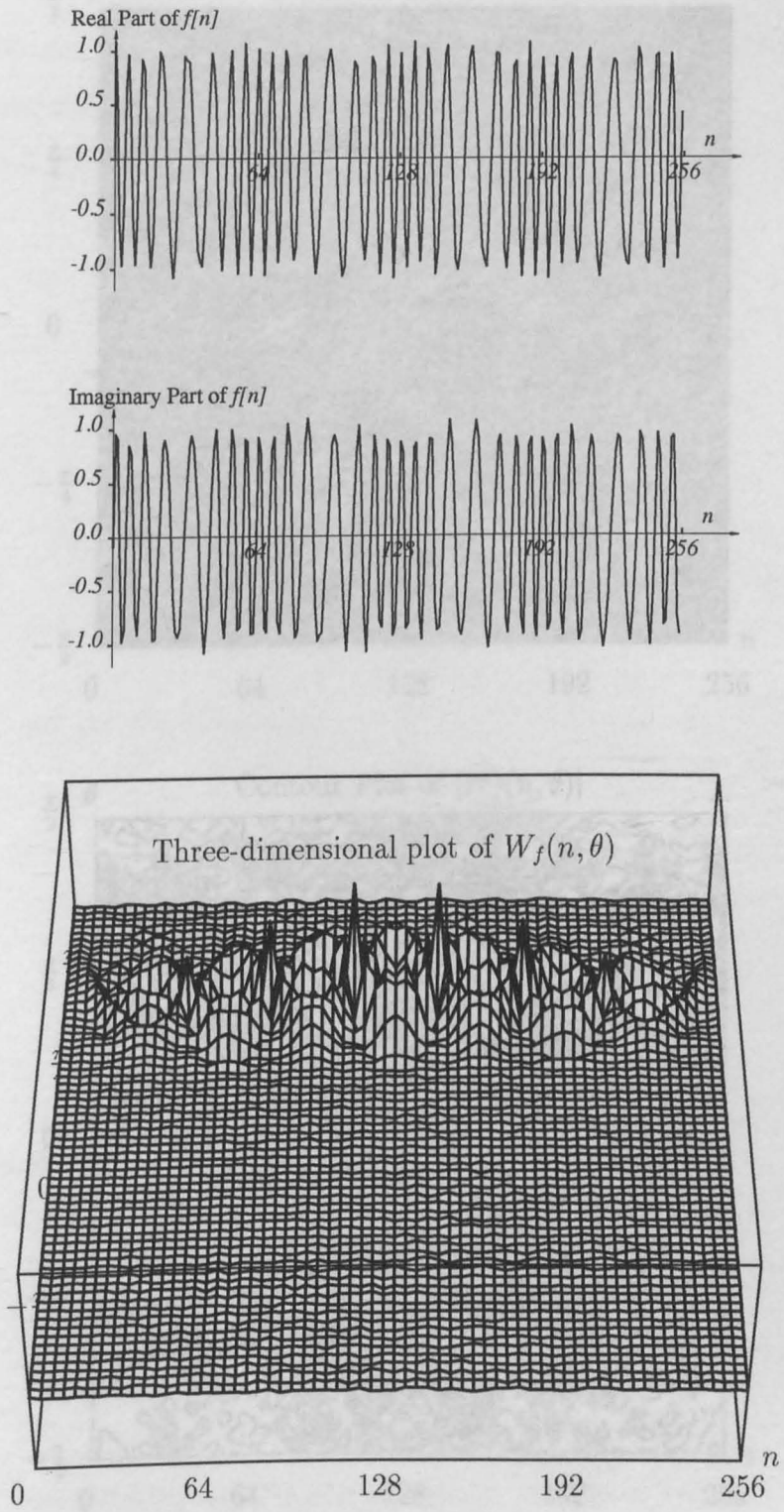

Figure 3.8: A frequency modulated signal with noise and its DWD

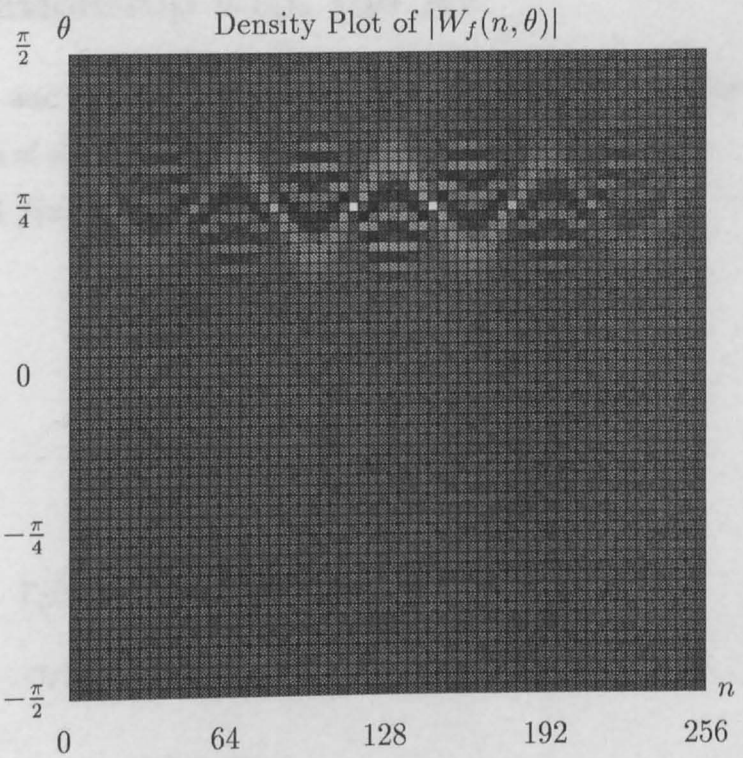

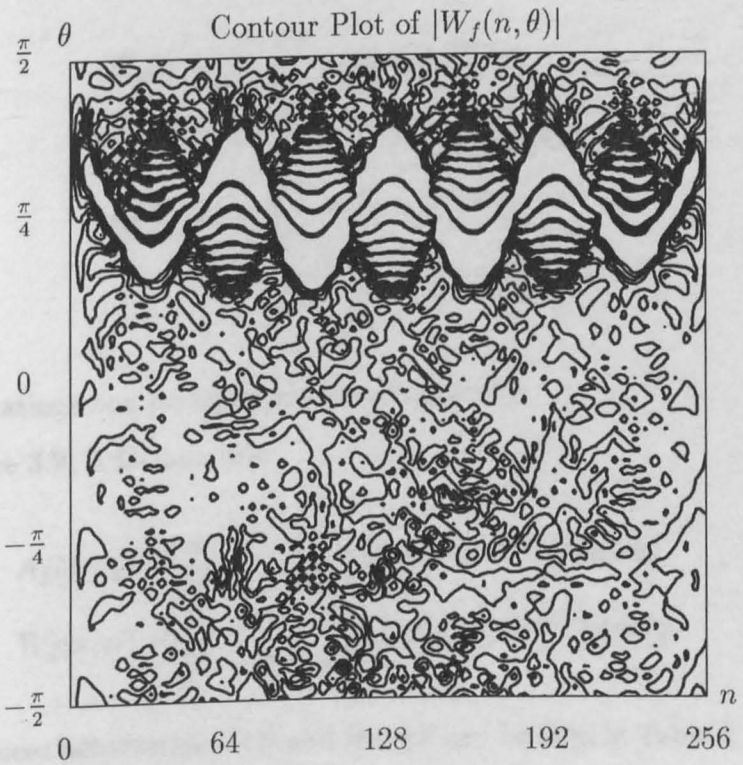

A frequency-modulated signal with noise and its DWD (continued)

3.5 Relationship with the AF

Both the WD and AF belong to mixed distance-frequency or time-frequency representations of signals, and are very closely related to each other.

For a signal $f(x)$ with the FT as $F(\varpi)$, let

$$\gamma_f(x,\chi) = f(x+\frac{\chi}{2})f^*(x-\frac{\chi}{2})$$
$$\Gamma_f(\varpi,\omega) = F(\omega+\frac{\varpi}{2})F^*(\omega-\frac{\varpi}{2})$$

so

$$\Gamma_f(\varpi,\omega) = \int_{-\infty}^{\infty}\int_{-\infty}^{\infty}\gamma_f(x,\chi)e^{-j\varpi x}e^{-j\omega\chi}dxd\chi \tag{3.83}$$
$$\gamma_f(x,\chi) = \frac{1}{4\pi^2}\int_{-\infty}^{\infty}\int_{-\infty}^{\infty}\Gamma_f(\varpi,\omega)e^{j\varpi x}e^{j\omega\chi}d\varpi d\omega \tag{3.84}$$

then the WD and AF are defined as

$$W_f(x,\omega) = \int_{-\infty}^{\infty}\gamma_f(x,\chi)e^{-j\omega\chi}d\chi \tag{3.85}$$
$$= \frac{1}{2\pi}\int_{-\infty}^{\infty}\Gamma_f(\varpi,\omega)e^{j\varpi x}d\omega \tag{3.86}$$
$$A_f(\varpi,\chi) = \int_{-\infty}^{\infty}\gamma_f(x,\chi)e^{-j\varpi x}dx \tag{3.87}$$
$$= \frac{1}{2\pi}\int_{-\infty}^{\infty}\Gamma_f(\varpi,\omega)e^{j\omega\chi}d\omega \tag{3.88}$$

The above equations can be represented in Figure 3.9

From Figure 3.9, it follows that

$$A_f(\varpi,\chi) = \frac{1}{2\pi}\int_{-\infty}^{\infty}\int_{-\infty}^{\infty}W_f(x,\omega)e^{-j\varpi x}e^{j\omega\chi}dxd\omega \tag{3.89}$$
$$W_f(x,\omega) = \frac{1}{2\pi}\int_{-\infty}^{\infty}\int_{-\infty}^{\infty}A_f(\varpi,\chi)e^{j\varpi x}e^{-j\omega\chi}d\varpi d\chi \tag{3.90}$$

The differences between the WD and the AF can be seen in Table 3.1. Shifting in spatial or frequency domain leads to a corresponding shifting in the WD; the effect on the AF is only a phase factor. Moreover, for a limited signal in

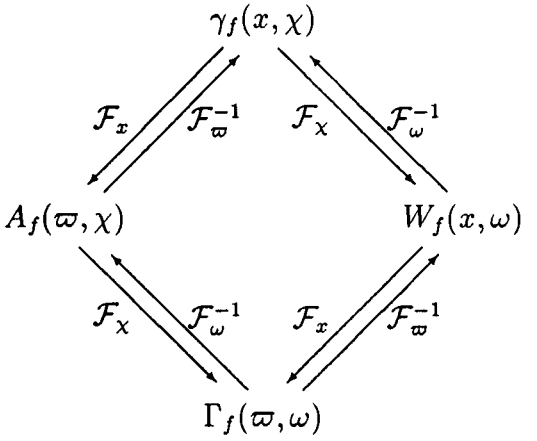

Figure 3.9: Relationship Amongst $W_f(x,\omega)$,$A_f(\varpi,\chi)$, $\gamma_f(x,\chi)$, and $\Gamma_f(\varpi,\omega)$

the spatial domain the WD is spatially limited and for a limited signal in the frequency domain the WD is frequency limited; while the AF does not have these properties. *For the WD, the interpretation of the spatial and frequency variable corresponds to that of the original signal, while it does not for the AF.* From these, it could be concluded that the WD is better than the AF in terms of analyzing both stationary and nonstationary signals. However, in order to verify this, both theoretical and practical application are investigated in Chapter 4 and Chapter 6.

Table 3.1 Relation among the FT, AF, and WD

	$f(x)$	$F(\omega)$	$A_f(\varpi,\chi)$	$W_f(x,\omega)$
	complex-valued	complex-valued	complex-valued	real-valued
Spatial Shifting	$f(x-x_0)$	$F(\omega)e^{-j\omega x_0}$	$A_f(\varpi,\chi)e^{-j\varpi x_0}$	$W_f(x-x_0,\omega)$
Frequency Shifting	$f(x)e^{j\omega_0 x}$	$F(\omega-\omega_0)$	$A_f(\varpi,\chi)e^{j\varpi_0\chi}$	$W_f(x,\omega-\omega_0)$
Spatial Limited	$[x_a,x_b]$ for x	$[-\infty,\infty]$ for ω	$[-(x_b-x_a),x_b-x_a]$ for χ	$[x_a,x_b]$ for x
Frequency Limitd	$[-\infty,\infty]$ for x	$[\omega_a,\omega_b]$ for ω	$[-(\omega_b-\omega_a),\omega_b-\omega_a]$ for ϖ	$[\omega_a,\omega_b]$ for ω
Convolution	$\int_{-\infty}^{\infty} f(\chi)h(x-\chi)d\chi$	$F(\omega)H(\omega)$	$\int_{-\infty}^{\infty} A_f(\varpi,x)A_h(\varpi,\chi-x)dx$	$\int_{-\infty}^{\infty} W_f(\chi,\omega)W_h(x-\chi,\omega)d\chi$
Modulation	$f(x)m(x)$	$\frac{1}{2\pi}\int_{-\infty}^{\infty} F(\varpi)M(\omega-\varpi)d\varpi$	$\frac{1}{2\pi}\int_{-\infty}^{\infty} A_f(\omega,\chi)A_m(\varpi-\omega,\chi)d\omega$	$\frac{1}{2\pi}\int_{-\infty}^{\infty} W_f(x,\varpi)W_m(x,\omega-\varpi)d\varpi$
Typical Stationary	$Ae^{j\omega_o x}$	$A2\pi\delta(\omega-\omega_o)$	$\lvert A\rvert^2 e^{-j\varpi_o\chi}2\pi\delta(\varpi)$	$\lvert A\rvert^2 2\pi\delta(\omega-\omega_o)$
Typical Non-stationary	$Ae^{j\frac{\alpha}{2}x^2}$	$A\frac{2\pi}{\alpha}e^{j\frac{\pi}{4}}e^{-\frac{j\omega^2}{2\alpha}}$	$\lvert A\rvert^2 2\pi\delta(\varpi-\alpha\chi)$	$\lvert A\rvert^2 2\pi\delta(\omega-\alpha x)$

Chapter 4

Extraction of Parameters from the WD

4.1 Introduction

In the previous chapter, the Wigner distribution, in both continuous and discrete forms, was studied, and it was suggested that the WD could be a realistic tool for representation and analysis of signals, especially non-stationary signals.

In this chapter, the WD is employed to analyse non-stationary signals and to extract relevant parameters. Two methods of extracting parameters are discussed. One is to employ the Hough transform; the other is to utilise local moments in frequency. More emphasis is put on the latter because it is simpler and easier to use, and more widely applicable.

Both chirp and frequency-modulated signals are tested here. These two types of signals are commonly found in engineering. Furthermore, frequency-modulated signals are in fact contained in the surface texture of a workpiece machined with the presence of tool vibration as will be shown later.

4.2 The Hough transform

4.2.1 Preliminary

The *Hough transform* deals with the detection of specific structural relationships between pixels in an image (therefore it can be used to extract valuable information from the WD). The Hough transform was first proposed by Hough (1962), later popularised by Duda and Hart (1972). A generalisation of the Hough transform for detecting arbitrary shapes has been proposed by Ballard (1981). Methods for reducing computational complexity have been investigated by Merlin and Farber (1975), and Davis (1982).

For an introduction to the Hough transform, suppose that given N points in an image, it is required to find subsets of these points that lie on straight lines. One method is to use the least-square fitting. However, this only works for very simple case, i.e. all the points are very close on one single line. Another method is to find all $N(N-1)/2$ possible lines first, then to perform $(N-2)N(N-1)/2$ comparison of all points to each line. The complexity of this algorithm is $O(N^3)$ or at least $O(N^2)$. As a result, this method is computationally prohibitive in all but the most trivial cases.

4.2.2 Fundamentals

This problem for detection lines can be solved efficiently by the Hough transform. For a fixed point (x_i, y_i) in xy plane (the image plane), there is an infinite number of lines that pass through (x_i, y_i) and they all have the line equation in slope-intercept form as

$$y_i = ax_i + b$$

for various values of a and b, or

$$b = -ax_i + y_i$$

which is the equation of a single line in the ab plane (*the parameter space*). In other words, each point in the xy plane corresponds to a straight line in the ab plane. It can be deduced that

1. the set of lines in the ab plane, having the same values for a or b, means that those corresponding points in the xy plane have the same slope or intercept, respectively.

2. each intersection of these lines in the ab plane means that those corresponding points in the xy plane are on the same line.

Therefore, to detect lines in the xy plane, it is only necessary to find those intersections of lines in the ab plane.

The algorithm can be described as:

1. Let $(a_{\min}, a_{\max})$ and $(b_{\min}, b_{\max})$ be the expected ranges of slope and intercept values, then quantise $(a_{\min}, a_{\max})$ and $(b_{\min}, b_{\max})$ into KL squares. Create a two-dimensional array $C[K][L]$ (This is in C language). and initialise C to zero.

2. Then for every point (x_i, y_i) in the image plane, let the parameter a equal each of the allowed subdivision values a_k on the axis and solve for the corresponding b's by using the equation $b = -x_i a + y_i$. The resulting b's are then rounded off to the nearest allowed values b_l in the b axis. Then $C[k, l]$ is increased by 1.

3. At the end of this procedure, a value of P in $C[k][l]$ corresponds to P points in the xy plane lying on the line $y = a_k x + b_l$. To find a line passing most of points in the xy plane is only necessary to find the maximum value of P in $C[k][l]$.

For N points, there are NK values of b to compute, therefore, the complexity is $O(N)$ provided that K is small.

4.2.3 Examples

Take for example a chirp signal. The result is good because the parameter α can be extracted quite simply from the graph. See Figure 4.1 and Figure 4.2.

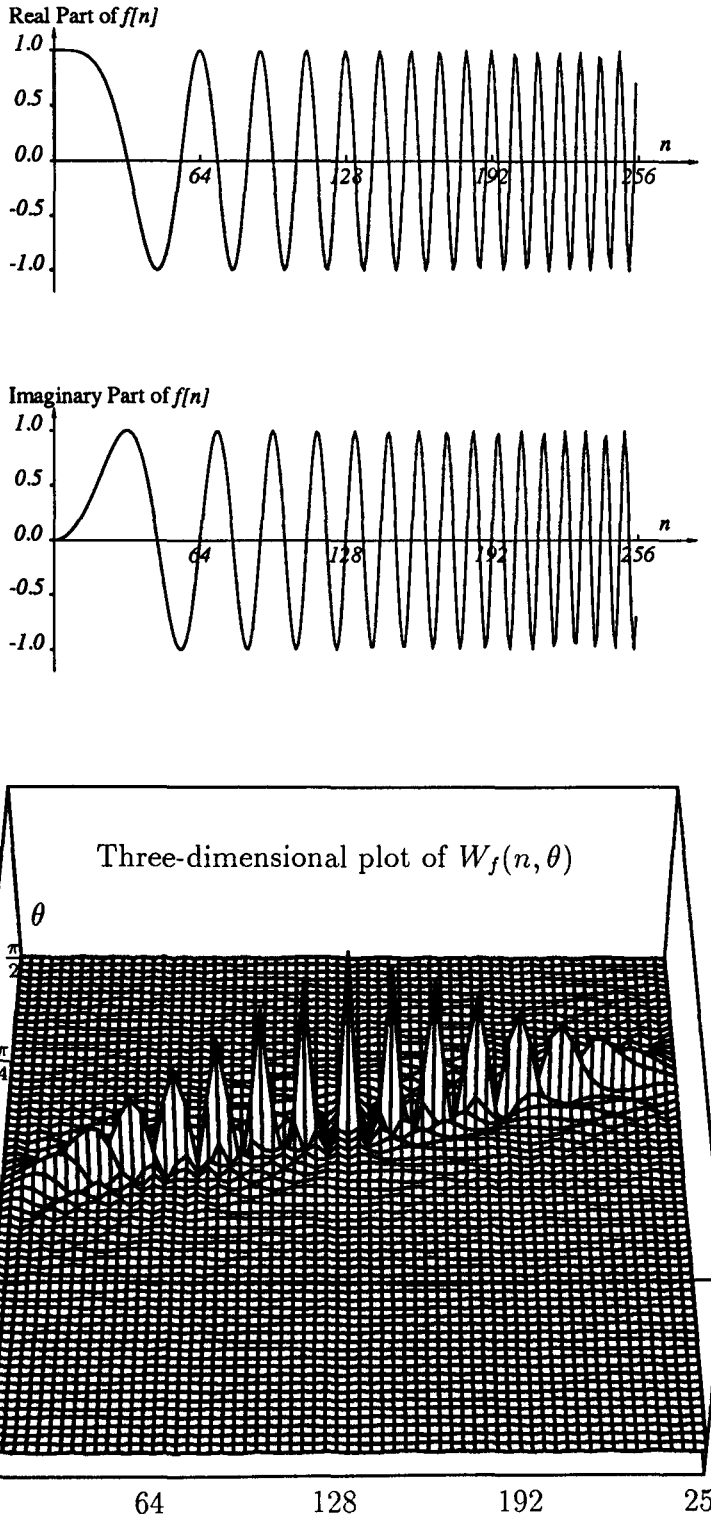

Figure 4.1: The signal f[n] and its DWD

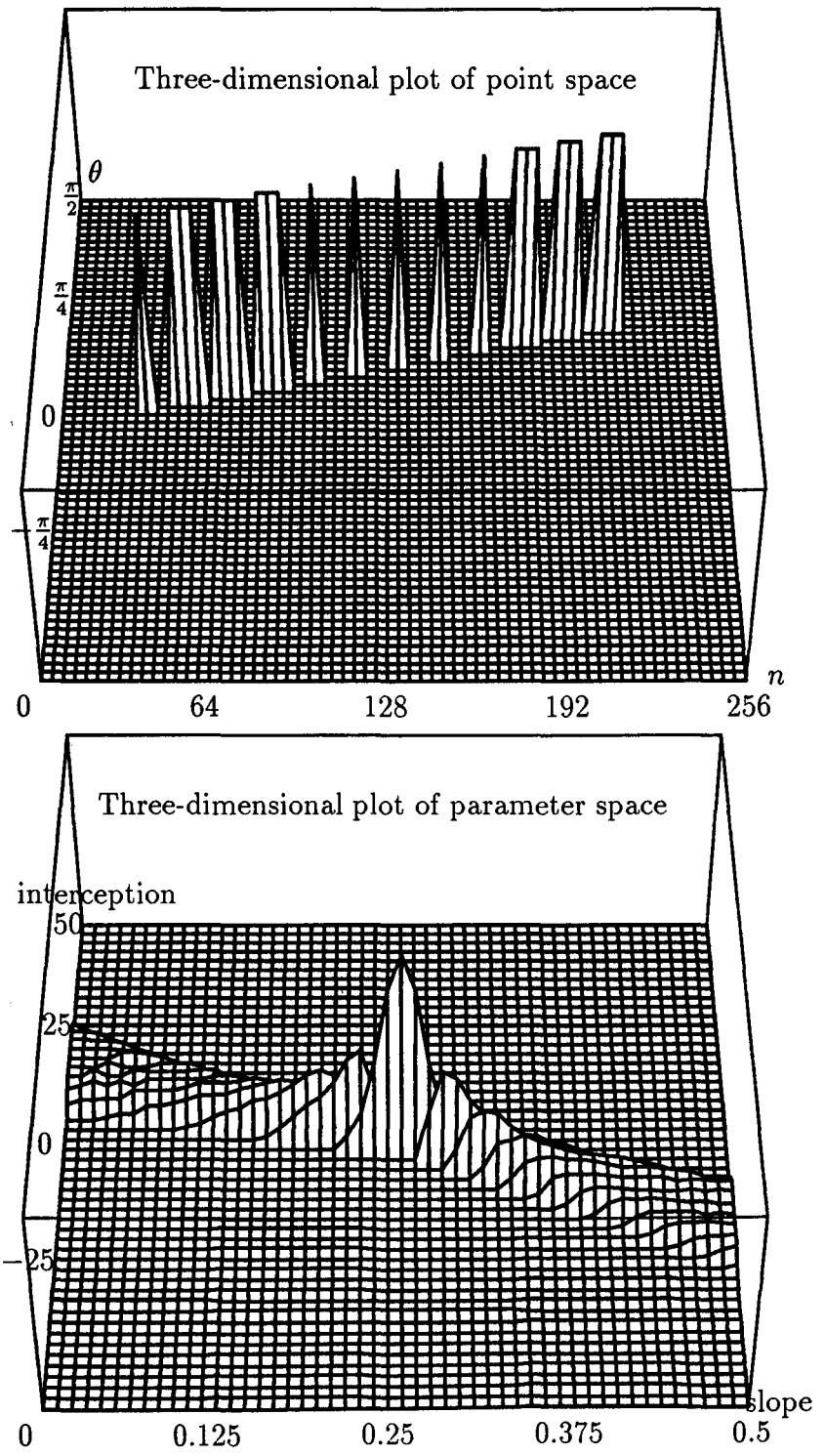

Figure 4.2: The Hough transform. True: $\alpha = \frac{0.250\pi}{N}$; extracted: $\alpha = \frac{0.245\pi}{N}$

4.2.4 Conclusion

Although the Hough transform is effective in extracting information from the DWD for chirp signals, its usage is limited for more complicated signals, such as frequency-modulated (FM) signals, this is because

1. For FM signals, the instantaneous frequency is not linearly increasing any more, in fact, it is changing sinusoidally. Therefore, to describe it, the curve equation should be

$$y = a + b\sin(\omega x + \phi)$$

   which has four parameters rather than two. This results in more complicated parameter spaces which can have computation problems.

2. For FM signals, at a fixed distance or time, the local spectrum is not only concentrating on the instantaneous frequency, but also fluctuates at nearby. This complicates image spaces.

3. Some tricks (such as low pass filters) can be used to mask out those fluctuation so that the HT can still be used. However, this is messy and a bit complicated.

To overcome these problems, a new method is adopted instead. This involves the usage of the local moments in frequency and yields good results for various nonstationary signals. This will be described in the rest of this chapter.

4.3 Local moments in frequency

For a complex-valued signal $f(x) = a(x)e^{j\phi(x)}$ where $a(x)$ and $\phi(x)$ are real-valued, let $W_f(x,\omega)$ be its WD. Let $p_f(x)$ and $\Omega_f(x)$ be the 0th- and 1st-order local moments in frequency of the WD, then

$$p_f(x) = a^2(x) \tag{4.1}$$

$$\Omega_f(x) = \phi'(x) \tag{4.2}$$

which means that the 0th-order moment in frequency is the instaneous power and the 1st-order moment in frequency is the instaneous frequency.

For a chirp signal $f(x) = ae^{j\frac{\alpha}{2}x^2}$,

$$p_f(x) = a^2 \tag{4.3}$$

$$\Omega_f(x) = \alpha x \tag{4.4}$$

and a FM signal $f(x) = Ae^{j(\omega_o x+\phi_o+b\sin(\omega_m x+\phi_m))}$,

$$p_f(x) = A^2 \tag{4.5}$$

$$\Omega_f(x) = \omega_o + b\omega_m \cos(\omega_m x + \phi_m) \tag{4.6}$$

If both $p_f(x)$ and $\Omega_f(x)$ are known, then it is trivial to extract relevant information about both chirp and FM signals (a, α; a, b, ω_o, ω_m). Since $p_f(x)$ and $\Omega_f(x)$ can be easily computed from the WD, so are the parameters. Furthermore, this method can be applied to other types of nonstationary signals as well.

Although it is straightforward to extract parameters for the complex-valued signal, it is the real-valued signal which is often encounted in engineering and for which the moment method can not be applied directly. However, if its corresponding analytical signals are used, then this method can still be used.

4.4 Complex-valued chirp signals

Fig 4.3, $\cdots$, 4.7 show five cases to extract parameters from complex-valued chirp signals.

The tested signals are of form

$$f[n] = \begin{cases} ae^{j\frac{\alpha}{2}n^2} & 0 \leq n < N \\ 0 & \text{otherwise} \end{cases} \tag{4.7}$$

where $N = 256$ and $n = \cdots, -2, -1, 0, 1, 2, \cdots$. Its moments are

$$p_f[n] = a^2 \tag{4.8}$$

$$\Theta_f[n] = \alpha n \mod \pi \tag{4.9}$$

where $0 \leq n < N$.

Note that the extracted values for a are the same as original values within three significant digits. Both extracted and true values for α are listed in Table 4.1

Table 4.1: Extraction results

true value ($\frac{\pi}{N}$)	0.100	0.200	0.300	0.400	0.500
extracted value ($\frac{\pi}{N}$)	0.098	0.195	0.293	0.391	0.488
error (%)	2.0	2.5	2.3	2.3	2.4

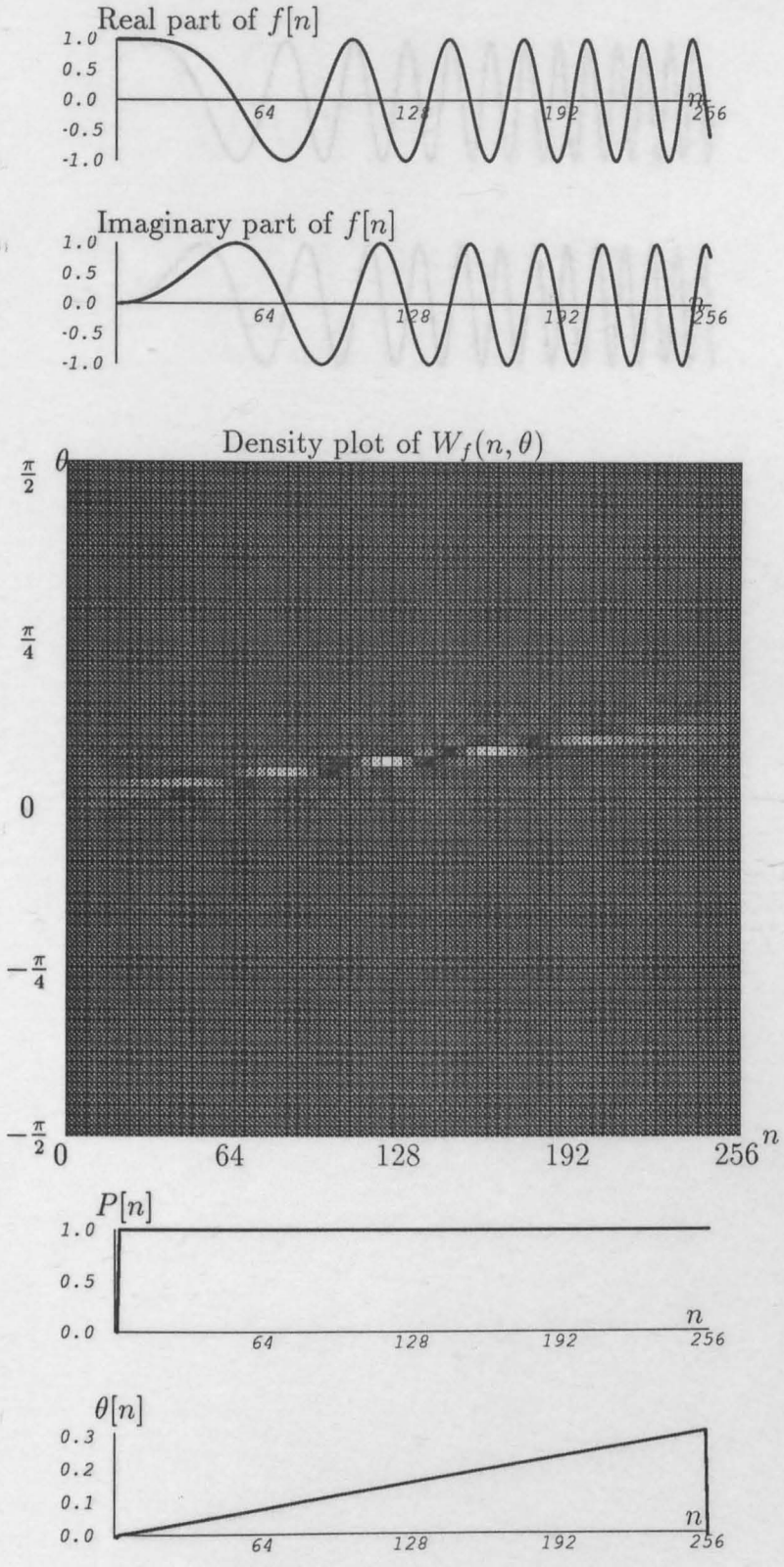

Figure 4.3: true: $a = 1.000$, $\alpha = \frac{0.100\pi}{N}$, Extracted: $a = 1.000$, $\alpha = \frac{0.098\pi}{N}$.

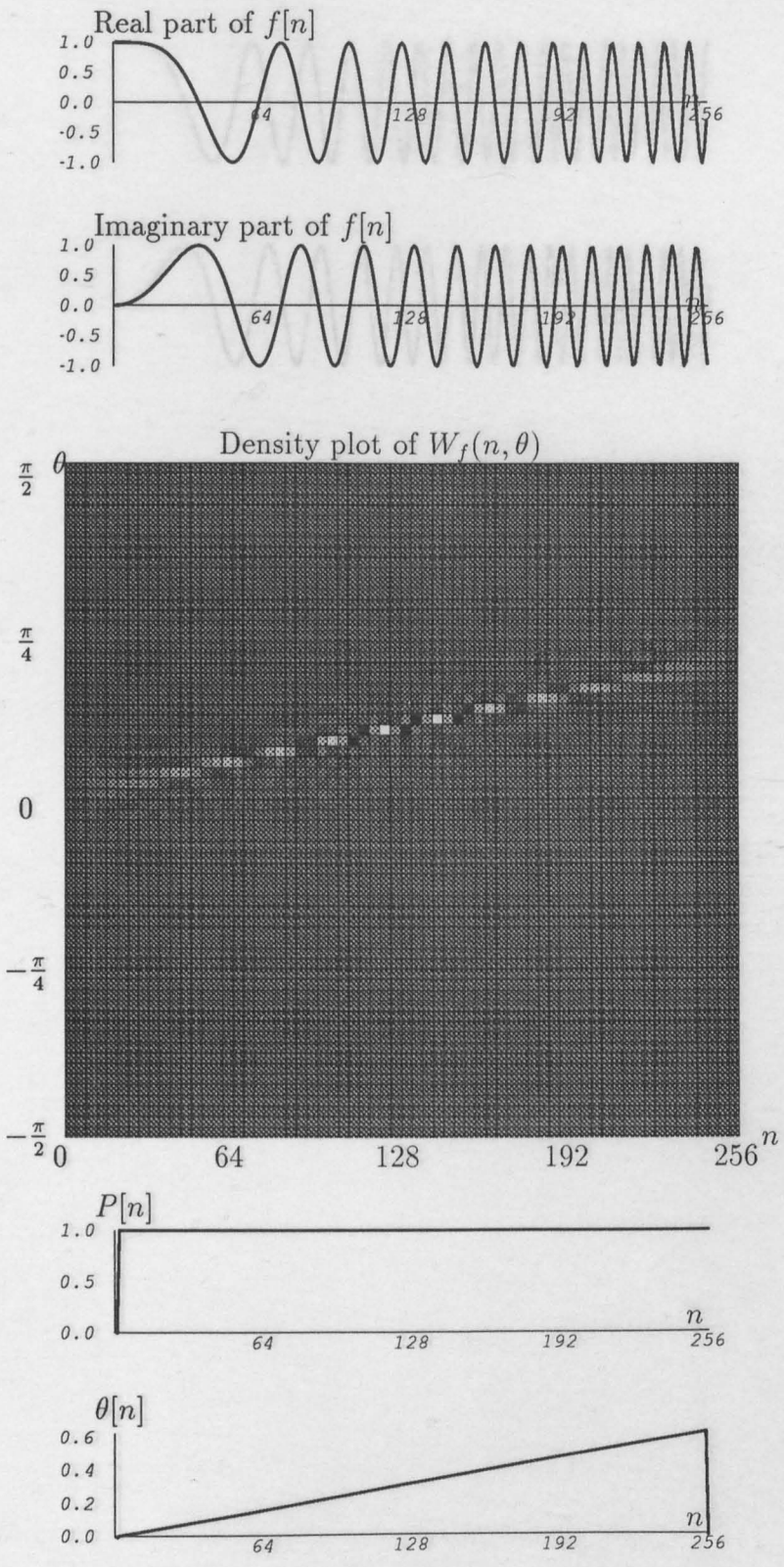

Figure 4.4: True: $a = 1.000$, $\alpha = \frac{0.200\pi}{N}$, Extracted: $a = 1.000$, $\alpha = \frac{0.195\pi}{N}$.

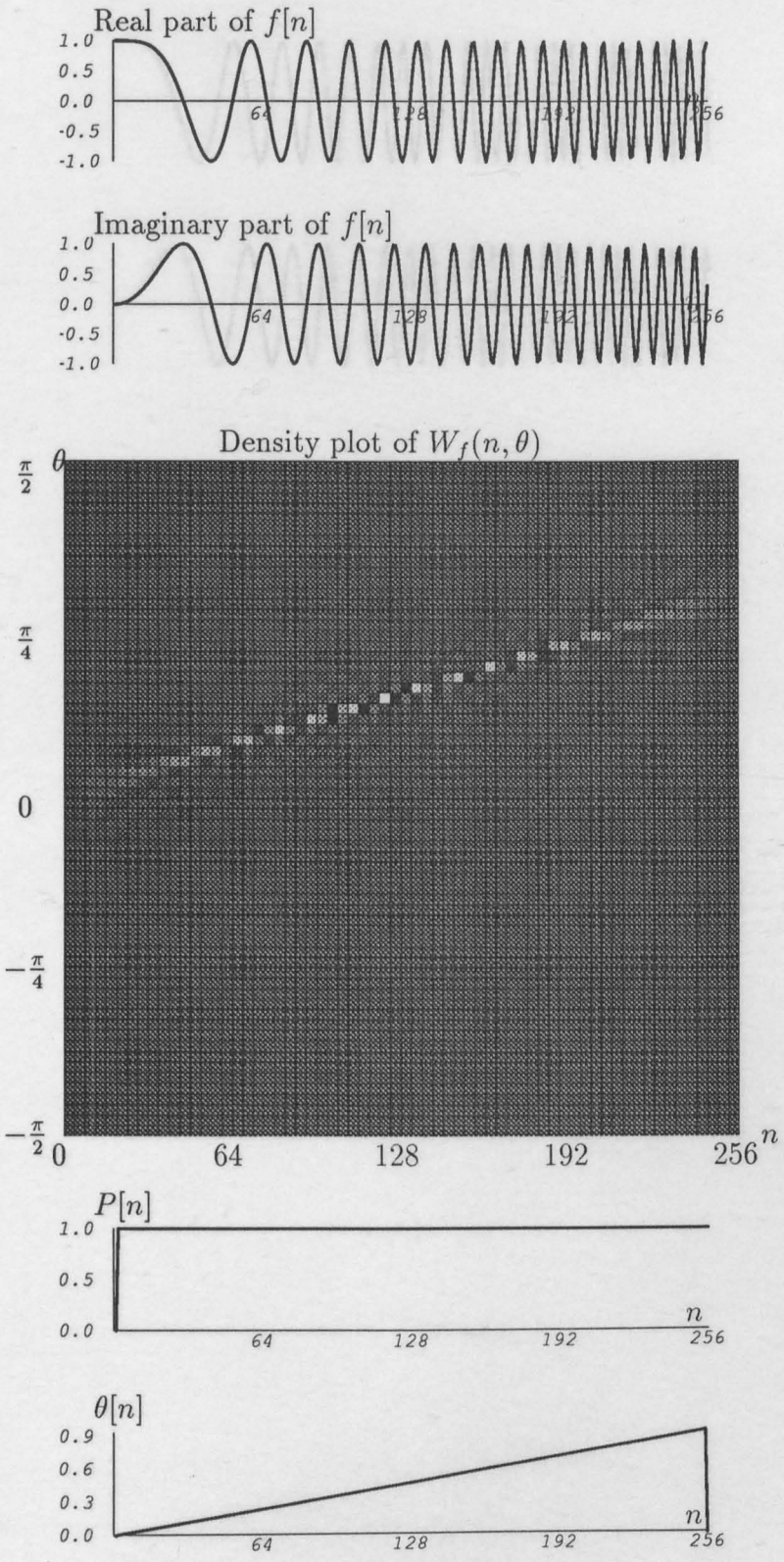

Figure 4.5: True: $a = 1.000$, $\alpha = \frac{0.300\pi}{N}$, Extracted: $a = 1.000$, $\alpha = \frac{0.293\pi}{N}$.

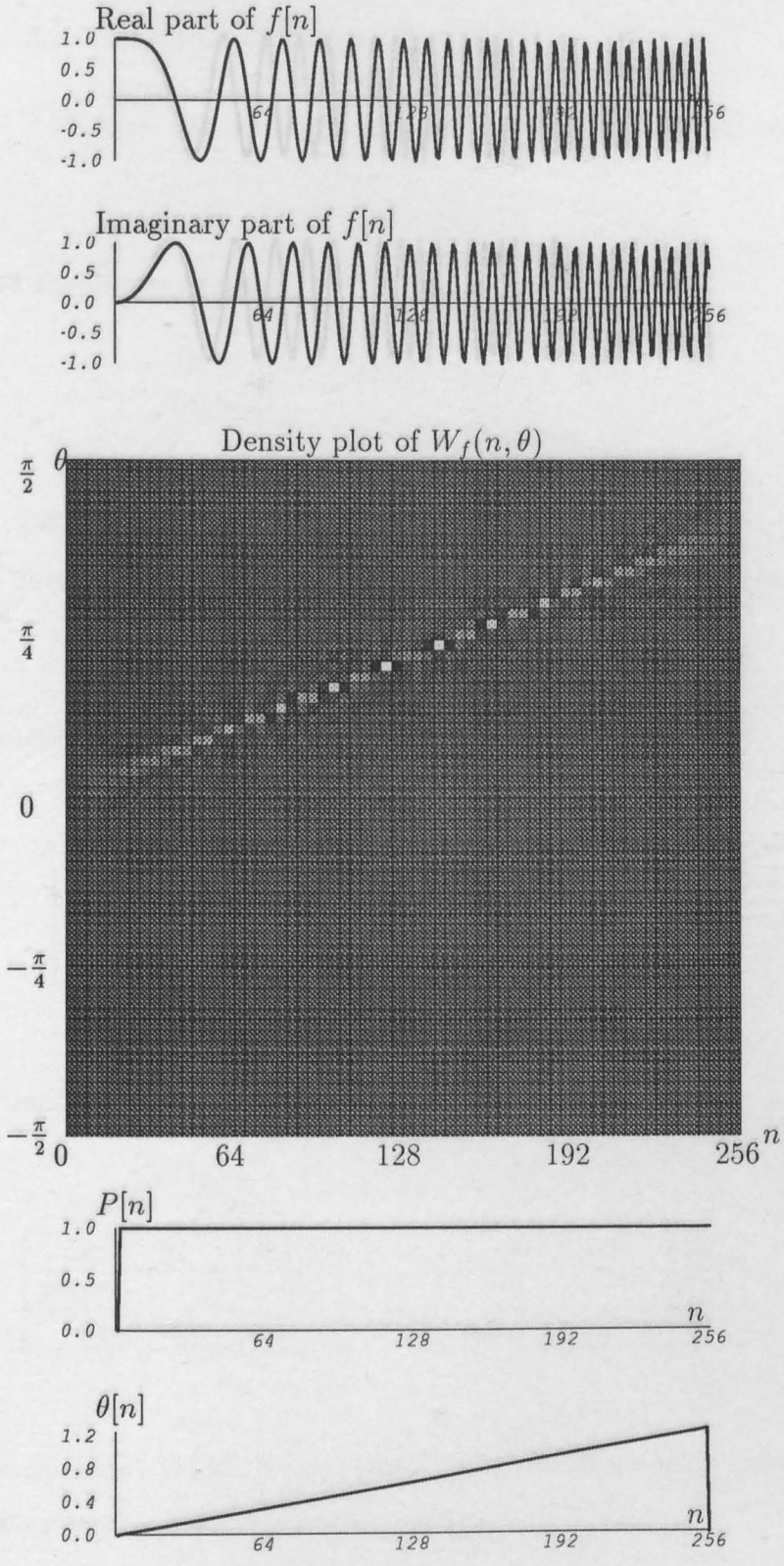

Figure 4.6: True: $a = 1.000$, $\alpha = \frac{0.400\pi}{N}$, Extracted: $a = 1.000$, $\alpha = \frac{0.391\pi}{N}$.

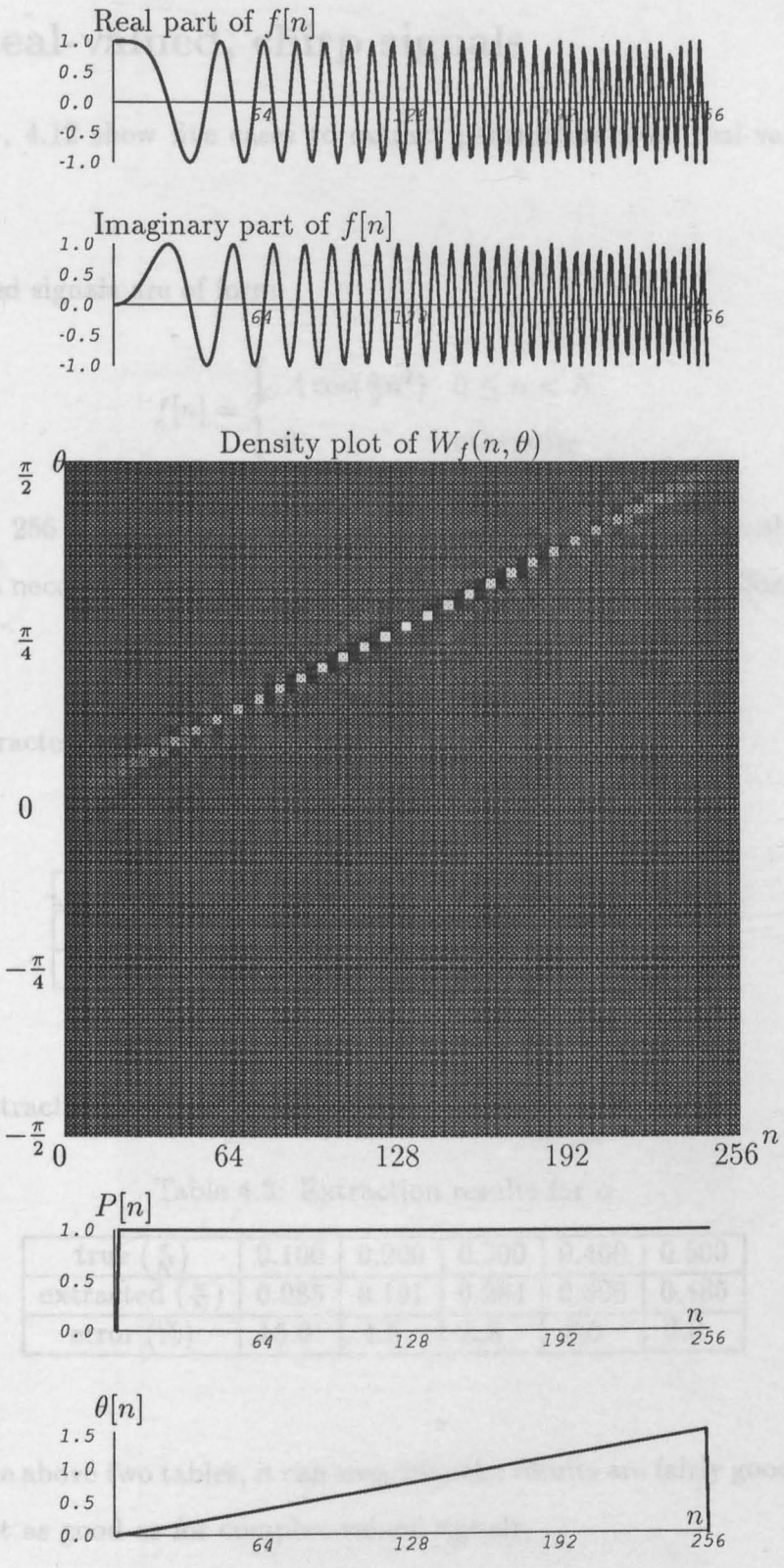

Figure 4.7: True: $a = 1.000$, $\alpha = \frac{0.500\pi}{N}$, Extracted: $a = 1.000$, $\alpha = \frac{0.488\pi}{N}$.

4.5 Real-valued, chirp signals

Fig 4.8, $\cdots$, 4.12 show five cases to extract parameters from real-valued chirp signals.

The tested signals are of form

$$f[n] = \begin{cases} A\cos(\frac{\alpha}{2}n^2) & 0 \le n < N \\ 0 & \text{otherwise} \end{cases} \tag{4.10}$$

where $N = 256$ and $n = \cdots, -2, -1, 0, 1, 2, \cdots$. Because these signals are real-valued, it is necessary to convert them to their analytical signals before applying the WD.

Both extracted and true values for a are listed in Table 4.2

Table 4.2: Extraction results for a

true	1.000	1.000	1.000	1.000	1.000
extracted	1.038	1.024	1.025	1.016	1.014
error (%)	3.8	2.4	2.5	1.6	1.4

Both extracted and true values for α are listed in Table 4.3

Table 4.3: Extraction results for α

true $(\frac{\pi}{N})$	0.100	0.200	0.300	0.400	0.500
extracted $(\frac{\pi}{N})$	0.085	0.191	0.284	0.366	0.485
error (%)	15.0	4.5	5.3	8.5	3.0

From the above two tables, it can seen that the results are fairly good although they are not as good as for complex-valued signals.

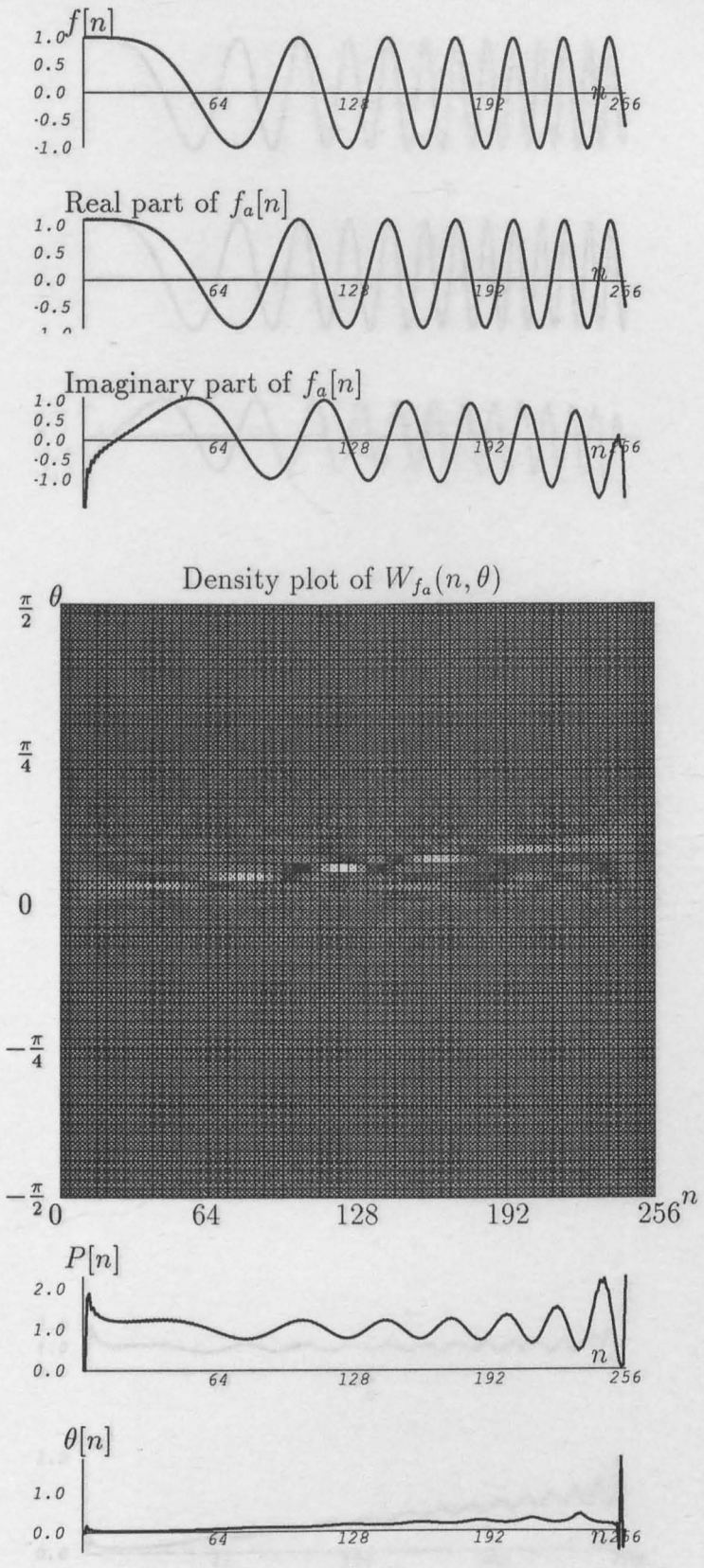

Figure 4.8: True: $a = 1.000$, $\alpha = \frac{0.100\pi}{N}$, Extracted: $a = 1.038$, $\alpha = \frac{0.085\pi}{N}$.

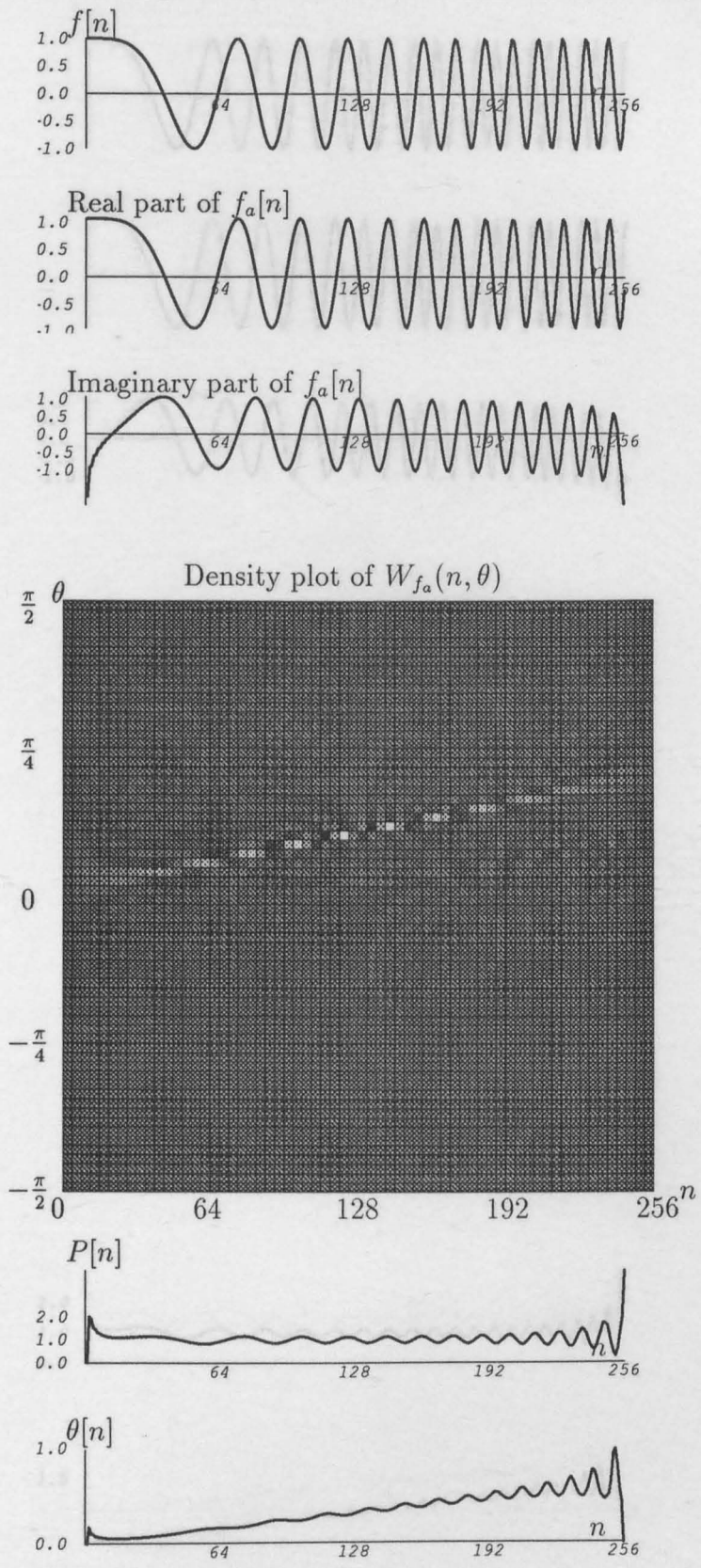

Figure 4.9: True: $a = 1.000$, $\alpha = \frac{0.200\pi}{N}$, Extracted: $a = 1.024$, $\alpha = \frac{0.191\pi}{N}$.

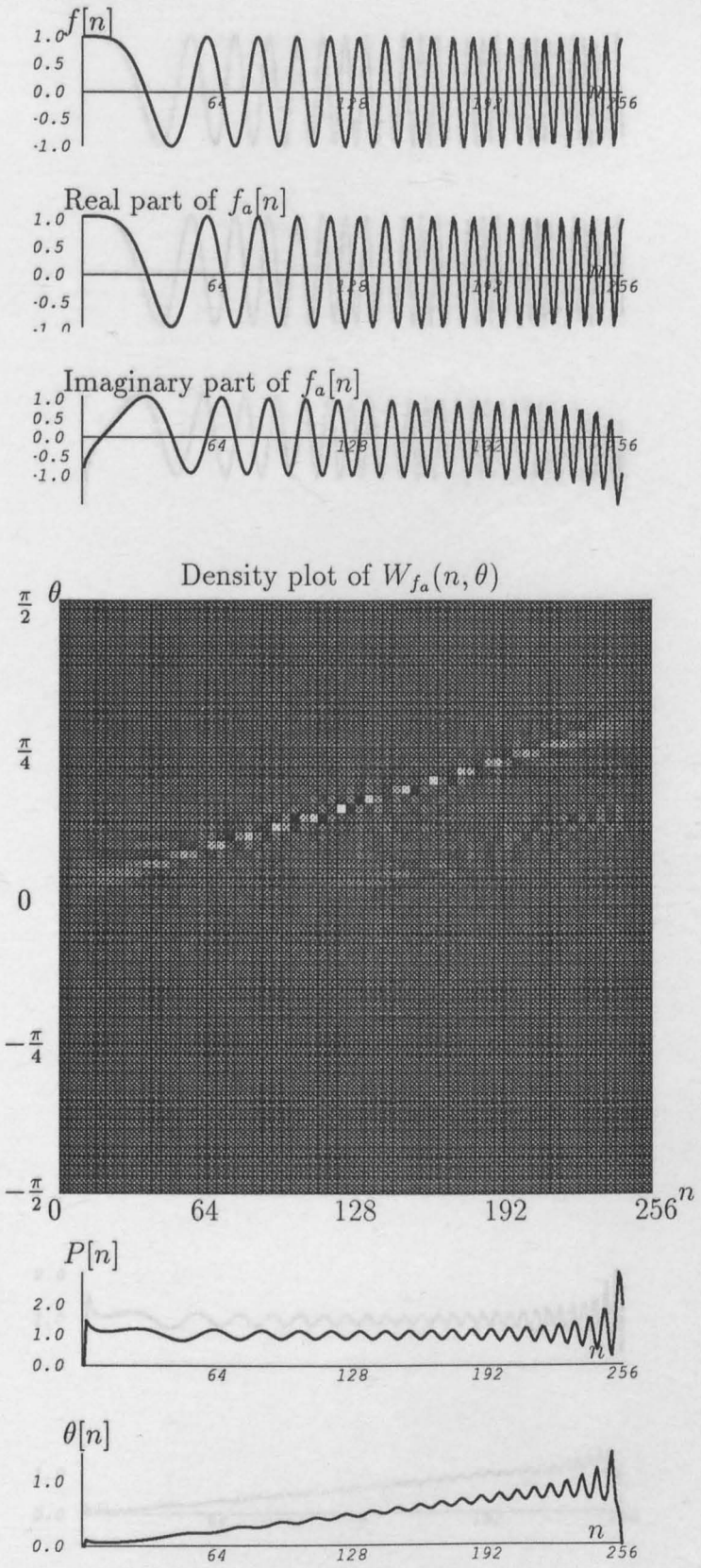

Figure 4.10: True: $a = 1.000$, $\alpha = \frac{0.300\pi}{N}$, Extracted: $a = 1.025$, $\alpha = \frac{0.284\pi}{N}$.

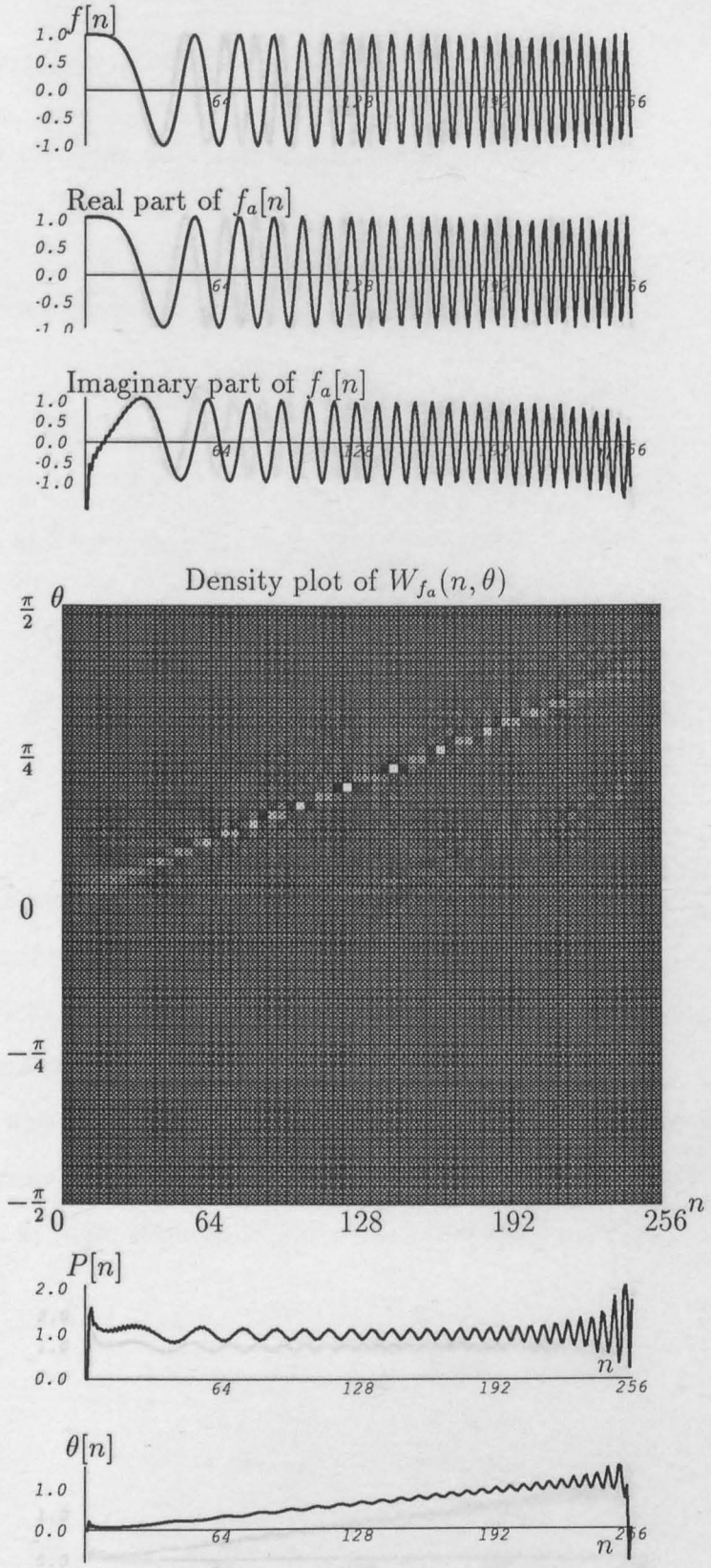

Figure 4.11: True: $a = 1.000$, $\alpha = \frac{0.400\pi}{N}$, Extracted: $a = 1.016$, $\alpha = \frac{0.366\pi}{N}$.

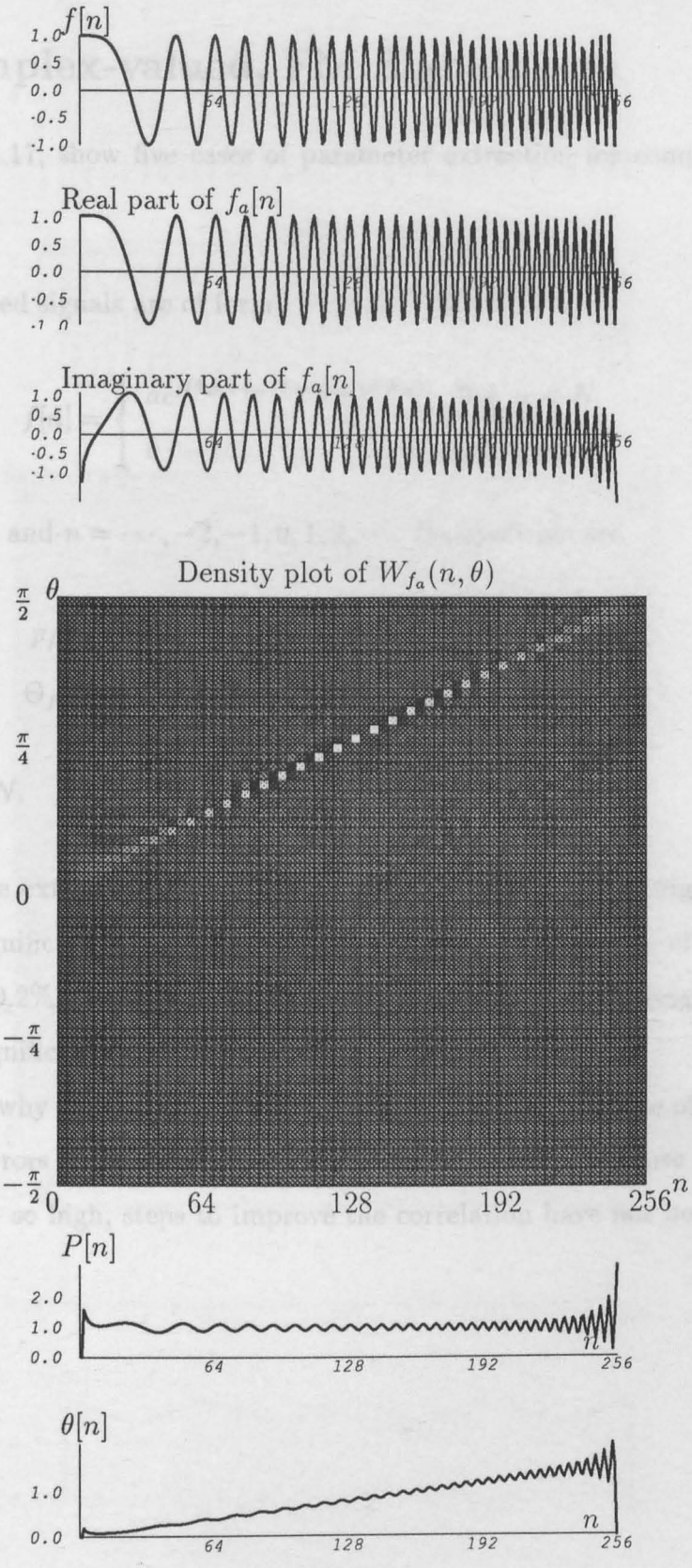

Figure 4.12: True: $a = 1.000$, $\alpha = \frac{0.500\pi}{N}$, Extracted: $a = 1.014$, $\alpha = \frac{0.485\pi}{N}$.

4.6 Complex-valued, FM Signals

Fig 4.13, $\cdots$, 4.17, show five cases of parameter extraction for complex-valued FM signals.

Here the tested signals are of form

$$f[n] = \begin{cases} ae^{j(\theta_o n + \phi_o + b\sin(\theta_m n + \phi_m))} & 0 \le n < N \\ 0 & \text{otherwise} \end{cases} \tag{4.11}$$

where $N = 256$ and $n = \cdots, -2, -1, 0, 1, 2, \cdots$. Its moments are

$$p_f[n] = a^2 \tag{4.12}$$

$$\Theta_f[n] = \theta_o + b\sin\theta_m \cos(\theta_m n + \phi_m) \mod \pi \tag{4.13}$$

when $0 \le n < N$.

Note that the extracted values for k_o and k_m are the same as original values within three significant digits (except for k_m in Fig 4.17). The error of extraction for a is about 0.2%. The extracted values for b are the same as original values within three significant digits.

The reason why the agreement is not exact, is probably because of numerical rounding off errors in the computer evaluation. However, because the agreement is already so high, steps to improve the correlation have not been deemed necessary.

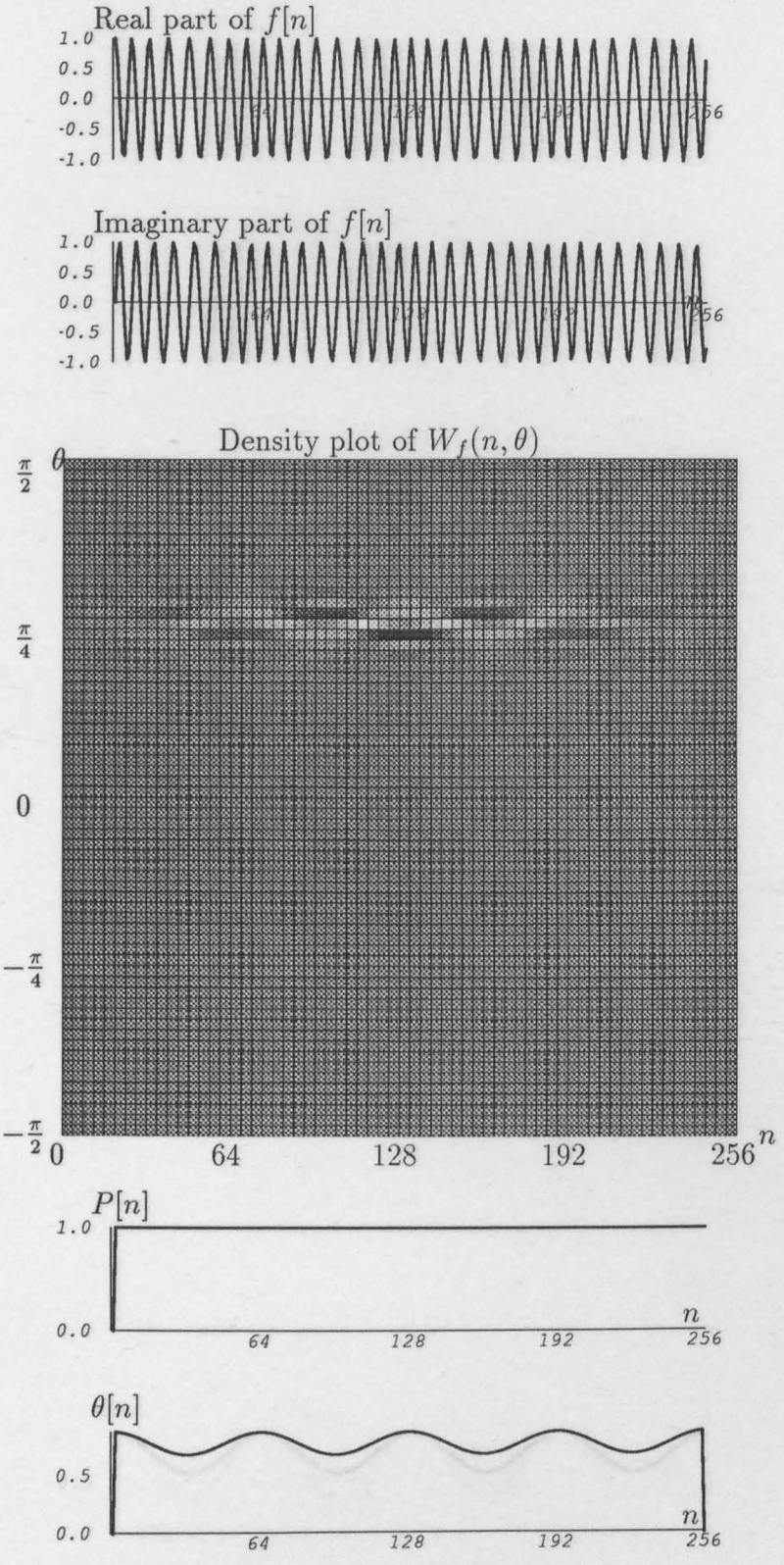

Figure 4.13: True: $a = 1.000$, $\theta_o = 32.0\frac{2\pi}{N}$, $b = 1.000$, $\theta_m = 4.0\frac{2\pi}{N}$, Extracted: $a = 0.998$, $\theta_o = 32.0\frac{2\pi}{N}$, $b = 1.000$, $\theta_m = 4.0\frac{2\pi}{N}$.

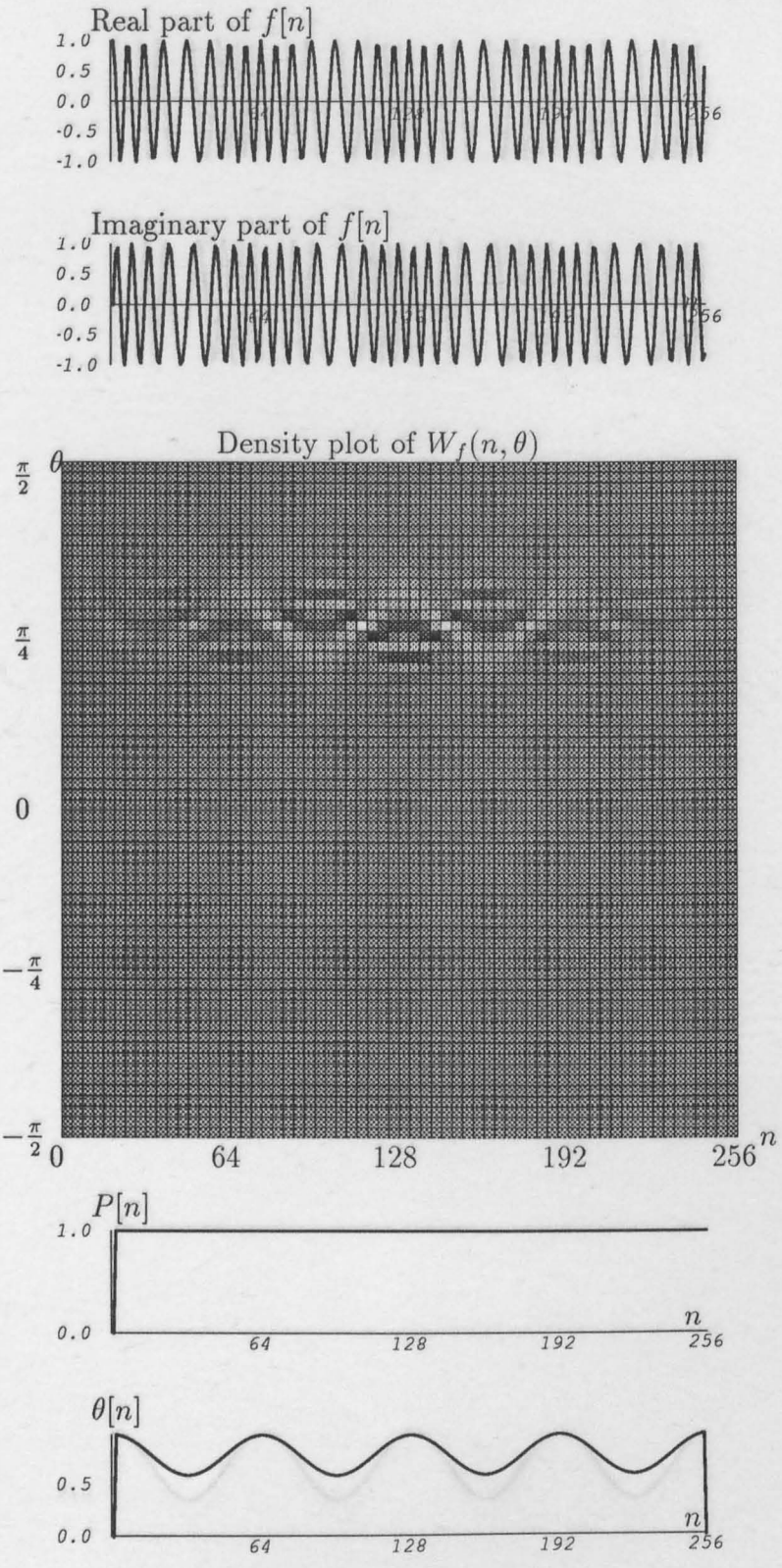

Figure 4.14: True: $a = 1.000$, $\theta_o = 32.0\frac{2\pi}{N}$, $b = 2.000$, $\theta_m = 4.0\frac{2\pi}{N}$, Extracted: $a = 0.998$, $\theta_o = 32.0\frac{2\pi}{N}$, $b = 2.000$, $\theta_m = 4.0\frac{2\pi}{N}$.

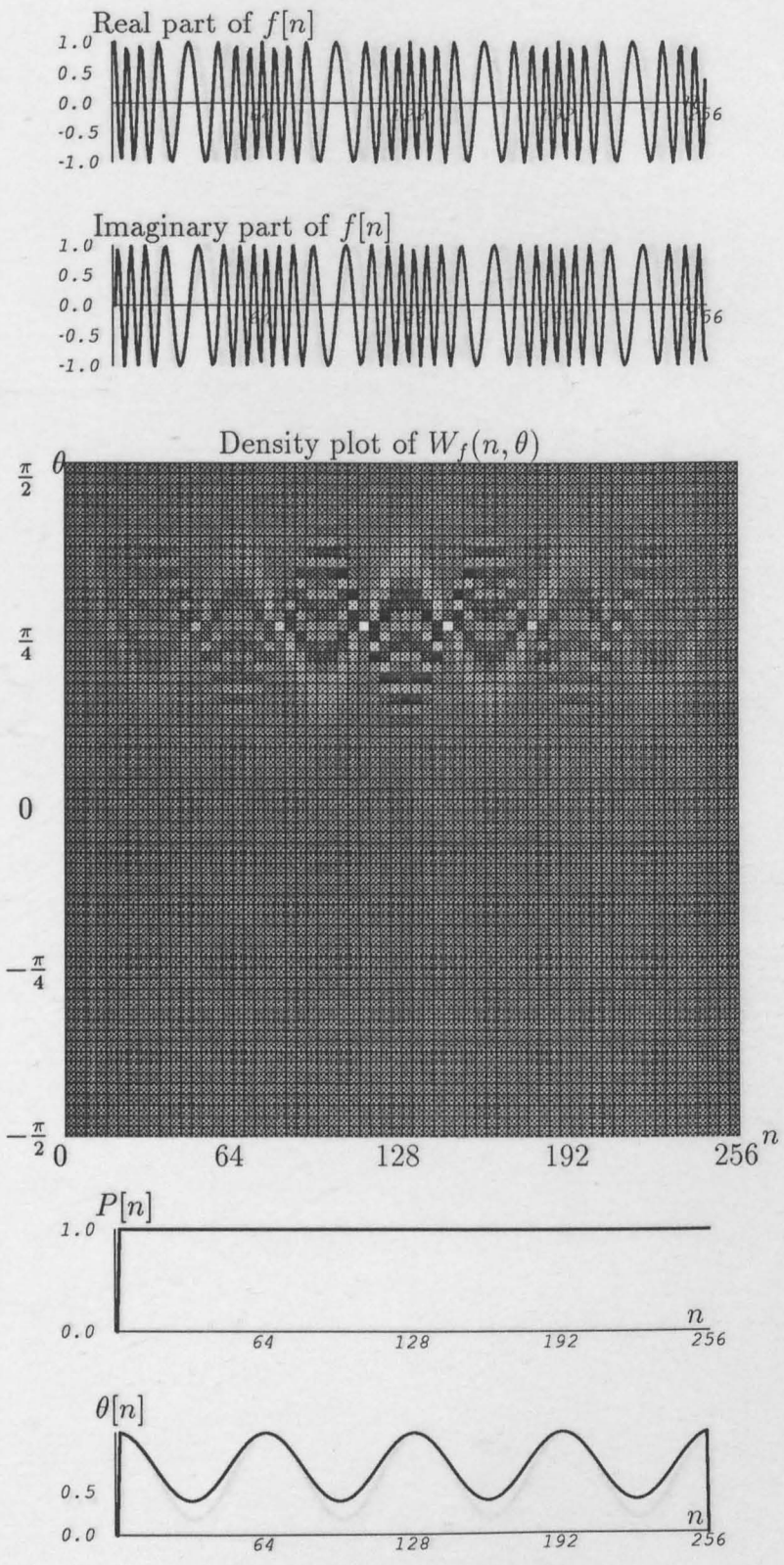

Figure 4.15: True: $a = 1.000$, $\theta_o = 32.0\frac{2\pi}{N}$, $b = 4.000$, $\theta_m = 4.0\frac{2\pi}{N}$, Extracted: $a = 0.998$, $\theta_o = 32.0\frac{2\pi}{N}$, $b = 4.000$, $\theta_m = 4.0\frac{2\pi}{N}$.

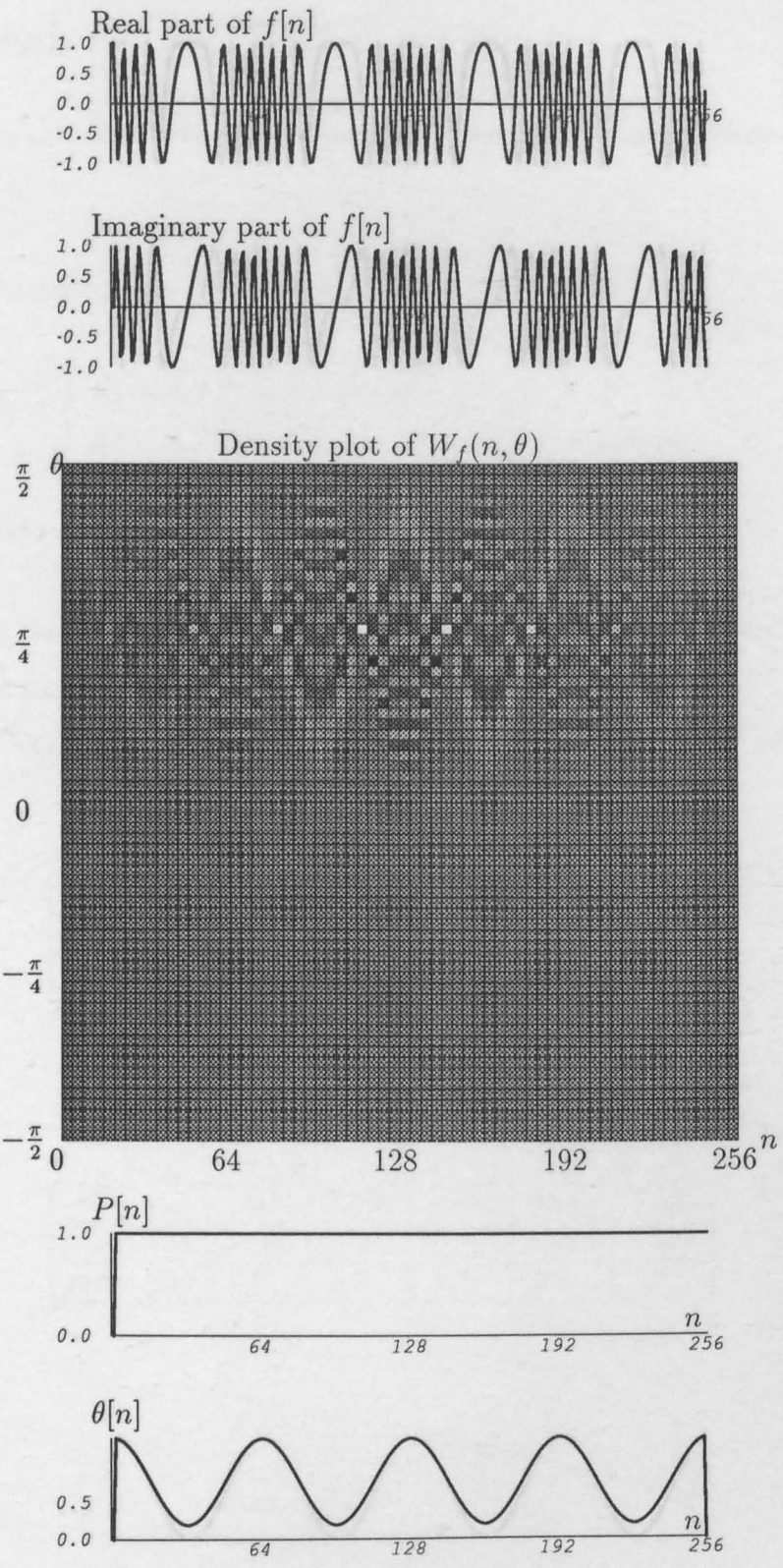

Figure 4.16: True: $a = 1.000$, $\theta_o = 32.0\frac{2\pi}{N}$, $b = 6.000$, $\theta_m = 4.0\frac{2\pi}{N}$, Extracted: $a = 0.998$, $\theta_o = 32.0\frac{2\pi}{N}$, $b = 6.000$, $\theta_m = 4.0\frac{2\pi}{N}$.

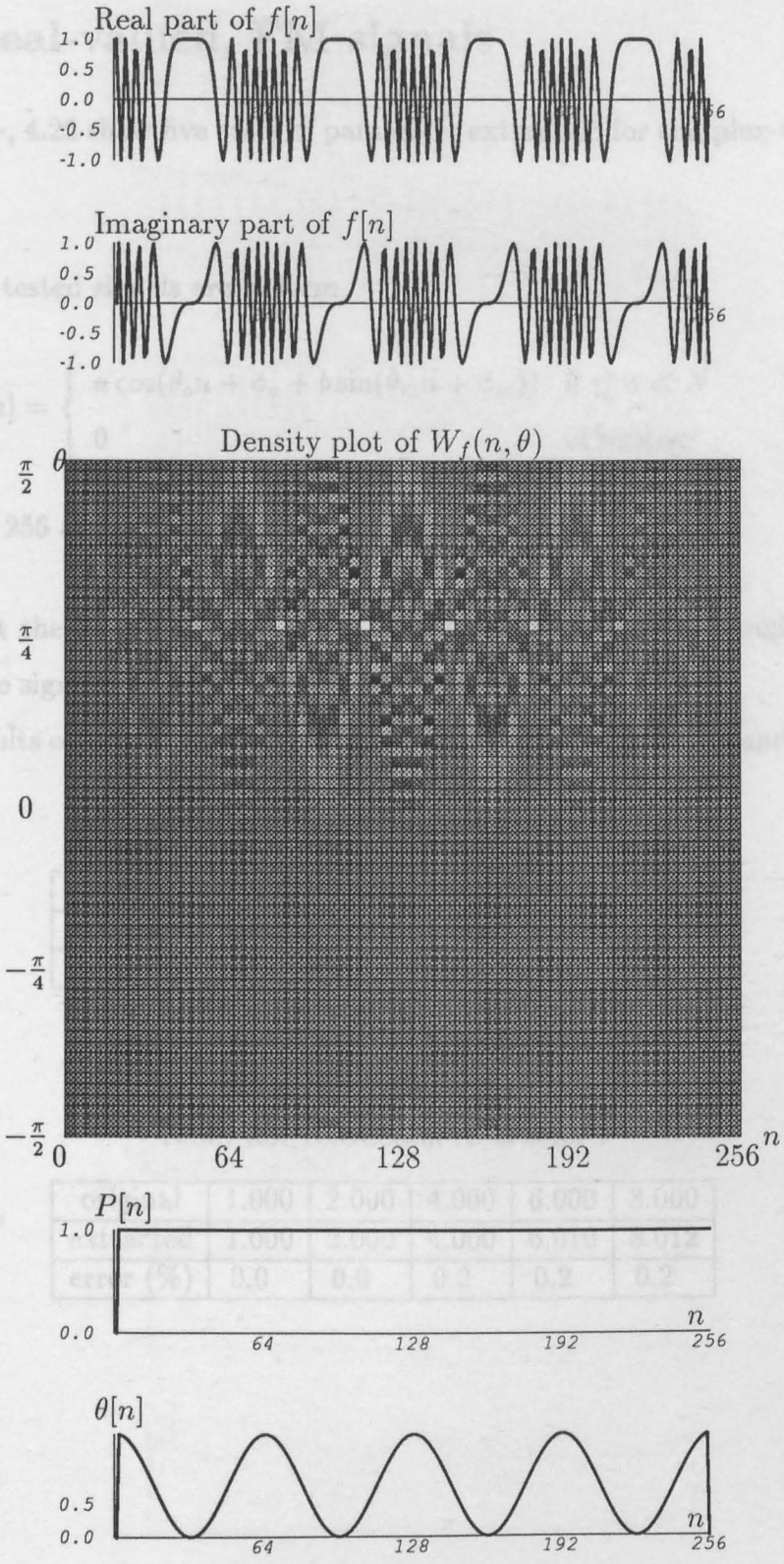

Figure 4.17: True: $a = 1.000$, $\theta_o = 32.0\frac{2\pi}{N}$, $b = 8.000$, $\theta_m = 4.0\frac{2\pi}{N}$, Extracted: $a = 0.998$, $\theta_o = 31.0\frac{2\pi}{N}$, $b = 8.000$, $\theta_m = 4.0\frac{2\pi}{N}$.

4.7 Real-valued, FM signals

Fig 4.18, $\cdots$, 4.22 show five cases of parameter extraction for complex-valued FM signals.

Here the tested signals are of form

$$f[n] = \begin{cases} a\cos(\theta_o n + \phi_o + b\sin(\theta_m n + \phi_m)) & 0 \le n < N \\ 0 & \text{otherwise} \end{cases} \tag{4.14}$$

where $N = 256$ and $n = \cdots, -2, -1, 0, 1, 2, \cdots$.

Note that the extracted values for k_o and k_m are the same as original values within three significant digits.

The results of extraction for both a and b are listed in Table 4.4 and Table 4.5

Table 4.4: Extraction results for a

original	1.000	1.000	1.000	1.000	1.000
extracted	0.998	0.998	0.998	1.008	1.128
error (%)	0.2	0.2	0.2	0.8	12.8

Table 4.5: Extraction results for b

original	1.000	2.000	4.000	6.000	8.000
extracted	1.000	2.000	4.000	6.010	8.012
error (%)	0.0	0.0	0.0	0.2	0.2

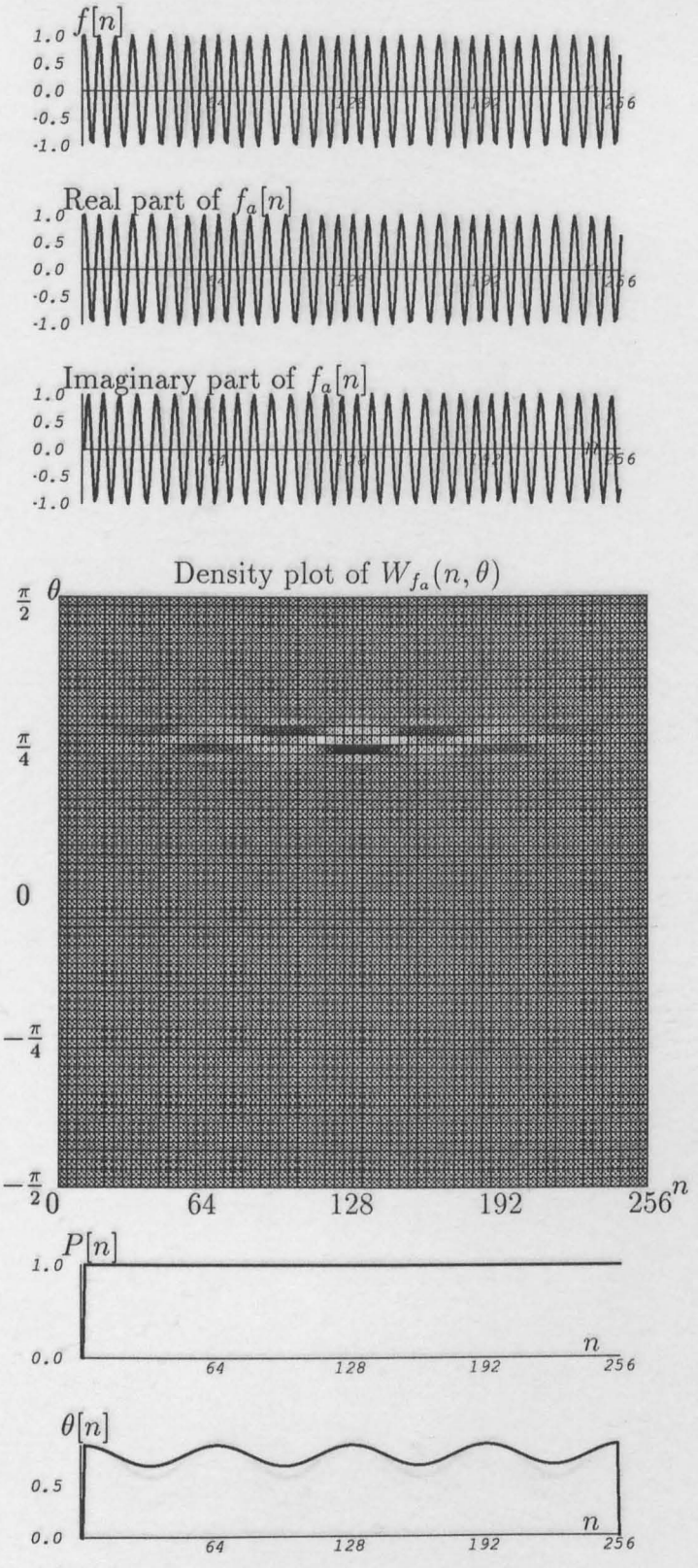

Figure 4.18: True: $a = 1.000$, $\theta_o = 32.0\frac{2\pi}{N}$, $b = 1.000$, $\theta_m = 4.0\frac{2\pi}{N}$, Extracted: $a = 0.998$, $\theta_o = 32.0\frac{2\pi}{N}$, $b = 1.000$, $\theta_m = 4.0\frac{2\pi}{N}$.

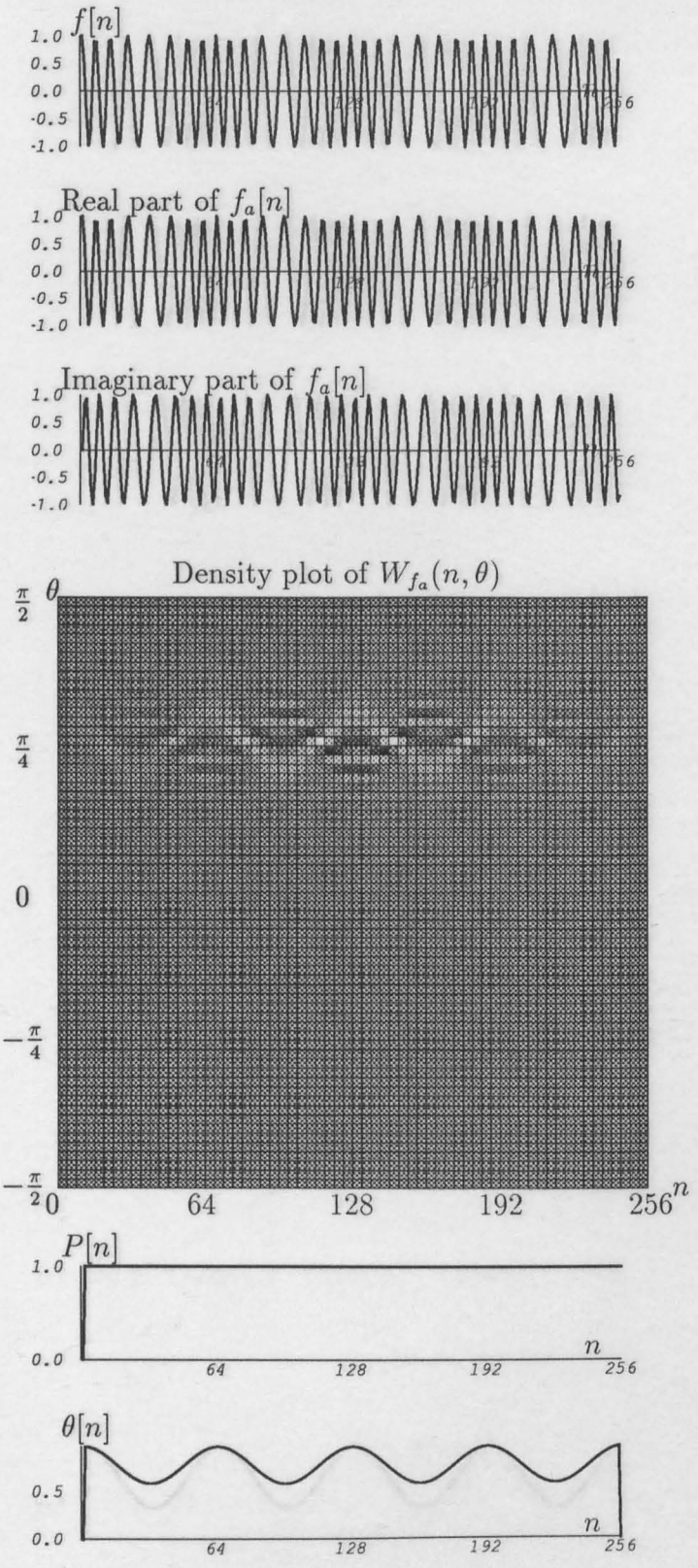

Figure 4.19: True: $a = 1.000$, $\theta_o = 32.0\frac{2\pi}{N}$, $b = 2.000$, $\theta_m = 4.0\frac{2\pi}{N}$, Extracted: $a = 0.998$, $\theta_o = 32.0\frac{2\pi}{N}$, $b = 2.000$, $\theta_m = 4.0\frac{2\pi}{N}$.

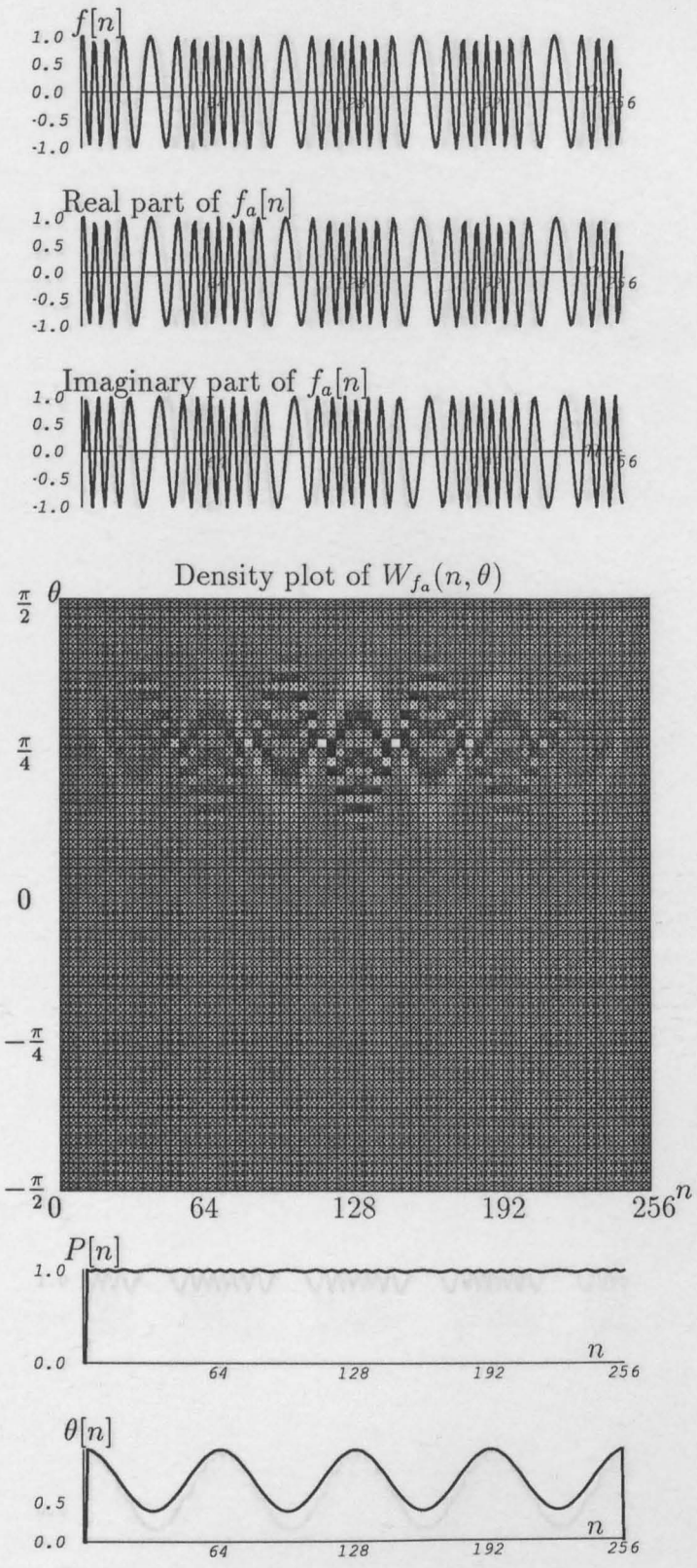

Figure 4.20: True: $a = 1.000$, $\theta_o = 32.0\frac{2\pi}{N}$, $b = 4.000$, $\theta_m = 4.0\frac{2\pi}{N}$, Extracted: $a = 0.998$, $\theta_o = 32.0\frac{2\pi}{N}$, $b = 4.000$, $\theta_m = 4.0\frac{2\pi}{N}$.

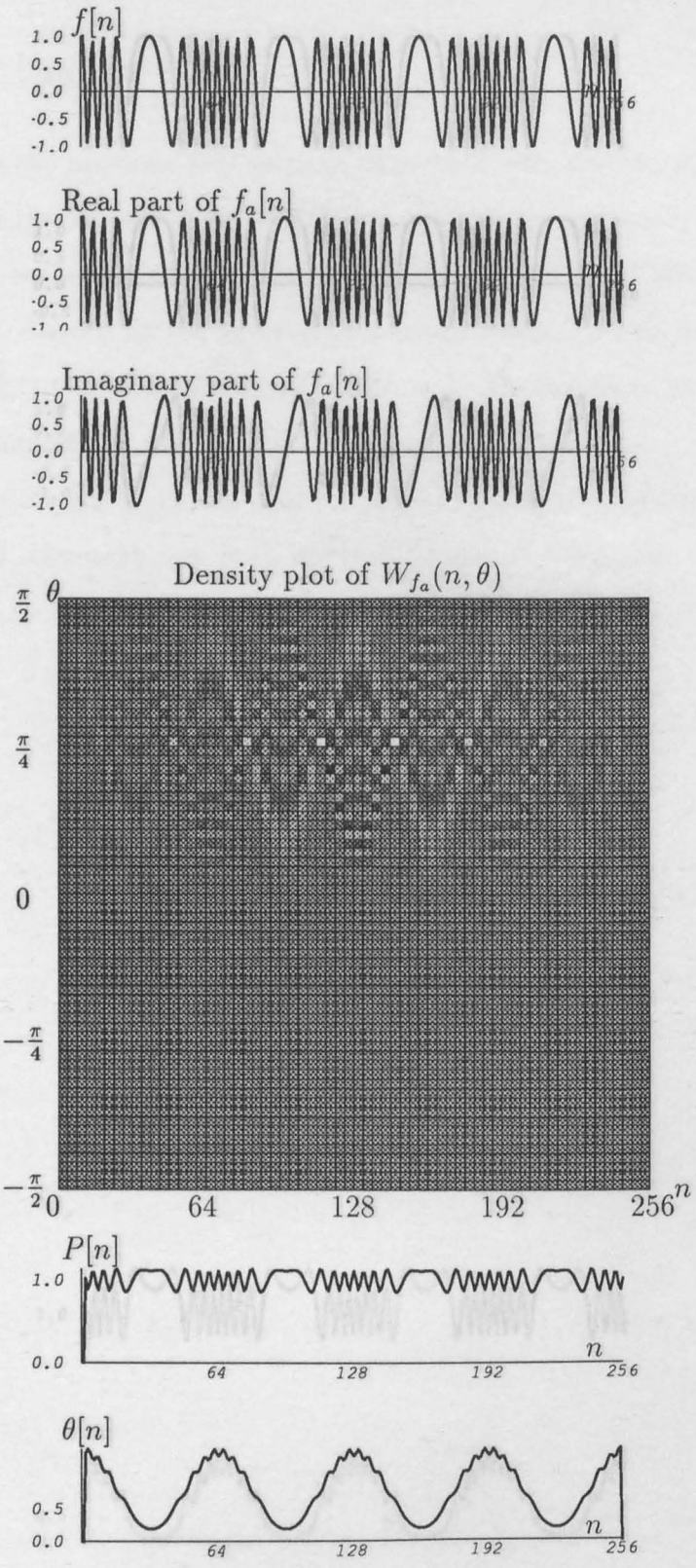

Figure 4.21: True: $a = 1.000$, $\theta_o = 32.0\frac{2\pi}{N}$, $b = 6.000$, $\theta_m = 4.0\frac{2\pi}{N}$, Extracted: $a = 1.008$, $\theta_o = 32.0\frac{2\pi}{N}$, $b = 6.010$, $\theta_m = 4.0\frac{2\pi}{N}$.

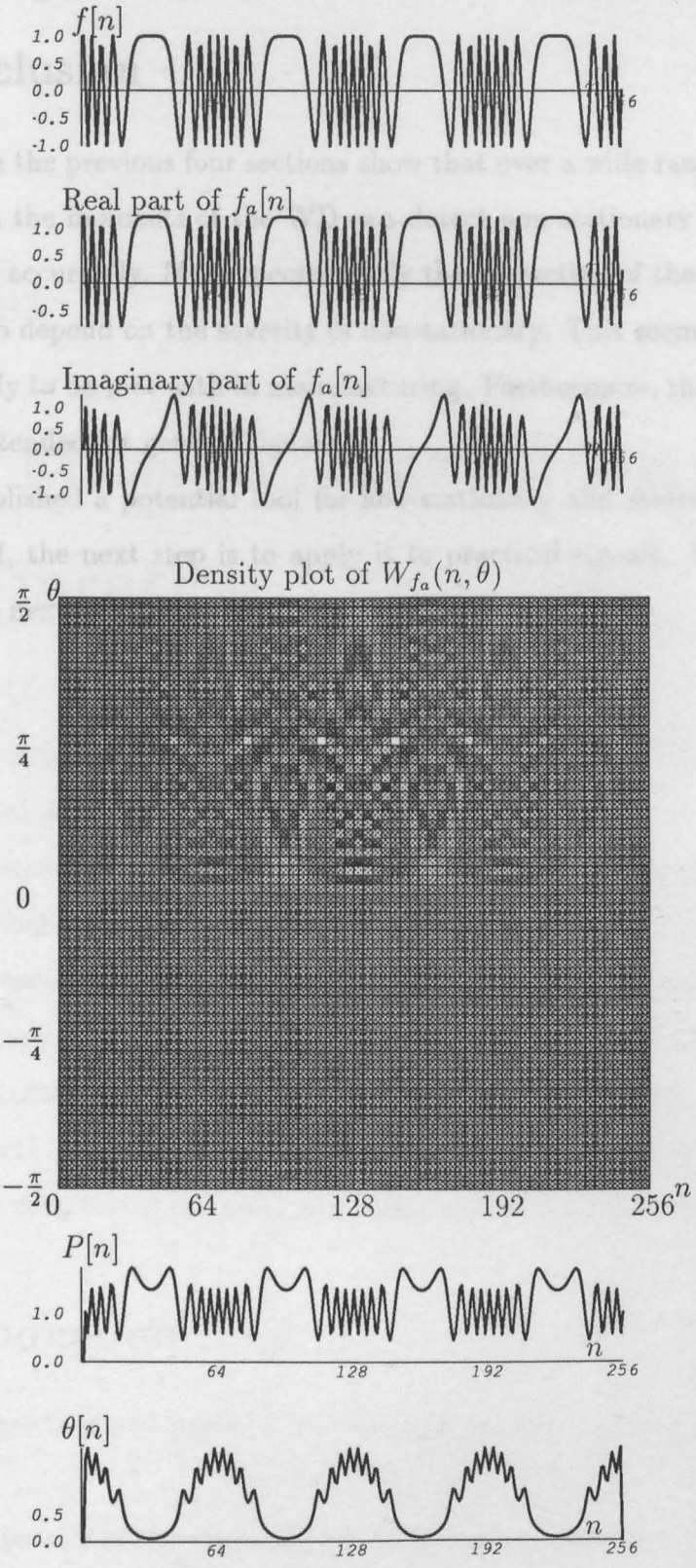

Figure 4.22: True: $a = 1.000$, $\theta_o = 32.0\frac{2\pi}{N}$, $b = 8.000$, $\theta_m = 4.0\frac{2\pi}{N}$, Extracted: $a = 1.128$, $\theta_o = 32.0\frac{2\pi}{N}$, $b = 8.012$, $\theta_m = 4.0\frac{2\pi}{N}$.

4.8 Conclusion

The results from the previous four sections show that over a wide range the algorithms based on the moments of the WD can detect non-stationary parameters successfully and accurately. More spectacularly the extraction of the parameters does not seem to depend on the severity of nonstationary. This seems to be true for all cases likely to be met with in manufacturing. Furthermore, this technique can be easily extended for general signals.

Having established a potential tool for non-stationary and stationary evaluation of a signal, the next step is to apply it to practical signals. This will be described in the next two chapters.

Chapter 5

Direct Measurement of Cutting Tool Vibration

In the previous chapter, the WD and its moments were successfully applied to simulated signals. However, this thesis is about the application of the WD to machine tool monitoring, in particular, to use the WD to extract vibration information from surface texture of a machined workpiece and use it for machine tool monitoring and control. In order to demonstrate the feasibility of this technique, it is necessary to review certain aspects of cutting tool vibration characteristics and more importantly how to measure it. This is done in this chapter. In the next chapter this practical vibration data will be used to validate the WD approach for machine tool monitoring (Chapter 6) (Zheng and Whitehouse 1992).

5.1 Introduction

This chapter consists of two parts: a discussion of cutting tool vibration and its measurement.

Some fundamentals of the vibration need to be examined, for it is the vibration that is going to be employed to monitor the machine-tool. Although much work has gone into understanding the mechanics of vibration, due to the very complicated dynamic characteristics of the machine tool, cutting tool and work-

piece, it is still not fully explained. Therefore, this chapter attempts to clarify some of the relevant fundamentals of cutting tool vibration, In Sections 5.2 to 5.6, an analysis of vibration is presented, following Tobias (1965) and Sweeney (1971).

The remainder of this chapter describes the instrument for cutting tool vibration measurement, developed by the author. To measure vibration, a piezoelectric accelerometer is usually employed, but it is not suitable for cutting tool vibration because 1) the dynamic range is not large enough for the strong vibration of a cutting tool and 2) it is difficult to mount an accelerometer on a cutting tool. Therefore, an instrument has had to be built especially for vibration measurement. Its construction and performance will be described in detail in the second part of this chapter.

5.2 Elementary vibratory systems

5.2.1 The equation of systems with one-degree of freedom

The simplest vibratory system is an idealised one-degree (1-D) of freedom, vibratory system as shown in Figure 5.1. It consists of a spring c, a mass m and a dashpot ρ (Tobias 1965, p 5).

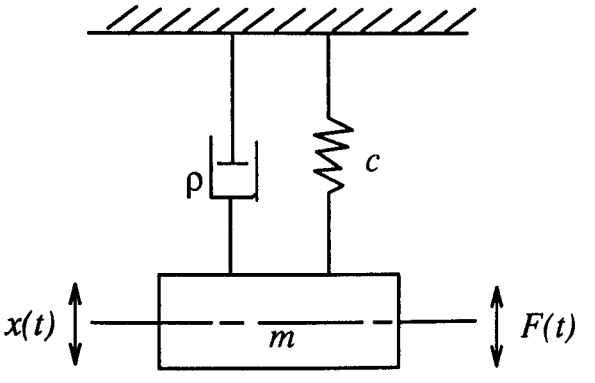

Figure 5.1: One degree of freedom system.

If the mass m is displaced from its position of rest, it will be acted upon by the following forces: the weight of mass m, the restoring force of the spring c, the

damping force of the dashpot ρ and the external exciting force $F(t)$.

From Newton's second law of motion,

$$m\ddot{x} = F(t) - cx - \rho\dot{x} \tag{5.1}$$

where x is the displacement from the rest position (therefore the weight of the mass is balanced by the initial movement of the spring).

Rewriting,

$$m\ddot{x} + \rho\dot{x} + cx = F(t) \tag{5.2}$$

which is the basic equation for a system with 1-D of freedom. Let

$$\delta = \frac{\rho}{2m}$$
$$\omega_0^2 = \frac{c}{m}$$
$$\mathbf{D} = \frac{\delta}{\omega_0}$$

then Eqn 5.2 can be written as

$$\ddot{x} + 2\delta\dot{x} + \omega_0^2 x = \frac{F(t)}{m} \tag{5.3}$$

or

$$\ddot{x} + 2\mathbf{D}\omega_0\dot{x} + \omega_0^2 x = \frac{F(t)}{m} \tag{5.4}$$

- When $F(t) = 0$, it is called *free vibration.*
- When $F(t) \neq 0$, it is called *forced vibration.*

5.2.2 Stability

In order to operate properly, a machine-tool has to be stable. There are two kinds of stability: static and dynamic.

Static stability

A system is said to be *statically stable* only if it will return to its original equilibrium after the cessation of a static disturbance. This means that there must exist a force (so called *restoring force*) which tends to restore the system to its equilibrium condition. For a 1-D vibratory system ,

- if $c > 0$, it is statically stable;
- otherwise it is not.

It is an intrinsic requirement that the machine-tool should be statically stable.

Dynamic stability

After an impact or other disturbances, a system in a steady-state condition of uniform motion may vibrate. If the vibration dies away and the uniform motion is thus restored, then it is said to be *dynamically stable.* However, it can also happen that the vibration will increase continuously. This type of system is termed as dynamically unstable. For a 1-D vibratory system with $c > 0$,

- if $\delta > 0$, it is dynamically stable;
- otherwise, it is not.

For machine-tool vibrations, some are dynamically stable, others are not, such as the case of self-induced vibration.

5.3 Free-vibrations

For free-vibrations, Eqn 5.4 turns out to be

$$\ddot{x} + 2\mathrm{D}\omega_0\dot{x} + \omega_0^2 x = 0 \tag{5.5}$$

with the initial condition as $x(0) = x_0$ and $\dot{x}(0) = \dot{x}_0$.

5.3.1 Weak damping

For weak damping, with the damping ratio **D** in the interval $(-1, 1)$, the solution for Eqn 5.5 is

$$x = e^{-\delta t}(C_1 \cos \omega_d t + C_2 \sin \omega_d t) \tag{5.6}$$

where $\omega_d = \sqrt{\omega_0^2 - \delta^2}$, $C_1 = x_0$ and $C_2 = \frac{\dot{x}_0 + \delta \dot{x}_0}{\omega_d}$

5.3.2 Critical damping

When $|\mathbf{D}| = 1$,

$$x = e^{-\delta t}(C_1 + C_2 t) \tag{5.7}$$

where C_1 and C_2 are determined by the initial conditions of displacement and velocity.

5.3.3 Heavy damping

When $|\mathbf{D}| > 1$,

$$x = C_1 e^{(-\delta + \sqrt{\delta^2 - \omega_0^2})t} + C_2 e^{(-\delta - \sqrt{\delta^2 - \omega_0^2})t} \tag{5.8}$$

where C_1 and C_2 are determined by the initial conditions of displacement and velocity.

For a machine tool, free-vibrations can be induced by a shock or similar means.

5.4 Forced-vibrations

Because the disturbing force can be resolved into a finite or infinite number of components varying harmonically with time, it is therefore sufficient to solve

$$\ddot{x} + 2\delta \dot{x} + \omega_0^2 x = \frac{F_n}{m} \cos(\omega_n t + \phi_n) \tag{5.9}$$

The general solution for other types of $F(t)$ can then be constructed because Eqn 5.4 is linear.

For Eqn 5.9, the solution (for weak damping) is

$$x = e^{-\delta t}(C_1 \cos \omega_d t + C_2 \cos \omega_d t) + \frac{F_n}{m} \frac{1}{\sqrt{(\omega_0 2 - \omega_n^2)^2 + 4\delta^2 \omega_n^2}} \cos(\omega_n t - \phi_n)$$

where C_1 and C_2 are determined by the initial conditions of displacement and velocity.

For a machine-tool, forced vibration is usually caused by an out-of-balanced force associated with a component integral with, or external to the machine tool. There are four methods of tackling machine tool forced vibration:

1. by eliminating the exciting force at source,
2. by vibration isolation,
3. by an undamped dynamic vibration absorber,
4. or by a Lanchester vibration absorber.

5.4.1 Vibration isolations

There are two methods for isolating the machine-tool from the disturbing vibration. The first is by preventing the vibration passing from the source into the machine foundation. The second is by preventing vibration transmitted through the ground from entering the machine-tool. The former is termed active isolation and the latter passive isolation.

5.4.2 Undamped dynamic vibration absorbers

This involves attaching an additional mass to the original system through a spring. The secondary system is so designed that it supplies a force at the dis-

turbing frequency which will be against the disturbing force.

5.4.3 Lanchester vibration absorbers

Instead of a spring, a damper can be used to couple a mass to the machine tool structure. This increases the damping and suppresses the amplitude at resonance. This absorber is normally called a *Lanchester vibration absorber.*

Of course, it is possible to connect the absorber mass to the main mass through both a spring and damper to give a damped dynamic vibration absorber, which offers certain advantages over the undamped type.

Theoretically, both free and forced vibrations can be eliminated provided that the causes responsible for inducing it have been identified (however, it is not always possible that the remedy can be practically realised). Moreover, vibrations of these two types are usually detected in the maker's works, therefore necessary counter-measures can be devised while the machine is still in the development stage.

There exists another type of vibration called *self-excited vibration* or *chatter*, which is far more difficult to cope with than free and forced vibrations. This will be discussed more in the next section.

5.5 Self-excited vibrations

Self-excited vibration is spontaneous. It is not induced by external periodic forces, but the forces generated in the vibratory processes itself. For a 1-D vibratory system, if it is dynamically unstable, then its vibration is self-induced. For the machine tool, the self-excited vibration is the result of interaction between the cutting force dynamics and the machine tool structure dynamics. It draws the energy for its maintenance from the tool or workpiece drive.

In machining, self-induced vibrations can occur in the following two ways:

1. Under certain conditions, the cutting process is basically, dynamically un-

stable. As a result, any slight displacement of the tool relative to the workpiece can rapidly build into a large-amplitude vibration.

2. The second way in which self-induced vibrations can occur is more complicated but more common. In this case, the cutting process is basically dynamically stable. However, because of overlapping cuts, the forced vibration resulting from the machining of the wavy surface from the previous stroke or revolution of the workpiece or tool can amplify the previous vibration. This type of vibration is called *regenerative chatter.*

5.6 The cantilever

As a first approximation, the cutting tool can be treated as a cantilever. A cantilever is a member fixed at one end and subjected to loads applied transverse to the long dimension causing the member to bend. See Figure 5.2.

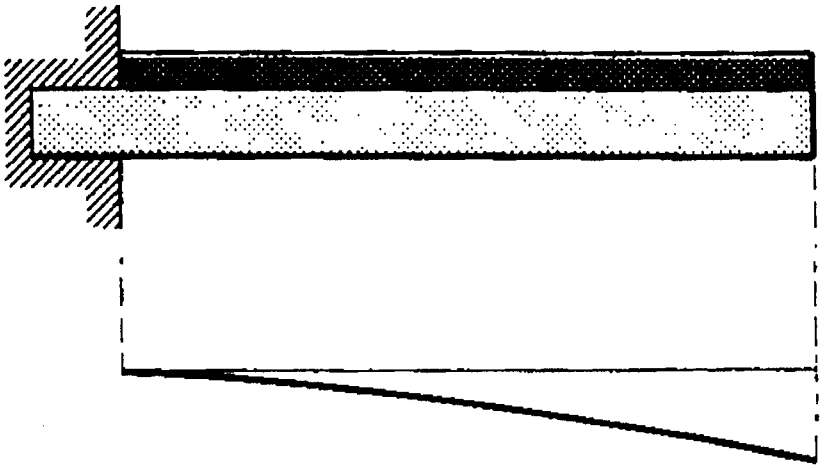

Figure 5.2: The cantilever.

5.6.1 The equation for a cantilever

To derive the differential equation for a cantilever, consider the forces and moments acting on an element shown in Figure 5.3.

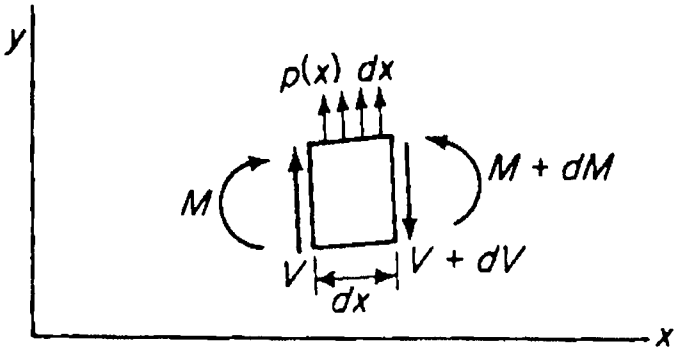

Figure 5.3: One element of the cantilever.

$p(x)$ represents the loading per unit length of the beam.

$V(x)$ and $M(x)$ are shear and bending moments at x, respectively.

The forces in the y direction satisfy

$$V + p(x)\,dx - (V + dV) = 0 \tag{5.10}$$

from which

$$\frac{dV}{dx} = p(x) \tag{5.11}$$

For the moments about any point on the right face of the element,

$$M + dM - M - V dx - \frac{1}{2}p(x)(dx)^2 = 0 \tag{5.12}$$

In the limiting process, it follows that

$$\frac{dM}{dx} = V(x) \tag{5.13}$$

Let $y(x)$ be the curve of a cantilever, then (Higdon et al 1985, p 358)

$$EI\frac{d^2y}{dx^2} = M(x) \tag{5.14}$$

where E is Young's Modulus, and $I(x)$ the moment of inertia — the second moment of the cross-sectional area with respect to the centroidal axis.

Combining 5.11, 5.13 and 5.14, it follows that

$$EI\frac{d^4y}{dx^4} = p(x) \tag{5.15}$$

where $I(x)$ is assumed to be independent of x,

Since $p(x)$ is the force of inertia acting on the element per unit length, it then follows

$$p(x) = -\frac{\sigma A}{g}\frac{\partial^2 y}{\partial t^2} \tag{5.16}$$

where σ is the weight per unit volume of the beam, A is the beam cross-section, and g is the acceleration due to gravity.

Combining Eqn 5.15 and Eqn 5.16, we then have

$$\frac{\partial^2 y}{\partial t^2} + a^2\frac{\partial^4 y}{\partial x^4} = 0 \tag{5.17}$$

where $a = \frac{EIg}{A\sigma}$

Eqn 5.17 is the basic differential equation for the cantilever, from which natural frequencies can be calculated.

5.6.2 The natural frequencies

Eqn 5.17 is a partial differential equation, so it can be assumed that

$$y = X(x)T(t) \tag{5.18}$$

Substituting this with Eqn 5.17 gives

$$\frac{d^2T(t)}{dt^2} + \omega^2 T(t) = 0 \tag{5.19}$$

$$\frac{d^4X(x)}{dx^4} - \frac{\omega^2}{a^2}X(x) = 0 \tag{5.20}$$

with a constant ω, whose solutions are given by

$$T(t) = B_1 \cos\omega t + B_2 \sin\omega t \tag{5.21}$$

$$X(x) = C_1 \sin kx + C_2 \cos kx + C_3 \sin hx + C_4 cos hkx \tag{5.22}$$

with constants B_1 and B_2 determined by initial conditions, constants C_1, C_2, C_3, and C_4 determined by the end conditions, and $k^4 = \frac{\omega^2}{a^2} = \frac{\omega^2 A\sigma}{EIg}$.

For the cantilever, at the clamped end

$$y = 0 \qquad \frac{dy}{dx} = 0$$

at the free end

$$\frac{d^2y}{dx^2} = 0 \qquad \frac{d^3y}{dx^3} = 0$$

Eqn 5.22 has the solutions as

$k_1 l$	$k_2 l$	$k_3 l$	$k_4 l$	$\cdots$
1.875	4.694	7.855	10.966	$\cdots$

(5.23)

Since $k^4 = \frac{\omega^2}{a^2} = \frac{\omega^2 A\sigma}{EIg}$, it follows that

$$f_n = \frac{k_n^2}{2\pi}\sqrt{\frac{EIg}{A\sigma}}$$

Moreover if the cross-section of the cantilever is rectangular with b and h as the width and height respectively then

$$f_n = \frac{k_n^2}{2\pi}\sqrt{\frac{Eg}{A\sigma}\frac{bh^3}{12}}$$

For a cantilever of steel with $b = h = 1$ cm, $l = 6.5$ cm, and let $E = 2.0 \times 10^7$ N/cm^2, $g = 980$ cm/s^2, $\sigma = 0.0764$ N/cm^3, then

$$f_1 = 1.9\text{kHz}.$$

which is close to cutting tool vibration frequency (about 1.8 kHz) in practice.

5.7 Measurement of vibration

5.7.1 Traditional method

For measurement of vibration, a vibration transducer is required to convert the mechanical vibration signal into an electrical form. There are various types of vibration transducers, such as proximity probes to sense displacement (mechanical lever, eddy current or proximity probe), velocity probes to sense velocity, and accelerometers to sense acceleration. Because displacement, velocity, and acceleration are interrelated in theory, any type of transducers can be used. However, in practice, the accelerometer is usually employed.

Properties of accelerometers

The accelerometer has the following advantages:

1. no moving parts, no wear;
2. compact, often low weight;
3. rugged;
4. very large dynamic range;
5. wide frequency range.

Displacement and velocity can be obtained from it by a simple analogue electronic integration technique. The disadvantage of an accelerometer is its high output impedance and no true DC response.

Application of accelerometers

As explained in the last section, an accelerometer was originally chosen to measure the vibration of the cutting tool, See Figure 5.4. The accelerometer selected was of type 8307 from Bruel and Kjaer, the output signal from which was then further amplified by a charge amplifier, and displayed on a oscilloscope.

It was found that the dynamic range of the above accelerometer was not large enough for the violent vibration of a cutting tool. For a typical case, the displacement amplitude was about 100 μm, the frequency was around 2 kHz, so the acceleration was between -1500 g and 1500 g (where g is the acceleration of gravity). Furthermore, mounting the accelerometer on the cutting tool was difficult. As a result, this standard method for measuring vibration did not work very well for the cutting tool vibration.

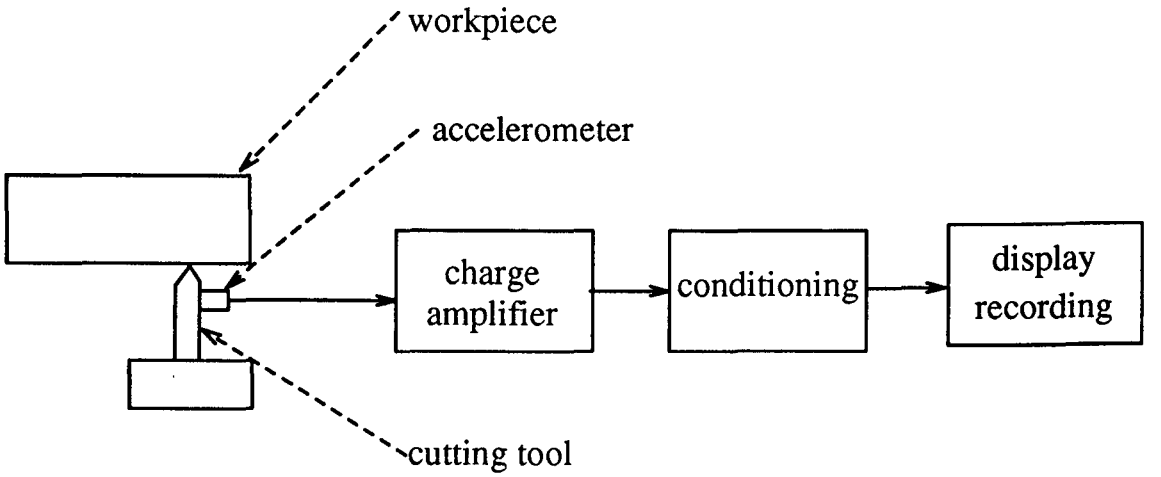

Figure 5.4: Measurement of vibration by the accelerometer.

Another approach

After considering many other possible methods, an instrument based on the linear variable differential transformer (LVDT) was developed. This instrument is able to get rid of some of the disadvantages mentioned above. See Figure 5.5 for its schematic diagram.

In the rest of this chapter, the components of this instrument are explained

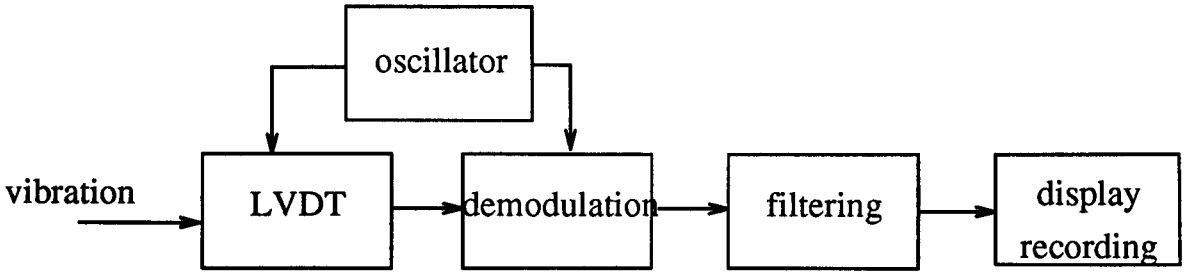

Figure 5.5: Measurement of vibration by the LVDT.

in detail and the performance of the instrument is described.

5.8 The linear variable differential transformer

5.8.1 Operating Principle

The linear variable differential transformer (LVDT) is a mechanical displacement transducer. Its construction is simple, including only two parts:

1. a primary coil and two identical secondary coils on a common former,
2. a movable magnetic armature or core.

Figure 5.8.1 shows a schematic diagram for the LVDT.

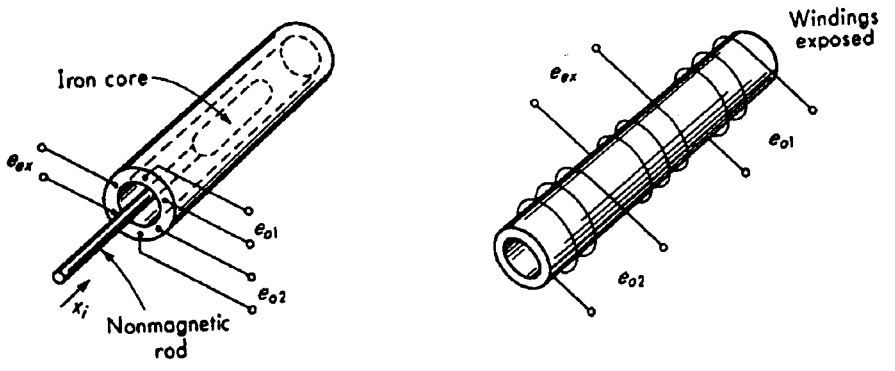

Figure 5.6: The schematic digram of a LVDT (Doebelin 1983, p 240).

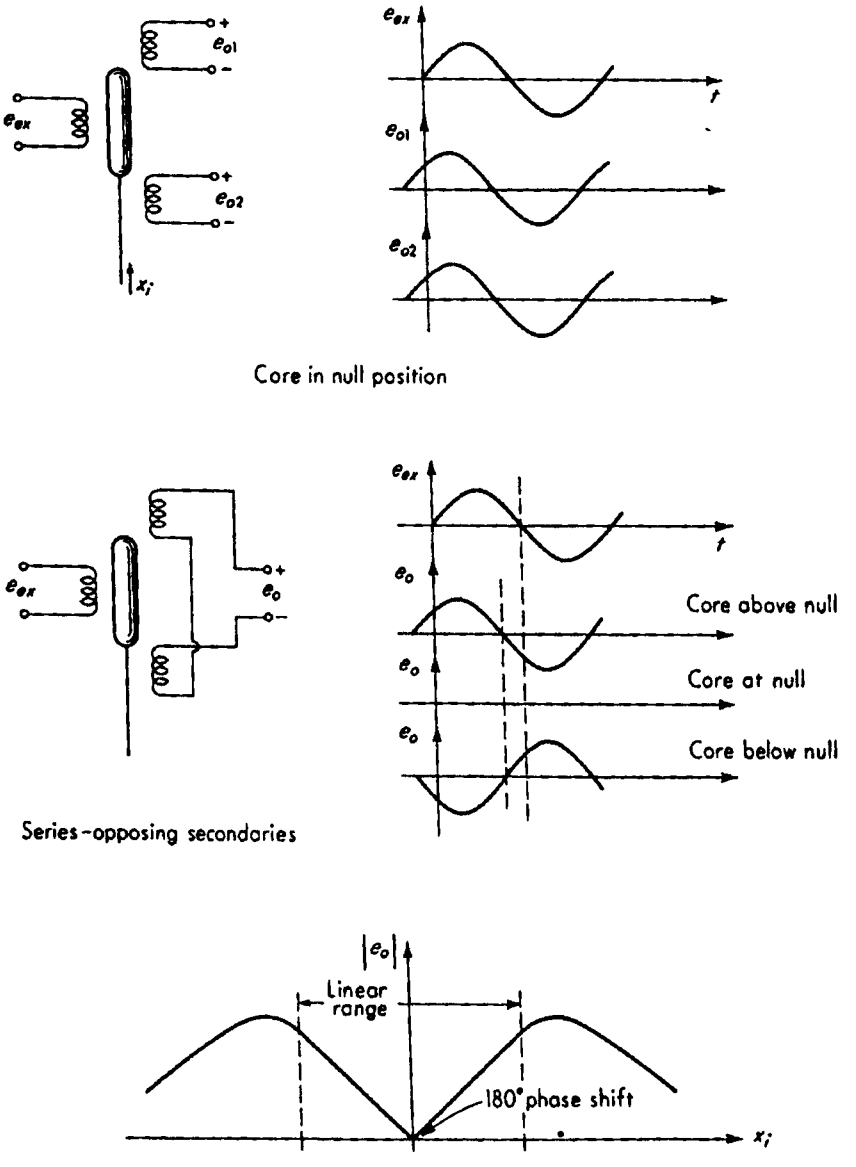

Figure 5.7: The circuit digram of a LVDT (Doebelin 1983, p240).

To operate the LVDT, the primary coil is normally excited with a sinusoidal voltage of 3 to 15 V rms amplitude and frequency of 60 to 20,000 Hz. Through the mutual coupling, the sinusoidal voltages in the secondary coils are induced, which have the same frequency as the excitation, but whose amplitudes vary with the position of the iron core. There is a position, called *null position* for the core, at which the output e_o is essentially zero, for the secondary coils are connected in series opposition. As the core moves away from the null position, the mutual inductances of the secondary coils are varying: one increases as the other decreases. As a result, e_o varies (in fact, *linearly*) with the displacement of the iron core. See Figure 5.8.1

5.8.2 Circuit Analysis

For completeness, a condensed analysis of the LVDT is given here.

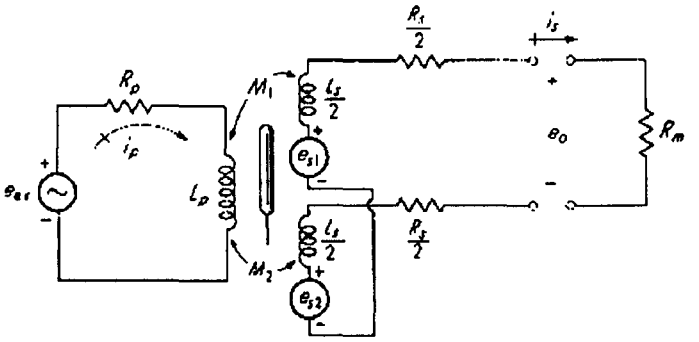

Figure 5.8: Circuit analysis (Doebelin 1983, p241).

Let

R_p, L_p are the resistor and inductance of the primary coil, respectively,

R_s, L_s are the total resistor and inductance of the secondary coils,

M_1, M_2 are the two mutual inductances between the secondary coils and the primary coil,

R_m is the load,

i_p, i_s are the currents in the primary coil and the secondary coils

e_{ex} is the active sinusoidal voltage source,

e_o is the output voltage, which is varying as the core moves in and out.

Applying Kirchhoff's voltage law, it is obtained from Figure 5.8.2 that

$$\begin{cases} i_p R_p & +L_p \frac{di_p}{dt} & +(M_1 - M_2)\frac{di_s}{dt} & = e_{ex} \\ i_s(R_s + R_m) & +L_s \frac{di_s}{dt} & +(M_1 - M_2)\frac{di_p}{dt} & = 0 \\ -i_s R_m & & & = e_o \end{cases} \tag{5.24}$$

If let I_p, I_s, E_{ex}, E_o are the Fourier transform of i_p, i_s, e_{ex}, e_o respectively, then Fourier transforming the above equations leads to

$$\begin{cases} I_p R_p & +L_p j\omega I_p & +(M_1 - M_2)j\omega I_s & = E_{ex} \\ I_s(R_s + R_m) & +L_s j\omega I_s & +(M_1 - M_2)j\omega I_p & = 0 \\ -I_s R_s & & & = E_o \end{cases} \tag{5.25}$$

Solving for E_o,

$$E_o = \frac{R_m(M_1 - M_2)j\omega \cdot E_{ex}}{[L_p L_s - (M_1 - M_2)^2]\omega^2 + [L_p(R_s + R_m) + L_s R_p]j\omega + (R_s + R_m)R_p} \tag{5.26}$$

Because R_m is very large,

$$E_o \approx \frac{(M_1 - M_2) \cdot E_{ex}}{L_p + \frac{R_p}{j\omega}} \tag{5.27}$$

i.e.

$$e_o \approx \frac{(M_1 - M_2) \cdot e_{ex}}{L_p + \frac{R_p}{j\omega}} \tag{5.28}$$

5.8.3 Modulation

According to electric circuit theory, $M_1(t) - M_2(t)$ is proportional to the position of the core, $x_i(t)$, provided that both take the value 0 simultaneously. So,

$$M_1(t) - M_2(t) = C_m \cdot x_i(t) \tag{5.29}$$

where C_m is a constant, which mainly depends on the winding of coils and the iron core.

From the above equation and $e_{ex} = A\cos(\omega_c t)$ where $w_c = 2\pi f_c$, then Eqn 5.28 becomes

$$e_o(t) = C \cdot x_i(t) \cdot \cos(\omega_c t) \tag{5.30}$$

where $C = \frac{C_m A}{L_p + \frac{R_p}{j\omega}}$.

Eqn 5.30 means that output from LVDT is actually amplitude modulated signal with the displacement of the core $x_i(t)$ as the modulating signal.

5.8.4 Features of an LVDT and its justification for tool vibration application

The LVDTs used are of type D5/25 from RDP Electronics Ltd, Wolverhampton, England. For a typical LVDT calibrated under temperature 20 ^0C, with energising supply as 5 V rms, 5 kHz,

linear range is ± 635 μm, which is large enough for machine tool vibration whose amplituded is around 100 μm.

linearity is 0.27%.

sensitivity is 65.66 mV/V/mm.

If the LVDT is energised by a sinusoidal voltage of frequency as 15 kHz, this frequency will be large enough for the cutting tool vibration whose frequency is of 0.5 to 5 kHz. In the application, the LVDT can measure the vibration amplitudes

with an absolute error of $\pm 0.25\mu$m and measure the vibration frequencies with an absolute error of ± 7 Hz.

5.9 Demodulation

As shown in the last section, the output from the LVDT is a modulated electrical signal:

$$g(t) = f(t)\cos(\omega_c t) \tag{5.31}$$

where $f(t) = Cx_i(t)$. Let $G(\omega)$ and $F(\omega)$ be the FTs of $g(t) and f(t)$ respectively, then

$$G(\omega) = \frac{1}{2}F(\omega + \omega_c) + \frac{1}{2}F(\omega - \omega_c) \tag{5.32}$$

which means that $g(t)$ is simply a translation of the frequency spectrum of $f(t)$ by $\pm\omega_c$ without changing the shape.

In order to make use of $g(t)$, $f(t)$ has to be extracted from it. This is achieved by a demodulation technique in communication theory. It is done by using $g(t)$ to modulate $\cos(\omega_c t)$ again, then passing through a low pass fiter.

Let

$$h(t) = g(t)\cos(\omega_c t) \tag{5.33}$$

then

$$H(\omega) = \frac{1}{2}F(\omega) + \frac{1}{4}F(\omega - 2\omega_c) + \frac{1}{4}F(\omega + 2\omega_c)$$

where $H(\omega)$ is the FT of $h(t)$. This means that $h(t)$ has two components, one is $f(t)$(low frequency), the other is $\frac{1}{4}(f(t)e^{j2\omega_c} + f(t)e^{-j2\omega_c})$ (high frequency). Therefore, $f(t)$ is obtained by passing $h(t)$ through a low-pass filter. NOTE: during the above discussion, $f(t)$ must vary slowly with respect to ω_c.

Instead of the demodulation using the same waveform carrier as the original carrier, any other periodic signal can be used as carrier provided that its period is ω_c. Let $\sum_{n=-\infty}^{\infty} c_n e^{-j\omega_c n x}$ be any carrier, then its FT can be written as

$\sum_{n=-\infty}^{\infty} c_n \delta(\omega - \omega_c n)$, so

$$
\begin{aligned}
H(\omega) &= \int_{-\infty}^{\infty} G(\omega - \varpi) \sum_{n=-\infty}^{\infty} c_n \delta(\varpi - \omega_c n) d\varpi \\
&= \sum_{n=-\infty}^{\infty} c_n G(\omega - \omega_c n) \\
&= \sum_{n=-\infty}^{\infty} c_n' F(\omega - \omega_c n)
\end{aligned}
$$

After passing a low-pass filter, $f(t)$ can be extracted.

In practice, in the instrument, the sinusoidal signal is used in the LVDT while the square wave is used during demodulation.

In the equipment, the sinusoidal signal is generated from the oscillator, so is the square wave. The demodulation and lowpass filtering is done by the demodulator. Both oscillators and demodulators are purchased from RS (Radio Spares).

5.10 A low-pass filter

The signal from the demodulator normally has high frequency ripples. In order to reduce these ripples, a low-pass filter is used. A typical configuration is shown in shown Figure 5.9

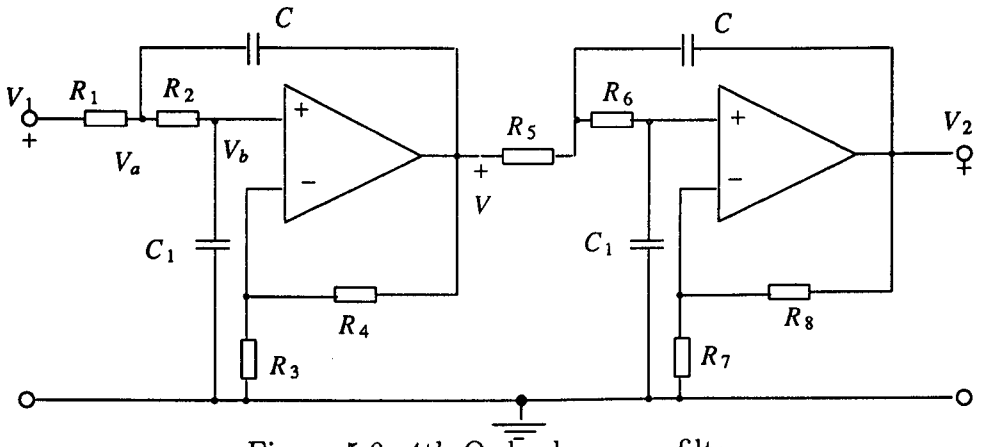

Figure 5.9: 4th-Order low-pass filter

This consists of two second-order low-pass filters which are of the type invented by Sallen and Key (Hilburn and Johnson 1973).

For the first part, we have

$$\begin{aligned} V_b &= V\frac{R_3}{R_3+R_4} \\ V_a &= V_b(1+j\omega C_1 R_2) \\ \frac{V_1-V_a}{R_1} &= (V_a-V)j\omega C + V_b j\omega C_1 \end{aligned}$$

from which

$$\frac{V}{V_1} = \frac{R_3+R_4}{-CC_1R_1R_2R_3\omega^2 + C_1R_1R_3j\omega + C_1R_2R_3j\omega - CR_1R_4j\omega + R_3} \tag{5.34}$$

i.e.

$$\frac{V(\omega)}{V_1(\omega)} = \frac{K_1}{-\omega^2 + ja_1\omega + b_1} \tag{5.35}$$

where $K_1 = \frac{R_3+R_4}{R_1R_2R_3CC_1}$, $a_1 = \frac{1}{R_1C} + \frac{1}{R_2C} - \frac{R_4}{R_2R_3C_1}$, and $b_1 = \frac{1}{R_1R_2CC_1}$.
For the second part,

$$\frac{V_2(\omega)}{V(\omega)} = \frac{K_2}{-\omega^2 + ja_1\omega + b_1} \tag{5.36}$$

where $K_2 = \frac{R_7+R_8}{R_5R_6R_7CC_1}$, $a_2 = \frac{1}{R_5C} + \frac{1}{R_6C} - \frac{R_8}{R_6R_7C_1}$, and $b_2 = \frac{1}{R_5R_6CC_1}$.
Combining the last two equations, and choosing suitable values for the resisters and capacitances, a Butterworth filter is then obtained

$$\frac{V_2(\omega)}{V_1(\omega)} = \frac{K}{\sqrt{1+(\frac{\omega}{\omega_c})^4}} \tag{5.37}$$

where ω_c is the cut-off frequency. Even though its cut-off characteristics are not sharp compared to other types of filters, such as the Chebychev filter, the Butterworth filter has a maximally flat, monotonic frequency response in the passband, which is very important for cutting tool vibration. Figure 5.10 shows the frequency response for a typical filter.

After this 4th-Order low-pass filter, the high frequency ripples are greatly reduced. Therefore there is no need to use higher order low-pass filters.

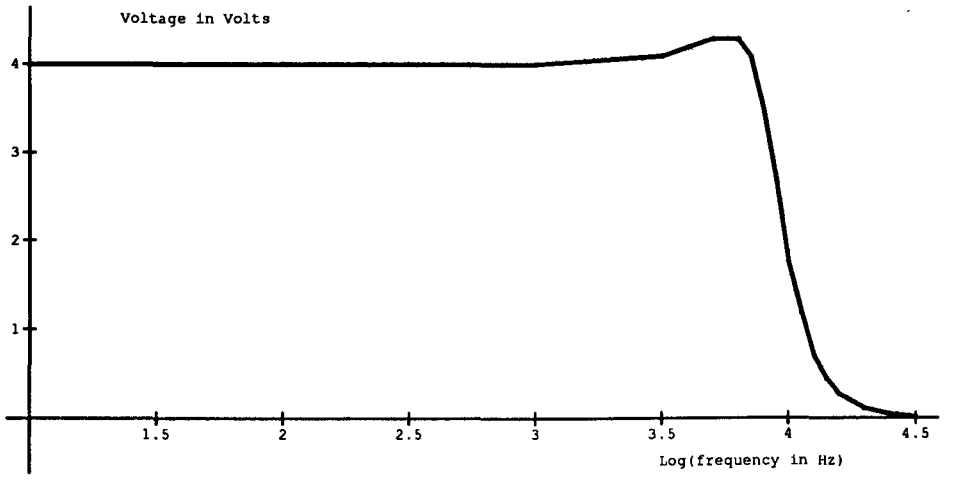

Figure 5.10: LVDT

Figure 5.11: The frequency response for an 4th-order Butterworth filter.

One set consisting of a LVDT, a demodulation chip, and a filter was built up for measuring vibration in the vertical y direction, and another set for measuring vibration in the horizontal z direction. A single oscillator chip provides the sinusoidal signal for both LVDTs. This has two advantages: 1) being cheap and simple; 2) reducing interference between the two LVDTs. For measurement in the y direction, the noise level is 10 mV and the sensitivity is 29.0 mV/μmwhile for measurement in the z direction, the noise level is 25 mV and the sensitivity is 44.0 mV/μm.

5.11 Data display and further processing

The two outputs from the low-pass filters were then displayed on the oscilloscope. Here, a Digital Storage Oscilloscope 1421 from Gould was used to monitor vibration signals in real-time, to record them, and later on to replay them.

The recorded data from the Gould 1421 was also sent to the MINC (Modular

INstrument Computer). Despite its many disadvantage (mainly the memory), the MINC was easy to interface. Here, the MINC was used to store the data on a disk for future use and compute amplitudes and frequencies of cutting tool vibration. These were obtained through spectrum analysis, including the following stages

1. the signal was weighted by a Hanning window, so that leakage was reduced;
2. its power spectrum was then computed by the FFT (For the program, see Appendix A);
3. Amplitudes and frequencies were then obtained by finding out the peak of the power spectrum.

The program for carrying out these calculations was written in BASIC for this was the only available language on the MINC.

5.12 Experiments

5.12.1 Equipments

In the experiments, the following equipment was used:

- the machine was a Hardinge CNC Lathe, Model HNC;
- all the cutting tools were from Sandvik Coromant,

$$\begin{aligned} 3 \quad & S10K - STFCR09 \\ 1 \quad & S12M - STFCR09 \\ 1 \quad & S12M - STFCR11 \end{aligned}$$

- The inserts were from Sandvik Coroman, TCMT090208UR Grad H13A;

- The material of workpiece was EN24T which contains (in percentage) the following elements,

.36 ~ .44	.10 ~ .35	.45 ~ .77	1.30 ~ 1.70	1.00 ~ 1.40	.20 ~ .35
Carbon	Silicon	Manganese	Nickel	Chromium	Molybdenum

5.12.2 Set up

The two LVDTs were located at the end of a tutting tool as shown in Figure 5.12 by the two thick lines on the cutting tool.

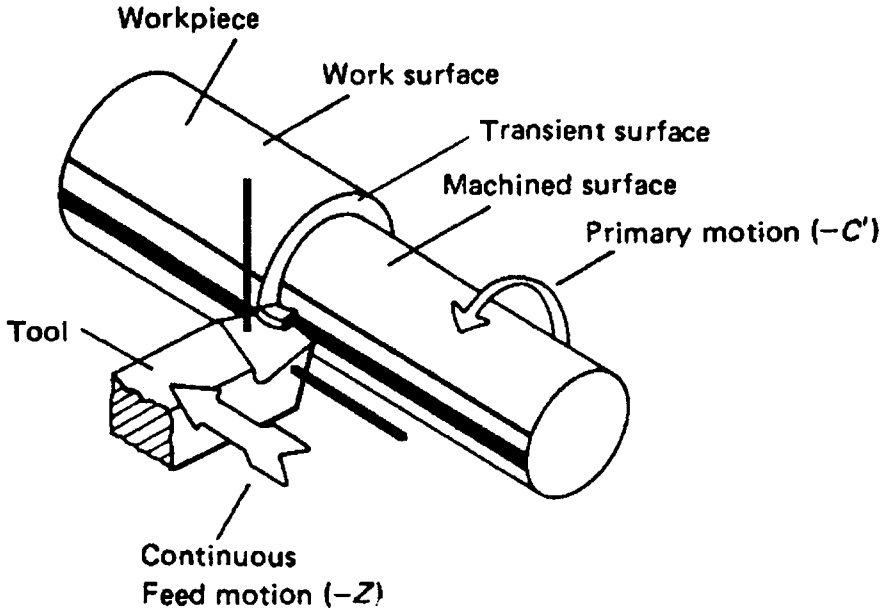

Figure 5.12: The two LVDTs for measuring the tool vibration.

Photo 1: The two LVDTs and the lathe.

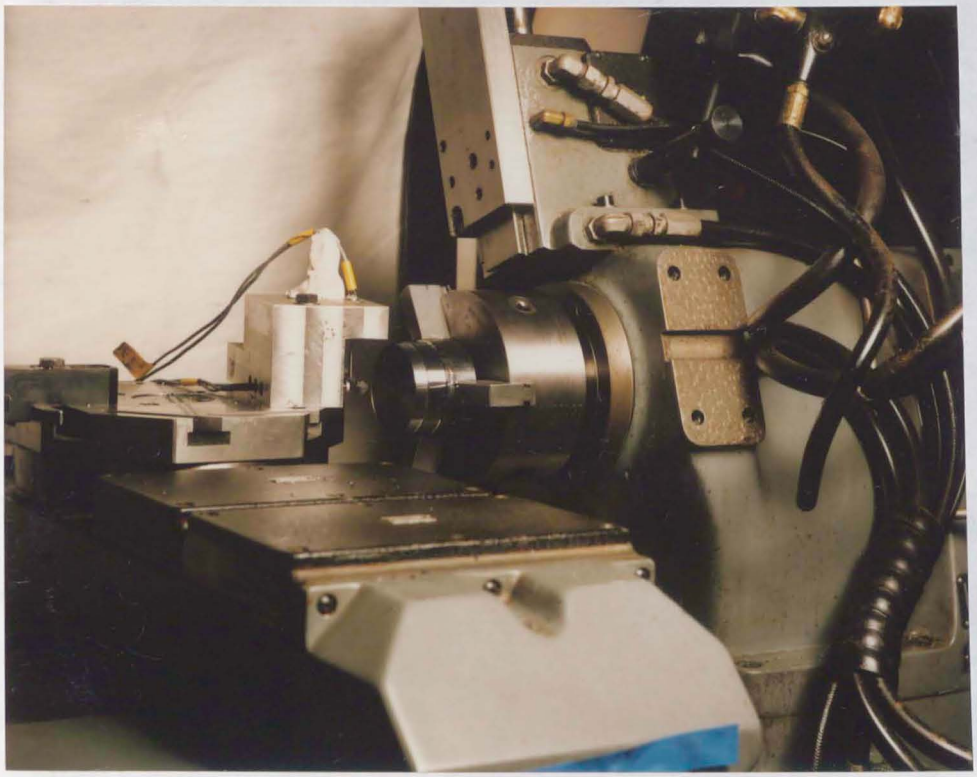

Photo 2: Two sets of modulation and demodulation and filtering.

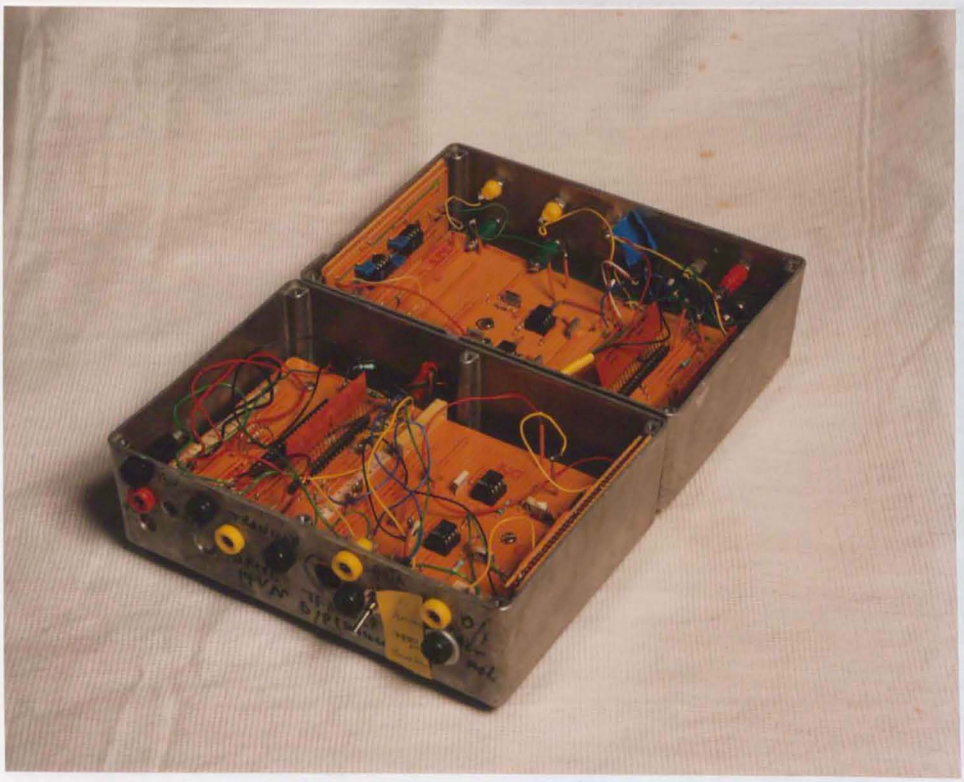

Photo 3: Gould 1421 for displaying vibration signals.

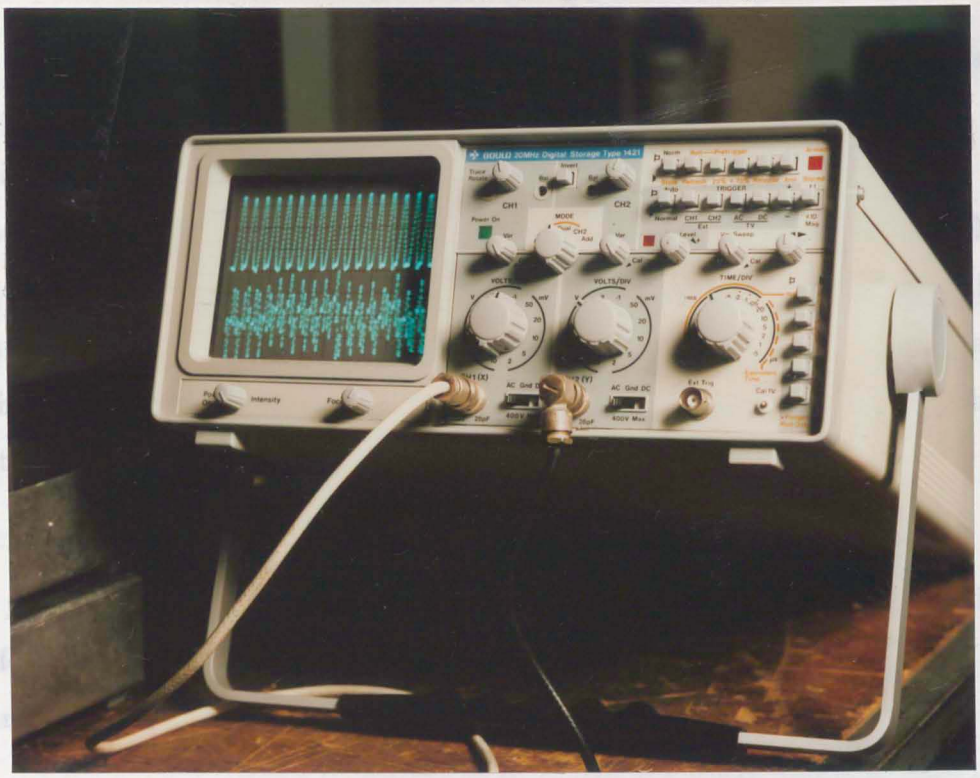

Photo 4: The MINC.

5.12.3 Results

Table 5.1 and Table 5.2 5.2 are two typical sets of values measured. The cutting conditions were: feed = 200 μm, RPM = 935; overhang = 6.5 cm; radius of workpiece = 32 cm, radius of a insert tip = 800 μm.

The positions where horizontal and vertical vibration were measured were 0.5 cm and 1.5 cm respectively away from the cutting tool tip. For a_y and a_z, the absolute error is less than ± 0.25 μm; for f_y and f_z, the absolute error is less than ± 7 Hz. Note the measured vibration amplitudes have been corrected. This correction is based on

$$y(x) = \frac{P}{EI}(\frac{x^2 L}{2} - \frac{x^3}{6})$$

where $y(x)$ is the deflection along the cutting tool x, L is the overhang, P is the point force at the end of the cutting tool, I is the the moment of inertia, and E is Young's Modulus.

Table 5.1: Group 1

	horizontal		vertical	
	amplitude	frequency	amplitude	frequency
	μm	kHz	μm	kHz
1	12.5	1.7	40.7	1.7
2	11.9	1.7	40.3	1.7
3	13.1	1.7	40.3	1.7
4	11.5	1.7	38.9	1.7

Table 5.2: Group 2

	horizontal		vertical	
	amplitude	frequency	amplitude	frequency
	μm	kHz	μm	kHz
1	9.4	1.7	39.8	1.7
2	7.0	1.7	38.5	1.7
3	10.8	1.7	38.5	1.7
4	9.3	1.7	38.6	1.7

5.13 Discussion

Because the vibration was measured away from the tool tip, it is different from the vibration at the tool tip. The measured amplitudes are much smaller compared with those at the tool tip although the measured frequencies are the same as those at the tool tip.

On one hand, it is difficult to measure the vibration of a cutting tool tip directly. On the other hand, analysing the surface texture by the WD can reveal the direct effect of tool vibration, which makes this technique more attractive. This will be discussed in detail in the next chapter and the extracted results will be compared with those in Table 5.1 and Table 5.2

Chapter 6

Extraction of Cutting Tool Vibration by WD Analysis of Surface Texture

6.1 Introduction

The vibration of a cutting tool can be measured by using instruments such as the one discussed in the previous chapter, then used to monitor the cutting process. However, there are some drawbacks about this technique:

1. it needs specific and expensive equipments, such as accelerometers, amplifiers, and so on;

2. it requires mounting and dismounting equipments.

To overcome these problems, a new approach developed by the author is described here. This is to analyse the surface texture of a turned workpiece by the WD, and then to extract cutting tool vibration information, which can be used for machine tool monitoring.

Although the surface texture contains much information about the cutting process and its malfunction, it is not true that all the surface texture in every direction can be used. For instance, the surface profile along the axis of a cylinder

is not suitable. This is because the vibration in this direction (order of 10 μm) is dwarfed by the feed (order of 100 μm). Therefore it is necessary to choose the surface texture in the most sensitive direction. Here, the out of roundness is used.

The roundness of a workpiece is derived through a mathematical model for the tool vibration, with the conclusion that the roundness is just a typical nonstationary signal — a frequency-modulated signal which is amenable to be analysed by the WD. Next the roundness from a real workpiece is measured, processed, and analysed by the WD. Then through the local moments of the WD, the vibration data for the cutting process is extracted, which can be used to control cutting processes.

In addition to this practical application, a computer simulation is presented in Section 9 (Zheng and Whitehouse 1992).

6.2 A mathematical model for cutting tool vibration

In this section, the roundness of a workpiece turned in the presence of the vibration is investigated. The variables used in this section are briefly explained below.

f_m feed, i.e., the displacement of the tool relative to the workpiece, in the direction of feed motion, per revolution of the workpiece.

n_w rotational frequency of the workpiece.

r_w the radius of a workpiece.

r_ϵ corner radius, i.e., the radius of a rounded tool corner.

a_y, f_y the amplitude and frequency of the cutting tool in vertical direction.

a_z, f_z the amplitude and frequency of the cutting tool in horizontal direction.

$r(\phi)$ the deviation of the actual radius of the workpiece from the ideal radius.

ϕ the angle about the workpiece axis of symmetry.

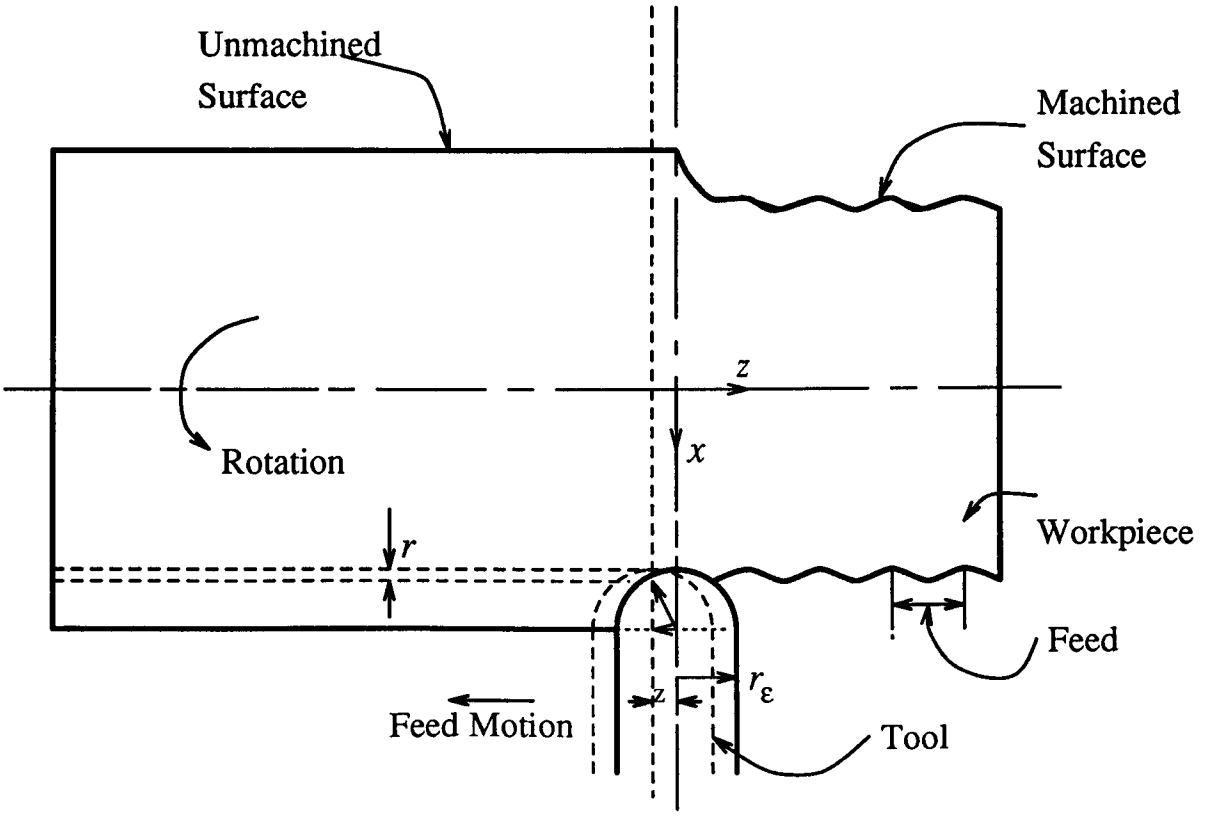

Figure 6.1: The fingerprint of turned workpiece in the presence of vibration.

From Figure 6.1, it follows that

$$r(\phi) = r_\epsilon - \sqrt{r_\epsilon^2 - z^2(\phi)} = r_\epsilon \left(1 - \sqrt{1 - \left(\frac{z(\phi)}{r_\epsilon}\right)^2}\right) \tag{6.1}$$

where $-\pi \leq \phi < \pi$. Since $\left(\frac{z(\phi)}{r_\epsilon}\right)^2$ is relatively small for a typical situation, $z(\phi) = 100\ \mu$m, then $r_\epsilon = 800\ \mu$m, $\left(\frac{z(\phi)}{r_\epsilon}\right)^2 = \frac{1}{64}$,

$$r(\phi) \approx r_\epsilon \left(1 - \left(1 - \frac{1}{2}\left(\frac{z(\phi)}{r_\epsilon}\right)^2\right)\right) \tag{6.2}$$

i.e.

$$r(\phi) \approx \frac{1}{2r_\epsilon} \cdot z^2(\phi) \tag{6.3}$$

6.2.1 Without any vibration

Since the position of the cutting tool is uniquely determined by the feed rate.

$$z(\phi) = -\frac{f_m \phi}{2\pi} \tag{6.4}$$

so

$$r(\phi) = \frac{1}{2r_\epsilon}\left(\frac{f_m \phi}{2\pi}\right)^2 = \frac{f_m^2 \phi^2}{8\pi^2 r_\epsilon} \tag{6.5}$$

6.2.2 With z vibration only

An additional cosine term is added to Eqn 6.4 to represent the vibration,

$$z(\phi) = -\left(a_z \cos\left(\frac{f_z \phi}{n_w} + \phi_z\right) + \frac{f_m \phi}{2\pi}\right) \tag{6.6}$$

so

$$\begin{aligned} r(\phi) &= \frac{1}{2r_\epsilon}\left(a_z \cos\left(\frac{f_z \phi}{n_w} + \phi_z\right) + \frac{f_m \phi}{2\pi}\right)^2 \\ &= \frac{a_z^2}{2r_\epsilon}\cos^2\left(\frac{f_z \phi}{n_w} + \phi_z\right) + \frac{a_z f_m \phi}{2\pi r_\epsilon}\cos\left(\frac{f_z \phi}{n_w} + \phi_z\right) + \frac{f_m^2 \phi^2}{8\pi^2 r_\epsilon} \end{aligned} \tag{6.7}$$

6.2.3 With z and y vibrations

From the point of view of theoretical mechanics, the situation with the cutting tool vibrating in both the z and y directions can be treated to be equivalent to the one with the cutting tool vibrating in the z direction and the workpiece (combined with the spindle) vibrating rotationally. So using Eqn 6.6 and allowing ϕ to vibrate,

$$\begin{aligned} z(\phi) &= -\left(a_z \cos\left(\frac{f_z(\phi + \frac{a_y}{r_w}\sin(\frac{f_y \phi}{n_w} + \phi_y))}{n_w} + \phi_z\right) + \frac{f_m(\phi + \frac{a_y}{r_w}\sin(\frac{f_y \phi}{n_w} + \phi_y))}{2\pi}\right) \\ &= -\left(a_z \cos\left(\frac{f_z(\phi + \frac{a_y}{r_w}\sin(\frac{f_y \phi}{n_w} + \phi_y))}{n_w} + \phi_z\right)\right. \end{aligned}$$

$$+\frac{f_m\phi}{2\pi}+\frac{f_m a_y}{2\pi r_w}\sin\left(\frac{f_y\phi}{n_w}+\phi_y\right)\Bigg) \tag{6.8}$$

Since $\frac{f_m a_y}{2\pi r_w}$ is small compared with a_z, for a typical case, $a_y = 60\ \mu\text{m}, a_z = 10\ \mu\text{m}, r_w = 30\ \text{mm} = 30000\ \mu\text{m}, f_m = 200\ \mu\text{m}$,

$$\frac{f_m a_y}{2\pi r_w a_z} = \frac{200\cdot 60}{2\pi\cdot 30000\cdot 10} = \frac{1}{50\pi}$$

so

$$z(\phi)\approx a_z\cos\left(\frac{f_z\phi}{n_w}+\frac{f_z a_y}{n_w r_w}\sin\left(\frac{f_y\phi}{n_w}+\phi_y\right)+\phi_z\right)+\frac{f_m\phi}{2\pi}$$

therefore

$$\begin{aligned} r(\phi) = {} & \frac{a_z^2}{2r_\epsilon}\cos^2\left(\frac{f_z\phi}{n_w}+\frac{f_z a_y}{n_w r_w}\sin\left(\frac{f_y\phi}{n_w}+\phi_y\right)+\phi_z\right) \\ & +\frac{a_z f_m\phi}{2\pi r_\epsilon}\cos\left(\frac{f_z\phi}{n_w}+\frac{f_z a_y}{n_w r_w}\sin\left(\frac{f_y\phi}{n_w}+\phi_y\right)+\phi_z\right)+\frac{f_m^2\phi^2}{8\pi^2 r_\epsilon} \end{aligned} \tag{6.9}$$

which will be discussed in the next two sections.

6.2.4 Vibrations in the x directions

The above equation does not include vibrations directly in x. Because of the large stiffness in this direction, the vibration in x is very small compared to those in y and z directions.

6.3 Roundness measurement

The roundness of a workpiece is measured by Talyrond 200 manufactured by Rank Taylor Hobson. See Figure 6.2.

A Talyrond 200 consists of the following three parts:

1. The turntable, on which the workpiece is placed. The turntable can be rotated manually as well as automatically.

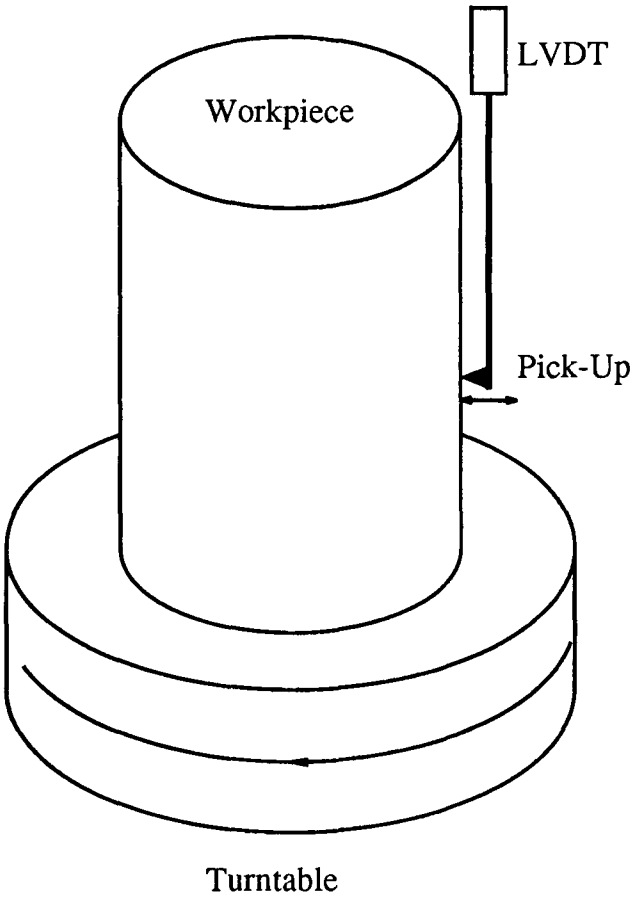

Figure 6.2: Talyrond 200

2. The pick-up. As the workpiece rotates with the turntable, the pick-up will move radially in response to workpiece irregularities.

3. The processing unit. Radial motion is converted into an electrical signal, which is amplified, filtered, plotted and transferred to the MINC.

In order to achieve accuracy, attention must be paid to the following important points:

1. The base of the workpiece should be ground smooth so that it is stable during measurement.

2. The stylus arm should be placed so that stylus displacements are normal to the surface.

3. The filter should be set to 1-500 u.p.r.[1] so that all undulations within the instrument bandwidth are recorded.

4. The magnification should be set as high as possible.

During the measurement, the magnification was set at 5000 or 10000, the filter was 1-500 u.p.r. For each revolution, $L = 2048$ points are sampled. The sampled data were plotted out and also transferred to the MINC computer.

[1] u.p.r. stands for undulations per revolution

Photo 5 and 6: The measurement of roundness.

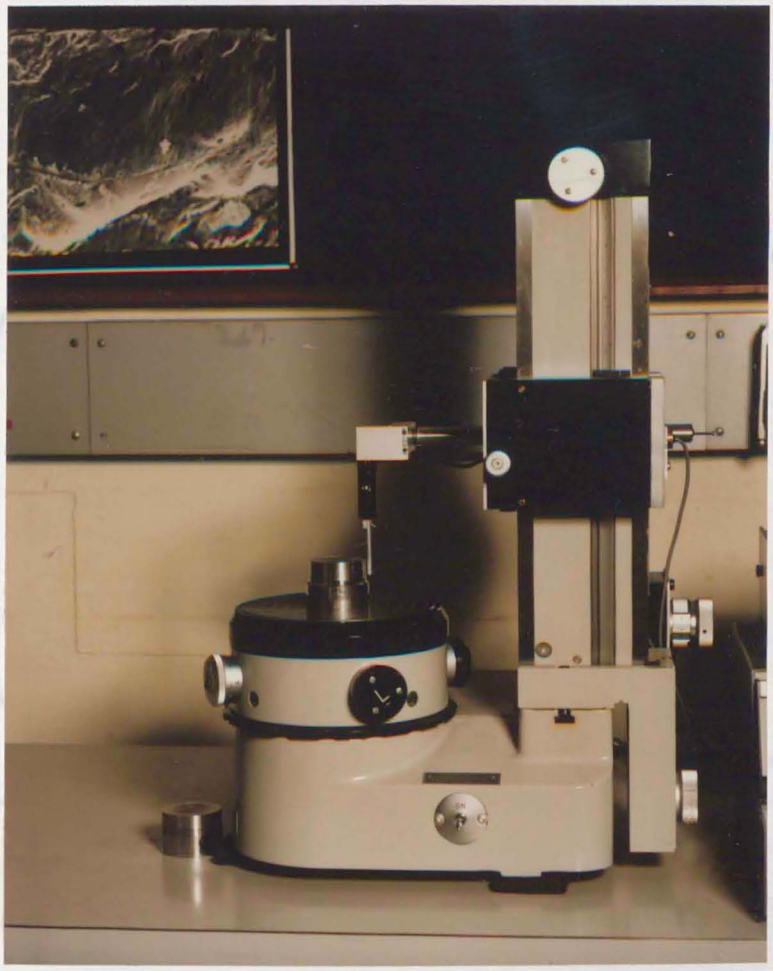

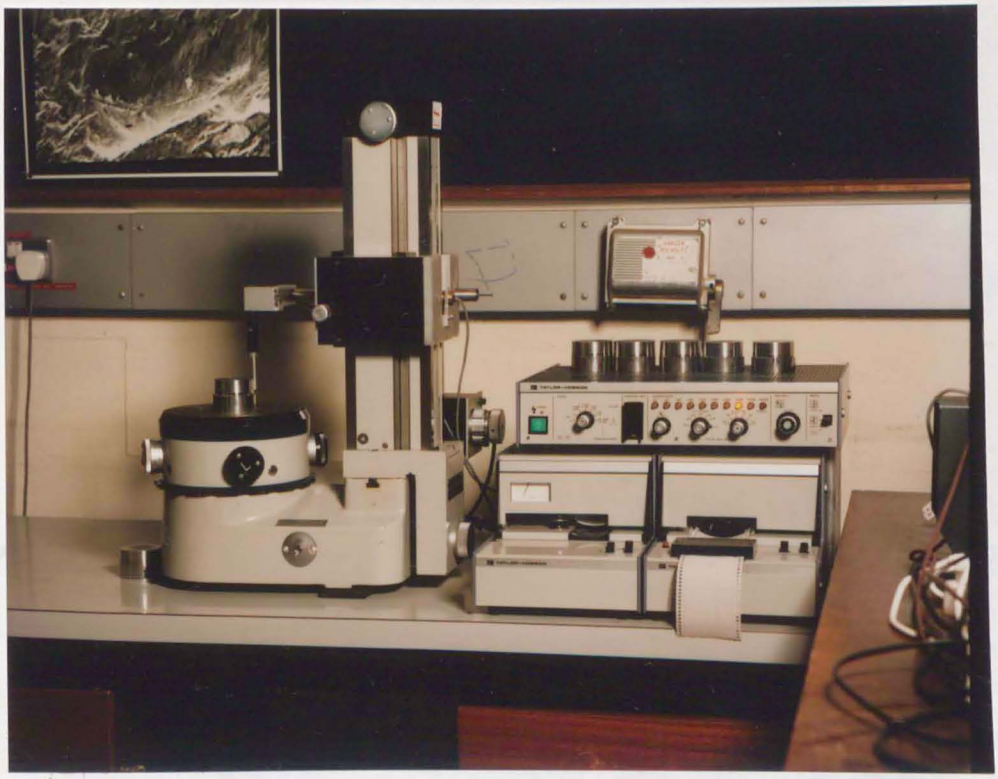

Here is one of the typical plot of roundness for a turned workpiece.

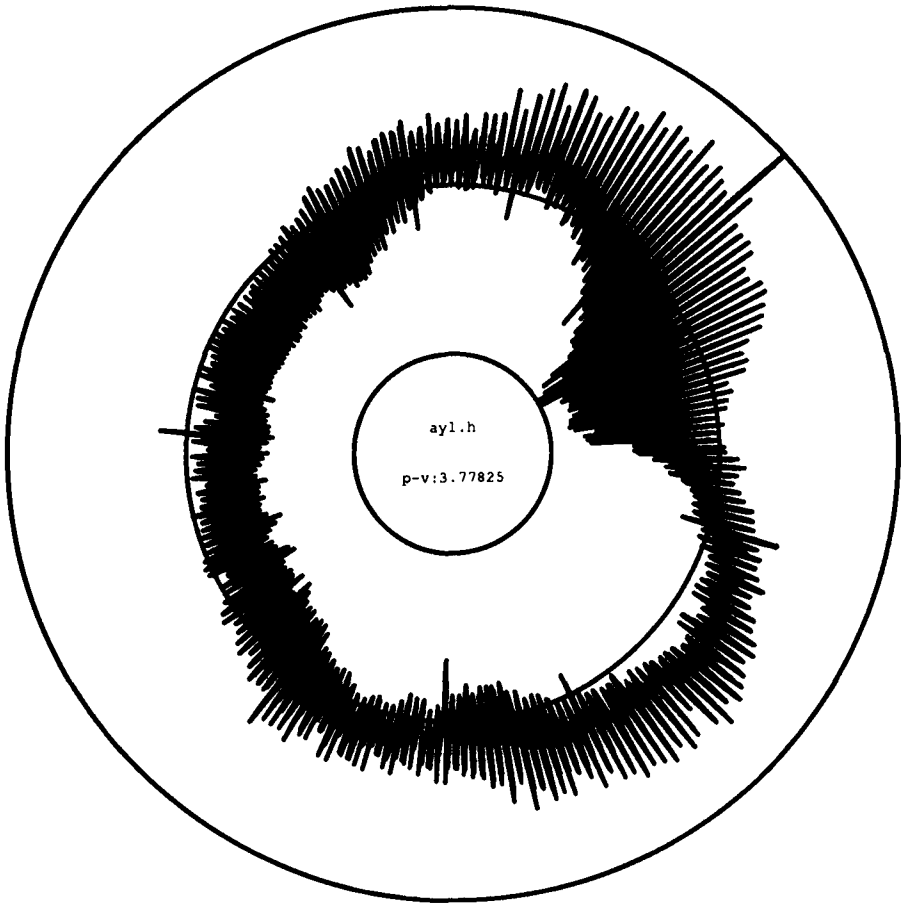

Figure 6.3: A typical roundness graph.

After measurement, the roundness takes the following form

$$
\begin{aligned}
r[n] = {} & \frac{a_z^2}{2r_\epsilon}\cos^2\left(\frac{f_z}{n_w}\phi[n] + \frac{f_z a_y}{n_w r_w}\sin\left(\frac{f_y}{n_w}\phi[n] + \phi_y\right) + \phi_z\right) \\
& + \frac{f_m a_z}{2\pi r_\epsilon}\phi[n]\cos\left(\frac{f_z}{n_w}\phi[n] + \frac{f_z a_y}{n_w r_w}\sin\left(\frac{f_y}{n_w}\phi[n] + \phi_y\right) + \phi_z\right) \\
& + \frac{f_m^2}{8\pi^2 r_\epsilon}(\phi[n])^2
\end{aligned}
$$

where $\phi[n] = \frac{2\pi n}{L}$ and $-\frac{L}{2} \leq n < \frac{L}{2}$.

6.4 Band pass filtering

Before applying the WD to analyse the roundness, there are a few preliminary things to do, in order to remove aspects of the signal that are unconcerned with the information concerning vibration, and to transform it into an analytical signal for the ease of computation. These include

1. choosing one section of the roundness for analysis, and if necessary more than one,
2. preprocessing the roundness data,
3. and transforming the roundness signal into its analytical form by means of the Hilbert transform.

Per revolution, there are $L = 2048$ sampled data points. In order to reduce computation time, one section of a revolution is chosen. It is found out that $\frac{1}{8}$ of a revolution is large enough for extraction of vibration information. The part of revolution is chosen as

$$\begin{aligned} f[n] = & \frac{f_m^2}{8r_\epsilon} \\ & + \frac{a_z^2}{2r_\epsilon}\cos^2\left(\frac{f_z}{n_w}\phi[n] + \phi_z + \frac{f_z a_y}{n_w r_w}\sin\left(\frac{f_y}{n_w}\phi[n] + \phi_y\right)\right) \\ & + \frac{f_m a_z}{2r_\epsilon}\cos\left(\frac{f_z}{n_w}\phi[n] + \phi_z + \frac{f_z a_y}{n_w r_w}\sin\left(\frac{f_y}{n_w}\phi[n] + \phi_y\right)\right) \end{aligned} \tag{6.10}$$

where $\phi[n] = \frac{2\pi(\frac{L-N}{2}+n)}{L}$, $n = 0, 1, 2, \cdots, N-1$, and $N = 256$.

Let

$$a = \frac{f_m a_z}{2r_\epsilon} \tag{6.11}$$

$$b = \frac{f_z a_y}{n_w r_w} \tag{6.12}$$

$$k_o = \frac{f_z}{n_w}\frac{N}{L} \tag{6.13}$$

$$k_m = \frac{f_y}{n_w}\frac{N}{L} \tag{6.14}$$

$$\varphi_y = \frac{f_y \pi}{n_w}\frac{L-N}{L} + \phi_y \tag{6.15}$$

$$\varphi_z = \frac{f_z \pi}{n_w}\frac{L-N}{L} + \phi_z \tag{6.16}$$

then

$$\begin{aligned} f[n] = & \frac{f_m^2}{8r_\epsilon} \\ & + \frac{a_z^2}{2r_\epsilon}\cos^2\left(\frac{2\pi k_o n}{N} + \varphi_z + b\sin\left(\frac{2\pi k_m n}{N} + \varphi_y\right)\right) \\ & + a\cos\left(\frac{2\pi k_o n}{N} + \varphi_z + b\sin\left(\frac{2\pi k_m n}{N} + \varphi_y\right)\right) \end{aligned} \tag{6.17}$$

From Eqn 6.17, it can be seen that the roundness of workpiece turned with vibration consists of 3 parts:

1. $\frac{f_m^2}{8r_\epsilon}$
2. $\frac{a_z^2}{2r_\epsilon}\cos^2(\frac{2\pi k_o n}{N} + \varphi_z + b\sin(\frac{2\pi k_m n}{N} + \varphi_y))$
3. $a\cos(\frac{2\pi k_o n}{N} + \varphi_z + b\sin(\frac{2\pi m}{N} + \varphi_y))$

Since the first part $\frac{f_m^2}{8r_\epsilon}$ contains nothing about the vibration condition and is also slowly varying, therefore it can removed by using a high pass filter as shown in Figure 6.4.

Now, $\frac{a_z^2}{2r_\epsilon}$ is relatively small compared with $a = \frac{f_m a_z}{2r_\epsilon}$, for example, let $a_z = 10$ μmand $f_m = 200$ μm, then

$$\frac{\frac{a_z^2}{2r_\epsilon}}{\frac{f_m a_z}{2r_\epsilon}} = \frac{a_z}{f_m} = 0.05$$

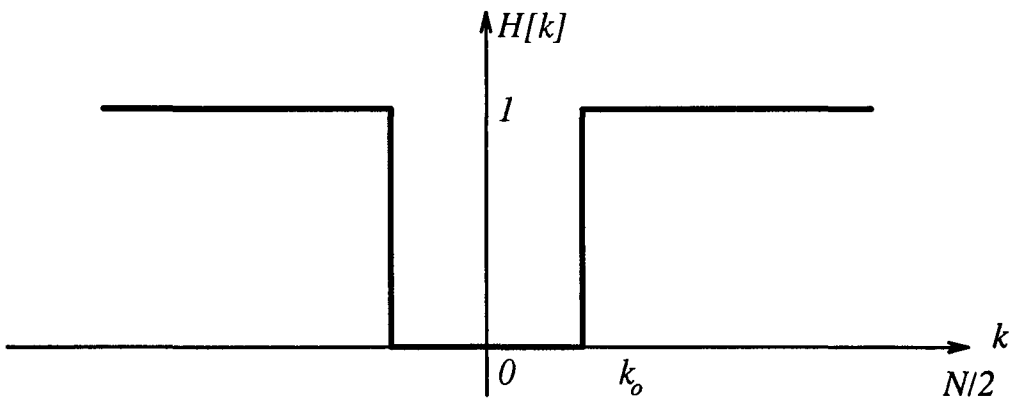

Figure 6.4: The high pass filter H[k] for removing terms like $\frac{f_m^2}{8r_e}$

Therefore it can be concluded that the dominant part in the roundness of the workpiece after the high pass filtering is

$$f[n] = a\cos(\frac{2\pi k_o n}{N} + \varphi_z + b\sin(\frac{2\pi k_m n}{N} + \varphi_y))$$

which is a FM signal. As explained in Chapter 3 and Chapter 4, this type of signal is amenable to be analysed by the WD.

However before analysing the roundness by the WD, it is necessary to convert it into its analytical form in order to remove the redundant spectrum in negative frequencies. This can be done by the Hilbert transform whose implementation requires a filter like the one shown in Figure 6.5

The roundness may also contain high frequency noise, for example, from the instrument electronic circuits. To reduce this noise and (or) to emphasize the term of FM, a lowpass pass filter can be used, See Fig 6.6.

The above three linear operations can be combined into a single bandpass filter such as shown in Figure 6.7

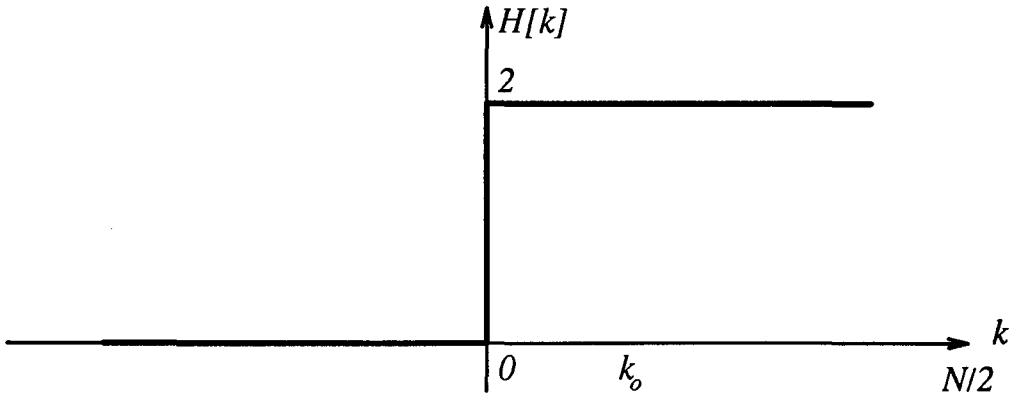

Figure 6.5: The filter H[k] for converting a real signal to its analytical signal.

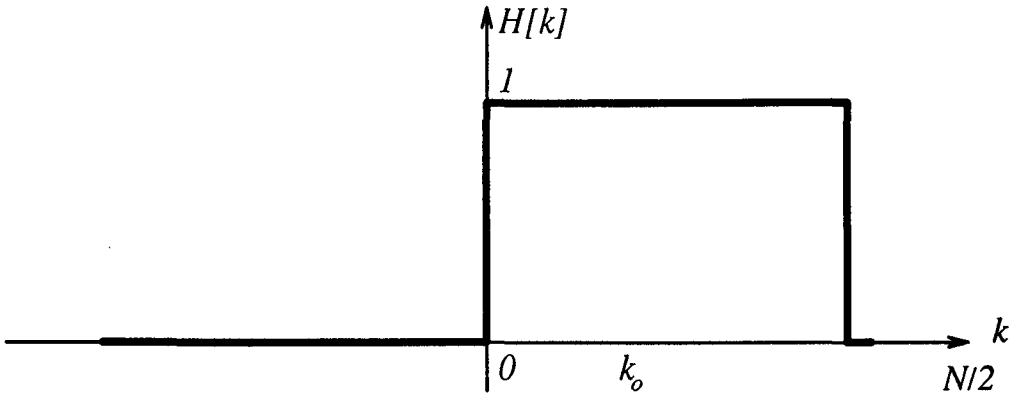

Figure 6.6: The low pass filter H[k] for removing high frequency noises.

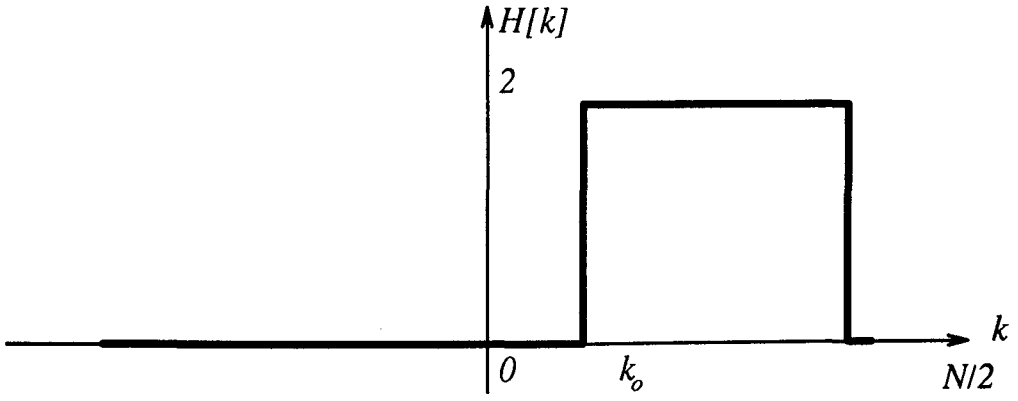

Figure 6.7: The combinded bandpass filter $H[k]$.

After this, the signal $f[n]$ would mainly contains

$$ae^{j(\frac{2\pi k_o n}{N}+\varphi_z+\frac{b}{2}\sin(\frac{2\pi k_m n}{N}+\varphi_y))} \tag{6.18}$$

6.5 The WD and its local moments

6.5.1 The WD

Since the roundness after the operations discussed in the previous section, $f[n]$, is restricted to $[0, N-1]$ (where $N = 256$), it is easy to compute its WD $W_f(n,\theta)$

$$W_f(n,\theta) = \sum_{m=-\infty}^{\infty} 2f[n+m]f^*[n-m]e^{-j2m\theta}$$

Because

$$\begin{cases} 0 \leq n+m \leq N-1 \\ 0 \leq n-m \leq N-1 \end{cases}$$

then

$$\begin{cases} 0 \leq n+m \leq N-1 \\ -(N-1) \leq -n+m \leq 0 \end{cases}$$

$$\begin{aligned} -(N-1) \leq & 2m \leq N-1 \\ -(\frac{N}{2}-1) \leq & m \leq \frac{N}{2}-1 \\ -M \leq & m \leq M \end{aligned}$$

where $M = \frac{N}{2} - 1$. Therefore

$$\begin{aligned} W_f(n,\theta) &= \sum_{m=-M}^{M} 2f[n+m]f^*[n-m]e^{-j2m\theta} \\ &= \sum_{m=0}^{N-1} 2f[n+m-M]f^*[n-m+M]e^{-j2(m-M)\theta} \end{aligned}$$

Let $\theta = \frac{k\pi}{N}$, then

$$W_f(n, \frac{k\pi}{N}) = \sum_{m=0}^{N-1} 2f[n+m-M]f^*[n-m+M]e^{\frac{-j2(m-M)k\pi}{N}}$$
$$= \frac{1}{\sqrt{N}} \sum_{m=0}^{N-1} 2f[n+m-M]f^*[n-m+M]e^{\frac{-j2mk\pi}{N}} \sqrt{N} e^{\frac{j2Mk\pi}{N}}$$

Therefore, to compute the WD is only necessary to compute

1. $2f[n+m-M]f^*[n-m+M]$ where $n, m = 0, 1, 2, \cdots, N-1$.
2. $\frac{1}{\sqrt{N}} \sum_{m=0}^{N-1} (2f[n+m-M]f^*[n-m+M))e^{\frac{-j2mk\pi}{N}}$ where $n, k = 0, 1, 2, \cdots, N-1$ by using Nag (numerical algorithm group) routine such as *c06ecf*.
3. $W_f(n, \frac{k\pi}{N}) = \left(\frac{1}{\sqrt{N}} \sum_{m=0}^{N-1} (2f[n+m-M]f^*[n-m+M])\right) \cdot \sqrt{N} e^{\frac{j2Mk\pi}{N}}$ for $n, k = 0, 1, 2, \cdots, N-1$.

6.5.2 The local moments in frequency

The 0th-order moment in frequency $p_f[n]$ is computed

$$p_f[n] = \frac{1}{2\pi} \int_{-\frac{\pi}{2}}^{\frac{\pi}{2}} W_f(n, \theta) d\theta$$
$$\approx \frac{1}{2N} \sum_{0}^{N-1} W_f(n, \frac{k\pi}{N})$$

The 1st-order moment in frequency $\Theta_f[n]$:

$$\Theta_f[n] = \frac{1}{2} \arg \left(\int_{-\frac{\pi}{2}}^{\frac{\pi}{2}} e^{j2\theta} W_f(n, \theta) d\theta \right)$$
$$\approx \frac{1}{2} \arg \left(\sum_{0}^{N-1} e^{j\frac{2k\pi}{N}} W_f(n, \frac{k\pi}{N}) \right)$$

6.6 Extraction of vibration information

Since

$$f[n] = ae^{j(\frac{2\pi k_o n}{N}+\varphi_x+\frac{b}{2}\sin(\frac{2\pi k_m n}{N}+\varphi_y))} \tag{6.19}$$

where $a = \frac{f_m a_z}{2r_\epsilon}$, $b = \frac{f_z a_y}{n_w r_w}$, $k_o = \frac{f_z}{n_w}\frac{N}{L}$, and $k_m = \frac{f_y}{n_w}\frac{N}{L}$. so

$$p_f(n) = a^2 \tag{6.20}$$

$$\Theta_f(n) = \frac{2\pi k_o}{N} + \frac{b}{2}\sin(\frac{2\pi k_m}{N})\cos(\frac{2\pi k_m n}{N} + \varphi_y) \tag{6.21}$$

6.6.1 a_z and f_z

If we let $\overline{p_f}$ and $\overline{\Theta_f}$ be the mean value for $p_f[n]$ and $\Theta_f[n]$ respectively, i.e.

$$\overline{p_f} = \frac{1}{N}\sum_{n=0}^{N-1} p_f[n]$$

$$\overline{\Theta_f} = \frac{1}{N}\sum_{n=0}^{N-1} \Theta_f[n]$$

it follows that

$$\overline{p_f} = a^2 = (\frac{f_m a_z}{2r_\epsilon})^2$$

$$\overline{\Theta_f} = \frac{2\pi k_o}{N} = \frac{2\pi f_z}{n_w L}$$

from which

$$a_z = \frac{2r_\epsilon\sqrt{\overline{p_f}}}{f_m}$$

$$f_z = \frac{n_w L\overline{\Theta_f}}{2\pi}$$

6.6.2 a_y and f_y

By finding the local maximum of the DFT of $\Theta_f[n]$ it is easy to obtain the values for $\frac{b}{2}\sin\left(\frac{2\pi k_m}{N}\right)$ and k_m. So a_y and f_y can be obtained through

$$a_y = \frac{n_w r_w b}{f_z}$$
$$f_y = \frac{n_w L k_m}{N}$$

6.7 An example of extracting vibration data from roundness

Figure 6.7 and Figure 6.9 present a complete example of extracting vibration data from a measured roundness.

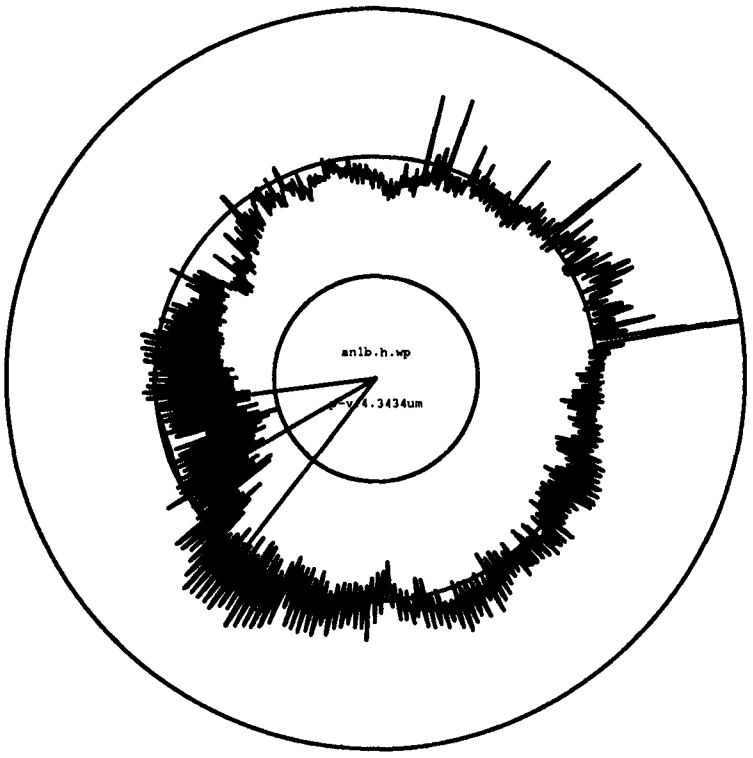

Figure 6.8: The measured roundness and the section chosen for extraction vibration data

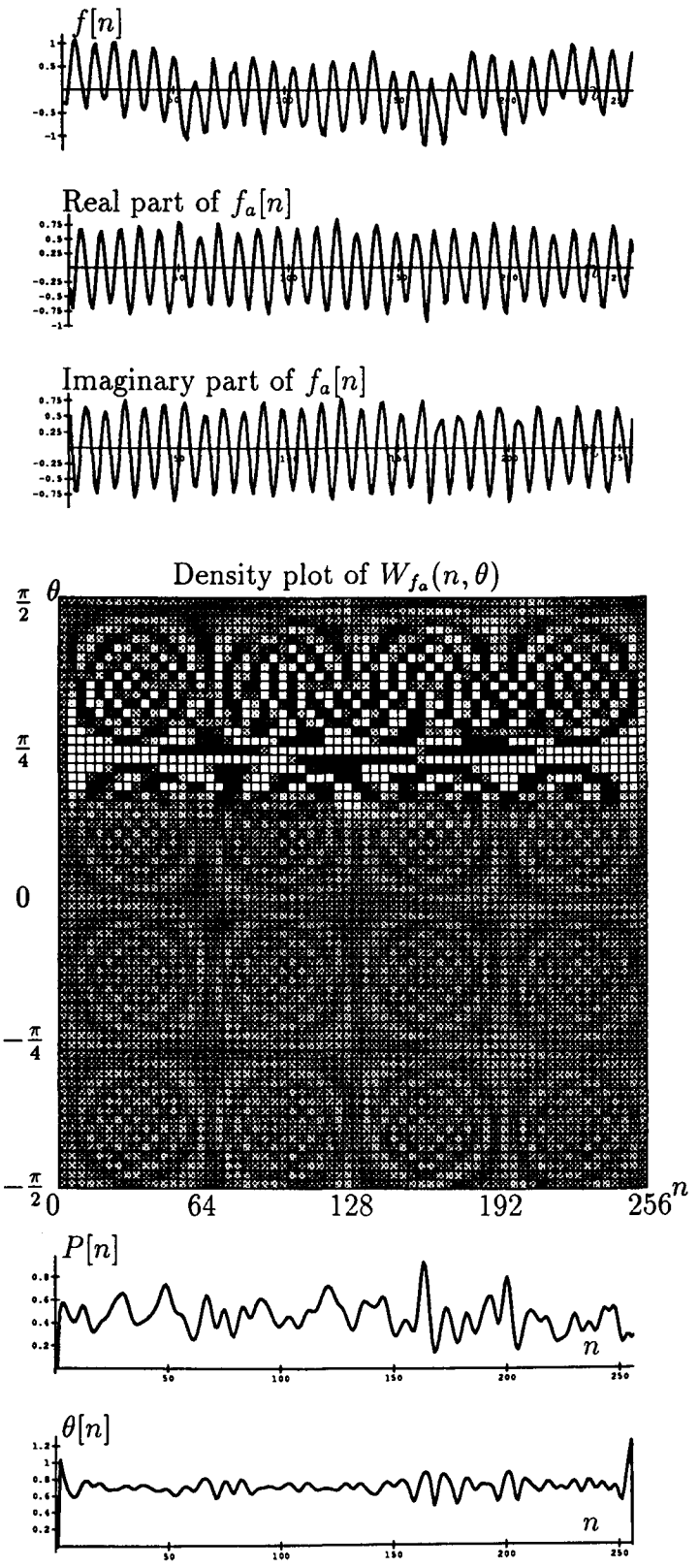

Figure 6.9: Measured: $a_z = 8.3$, $f_z = 3600.0$, $a_y = 22.6$, $f_y = 3600.0$. Extracted: $a_z = 10.8$, $f_z = 3615.3$, $a_y = 34.7$, $f_{..} = 3615.3$.

6.8 Results

Here are three cases of extracting vibration parameters from roundness data via the WD. As for the measured a_y and a_z, the absolute error is about $\pm 0.25\mu$m; while for the measured f_y and f_z, the absolute error is about ± 7 Hz. Note that for y direction the vibration was measured 1.5 cm away from the tip; for z direction it was 0.5 cm away from the tip. Therefore the measured vibration amplitudes have been corrected, see Section 5.12.3.

Case 1 With the cutting condition as

cutting tool: S10K-STFCR09

overhang = 45 mm,

depth of cut = 200 μm, feed = 100 μm, rpm = 935,

radius of workpiece = 32 mm, radius of tool tip = 800 μm,

the results are listed in Table 6.1.

Table 6.1: Experimental results: case 1

	a_z μm	f_z kHz	a_y μm	f_y kHz
measured	6.6	3.60	11.4	3.60
extracted	10.2	3.49	31.1	3.49
extracted	10.7	3.62	35.9	3.49
extracted	11.0	3.49	28.0	3.49
$\frac{\text{extracted}}{\text{measured}}$ in average	1.60	0.98	2.80	0.97

Case 2 With the cutting condition as

cutting tool: S10K-STFCR09

overhang = 65 mm,

depth of cut = 50 μm, feed = 100 μm, rpm = 935,

radius of workpiece = 32 mm, radius of tool tip = 800 μm,

the results are listed in Table 6.2.

Table 6.2: Experimental results: case 2

	a_z μm	f_z kHz	a_y μm	f_y kHz
measured	10.2	1.60	72.2	1.60
extracted	26.2	1.62	234.8	1.62
extracted	24.0	1.62	235.0	1.62
extracted	30.7	1.62	239.4	1.62
$\frac{\text{extracted}}{\text{measured}}$ in average	2.65	1.01	3.28	1.01

Case 3 With the cutting condition as

cutting tool: S10K-STFCR09

overhang = 65 mm,

depth of cut = 50 μm, feed = 100 μm, rpm = 935,

radius of workpiece = 32 mm, radius of tool tip = 800 μm,

the results are listed in Table 6.3.

From Table 6.1 to Table 6.3, a number of points emerge. One concerns the validity of the cantilever model for the cutting tool vibration. This says that the natural frequency even during cutting is given by f_1

$$f_1 = \frac{k_1^2}{2\pi}\sqrt{\frac{Eg}{A\sigma}\frac{bh^3}{12}}$$

Table 6.3: Experimental results: case 3

	a_z μm	f_z kHz	a_y μm	f_y kHz
measured	9.4	1.70	39.8	1.70
extracted	39.7	1.75	153.7	1.75
$\frac{\text{extracted}}{\text{measured}}$	4.23	1.03	3.86	1.03
measured	7.0	1.70	38.6	1.70
extracted	33.5	1.75	130.1	1.75
$\frac{\text{extracted}}{\text{measured}}$	4.8	1.03	3.37	1.03
measured	9.3	1.70	38.6	1.70
extracted	26.2	1.87	174.7	1.87
$\frac{\text{extracted}}{\text{measured}}$	2.83	1.10	4.52	1.10
$\frac{\text{extracted}}{\text{measured}}$ in average	3.95	1.05	3.92	1.05

where $k_1 = \frac{1.875}{l}$. For the Sandvic cutting used, $E = 2.0 \times 10^7$ N/cm^2, $g = 980$ cm/s^2, $\sigma = 0.0764$ N/cm^3, $b = h = 1$ cm, $A = 1cm^2$, and l, the effective overhang of the tool which in the case of this experiment took two values 4.5 cm and 6.5 cm,

$$f_1 = \begin{cases} 3.9\text{kHz} & l = 4.5\text{cm} \\ 1.9\text{kHz} & l = 6.5\text{cm} \end{cases} \tag{6.22}$$

These are compared well with the measured values of 3.6 kHzand 1.7 kHz, respectively. The small reduction is attributable to the damping of the cutting process. These results show that within the errors of this experience the model is satisfactory and that vibration due to the tool column is not significant when compared with that of the tool.

A comparison between the measured vibration frequencies and those picked out by the Wigner Moment Analysis of the roundness graphs is very encouraging. The relative errors are within a few percent only. This proves that the Wigner distribution can be used as an indirect measure of tool vibration.

That the amplitude of the measured vibration is small compared with those

determined by the WD is predictable. This is due to the fact the LVDT measuring the vibration cannot be located at the tool tip. It therefore measures a smaller movement, and if higher order vibration modes are present, there may be a large ratio factor of the measured amplitude to the tool tip amplitude; however, this ratio should be constant for a given cutting condition. In fact, it is exactly for this reason that the indirect method is a better alternative to detect vibration than the more direct method. Furthermore, it is vibration at the workpiece which is important not the vibration anywhere along the tool shank. Producing the workpiece after all is the reason for using the machine tool.

6.9 Conclusions

It has been demonstrated that by using the Wigner distribution, a potentially useful new tool for detecting cutting tool vibration prior to machining failure has been developed. In this preliminary study turning has been chosen as the process to be monitored because it is more easily understood than, say grinding. Furthermore, it has been possible to measure the vibration directly to verify the method. The practical results so far obtained are limited and more work needs to be carried out in this area both for turning and for other processes, but the results obtained are encouraging.

It also seems plausible that an optical on-line instrument could be developed to monitor the surface without contact. This will be the object of further work in the use of the Wigner distribution for monitoring machine tool conditions.

6.10 Simulation

In this section, the roundness is simulated according to the mathematical model discussed previously. The input for the simulation program is the parameters about tool vibration, they are the amplitudes (a_z, a_y), the frequencies (f_z, f_y), and the initial phases (ϕ_z, ϕ_y) for both horizontal $(z)$and vertical (y) directions. The output is the extracted values for a_z, a_y, f_z and f_y.

For an example, with the RPM 900, the feed 200 μm, the radius of the workpiece 32 mm, and the radius of the insert tip 0.8 mm. The results are listed in Table 6.4 and Table 6.5.

Table 6.4: Simulation results of varying amplitudes

	a_z	f_z	a_y	f_y
unit	μm	kHz	μm	kHz
true	10.0	1.80	100.0	1.80
extracted	9.9	1.80	112.2	1.80
error (%)	1.0	0	12.2	0
true	15.0	1.80	150.0	1.80
extracted	14.8	1.80	166.1	1.80
error (%)	0.1	0	10.7	0
true	20.0	1.80	200.0	1.80
extracted	19.4	1.80	217.4	1.80
error (%)	3.0	0	8.7	0
true	25.0	1.80	250.0	1.80
extracted	23.7	1.80	265.2	1.80
error (%)	0.5	0	6.1	0
true	30.0	1.80	300.0	1.80
extracted	27.6	1.80	308.7	1.80
error (%)	3.0	0	2.9	0
maximum error (%) for all	3.0	0	12.2	0
average error (%) for all	1.5	0	8.1	0

Table 6.5: Simulation results of varying frequencies

	a_z	f_z	a_y	f_y
unit	μm	kHz	μm	kHz
true	10.0	1.50	100.0	1.50
extracted	9.9	1.56	110.3	1.56
error (%)	1.0	4.0	10.3	4.0
true	10.0	1.60	100.0	1.60
extracted	9.9	1.68	114.7	1.56
error (%)	1.0	5.0	14.7	4.0
true	10.0	1.70	100.0	1.70
extracted	9.9	1.68	118.1	1.68
error (%)	1.0	1.2	18.1	1.2
true	10.0	1.80	100.0	1.80
extracted	9.9	1.80	112.2	1.80
error (%)	1.0	0.0	12.2	0.0
true	10.0	1.90	100.0	1.90
extracted	9.9	1.92	111.4	1.92
error (%)	1.0	1.1	11.4	1.1
maximum error (%) for all	1.0	4.0	18.1	4.0
average error (%) for all	1.0	2.3	13.8	2.1

Notice that the frequencies f_z and f_y can be extracted by the WD quite accurately, with the relative error less than 4.0 percent. The error for extraction of a_y is usually less than 15 percent, this is due to the fact that preprocessing the roundness data has not completely removed the low and high frequency parts. If necessary, more refined bandpass filters can be used. Extraction of a_z is successful, with its error less than 3 percent. This is rather encouraging for the deviation from roundness is mainly due to a_z (with the feed) rather than a_y.

Chapter 7

Conclusions

One of the major constituents of computer integrated manufacturing is the field of machine tool capability and machine tool monitoring. This is economically a necessity because of the high cost of failure of the machine tool and also of failure to meet the quality requirements of the parts produced. This need has led to much work being carried out to detect incipient failure due to chatter, tool wear or breakage, slideway and bearing error. In particular, the monitoring of the cutting tool itself is emerging as one of the most important areas because of the increased use of precision manufacturing in nanotechnology and other high technology areas.

Basically there are two methods: direct (such as the actual measurement of tool wear using optical or radioactive methods), and indirect (involving measurement of parameters associated with the cutting process such as cutting forces, vibration, sound, acoustic emission, cutting temperature and surface texture). In this thesis, the surface analysis method is investigated because this serves a dual purpose. The surface geometry has to be controlled and preferably known in order to meet the functional requirements of the workpiece. It seems logical therefore to use the surface geometry not only to predict function but also to control manufacture.

During the early days (Reason 1944), a single number such as R_a was used to characterise the surface and predict the function of the workpiece. Despite

limited success, there were and are two problems associated with this approach. The first is that the change in the surface parameter did not necessarily identify the cause and the second is that this method was usually too slow to have stopped a large number of faulty components being made.

To overcome these problems, the concepts of random process analysis were introduced (Peklenik, 1968). This allowed a much better link between the geometry and the process to be made. By means of the power spectrum and the correlation function many aspects of manufacture could be identified.

However, even random process analysis as described has a conceptual limitation. This is due to the fact that it is presented either spatially (as a correlation function) or as a frequency plot (as the power spectrum). This is a disadvantage in some respects because it precludes the easy assessment of changes in the process. With the power spectrum or correlation function, it is difficult to measure the changes in the power spectrum in space i.e. over the surface of one workpiece. Therefore, what is needed is some function, probably based on Fourier and random process concepts, which is equally defined in the space and frequency domain; one which can characterise the surface geometry in space and frequency simultaneously and also preferably be realised instrumentally. There are at least two possibilities, the ambiguity function (AF) and the Wigner distribution (WD). After comparing these two functions in detail, the conclusion is reached that the Wigner distribution is the most likely to be useful as an analysing tool.

Although it is suitable for characterising both stationary and nonstationary signals, the WD contains too much information, which means data condensation is required. The Hough transform (HT) was tried. It turned out that the HT did not work very well despite its success with chirp signals. Next the method based on local moments in frequency for the WD was tested and found to be successful. This was verified for both simulated and real data (Zheng and Whitehouse 1992).

The technique of cutting tool monitoring by the WD has several advantages:

1. It is straightforward in spite of the fact that the WD is more complicated than the Fourier transform (FT).

2. It does not interfere with cutting processes.

3. It is indirect, but can reveal the direct effect of cutting condition, in particular, tool vibration.

4. Besides being able to extract tool vibration, it can be extended to extract other information such as tool wear and breakage.

5. It is possible to build an in-process integrated machine tool diagnosis system from this technique. This may be achieved by measuring the roundness optically, computing its WD and extracting parameters optically. It can also be realised by on-line measuring the roundness, and using a microcomputer for computation and control.

Despite the above advantages, this technique has its drawbacks:

- It is computationally more expensive than the FT because the WD is a function of two variables

- At present it is not in-process although it can be extended to in-process.

In conclusion, after comparing the FT, the AF, and the WD, it has been demonstrated that the WD is a very useful analysising tool which can be successfully used for cutting tool monitoring by extracting vibration data.

In addition to this application, a number of developements are possible in future. Potential usage of local spatial moments and global moments should be explored more fully. For example the first local spatial moment can be used as an indication of the position of freak behaviour on the surface, and the second local spatial moment can be used as a measure of the size of the freak. This has obvious implications for process control and flaw detection.

An in-process instrument based on the WD can be built. This is because the WD is in fact the Fourier transform of $f(x + \frac{x}{2})f^*(x - \frac{x}{2})$ provided that x is treated as a fixed parameter. Hence, the WD can be achieved through optical transformation, i.e. in an optical instrument.

Application to grinding should be explored. In principle, the WD will work as well for a statistical signal as for a deterministic signal, so the problem should be tractable. The problem of wear should also be tractable, since it can be divided into a combination of texture analysis; as the microscopic shape of the surface changes during wear, and flaw detection; as for example, the detection of pit formation. The WD also forms a rather complete description of surface texture. It may therefore be possible to relate this quantitatively to frictional properties of surfaces.

Its application is not restricted to surface analysis and indeed a project has recently commenced at Warwick University on its application to X-ray reflectivity data.

Futher applications of the WD, such as flaw detection, wear, friction, should be explored.

Even from the limited amount of work carried out in this thesis it could be concluded that the WD provides powerfull mathematical framework for application to machine tool condition monitoring.

References

Akgerman, N. and Frisch, J. 1971. *The use of a cutting force spectrum for tool wear compesation during turning.* Proceedings of 12th International Machine Tool Design and Research Conference v 2 n 8 p 517-526.

Allen, J. B. and Rabiner, L. R. 1977. *A unified approach to short-time Fourier analysis and Synthesis.* Proceedings of the IEEE v 65 n 11 p 1558-1564.

Bastiaans, M. J. 1978. *The Wigner distribution applied to optical signals and systems.* Optics Communications v 25 n 1 p 26-30.

Bastiaans, M. J. 1979. *Transport equations for the Wigner distribution function.* Optica Acta v 26 n 10 p 1265-1272.

Bath, M. and Sharp, R. 1968. *In-process control of lathes improves accuracy and productivity.* Proceedings of 9th International Machine Tool Design and Research Conference v 22 p 1209-1221.

Bhattacharyya, A. and Ham, I. 1969. *Analysis of tool wear part 1: theoretical models of flank wear.* Journal of Engineering for Industry, Transactions ASME v 22 p 790-798.

Boashash, B. 1988. *Note on the use of the Wigner distribution for time-frequency signal analysis.* IEEE Transactions on Acoustics, Speech, and Signal Processing v 36 n 9 p 1518-1521.

Boashash, B. and Black, P. J. 1987. *An efficient eeal-time implementation of the Wigner-Ville distribution.* IEEE Transactions on Acoustics, Speech, and Signal Processing v ASSP-35 n 11 p 1611-1618.

Boctor, S. A. 1987. *Electric Circuit Analysis.* Prentice-Hall, Inc.

Boothroyd, G. 1975. *Fundamentals of metal maching and machine tools.* McGraw-Hill.

Boothroyd, G.; Eagle, J. M. and Chisholm, W. J. 1967. *Effect of tool tlank wear on the temperatures generated during metal cutting.* Proceedings of 8th International Machine Tool Design and Research Conference v ASSP-35 n 11 p 667-680.

Boudreaux-Bartels G. F. and Parks, T. W. 1980. *Time-varying filtering and signal estimation using Wigner distribution synthesis techniques.* IEEE Transactions on Acoustics, Speech, and Signal Processing v ASSP-34 n 3 p 442-451.

Brigham, E. O. 1988. *The Fast fourier transform and its applications.* Prentice-Hall.

Broch, J. T. 1980. *Mechanical Vibration and Shock Measurement.* Bruel & Kjaer.

Bruck, Y. M. and Sodin, L. G. 1979. *On the ambiguity of the image reconstruction problem.* Optics Communications v 30 n 3 p 304-308.

Bulletin of Japan Society of Mechanical Engineers v 24 p 748-755.

Carlson, A. B. 1986. *Communication Systems.* McGraw-Hill, Inc.

Classen, T. A. C. M. and Meeklenbrauker, W. F. G. 1980. *The Wigner distribution: a tool for time-frequency signal analysis, part 1: continuous time signals.* Philips J Res v 35 p 217-250.

Classen, T. A. C. M. and Meeklenbrauker, W. F. G. 1980. *The Wigner distribution: a tool for time-frequency signal analysis, part 2: discrete time signals.* Philips J Res v 35 p 276-350.

Classen, T. A. C. M. and Meeklenbrauker, W. F. G. 1980. *The Wigner distribution: a tool for time-frequency signal analysis, part 3: relations with other time-frequency signal transformations.* Philips J Res v 35 p 372-389.

Classen, T. A. C. M. and Meeklenbrauker, W. F. G. 1983. *The aliasing problem in discrete-time Wigner distributions.* IEEE Transactions on Acoustics, Speech, and Signal Processing v ASSP-31 n 5, p 1067-1072.

Collacott, R. A. 1979 *Vibration Monitoring and Diagnosis.* George Godwin Limited, London.

Colwell, L. V. 1971. *Methods for sensing the rate of tool wear.* CIRP Annals v 19 p 647-651.

Colwell, L. V. 1975. *Cutting temperature versus tool wear.* CIRP Annals v 24 p 73-76.

Cook, N. H. 1980. *Tool wear sensors.* Wear v 62 p 49-57.

Cook, N. H. and Subramanian, K. 1978. *Micro-isotope tool wear sensor.* CIRP Annals v 27 p 73-78.

Cooley, J. W. and Tukey, J. W. 1965. An algorithm for the machine calculation of complex fourier series. Math. Computation, v 19 p 297-301.

Dalpiaz, G. and Remondi, M. 1988. *Use of acoustic emission for cutting process monitoring in turning.* The Journal of Condition Monitoring v 1 p 1-26.

Danai, K. and Ulsoy, A. G. 1987. *A Dynamic state model for on-line tool estimation in turning.* Journal of Engineering for Industry, Transactions ASME v 109 p 396-399.

De Bruijn, N. G. 1973. *A theory of generalized functions with applications to Wigner distribution and Weyl correspondence.* v XXI p 205-280.

De Bruijn, N. G. *Uncertainty principles in Fourier analysis.*

Del Taglia, A.; Portunato, S. and Toni, P. 1976. *An Approach to on-line measurement of tool wear by spectrum analysis.* Proceedings of 17th International Machine Tool Design and Research Conference v 107 p 141-148.

Diei, E. N.; and Dornfeld, D. A. 1987. *A model of tool fracture generated.*

Doebelin, E. O. 1983. *Measurement Systems: Application and Design.* McGraw-Hill, Inc.

Duda, R. O. and Hart, P. E. 1972. *Use of the Hough transformation to detect lines and curves in pictures.* Communications of ACN v 15 n 1 p 11-15.

El Gomayel, J. L. and Bregger, K. D. 1986. *On-line tool wear sensing for turning operations.* Journal of Engineering for Industry, Transactions ASME v 108 p 44-47.

Emel, E. and Kannatey-Asibu Jr, E. 1988. *Tool failure monitoring in turning by pattern recognition analysis of AE signals.* Journal of Engineering for Industry, Transactions ASME v 110 p 137-145.

Giusti, F. and Santochi, M. 1979. *Developement of a fibre optic sensor for in process measurement of tool flank wear.* Proceedings of 20th International Machine Tool Design and Research Conference v 35 p 351-360.

Giusti, F.; Santochi, M. and Tantussi, G. 1984. *A flexible tool wear sensor for NC lathes.* CIRP Annals v 33 p 229-232.

Groover, M. P.; Karpovich, R. J. and Levy, E. K. 1977 *A study of the relationship between remote thermocouple temperatures and tool wear in machining.* International Journal of Production Research v 25 p 129-141.

Guigay, J. P. 1978. *The ambiguity function in diffraction and isoplanatic imaging by partially coherent beams.* Optics Communications v 26 n 2 p 129-41.

Higdon, A. and et al, 1985. *Mechanics of Materials.* John Wiley & Sons.

Hilburn, J. L. and Johnson, D. E. 1973. *Manual of Active Filter Design.* McGraw-Hill.

Hingle, H. T. and Rakels, J. H. 1983. *The Practical application of diffraction techniques to assess surface finish of diamond turned parts.* CIRP Annals v 32 p 499-501.

Hingle, H. T. 1986. *Tool wear monitoring by the component.* International conference on "Modern Production and Production Metrology"

Hough, P. V. C. 1962. *Methods and means for recognizing complex pattern.* U.S. Patent 3,069,654.

Iwata, K. and Moriwaki, T. 1976. *An Application of Acoustic Emission Measurement to In-Process Sensing of Tool Wear.* CIRP Annals v 25 p 21-26.

Jeon, J. U. and Kim, W. 1988. *Optical flank wear monitoring of cutting tool by image processing.* Wear v 127 p 207-217.

Jones, Barry E. 1989. *Industrial metrology and sensors.* COMPEURO '89 - 3rd Annual European Computer Conference. VLSI and Computer Peripherals. p 3/1-8.

Kegg, R. L. 1984. *On-line machine and process diagnostics.* CIRP Annals v 32 p 469-473.

Koren, Y. 1978. *Flank wear model of cutting tools using control theory.* Journal of Engineering for Industry, Transactions ASME v 100 p 103-109.

Koren, Y. *et al* 1970. *Mathematical model for the flank wear while turning steel with carbide tools.* CIRP Annals v 21 p 19-20.

Koren, Y.; Uisoy, A.G. and Danai, K. 1986. *Tool wear and breakage detection using a process model.* CIRP Annals v 35 p 283-288.

Kramer, B. M. and Suh, N. P. 1980. *Tool wear solution: a quantitative understanding.* Journal of Engineering for Industry, Transactions ASME v 102 p 303-309.

Lan. M. S. and Dornfeld, D. A. 1984 *In-process tool fracture detection.* Journal of Engineering Material and Technology, Transactions ASME v 106 p 111-118.

Lee, J. L. et al 1980. *Ambiguity processing by joint Fourier transform holography.* Applied Optics v 19 n 6 p 895-899.

Lee, L. C. 1986. *A Study of noise emission for tool failure prediction.* International Journal of Machine Design and Research v 26 p 205-215.

Lenz, E.; Katz, Z. and Rubenstein, C. 1976. *The influence of tool/chip contact length on cutting behavior and its use in tool selection.* CIRP Annals v 25 p 33-38.

Li, D. and Mathew, J. 1990. *Tool wear and failure monitoring techniques for turning — a review.* International Journal of Machine Tools & Manufacture v 30 n 3 p 579-598.

Mackinnon, R.; Wilson, G. E. and Wilkinson, A. J. 1986. *Tool condition monitoring using multi-component force measuremnts.* Proceedings of 26th International Machine Tool Design and Research Conference v 10 p 317-324.

Marks II, R. J. and Hall, M. W. 1979. *Ambiguity function display using a single 1-D input.* Applied Optics v 18 n 15 p 2539-2540.

Marks II, R. J.; Walkup, J. F. and Krile, T. F. 1977. *Ambiguity function display: an improved coherent processor.* Applied Optics v 16 n 3, p 1777-1777.

Martin, K. F. *et al* 1986. *A Comparison of in-process tool wear measurement methods in turning.* Proceedings of 26th International Machine Tool Design and Research Conference v 16 n 3, p 289-296.

Martin, K. F. *et al* 1986. *A Comparison of in-process tool wear measurement methods in turning.* Proceedings of 26th International Machine Tool Design and Research Conference v 16 n 3, p 289-296.

Martin, P.; Mutel, B. and Drapier, J. P. 1974. *Influence of lathe tool wear on the vibrations sustained in cutting.* Proceedings of 15th International Machine Tool Design and Research Conference v 16 n 3, p 251-257.

Matsushima, K.; Kawabata, T. and Sata, T. 1979. *Recognition and control of the morphology of tool failures.* CIRP Annals v 28 n 1 p 43-47.

Matsushima, K.; Bertok, P. and Sata, T. 1982. *In-process detection of tool breakage by monitoring the spindle motor current of a machine tool.* Measurement and Control for Batch Manufacturing, ASME, p 145-154.

Merlin, P. M. and Farber, D. J. 1975. *A parallel mechanism for detecting curves in pictures.* IEEE Transactions on Computer v C-24 n 1 p 96-98.

Metel'kov, V. P. and Liberman, Ya. L 1989. *On setting up a system for automatic detection of cutting tool breakage from the current of the main machine tool drive.* Soviet Engineering Research v 9 n 6 p 61-65.

Micheletti, G. F.; Keonig, W. and Victor, H. G. 1976. *In process tool wear sensors for cutting operations.* CIRP Annals v 25 p 483-496.

Micheletti, G. F.; De Filippi, A. and Ippolito, R. 1968. *Tool wear and cutting forces in steel turning.* CIRP Annals v 16 p 353-360.

Novak, A. and Ossbahr, G. 1986. *Reliability of the cutting force monitoring in FMS-instalations.* Proceedings of 26th International Machine Tool Design and Research Conference v 81 p 325-329.

Oppenheim, A. V. 1983. *Signals and systems.* Prentice-Hall.

Pandit,S. M. 1977. *Stochastic linearization by data dependent systems.* Journal of Engineering for Industry, Transactions ASME v 27 p 221-226.

Pandit,S. M. 1978. *Data dependent systems approach to stochastic tool life and reliability.* Journal of Engineering for Industry, Transactions ASME v 100 p 318-322.

Pandit,S. M. and Kashou,S. 1982. *A Data dependent systems of on-line tool wear sensing.* Journal of Engineering for Industry, Transactions ASME v 104 p 217-223.

Papoulis, A. 1974. *Ambiguity function in fourier optics.* Journal of the Optical Society of America v 64 n 6 p 779-788.

Papoulis, A. 1984. *Signal analysis.* McGraw-Hill.

Papoulis, A. 1962. *The Fourier integral and its application.* McGraw-Hill.

Pedersen, K. B. 1990. *Wear measurement of cutting tools by computer vision.* International Journal of Machine Tools & Manufacture v 30 n 1 p 131-139.

Peyrin, F. and Prost, R. 1986. *A unified definition for the discrete-time, discrete-frequency, and discrete-time/frequency Wigner distributions.* IEEE Transactions on Acoustics, Speech, and Signal Processing v ASSP-34 n 4 p 858-867.

Raja, J. and Whitehouse, D. J. 1983. *Application of complex demodulation techniques to surface analysis.* Precision Engineering v 5 n 1 p 17-21.

Raja, J. and Whitehouse, D. J. 1984. *An investigation into the possibility of using surface profiles for machine tool surveillance.* International Journal of Production Research v 22 n 3 p 453-466.

Rakels, J. H. and Hingle, H. T. 1986. *The use of optical diffraction techniques to obtain information about surface finish, tool shape and machine tool condition.* Wear v 109 p 259-266.

Ramalingam, S. and Watson, J. D. 1978. *Tool life distributions part 4: minor phases in work material and multiple-injury tool failure.* Journal of Engineering for Industry, Transactions ASME v 100 p 201-209.

Ramalingam, S.; Peng, Y. I. and Watson, J. D. 1978. *Tool life distributions part 3: mechanism of single injury tool failure and tool life distribution in*

in interrupted cutting. Journal of Engineering for Industry, Transactions ASME v 100 p 193-200.

Rau, N. and Huebner, G. 1986. *Optical measurements of chatter marks.* Wear v 109 p 225-239.

Reis, F. B. 1962. *A linear transformation of the ambiguity function plane.* IRE Trans. on Information Theory v 8 n 1 p 59.

Rudin, W. 1973. *Functional analysis.* McGraw-Hill.

Rudin, W. 1976. *Principles of mathematical analysis.* McGraw-Hill.

Rudin, W. 1986. *Real and complex analysis.* McGraw-Hill.

Sadat,A. B. and Raman,S. 1987. *Detection of tool flank wear using acoustic signature analysis.* Wear v 115 p 265-272.

Said, R. A. K. and Cooper, D. C. 1973. *Crosspath real-time optical correlator and ambiguity function processer.* Proceedings of IEE v 120 n 4 p 423-428.

Sakuma, K. and Seto, M. 1981. *Tool wear in cutting glass-fiber-reinforced-pl astics(the relation between cutting temperature and tool wear.*

Shillam, N. F. 1971. *The On-line control of cutting condition using direct feedback.* Proceedings of th International Machine Tool Design and Research Conference v 28 p 15-21.

Siebert, W. M. 1958. *Studies of Woodward's uncertainty function.* Quarterly Progress Report - Res. Lab. of Electronics, MIT v 28 p 15-21.

Stein, J. L. *et al* 1984. *Current Monitoring on DC servo machine tool feed drives.* "Sensors and Control for Automated Manufacturing and Robtics" edited by Stelson, A. and Sweet, L. M. ASME p 45-65.

Stoferle, T. H. and Bellmann, B. 1975. *Continuous measuring of flank wear.* Proceedings of 16th International Machine Tool Design and Research Conference v 29 p 573-578.

Stutt, C. A. 1959. *A note on invariant relations for ambiguity.* IRE Trans. on Information Theory v IT-4 p 164-167.

Stutt, C. A. 1964. *Some results on real-part/imaginary-part and magnitude-phase relations in ambiguity functions.* IEEE Trans. on Information Theory v IT-10 p 321-327.

Sussman, S. M. 1962. *Least-square synthesis of radar ambiguity functions.* IRE Trans. on Information Theory v IT-2, p 246-254.

Suzuki, H. and Weinamann, K. J. 1985. *An on-line tool wear sensor for straight turning operations.* Journal of Engineering for Industry, Transactions ASME v 107 p 397-399.

Sweeney, G. 1971. *Vibration of Machine Tools.* The Machinery Publishing Co. , Ltd.

Tönshoff, H. K. *et al* 1988. *Developments and trends in monitoring and control of machining processes* CIRP Annals v 37 n 2 p 611-622.

Titlebaum, E. L. 1966. *A generalization of two-fimensional fourier transform property for ambiguity functions.* IRE Trans. on Information Theory v IT-6 p 80-81.

Tlusty, J. and Andrews, G. C. 1983. *A critical review of sensors for unmanned machining.* CIRP Annals v 32 p 563-572.

Tlusty, J. and Masood, Z. 1978. *Chipping and breakage of carbide tools.* Journal of Engineering for Industry, Transactions ASME v 100 p 403-412.

Tobias, S. A. 1965. *Machine-Tool Vibration.* Blackie.

Tsao, K. C.; Husein, A. B. and Wu, S. M. 1968. *Cutting tool crater wear measurement by the lapping-comparator technique.* International Journal of Machine Tools & Manufacture v 8 p 15-26.

Uehara, K.; Kiyosawa, F. and Takeshita, H. 1979. *Automatic tool wear monitoring in NC turning.* CIRP Annals v 28 p 39-42.

Usui, E. and Hirota, A. 1978. *Analytical prediction of three dimensional cutting process part 2: chip formation and cutting force with conventional single-point tool.* Journal of Engineering for Industry, Transactions ASME v 100 p 229-243.

Vijaya Kumar, B. V. K.; Neuman, C. P. and DeVos, K. J. 1986. *Signal Processing.* v 11 p 277-304.

Ville, J. 1948. *Theories et application de la notion de signal analytique.* Cables Et Transmission v 2 p 61-74.

Weller, E. J. *et al* 1969. *What sound can be expected from a worn tool?.* Journal of Engineering for Industry, Transactions ASME v 25 p 525-534.

Whitehouse, D. J. 1978. *Beta functions for surface typologie?* CIRP Annals v 27 p 491-497.

Whitehouse, D. J. 1978. *Surfaces — A link between manufacture and function.* Proceedings of Institution of Mechanical Engineers v 192 p 179.

Whitehouse, D. J. and Zheng, K. G., 1992. *The use of space-frequency functions in machine tool monitoring.* Journal of Physics, Part A General. In press.

Wigner, E. 1932. *On the quantum correction for thermo-dynamic equilibrium.* Phys. Rev. v 40 p 749-759.

Woodward, P. M. 1953. *Probability and information theory with application to radar.* Pergamon.

Wu, S. M. 1964. *Tool-life testing by response surface methodology– part 1.* Journal of Engineering for Industry, Transactions ASME v 40 p 105-110.

Yu, K. B. and Cheng, S. L. 1987. *Signal synthesis from pseudo-Wigner distribution and application.* IEEE Transactions on Acoustics, Speech, and Signal Processing v ASSP-35 n 9 p 1293-1302.

Zakaria, A. A. and El Gomayel, J. I. 1975. *On the reliability of the cutting temperature for monitoring tool wear.* International Journal of Machine Tool Design and Research v 15 p 195-208.

Zheng, K. G. and Whitehouse, D. J. 1992. *The application of the Wigner distribution to machine tool monitoring.* Proceedings of the Institution of Mechanical Engineers. In press.

Appendix A

The Fast Fourier Transform

The fast Fourier transform is an algorithm of efficiently computing

$$F[k] = \sum_{n=0}^{N-1} f[n] e^{\frac{j2\pi kn}{N}} \tag{A.1}$$

For $N = 2^r$, this is derived here (Brigham 1988).

Let k and n be represented in binary form as

$$k = k_{r-1}\, 2^{r-1} + k_{r-2}\, 2^{r-2} + \cdots + k_0$$

$$n = n_{r-1}\, 2^{r-1} + n_{r-2}\, 2^{r-2} + \cdots + n_0$$

and $W = e^{\frac{j2\pi}{N}}$, then

$$\begin{aligned} F[k_{r-1},\, k_{r-2},\, \cdots,\, k_0] = \sum_{n_0=0}^{1} \sum_{n_1=0}^{1} \cdots \sum_{n_{r-1}=0}^{1} & f[n_{r-1},\, n_{r-2},\, \cdots,\, n_0] \\ & \times W^{k_0\, n_{r-1} 2^{r-1}} \times W^{(k_1 2^1 + k_0)\, n_{r-2} 2^{r-2}} \\ & \times \cdots \\ & \times W^{(k_{r-1} 2^{r-1} + k_{r-2} 2^{r-2} + \cdots + k_0)\, n_0} \end{aligned}$$

Performing each of the summations separately and labelling the intermediate results, we obtain

$$
\begin{aligned}
F_0[n_{r-1}, n_{r-2}, \cdots, n_0] &= f[n_{r-1}, n_{r-2}, \cdots, n_0] \\
F_1[k_0, n_{r-2}, \cdots, n_0] &= \sum_{n_{r-1}=0}^{1} F_0[n_{r-1}, n_{r-2}, \cdots, n_0] W^{k_0 n_{r-1} 2^{r-1}} \\
F_2[k_0, k_1, \cdots, n_0] &= \sum_{n_{r-2}=0}^{1} F_1[k_0, n_{r-2}, \cdots, n_0] W^{(k_1 2^1 + k_0) n_{r-2} 2^{r-2}} \\
&\vdots \\
F_r[k_0, k_1, \cdots, k_{r-1}] &= \sum_{n_0=0}^{1} F_{r-1}[k_0, k_1, \cdots, n_0] W^{(k_{r-1} 2^{r-1} + k_{r-2} 2^{r-2} + \cdots + k_0) n_0} \\
F[k_{r-1}, k_{r-2}, \cdots, k_0] &= F_r[k_0, k_1, \cdots, k_{r-1}]
\end{aligned}
$$

$N \log_2(N)$ complex multiplications are required to computer Equation A.1 through the above equations indirectly, while N^2 complex multiplications are required to compute Equation A.1 directly. Therefore, the FFT is very efficient for large N.

The FFT — Makefile

```
OBJ =  dft.o input.o fft.o store_data.o
FLAGS = -g
EXEC = dft
$(EXEC): $(OBJ)
        cc $(FLAGS) $(OBJ) -o $(EXEC) -lm

dft.o: dft.h Makefile
        cc $(FLAGS) -c dft.c -o dft.o
input.o: dft.h Makefile
        cc $(FLAGS) -c input.c -o input.o
fft.o: dft.h Makefile
        cc $(FLAGS) -c fft.c -o fft.o
store_data.o: dft.h Makefile
        cc $(FLAGS) -c store_data.c -o store_data.o
```

The FFT — dft.h

```
#include        <stdio.h>
#include        <math.h>
#include        <strings.h>

#define N       256
#define NU      8

extern  void    input();
extern  void    fft();
extern  void    store_data();
```

The FFT — dft.c

```
#include        "dft.h"

main()
{
        double  f[2][N];
        char    type_of_signal[25];
        char    file_name[250];


        input(f[0], f[1], type_of_signal);

        strcpy(file_name, "/home/hawk/eng/es036/work/fft/Data/");
        strcat(file_name, type_of_signal);
        strcat(file_name, ".sig");
        store_data(f[0], f[1], file_name);


        printf("\n\nDoing FFT ....\n\n");
        fft(f[0], f[1], N, NU);


        strcpy(file_name, "/home/hawk/eng/es036/work/fft/Data/");
        strcat(file_name, type_of_signal);
        strcat(file_name, ".dft");
        store_data(f[0], f[1], file_name);
}
```

The FFT — input.c

```
#include        "dft.h"

void    input(real, imag, type_of_signal)
double  real[], imag[];
char    type_of_signal[];
{
        double  arg;
        int     i;

        printf("\n");
        printf("Choose a signal from:\n");
        printf("    a  sinusoidal signal\n");
        printf("    b  sum of three sinusoidal signals\n");
        printf("    c  chirp signal\n");
        printf("    d  frequency-modulated signal\n");
        printf("\n");
        scanf("%s", type_of_signal);

        if ( type_of_signal[0] == 'a' )
        {       arg = 2.0*3.14159265*32.0/N;
                for (i=0; i < N; i++)
                {       real[i] = cos(arg*i);
                        imag[i] = sin(arg*i);
                }
                strcpy(type_of_signal, "sinu1");
        }
        else if (type_of_signal[0] == 'b')
        {       arg = 2.0*3.14159265/N;
                for (i=0; i < N; i++)
                {       real[i] = 0.5*cos(arg*16.0*i) + cos(arg*32.0*i)
                                + 0.25*cos(arg*48.0*i);
                        imag[i] = 0.5*sin(arg*16.0*i) + sin(arg*32.0*i)
                                + 0.25*sin(arg*48.0*i);
                }
                strcpy(type_of_signal, "sinu3");
        }
        else if (type_of_signal[0] == 'c')
        {       arg = 3.14159265/(2.0*N);
                for (i=0; i < N; i++)
                {       real[i] = cos(arg*0.5*i*i);
                        imag[i] = sin(arg*0.5*i*i);
                }
                strcpy(type_of_signal, "chirp");
        }
        else if (type_of_signal[0] == 'd')
        {       arg = 2.0*3.14159265/N;
                for (i=0; i < N; i++ )
                {       real[i] = 1.0*cos(arg*32.0*i + 3.0 * sin(arg*4.0*i));
                        imag[i] = 1.0*sin(arg*32.0*i + 3.0 * sin(arg*4.0*i));
```

```
                }
                strcpy(type_of_signal, "fm");
        }
        else
        {       printf("Wrong choice!!!\n");
                exit(1);
        }
}
```



```
#include <math.h>

/*********************************************/
/*              Cooley-Tukey's FFT           */
/*********************************************/
/*      For more, see "The Fast Fourier      */
/*      Transform and its Application"       */
/*      by E.O. Brigham.                     */
/*********************************************/

/*********************************************/
/*********************************************/

void    fft(xreal, ximag, n, nu)
double  xreal[], ximag[];
int     n, nu;
{
        extern  int     ibitr();

        int     n2, i, l, k, m;
        double  treal, timag, p, arg, c, s;


        n2 = n/2;
        k = 0;
        for (l=1; l <= nu; l++)
        {
            while (k < n)
            {   for (i=1; i <= n2; i++)
                {       m = k/n2;
                        p = ibitr(m, nu);
                        arg = 6.283185 * p /n;
                        c = cos(arg);
                        s = sin(arg);
                        treal = xreal[k+n2]*c + ximag[k+n2]*s;
                        timag = ximag[k+n2]*c - xreal[k+n2]*s;
                        xreal[k+n2] = xreal[k] -treal;
                        ximag[k+n2] = ximag[k] -timag;
                        xreal[k] = xreal[k] + treal;
                        ximag[k] = ximag[k] + timag;
                        k++;
                }
                k += n2;
            }

            k = 0;
            n2 /= 2;
        }
```

The FFT — fft.c

```
        for (k=0; k<n; k++)
        {       i = ibitr(k, nu);
                if (i>k)
                {       treal = xreal[k];
                        timag = ximag[k];
                        xreal[k] = xreal[i];
                        ximag[k] = ximag[i];
                        xreal[i] = treal;
                        ximag[i] = timag;
                }
        }
}

/*************************************************/

int     ibitr(j, nu)
int     j, nu;
{
        int     i, j1, j2, k;

        j1 = j;
        k = 0;
        for (i=1; i<= nu; i++)
        {
                j2 = j1 / 2;
                k = k*2 + (j1- 2*j2);
                j1 = j2;
        }

        return (k);
}

/*************************************************/
/*************************************************/
```

The FFT — store_data.c

```
#include        "dft.h"

void    store_data(real, imag, file_name)
double  real[], imag[];
char    file_name[];
{

        FILE    *fp, *fopen();
        int     i;

        fp = fopen(file_name, "w");
        for (i=0;  i < N; i++)
        {       fprintf(fp, "%12.4f  %12.4f\n", real[i], imag[i]);
        }
        fclose(fp);
}
```

Appendix B

The Ambiguity Function

This is to demonstrate the AF for various signals.

The AF — Makefile

```
OBJ =   ambiguity.o input.o store_signal.o af.o store_af.o misce.o
FLAGS = -g
EXEC = ambiguity

$(EXEC): $(OBJ)
        cc $(FLAGS) $(OBJ) -o $(EXEC) -lnag -lF77 -lI77 -lU77 -lm

ambiguity.o: ambiguity.h Makefile
        cc $(FLAGS) -c ambiguity.c -o ambiguity.o
input.o: ambiguity.h Makefile
        cc $(FLAGS) -c input.c -o input.o
store_signal.o: ambiguity.h Makefile
        cc $(FLAGS) -c store_signal.c -o store_signal.o
af.o: ambiguity.h Makefile
        cc $(FLAGS) -c af.c -o af.o
store_af.o: ambiguity.h Makefile
        cc $(FLAGS) -c store_af.c -o store_af.o
misce.o: ambiguity.h Makefile
        cc $(FLAGS) -c misce.c -o misce.o
```

The AF — ambiguity.h

```
/*********************************************/
/*              ambiguity.h                  */
/*********************************************/

/*****************************************/
#include        <math.h>
#include        <stdio.h>
#include        <strings.h>
#include        <malloc.h>
/*****************************************/
#define         N       256
#define         N2      128
#define         M       127
/*****************************************/
/*****************************************/
extern  void    input();
extern  void    store_signal();
extern  void    af();
extern  void    store_af();

extern  double  **dmatrix();
extern  void    free_dmatrix();
extern  void    nrerror();
/*****************************************/
```

The AF — ambiguity.c

```
/************************************************/
/*              AMBIGUITY FUNCTION              */
/************************************************/

#include        "ambiguity.h"

void    main()
{
        double  f[2][N];
        double** a[2];
        char    type_of_signal[25];
        char    file_name[250];
        char    noise[25];

        input(f[0], f[1], type_of_signal, noise);

        strcpy(file_name, "/home/hawk/eng/es036/work/ambiguity/Data/");
        if (noise[0] == 'y')
                strcat(file_name, "Noise.");
        strcat(file_name, type_of_signal);
        strcat(file_name, ".sig");
        store_signal(f[0], f[1], file_name);



        printf("\n\nComputing the AF ....\n\n");

        a[0] = dmatrix(-N2, M, 0, N-1);
        a[1] = dmatrix(-N2, M, 0, N-1);

        af(f[0], f[1], a[0], a[1]);

        strcpy(file_name, "/home/hawk/eng/es036/work/ambiguity/Data/");
        if (noise[0] == 'y')
                strcat(file_name, "Noise.");
        strcat(file_name, type_of_signal);
        strcat(file_name, ".af");
        store_af(a[0], a[1], file_name);

        free_dmatrix(a[0], -N2, M, 0, N-1);
        free_dmatrix(a[1], -N2, M, 0, N-1);
}
```

The AF — input.c

```
#include        "ambiguity.h"

void    input(real, imag, type_of_signal, noise)
double  real[], imag[];
char    type_of_signal[];
char    noise[];
{
        double  arg;
        int     i;

        printf("\n");
        printf("Choose a signal from:\n");
        printf("    a  sinusoidal signal\n");
        printf("    b  sum of three sinusoidal signals\n");
        printf("    c  chirp signal\n");
        printf("    d  frequency-modulated signal\n");
        printf("\n");
        scanf("%s", type_of_signal);

        if ( type_of_signal[0] == 'a' )
        {       arg = 2.0*3.14159265*32.0/N;
                for (i=0; i < N; i++)
                {       real[i] = cos(arg*i);
                        imag[i] = sin(arg*i);
                }
                strcpy(type_of_signal, "sinu1");
        }
        else if (type_of_signal[0] == 'b')
        {       arg = 2.0*3.14159265/N;
                for (i=0; i < N; i++)
                {       real[i] = 0.5*cos(arg*16.0*i) + cos(arg*32.0*i)
                                + 0.25*cos(arg*48.0*i);
                        imag[i] = 0.5*sin(arg*16.0*i) + sin(arg*32.0*i)
                                + 0.25*sin(arg*48.0*i);
                }
                strcpy(type_of_signal, "sinu3");
        }
        else if (type_of_signal[0] == 'c')
        {       arg = 3.14159265/(2.0*N);
                for (i=0; i < N; i++)
                {       real[i] = cos(arg*0.5*i*i);
                        imag[i] = sin(arg*0.5*i*i);
                }
                strcpy(type_of_signal, "chirp");
        }
        else if (type_of_signal[0] == 'd')
        {       arg = 2.0*3.14159265/N;
                for (i=0; i < N; i++ )
                {       real[i] = 1.0*cos(arg*32.0*i + 3.0 * sin(arg*4.0*i));
```

```
                imag[i] = 1.0*sin(arg*32.0*i + 3.0 * sin(arg*4.0*i));
        }
        strcpy(type_of_signal, "fm");
    }
    else nrerror("Wrong choice!!!");

    printf("\n");
    printf("Contain noise?(y/n)\n");
    scanf("%s", noise);
    printf("\n");

    if (noise[0] == 'y')
    for (i=0; i<N; i++)
    {       real[i] += 0.2 * random()/2147483647.0 - 0.1;
            imag[i] += 0.2 * random()/2147483647.0 - 0.1;
    }

}
```



```
/*********************************************/
/*              af.c                         */
/*********************************************/

#include        "ambiguity.h"


void    af(freal, fimag, afreal, afimag)
double  freal[], fimag[];
double  **afreal, **afimag;
{
        int     n, n1, m1, m2;
        int     I=N, ifail=0;

        for (n1=-N2; n1 < N2; n1++ )
        for (n=0; n<N; n++)
        {       m1 = n + n1;
                m2 = n - n1;
                if (-1<m1 && m1<N && -1<m2 && m2<N)
                {       afreal[n1][n] = freal[m1] * freal[m2]
                                        + fimag[m1] * fimag[m2];
                        afimag[n1][n] = fimag[m1] * freal[m2]
                                        - freal[m1] * fimag[m2];
                        afreal[n1][n] *= 2.0;
                        afimag[n1][n] *= 2.0;
                }
                else
                {       afreal[n1][n] = 0;
                        afimag[n1][n] = 0;
                }
        }

        for (n1=-N2; n1 < N2; n1++)
        {       c06ecf_(afreal[n1], afimag[n1], &I, &ifail);
                for (n=0; n<N; n++)
                {       afreal[n1][n] *= sqrt((double)N);  /* nag */
                        afimag[n1][n] *= sqrt((double)N);  /* nag */
                }
        }

}
```

The AF — store_af.c

```
#include        "ambiguity.h"

void    store_af(real, imag, file_name)
double  **real, **imag;
char    file_name[];
{
        FILE    *fp, *fopen();
        int     n1, k;


        fp = fopen(file_name, "w");

        for (k=N2; k< N+N2; k += 4)
        for (n1=-N2; n1<N2; n1 += 4)
        {
                fprintf(fp, "%f\n", sqrt( real[n1][k%N]*real[n1][k%N]
                        + imag[n1][k%N]*imag[n1][k%N] ));
        }
        fclose(fp);
}
```

The AF — store_signal.c

```
#include        "ambiguity.h"

void    store_signal(real, imag, file_name)
double  real[], imag[];
char    file_name[];
{

        FILE    *fp, *fopen();
        int     i;

        fp = fopen(file_name, "w");
        for (i=0;  i < N; i++)
        {       fprintf(fp, "%12.4f  %12.4f\n", real[i], imag[i]);
        }
        fclose(fp);
}
```

```
#include        "ambiguity.h"


extern  void    nrerror();

double  **dmatrix(nrl, nrh, ncl, nch)
int     nrl, nrh, ncl, nch;
{
        int     i;
        double  **m;

        m = (double**) malloc( (unsigned) (nrh-nrl+1)*sizeof(double*));
        if (!m) nrerror("Allocation failure 1 in dmatrix()");
        m -= nrl;

        for(i=nrl; i <= nrh; i++)
        {       m[i] = (double *)malloc((unsigned)(nch-ncl+1)*sizeof(double));
                if (!m[i]) nrerror("Allocation failure 2 in dmatrix()");
                m[i] -= ncl;
        }
        return m;
}

void    free_dmatrix(m, nrl, nrh, ncl, nch)
double  **m;
int     nrl, nrh, ncl, nch;
{
        int     i;

        for(i=nrh; i >= nrl; i--)
        {       free((char*)(m[i]+ncl));
        }

        free((char*) (m+nrl));
}


void    nrerror(error_text)
char    error_text[];
{
        void    exit();

        fprintf(stderr, "ERROR:  ");
        fprintf(stderr, "%s\n", error_text);
        exit(1);
}
```

Appendix C

The Wigner Distribution

To demonstrate the WDs for various signals.

The WD — Makefile

```
OBJ =   wigner.o input.o store_signal.o wd.o store_wd.o misce.o
FLAGS = -g
EXEC = wigner

$(EXEC): $(OBJ)
        cc $(FLAGS) $(OBJ) -o $(EXEC) -lnag -lF77 -lI77 -lU77 -lm

wigner.o: wigner.h Makefile
        cc $(FLAGS) -c wigner.c -o wigner.o
input.o: wigner.h Makefile
        cc $(FLAGS) -c input.c -o input.o
store_signal.o: wigner.h Makefile
        cc $(FLAGS) -c store_signal.c -o store_signal.o
wd.o: wigner.h Makefile
        cc $(FLAGS) -c wd.c -o wd.o
store_wd.o: wigner.h Makefile
        cc $(FLAGS) -c store_wd.c -o store_wd.o
misce.o: wigner.h Makefile
        cc $(FLAGS) -c misce.c -o misce.o
```

The WD — wigner.h

```
/*********************************************/
/*              wigner.h                     */
/*********************************************/

/*************************************/
#include        <math.h>
#include        <stdio.h>
#include        <strings.h>
#include        <malloc.h>
/*************************************/
#define         N       256
#define         N2      128
#define         M       127
/*************************************/
/*************************************/
extern  void    input();
extern  void    store_signal();
extern  void    wd();
extern  void    store_wd();

extern  double  **dmatrix();
extern  void    free_dmatrix();
extern  void    nrerror();
/*************************************/
```

```
/************************************************/
/*              WIGNER FUNCTION                 */
/************************************************/

#include        "wigner.h"

void    main()
{
        double  f[2][N];
        double** w[2];
        char    type_of_signal[25];
        char    file_name[250];
        char    noise[25];

        input(f[0], f[1], type_of_signal, noise);

        strcpy(file_name, "/home/hawk/eng/es036/work/wigner/Data/");
        if (noise[0] == 'y')
                strcat(file_name, "Noise.");
        strcat(file_name, type_of_signal);
        strcat(file_name, ".sig");
        store_signal(f[0], f[1], file_name);



        printf("\n\nComputing the WD ....\n\n");

        w[0] = dmatrix(0, N-1, 0, N-1);
        w[1] = dmatrix(0, N-1, 0, N-1);

        wd(f[0], f[1], w[0], w[1]);

        strcpy(file_name, "/home/hawk/eng/es036/work/wigner/Data/");
        if (noise[0] == 'y')
                strcat(file_name, "Noise.");
        strcat(file_name, type_of_signal);
        strcat(file_name, ".wd");
        store_wd(w[0], w[1], file_name);

        free_dmatrix(0, N-1, 0, N-1);
        free_dmatrix(0, N-1, 0, N-1);
}
```



```
#include        "wigner.h"

void    input(real, imag, type_of_signal, noise)
double  real[], imag[];
char    type_of_signal[];
char    noise[];
{
        double  arg;
        int     i;

        printf("\n");
        printf("Choose a signal from:\n");
        printf("    a  sinusoidal signal\n");
        printf("    b  sum of three sinusoidal signals\n");
        printf("    c  chirp signal\n");
        printf("    d  frequency-modulated signal\n");
        printf("\n");
        scanf("%s", type_of_signal);

        if ( type_of_signal[0] == 'a' )
        {       arg = 2.0*3.14159265*32.0/N;
                for (i=0; i < N; i++)
                {       real[i] = cos(arg*i);
                        imag[i] = sin(arg*i);
                }
                strcpy(type_of_signal, "sinu1");
        }
        else if (type_of_signal[0] == 'b')
        {       arg = 2.0*3.14159265/N;
                for (i=0; i < N; i++)
                {       real[i] = 0.5*cos(arg*16.0*i) + cos(arg*32.0*i)
                                + 0.25*cos(arg*48.0*i);
                        imag[i] = 0.5*sin(arg*16.0*i) + sin(arg*32.0*i)
                                + 0.25*sin(arg*48.0*i);
                }
                strcpy(type_of_signal, "sinu3");
        }
        else if (type_of_signal[0] == 'c')
        {       arg = 3.14159265/(2.0*N);
                for (i=0; i < N; i++)
                {       real[i] = cos(arg*0.5*i*i);
                        imag[i] = sin(arg*0.5*i*i);
                }
                strcpy(type_of_signal, "chirp");
        }
        else if (type_of_signal[0] == 'd')
        {       arg = 2.0*3.14159265/N;
                for (i=0; i < N; i++ )
                {       real[i] = 1.0*cos(arg*32.0*i + 3.0 * sin(arg*4.0*i));
```

```
                imag[i] = 1.0*sin(arg*32.0*i + 3.0 * sin(arg*4.0*i));
        }
        strcpy(type_of_signal, "fm");
    }
    else nrerror("Wrong choice!!!");


    printf("\n");
    printf("Contain noise?(y/n)\n");
    scanf("%s", noise);
    printf("\n");

    if (noise[0] == 'y')
    for (i=0; i<N; i++)
    {       real[i] += 0.2 * random()/2147483647.0 - 0.1;
            imag[i] += 0.2 * random()/2147483647.0 - 0.1;
    }
}
```



```
/*********************************************/
/*              wd.c                         */
/*********************************************/

#include        "wigner.h"


void    wd(freal, fimag, wdreal, wdimag)
double  freal[], fimag[];
double  **wdreal, **wdimag;
{
        int     n, m, m1, m2, k;
        int     I=N, ifail=0;
        double  treal, timag, arg, c, s;


        for (n=0; n<N; n++)
        for (m=0; m<N; m++)
        {       m1 = n + m -M;
                m2 = n - m +M;

                if (-1<m1 && m1<N && -1<m2 && m2<N)
                {       wdreal[n][m] = freal[m1] * freal[m2]
                                       + fimag[m1] * fimag[m2];
                        wdimag[n][m] = fimag[m1] * freal[m2]
                                       - freal[m1] * fimag[m2];
                        wdreal[n][m] *= 2.0;
                        wdimag[n][m] *= 2.0;
                }
                else
                {       wdreal[n][m] = 0;
                        wdimag[n][m] = 0;
                }
        }

        for (n=0; n<N; n++)
        {       c06ecf_(wdreal[n], wdimag[n], &I, &ifail);
        }

        for (k=0; k<N; k++)
        {       arg = 2.0 * M * 3.14159265358979323846;
                arg *= k;
                arg /= N;
                c = cos(arg);
                s = sin(arg);
                for (n=0; n<N; n++)
                {       treal = wdreal[n][k]*sqrt((double)N);  /* nag */
                        timag = wdimag[n][k]*sqrt((double)N);  /* nag */
```

The WD — wd.c

```
                        wdreal[n][k] = treal * c - timag * s;
                        wdimag[n][k] = treal * s + timag * c;
                }
        }
}
```

The WD — store_signal.c

```
#include        "wigner.h"

void    store_signal(real, imag, file_name)
double  real[], imag[];
char    file_name[];
{

        FILE    *fp, *fopen();
        int     i;

        fp = fopen(file_name, "w");
        for (i=0;  i < N; i++)
        {       fprintf(fp, "%12.4f  %12.4f\n", real[i], imag[i]);
        }
        fclose(fp);
}
```

The WD — store_wd.c

```
#include        "wigner.h"

void    store_wd(real, imag, file_name)
double  **real, **imag;
char    file_name[];
{
        FILE    *fp, *fopen();
        int     n, k;


        fp = fopen(file_name, "w");

        for (k=N2; k < N+N2; k += 4)
        for (n=0; n < N; n += 4)
        {
                fprintf(fp, "%f\n", real[n][k%N]);
        }

        fclose(fp);
}
```

The WD — misce.c

```
#include        "wigner.h"


extern  void    nrerror();

double  **dmatrix(nrl, nrh, ncl, nch)
int     nrl, nrh, ncl, nch;
{
        int     i;
        double  **m;

        m = (double**) malloc( (unsigned) (nrh-nrl+1)*sizeof(double*));
        if (!m) nrerror("Allocation failure 1 in dmatrix()");
        m -= nrl;

        for(i=nrl; i <= nrh; i++)
        {       m[i] = (double *)malloc((unsigned)(nch-ncl+1)*sizeof(double));
                if (!m[i]) nrerror("Allocation failure 2 in dmatrix()");
                m[i] -= ncl;
        }
        return m;
}

void    free_dmatrix(m, nrl, nrh, ncl, nch)
double  **m;
int     nrl, nrh, ncl, nch;
{
        int     i;

        for(i=nrh; i >= nrl; i--)
        {       free((char*)(m[i]+ncl));
        }

        free((char*) (m+nrl));
}


void    nrerror(error_text)
char    error_text[];
{
        void    exit();

        fprintf(stderr, "ERROR:  ");
        fprintf(stderr, "%s\n", error_text);
        exit(1);
}
```

Appendix D

The Hough Transform

The extraction of useful parameters from chirp signals

The HT — Makefile

```
OBJ =   Hough.o input.o wd.o \
        point_space.o para_space.o \
        extraction.o \
        suncore.o misce.o
FLAGS = -g
EXEC = Hough

$(EXEC): $(OBJ)
        cc $(FLAGS) $(OBJ) -o $(EXEC) \
         -lnag -lF77 -lI77 -lU77 -lcore -lsunwindow -lpixrect -lm

Hough.o: Hough.h Makefile
        cc $(FLAGS) -c Hough.c -o Hough.o
input.o: Hough.h Makefile
        cc $(FLAGS) -c input.c -o input.o
wd.o: Hough.h Makefile
        cc $(FLAGS) -c wd.c -o wd.o
suncore.o: Hough.h Makefile
        cc $(FLAGS) -c suncore.c -o suncore.o
point_space.o: Hough.h Makefile
        cc $(FLAGS) -c point_space.c -o point_space.o
para_space.o: Hough.h Makefile
        cc $(FLAGS) -c para_space.c -o para_space.o
extraction.o: Hough.h Makefile
        cc $(FLAGS) -c extraction.c -o extraction.o
misce.o: Hough.h Makefile
        cc $(FLAGS) -c misce.c -o misce.o
```

The HT — Hough.h

```
/*************************************************/
/*              Hough.h                          */
/*************************************************/

/*****************************************/
#include        <math.h>
#include        <stdio.h>
#include        <strings.h>
#include        <usercore.h>
/*****************************************/
#define         N       256
#define         N2      128
#define         M       127
/*****************************************/
extern  double  a;
extern  double  frac;

extern  double  a1;
extern  double  frac1;
/*****************************************/
extern  void    input();
extern  void    wd();
extern  void    point_space();
extern  void    para_space();
extern  void    extraction();

extern  void    store_sig_re();
extern  void    store_sig_im();
extern  void    store_vector();
extern  void    plot_vector();

extern  void    store_wd();
extern  void    store_point_space();
extern  void    store_para_space();
extern  void    plot_wd();
extern  void    plot_para_space();

extern  double  **dmatrix();
extern  void    free_dmatrix();
extern  void    error_message();
/*****************************************/
extern  void    set_up();
extern  void    clean_up();
extern  char*   io_by_keyboard();
extern  int     go_on_or_not();
extern  char    input_string[];
extern  int     seg;
/*****************************************/
extern  void    error_message();
```

The HT — Hough.h

```
/*****************************************/
```

The HT — Hough.c

```
/***********************************************/
/*      Parameter Extraction by the HT         */
/***********************************************/

#include        "Hough.h"

main()
{
        static  double  f[2][N];
        static  double  w[2][N][N];
        static  double  **xy;
        static  double  **ab;
        static  double  amin =0.0, da = 0.005;
        static  double  bmin = -50, db = 1;
        static  int     precision = 100;
        static  char    type_of_signal[25];
        static  int     finished = 0;


        set_up();

        while( !finished )
        {

                input(f[0], f[1], type_of_signal);
                store_sig_re(f[0], type_of_signal);
                store_sig_im(f[1], type_of_signal);

                set_viewport_2(0.0, 1.0, 0.65, 0.75);
                plot_vector(f[0], N, "n", "Real part of f[n]");

                set_viewport_2(0.0, 1.0, 0.55, 0.65);
                plot_vector(f[1], N, "n", "Imaginary part of f[n]");


                wd(f[0], f[1], w[0], w[1]);
                store_wd(w[0], type_of_signal);

                set_viewport_2(0.0, 1.0, 0.3, 0.55);
                plot_wd(w[0],"n", "k", "W[n,k]");


                xy = dmatrix(0, N-1, 0, N-1);
                point_space(w[0], xy);
                store_point_space(xy, type_of_signal);

                ab = dmatrix(0, precision, -precision/2, precision/2 -1);
                para_space(xy, ab, amin, da, bmin, db, precision);
                store_para_space(ab, precision, type_of_signal);
```

```
            set_viewport_2(0.0, 1.0, 0.05, 0.30);
            plot_para_space(ab, precision, "a", "b", "Parameter Space");



            extraction(ab, amin, da, bmin, db, precision);

            free_dmatrix(xy,0, N-1, 0, N-1);
            free_dmatrix(ab,0, precision, -precision/2, precision/2 -1);

            finished = go_on_or_not("Go on ?");

        }

        clean_up();

}
```



```
/*************************************************/
/*              input.c                          */
/*************************************************/

#include        "Hough.h"

double  a, frac;

void    input(real, imag, type_of_signal)
double  real[], imag[];
char    type_of_signal[];
{
        double  coef, arg;
        int     i;

        io_by_keyboard("Choose a, frac (Pi/N):", 0.2, 0.4);
        sscanf(input_string, "%lf %lf",  &a, &frac);

        coef = 0.5 * 3.141596 * frac/N;
        for (i=0; i<N; i++)
        {       arg = coef* i * i;
                real[i] = a * cos(arg);
                imag[i] = a * sin(arg);
        }

        sprintf(type_of_signal, "cc%.3fa_%.3ffrac", a, frac);
}
```

```
/************************************************/
/*              wd.c                            */
/************************************************/

#include        "Hough.h"


void    wd(freal, fimag, wdreal, wdimag)
double  freal[N], fimag[N];
double  wdreal[N][N], wdimag[N][N];
{
        int     n, m, m1, m2, k;
        int     I=N, ifail=0;
        double  treal, timag, arg, c, s;


        for (n=0; n<N; n++)
        for (m=0; m<N; m++)
        {       m1 = n + m -M;
                m2 = n - m +M;

                if (-1<m1 && m1<N && -1<m2 && m2<N)
                {       wdreal[n][m] = freal[m1] * freal[m2]
                                       + fimag[m1] * fimag[m2];
                        wdimag[n][m] = fimag[m1] * freal[m2]
                                       - freal[m1] * fimag[m2];
                        wdreal[n][m] *= 2.0;
                        wdimag[n][m] *= 2.0;
                }
                else
                {       wdreal[n][m] = 0;
                        wdimag[n][m] = 0;
                }
        }

        for (n=0; n<N; n++)
        {       c06ecf_(wdreal[n], wdimag[n], &I, &ifail);
        }

        for (k=0; k<N; k++)
        {       arg = 2.0 * M * 3.14159265358979323846;
                arg *= k;
                arg /= N;
                c = cos(arg);
                s = sin(arg);
                for (n=0; n<N; n++)
                {       treal = wdreal[n][k]*sqrt((double)N);  /* nag */
                        timag = wdimag[n][k]*sqrt((double)N);  /* nag */
```



```
                        wdreal[n][k] = treal * c - timag * s;
                        wdimag[n][k] = treal * s + timag * c;

                }
        }
}


void    plot_wd(w, xlabel, ylabel, zlabel)
double  w[N][N];
char    xlabel[], ylabel[], zlabel[];
{
        double  min, max, scale, shift;
        int     n, k;



        min = max = w[0][0];
        for (n=0; n<N; n++)
        {   for (k=0; k<N; k++)
            {   min = (w[n][k]<min) ? w[n][k] : min;
                max = (w[n][k]>max) ? w[n][k] : max;
            }
        }

        scale = 1.0 / (max - min);
        shift = (-min) * scale;
        /*******************************/
        set_window(-0.16, 1.7, -0.16, 1.7);
        create_retained_segment( ++seg );
                move_abs_3(0.0, 0.0,  shift);
                line_abs_3(1.0, 0.0,  shift);
                move_abs_3(0.0, 0.0,  shift);
                line_abs_3(0.0, 1.0,  shift);
                move_abs_3(0.0, 0.0,  shift);
                line_abs_3(0.0, 0.0,  shift+max*scale);
                for (n=0; n < N; n += 5)
                {   move_abs_3(n/((double)N), 0.0, w[n][0]*scale+shift );
                    for (k=0; k<N; k += 5)
                    {   line_abs_3(n/((double)N),k/((double)N),
                                w[n][k]*scale+shift);
                    }
                }
                move_abs_3(1.05, 0.0,  shift);
                text(xlabel);
                move_abs_3(0.0, 1.0,  shift+max*scale*0.2);
                text(ylabel);
                move_abs_3(0.0,0.0,  max*scale + shift);
                text(zlabel);
        close_retained_segment();
```

The HT wd.c

```
        /*********************************/

}


void    store_wd(real, type_of_signal)
double  real[N][N];
char    type_of_signal[];
{
        FILE    *fp, *fopen();
        int     n, k;

        char    file_name[100];

        strcpy(file_name, "Data/");
        strcat(file_name, type_of_signal);
        strcat(file_name, ".wd");


        fp = fopen(file_name, "w");

        for (k=N2; k < N+N2; k += 4)
        for (n=0; n < N; n += 4)
        {
                fprintf(fp, "%f\n", real[n][k%N]);
        }

        fclose(fp);
}
```

The HT point_space.c

```
#include        "Hough.h"

void    point_space(w, xy)
double  w[N][N];
double  **xy;
{
        double  peak, valley, threshold;
        int     i,j;

        peak = valley = w[0][0];
        for (i=0; i<N; i++)
        {       for (j=0; j<N; j++)
                {
                        if (peak < w[i][j] )
                                peak = w[i][j];
                        if (valley > w[i][j]);
                                valley = w[i][j];
                }
        }

        threshold = (peak-valley)*0.25 + valley;

        for (i=0; i<N; i++)
        {       for (j=0; j<N; j++)
                {       if (w[i][j] > threshold)
                                xy[i][j] = 1;
                        else
                                xy[i][j] = 0;
                }
        }
}

void    store_point_space(xy, type_of_signal)
double  **xy;
char    type_of_signal[];
{
        FILE    *fp, *fopen();
        int     n, k;

        char    file_name[100];

        strcpy(file_name, "Data/");
        strcat(file_name, type_of_signal);
        strcat(file_name, ".xy");


        fp = fopen(file_name, "w");

        for (k=N2; k < N+N2; k += 4)
```

The HT point_space.c

```
        for (n=0; n < N; n += 4)
        {
                fprintf(fp, "%d\n", (int) (xy[n][k%N]) );
        }

        fclose(fp);
}
```

The HT para_space.c

```
#include        "Hough.h"

void    para_space(xy, ab, amin, da, bmin, db, P)
double  **xy;
double  **ab;
double  amin, da, bmin, db;
int     P;
{
        int     i, j, ia, jb;

        double  a, b;
        int     counter;

        for (i=0; i<P; i++)
        {       for (j=-P/2; j<P/2; j++)
                {       ab[i][j] = 0;
                }
        }


        for (i=0; i<P; i++)
        for (j=-P/2; j<P/2; j++)
        if (xy[i][j] > 0.5)
        for (ia=0; ia<P; ia++)
        {
                a = amin + ia * da;
                b = -a * i + j;
                jb = (int) (b / db);
                ab[ia][jb] += 1;
        }

}


void    plot_para_space(ab, P, xlabel, ylabel, zlabel)
double  **ab;
int     P;
char    xlabel[], ylabel[], zlabel[];
{
        double  min, max, scale, shift, yshift;
        int     i, j;

        min = max = ab[0][-P/2];
        for (i=0; i<P; i++)
        for (j=-P/2; j<P/2; j++)
        {       min = (ab[i][j]<min) ? ab[i][j] : min;
                max = (ab[i][j]>max) ? ab[i][j] : max;

        }
```

```
        scale = 1.0 / (max - min);
        shift = (-min) * scale;
        /*******************************/
        yshift = 0.5;
        set_window(-0.16, 1.7, -0.16, 1.7);
        create_retained_segment( ++seg );
                move_abs_3(0.0, 0.0+yshift,  shift);
                line_abs_3(1.0, 0.0+yshift,  shift);
                move_abs_3(0.0, -0.5+yshift, shift);
                line_abs_3(0.0, 0.5+yshift,  shift);
                move_abs_3(0.0, 0.0+yshift,  shift);
                line_abs_3(0.0, 0.0+yshift,  shift+max*scale);
                for (i=0; i < P; i += 2)
                {   move_abs_3(i/((double)P), -0.5+yshift,
                                ab[i][-P/2]*scale+shift );
                    for (j=-P/2; j<P/2; j += 2)
                    {   line_abs_3(i/((double)P),j/((double)P) + yshift,
                                ab[i][j]*scale+shift);
                    }
                }

                move_abs_3(1.05, yshift,  shift);
                text(xlabel);
                move_abs_3(0.0, 0.6+yshift,  shift);
                text(ylabel);
                move_abs_3(0.0, yshift,  max*scale + shift);
                text(zlabel);
        close_retained_segment();

        /*******************************/

}

void    store_para_space(ab, p, type_of_signal)
double  **ab;
int     p;
char    type_of_signal[];
{
        FILE    *fp, *fopen();
        int     i, j;

        char    file_name[100];

        strcpy(file_name, "Data/");
        strcat(file_name, type_of_signal);
        strcat(file_name, ".ab");


        fp = fopen(file_name, "w");
```



```
        for (j=-p/2; j < p/2; j += 2)
        {       for (i=0; i < p; i += 2)
                {
                        fprintf(fp, "%d  ", (int) ab[i][j]);
                }
                fprintf(fp, "\n");
        }


        fclose(fp);
}
```

The HT — extraction.c

```
#include        "Hough.h"

double  a1, frac1;

void    extraction(ab, amin, da, bmin, db, P)
double  **ab;
double  amin, da, bmin, db;
int     P;
{
        int     counter;
        int     i, j, i0, j0;

        char    str[100];

        counter = ab[0][-P/2];
        i0 = 0;
        j0 = -P/2;

        for (i=0; i<P; i++)
        for (j=-P/2; j<P/2; j++)
        {       if (counter < ab[i][j])
                {       counter = ab[i][j];
                        i0 = i;
                        j0 = j;
                }
        }

        frac1 = amin + i0 * da;

        set_viewport_2(0.0, 1.0, 0.0, 0.05);
        set_window(-0.1, 1.1, -0.1, 1.1);
        create_retained_segment(++seg);
                move_abs_3(0.4, 0.0, 0.8);
                sprintf(str, "Original: frac=%.3f", frac);
                text(str);
                move_abs_3(0.4, 0.0, 0.4);
                sprintf(str, "Extracted: frac1=%.3f", frac1);
                text(str);
        close_retained_segment();
}
```

The HT — suncore.c

```
/*********************************************/
/*              suncore.c                    */
/*********************************************/

#include        "Hough.h"


extern  int     pixwindd();
struct  vwsurf
        vwsurf  = DEFAULT_VWSURF(pixwindd);

int     keyboard_number = 1;
char    input_string[80];
int     buffer_size = 80;
char    initial_string[80] = {"enter:"};
int     initial_cursor_position = 7;
double  echo_x, echo_y;
int     echo_type = 1;
int     length;

int     seg = 0;
/*********************************************/

void    set_up()
{
        initialize_core(DYNAMICC,SYNCHRONOUS,THREED);
        initialize_view_surface(&vwsurf,FALSE);
        select_view_surface(&vwsurf);

        set_view_reference_point(0.0,0.0,0.0);
        set_view_plane_normal(0.0,1.0,0.0);
        set_projection(PARALLEL, -1.0,1.732,-1.0);
        set_view_up_3(0.0,0.0,1.0);

        initialize_device(KEYBOARD,keyboard_number);
        set_echo(KEYBOARD,keyboard_number, echo_type);
        set_echo_surface(KEYBOARD,keyboard_number, &vwsurf);
}

/*********************************************/

void    clean_up()
{
        terminate_device(KEYBOARD,keyboard_number);
        deselect_view_surface(&vwsurf);
        terminate_core();
}

/*********************************************/
```

```
char*   io_by_keyboard(prompt, x, y)
char*   prompt;
double  x, y;
{
        int     MAXINT = 2147483647;
        char    str[80], *p;

        strcpy(initial_string, prompt);
        initial_cursor_position = strlen(initial_string)+ 5;
        echo_x = x;   echo_y = y;

        set_echo_position(KEYBOARD,keyboard_number,
                echo_x,echo_y);
        set_keyboard(keyboard_number,buffer_size,
                initial_string, initial_cursor_position);
        await_keyboard(MAXINT,keyboard_number,
                input_string, &length);

        input_string[ strlen(input_string)-1 ] = '\0';
        p = input_string;
        while( *p == ' ' || *p == '\t')
        {       p++;
        }
        strcpy(str, p);
        strcpy(input_string, str);

        return input_string;
}

/*************************************************/

int     go_on_or_not(text)
char    text[];
{
        io_by_keyboard("", 0.2, 0.4);
        while( seg > 0 )
        {       delete_retained_segment(seg--);
        }

        io_by_keyboard(text, 0.2, 0.4);
        if (input_string[0] == 'n')
                return 1;
        else if (input_string[0] == 'N')
                return 1;
        else
                return 0;
}

/*************************************************/
```



```
/*************************************************/
```

```
#include        "Hough.h"

void    store_sig_re(v, type_of_signal)
double  v[];
char    type_of_signal[];
{
        char    file_name[100];

        strcpy(file_name, "Data/");
        strcat(file_name, type_of_signal);
        strcat(file_name, ".sig.re");
        store_vector(v, N, file_name);
}

void    store_sig_im(v, type_of_signal)
double  v[];
char    type_of_signal[];
{
        char    file_name[100];

        strcpy(file_name, "Data/");
        strcat(file_name, type_of_signal);
        strcat(file_name, ".sig.im");
        store_vector(v, N, file_name);
}


void    store_vector(v, length, file_name)
double  v[];
int     length;
char    file_name[];
{

        FILE   *fp, *fopen();
        int    i;

        fp = fopen(file_name, "w");
        for (i=0;  i < length; i++)
        {       fprintf(fp, "%f\n", v[i]);
        }
        fclose(fp);
}


void    plot_vector(v, length, xlabel, ylabel)
double  v[];
int     length;
char    xlabel[], ylabel[];
{
```



```
        double  min, max;
        int     i;

        min = max = v[0];
        for (i=0; i<length; i++)
        {       if (min > v[i])
                {       min = v[i];
                }
                if (max < v[i])
                {       max = v[i];
                }
        }

        set_window(-0.1*length, 1.1*length,
                min-0.1*(max-min), max+0.1*(max-min) );
        create_retained_segment(++seg);
        {       move_abs_3(0.0, 0.0, 0.0);
                line_abs_3((double)length, 0.0, 0.0);
                move_abs_3(0.0, 0.0, min);
                line_abs_3(0.0, 0.0, max);

                move_abs_3(0.0, 0.0, v[0]);
                for (i=0; i<length; i++)
                {       line_abs_3( (double)i, 0.0, v[i]);
                }

                move_abs_3((double)length, 0.0, 0.0);
                text(xlabel);

                move_abs_3(0.0, 0.0, max+0.05*(max-min));
                text(ylabel);
        }
        close_retained_segment();
}

double  **dmatrix(nrl, nrh, ncl, nch)
int     nrl, nrh, ncl, nch;
{
        int     i;
        double  **m;

        m = (double**) malloc( (unsigned) (nrh-nrl+1)*sizeof(double*));
        if (!m) error_message("Allocation failure 1 in dmatrix()");
        m -= nrl;

        for(i=nrl; i <= nrh; i++)
        {       m[i] = (double *)malloc((unsigned)(nch-ncl+1)*sizeof(double));
                if (!m[i]) error_message("Allocation failure 2 in dmatrix()");
                m[i] -= ncl;
        }
```

```
        return m;
}

void    free_dmatrix(m, nrl, nrh, ncl, nch)
double  **m;
int     nrl, nrh, ncl, nch;
{
        int     i;

        for(i=nrh; i >= nrl; i--)
        {       free((char*)(m[i]+ncl));
        }

        free((char*) (m+nrl));
}

void    error_message(text)
char    text[];
{
        void    exit();

        fprintf(stderr, "ERROR:   ");
        fprintf(stderr, "%s\n", text);
        exit(1);
}
```

Appendix E

Extraction of Useful Parameters

The extraction of useful parameters from both chirp and FM signals.

Extraction — Makefile

```
OBJ =   Extraction.o choose.o input.o hilbert.o \
        moments.o wd.o extraction.o suncore.o misce.o
FLAGS = -g
EXEC = Extraction

$(EXEC): $(OBJ)
        cc $(FLAGS) $(OBJ) -o $(EXEC) \
        -lnag -lF77 -lI77 -lU77 \
        -lcore -lsunwindow -lpixrect -lm

Extraction.o: Extraction.h Makefile
        cc $(FLAGS) -c Extraction.c -o Extraction.o
choose.o: Extraction.h Makefile
        cc $(FLAGS) -c choose.c -o choose.o
input.o: Extraction.h Makefile
        cc $(FLAGS) -c input.c -o input.o
hilbert.o: Extraction.h Makefile
        cc $(FLAGS) -c hilbert.c -o hilbert.o
wd.o: Extraction.h Makefile
        cc $(FLAGS) -c wd.c -o wd.o
moments.o: Extraction.h Makefile
        cc $(FLAGS) -c moments.c -o moments.o
extraction.o: Extraction.h Makefile
        cc $(FLAGS) -c extraction.c -o extraction.o
suncore.o: Extraction.h Makefile
        cc $(FLAGS) -c suncore.c -o suncore.o
misce.o: Extraction.h Makefile
        cc $(FLAGS) -c misce.c -o misce.o
```

Extraction — Extraction.c

```
/*************************************************/
/*************************************************/
/*      Parameter Extraction                     */
/*************************************************/
/*************************************************/

#include        "Extraction.h"

main()
{
        static  double  f[2][N];
        static  double  w[2][N][N];
        static  double  p[N];
        static  double  theta[N];
        char    type_of_signal[25];

        int     finished = 0;

        set_up();

        while( !finished )
        {
                set_viewport_2(0.0, 1.0, 0.0, 0.75);
                choose(type_of_signal);


                input(f[0], f[1], type_of_signal);

                if (type_of_signal[0] == 'c')   /* complex-valued */
                {       set_viewport_2(0.0, 1.0, 0.65, 0.75);
                        plot_vector(f[0], N, "n", "Real part of f[n]");
                        store_sig_re(f[0], type_of_signal);

                        set_viewport_2(0.0, 1.0, 0.55, 0.65);
                        plot_vector(f[1], N, "n", "Imaginary part of f[n]");
                        store_sig_im(f[1], type_of_signal);
                }
                else
                {       set_viewport_2(0.0, 1.0, 0.68, 0.75);
                        plot_vector(f[0], N, "n", "f[n]");
                        store_sig_re(f[0], type_of_signal);

                        hilbert(f[0], f[1]);

                        set_viewport_2(0.0, 1.0, 0.615, 0.68);
                        plot_vector(f[0], N, "n", "Real part of f_a[n]");
                        store_ana_re(f[0], type_of_signal);

                        set_viewport_2(0.0, 1.0, 0.55, 0.615);
```

Extraction — Extraction.c

```
                plot_vector(f[1], N, "n", "Imaginary part of f_a[n]");
                store_ana_im(f[1], type_of_signal);
            }

            wd(f[0], f[1], w[0], w[1]);

            set_viewport_2(0.0, 1.0, 0.2, 0.55);
            plot_wd(w[0],"n", "k", "W[n,k]");
            store_wd(w[0], type_of_signal);

            moments(w[0], p, theta);

            set_viewport_2(0.0, 1.0, 0.125, 0.2);
            plot_vector(p, N, "n", "P");
            store_mom_p(p, type_of_signal);

            set_viewport_2(0.0, 1.0, 0.05, 0.125);
            plot_vector(theta, N, "n", "theta");
            store_mom_t(theta, type_of_signal);

            set_viewport_2(0.0, 1.0, 0.0, 0.05);
            extraction(p, theta, type_of_signal);

            finished = go_on_or_not("Go on ?");
        }

        clean_up();

}
```

Extraction — Extraction.h

```
/*********************************************/
/*              Extraction.h                 */
/*********************************************/

/*****************************************/
#include        <math.h>
#include        <stdio.h>
#include        <strings.h>
#include        <usercore.h>
/*****************************************/
#define         N       256
#define         N2      128
#define         M       127
/*****************************************/
extern  double  a, b;
extern  double  frac;
extern  double  k_o, phi_o, k_m, phi_m;

extern  double  a1, b1;
extern  double  frac1;
extern  double  k_o1, phi_o1, k_m1, phi_m1;
/*****************************************/
extern  void    choose();
extern  void    input();
extern  void    hilbert();
extern  void    wd();
extern  void    moments();
extern  void    extraction();

extern  void    store_sig_re();
extern  void    store_sig_im();
extern  void    store_ana_re();
extern  void    store_ana_im();
extern  void    store_mom_p();
extern  void    store_mom_t();
extern  void    store_wd();
extern  void    store_results();
extern  void    store_vector();
extern  void    plot_vector();
extern  void    plot_wd();
/*****************************************/
extern  void    set_up();
extern  void    clean_up();
extern  char*   io_by_keyboard();
extern  int     go_on_or_not();
extern  char    input_string[];
extern  int     seg;
/*****************************************/
extern  void    error_message();
```

Extraction — Extraction.h

```
/****************************************/
```

Extraction — choose.c

```
#include        "Extraction.h"

void    choose(type_of_signal)
char    type_of_signal[];
{
        set_viewport_2(0.0, 1.0, 0.0, 0.75);
        set_window(0.0, 1.0, 0.0, 1.0);
        create_retained_segment(++seg);
        {       move_abs_3(0.25, 0.0, 0.6);
                text("Choose a signal from:");
                move_abs_3(0.25, 0.0, 0.5);
                text("    cc  complex-valued, chirp signals");
                move_abs_3(0.25, 0.0, 0.45);
                text("    rc  real-valued, chirp signals");
                move_abs_3(0.25, 0.0, 0.4);
                text("    cf  complex-valued, FM signals");
                move_abs_3(0.25, 0.0, 0.35);
                text("    rf  real-valued, FM signals");
        }
        close_retained_segment();

        io_by_keyboard("Enter:  ", 0.25, 0.2);
        strncpy(type_of_signal, input_string, 5);

        delete_retained_segment(seg--);
}
```

Extraction — input.c

```
#include        "Extraction.h"

double  a, b;
double  frac;
double  k_o, phi_o, k_m, phi_m;

void    input(real, imag, type_of_signal)
double  real[], imag[];
char    type_of_signal[];
{
        double  coef, arg;
        int     i;

        if ( type_of_signal[1] == 'c')
        {       io_by_keyboard("a, frac (Pi/N):", 0.2, 0.4);
                sscanf(input_string, "%lf %lf",  &a, &frac);

                coef = 0.5 * 3.141596 * frac/N;
                for (i=0; i<N; i++)
                {       arg = coef* i * i;
                        real[i] = a * cos(arg);
                        if (type_of_signal[0] == 'c')
                        {       imag[i] = a * sin(arg);
                                sprintf(type_of_signal,
                                        "cc%.3fa_%.3ffrac",a,frac);
                        }
                        else if (type_of_signal[0] == 'r')
                        {       imag[i] = 0;
                                sprintf(type_of_signal,
                                        "rc%.3fa_%.3ffrac",a,frac);
                        }
                        else error_message("Wrong choice!!!");
                }
        }
        else if ( type_of_signal[1] == 'f')
        {       io_by_keyboard("a, k_o, phi_o(Deg):", 0.2, 0.4);
                sscanf(input_string, "%lf %lf %lf", &a, &k_o, &phi_o);
                phi_o /= 180.0/3.141596;
                io_by_keyboard("b, k_m, phi_m(Deg):", 0.2, 0.4);
                sscanf(input_string, "%lf %lf %lf", &b, &k_m, &phi_m);
                phi_m /= 180.0/3.141596;

                coef = 2.0 * 3.141596 /N;
                for (i=0; i<N; i++)
                {       arg = coef *k_o * i + phi_o;
                        arg += b * sin(coef *k_m * i + phi_m);
                        real[i] = a * cos(arg);
                        if (type_of_signal[0] == 'c')
```

Extraction — input.c

```
                        {       imag[i] = a * sin(arg);
                                sprintf(type_of_signal,
                                        "cf%.3fa_%dko_%.3fb_%dkm",
                                        a, (int)k_o, b, (int)k_m );
                        }
                        else if (type_of_signal[0] == 'r')
                        {       imag[i] = 0;
                                sprintf(type_of_signal,
                                        "rf%.3fa_%dko_%.3fb_%dkm",
                                        a, (int)k_o, b, (int)k_m );
                        }
                        else error_message("Wrong choice!!!");
                }
        }
        else error_message("Wrong choice!!!");
}
```

Extraction hilbert.c

```
/************************************************/
/*              hilbert.c                       */
/************************************************/

#include        "Extraction.h"

void    hilbert(real, imag)
double  real[], imag[];
{
        int     I=N, ifail=0;
        int     i;

        /********       FFT     *********/
        c06ecf_(real, imag, &I, &ifail);
        /*********************************/

        for (i=0; i<I; i++)
        {       if ( i >= N2)
                {       real[i] = 0.0;
                        imag[i] = 0.0;
                }
                else
                {       real[i] *= 2.0;
                        imag[i] *= 2.0;
                }

        }

        /*********************************/
        /********       IFFT    *********/
        c06gcf_(imag, &I, &ifail);
        c06ecf_(real, imag, &I, &ifail);
        c06gcf_(imag, &I, &ifail);
        /*********************************/
        /*********************************/
}
```

Extraction wd.c

```
/************************************************/
/*              wd.c                            */
/************************************************/

#include        "Extraction.h"


void    wd(freal, fimag, wdreal, wdimag)
double  freal[N], fimag[N];
double  wdreal[N][N], wdimag[N][N];
{
        int     n, m, m1, m2, k;
        int     I=N, ifail=0;
        double  treal, timag, arg, c, s;


        for (n=0; n<N; n++)
        for (m=0; m<N; m++)
        {       m1 = n + m -M;
                m2 = n - m +M;

                if (-1<m1 && m1<N && -1<m2 && m2<N)
                {       wdreal[n][m] = freal[m1] * freal[m2]
                                       + fimag[m1] * fimag[m2];
                        wdimag[n][m] = fimag[m1] * freal[m2]
                                       - freal[m1] * fimag[m2];
                        wdreal[n][m] *= 2.0;
                        wdimag[n][m] *= 2.0;
                }
                else
                {       wdreal[n][m] = 0;
                        wdimag[n][m] = 0;
                }
        }

        for (n=0; n<N; n++)
        {       c06ecf_(wdreal[n], wdimag[n], &I, &ifail);
        }

        for (k=0; k<N; k++)
        {       arg = 2.0 * M * 3.14159265358979323846;
                arg *= k;
                arg /= N;
                c = cos(arg);
                s = sin(arg);
                for (n=0; n<N; n++)
                {       treal = wdreal[n][k]*sqrt((double)N);  /* nag */
                        timag = wdimag[n][k]*sqrt((double)N);  /* nag */
```

Extraction wd.c

```
                        wdreal[n][k] = treal * c - timag * s;
                        wdimag[n][k] = treal * s + timag * c;

                }
        }
}
```

Extraction moments.c

```
/*************************************************/
/*              moments.c                        */
/*************************************************/

#include        "Extraction.h"

void    moments(w, p, theta)
double  w[N][N];
double  p[N];
double  theta[N];
{
        double  x[N], y[N], coef;
        int     n, k;

        /********** p  ******************/
        for (n=0; n<N; n++)
        {       p[n] = 0;
                for (k=0; k<N; k++)
                {       p[n] += w[n][k];
                }
                p[n] /= 2.0*N;
        }
        p[0] = 0; /* for the sake of plot */

        /********** x ***************/
        coef = 2.0 * 3.141596 /N;
        for (n=0; n<N; n++)
        {       x[n] = y[n] = 0.0;
                for (k=0; k<N; k++)
                {       x[n] += w[n][k] * cos(coef*k);
                        y[n] += w[n][k] * sin(coef*k);
                }
        }
        for (n=0; n<N; n++)
        {
                if (y[n] == 0 && x[n] > 0)
                {       theta[n] = 0;
                }
                else if (y[n] == 0 && x[n] < 0)
                {       theta[n] = 3.141596;
                }
                else if (y[n] == 0 && x[n] == 0)
                {       theta[n] = 0;
                }
                else if (x[n] < 0 )
                {       theta[n] = atan(y[n]/x[n]) + 3.141596;
                }
                else if (x[n] == 0 )
                {       if (y[n] > 0)
```

Extraction — moments.c

```
                        theta[n] = 3.141596/2.0;
                else if (y[n] < 0)
                        theta[n] = 3.0*3.141596/2.0;
                else
                        theta[n] = 0;
        }
        else
        {       theta[n] = atan(y[n]/x[n]);
        }

        theta[n] /= 2.0;
    }
}
```

Extraction — extraction.c

```
#include        "Extraction.h"

double  a1, b1;

double  frac1;

double  k_o1, k_m1, phi_o, phi_m;


void    extraction(p, theta, type_of_signal)
double  p[N];
double  theta[N];
char    type_of_signal[];
{
        extern  void    extraction_for_chirp();
        extern  void    results_for_chirp();
        extern  void    extraction_for_fm();
        extern  void    results_for_fm();

        char    file_name[100];

        strcpy(file_name, "Data/");
        strcat(file_name, type_of_signal);
        strcat(file_name, ".res.tex");

        if (type_of_signal[1] == 'c')
        {       extraction_for_chirp(p, theta);
                results_for_chirp(file_name);
        }
        else
        {       extraction_for_fm(p, theta);
                results_for_fm(file_name);
        }

}


void    extraction_for_chirp(p, theta)
double  p[N];
double  theta[N];
{
        char    str[100];
        double  t[6];
        int     n;

        /********       a1      ***********/
        a1 = 0;
        for (n=1; n < N; n++)
        {       a1 += p[n];
```

```
        }
        a1 /= N-1.0;
        a1 = sqrt(a1);

        /**********  frac1       *********/
        t[0] = t[1] = t[2] = t[3] = t[4] = t[5] = 0;
        for (n=0; n<N; n++)
        {       t[0] += n * n;
                t[1] += n;
                t[2] += theta[n] * n;
                t[3] += n;
                t[4] += 1;
                t[5] += theta[n];
        }
        frac1 = (t[2]*t[4] - t[1]*t[5])/(t[0]*t[4] - t[1]*t[3]);
        frac1 *= 256 / 3.141596;

        set_window(-0.1, 1.1, -0.1, 1.1);
        create_retained_segment(++seg);
                move_abs_3(0.30, 0.0, 0.8);
                sprintf(str,
                  "Original: a=%.3f, frac=%.3f", a, frac);
                text(str);
                move_abs_3(0.30, 0.0, 0.4);
                sprintf(str,
                  "Extracted: a1=%.3f, frac1=%.3f", a1, frac1);
                text(str);
        close_retained_segment();
        /*******************************/

}


void    extraction_for_fm(p, theta)
double  p[N];
double  theta[N];
{
        double  y[N];
        int     I=N, ifail=0;
        int     n, k;

        double  coef;
        double  tmp;

        char    str[80];

        /********       a1      ***********/
        a1 = 0;
        for (n=0; n<N; n++)
        {       a1 += p[n];
```



```
        }
        a1 /= N;
        a1 = sqrt(a1);
        /********       k_o1    ***********/
        k_o1 = 0.0;
        for (n=0; n<N; n++)
        {       k_o1 += theta[n];
        }
        k_o1 /= (2.0*3.141596);
        k_o1 = (int)(k_o1 + 0.5);
        /*******************************/
        tmp = 0.0;
        for (n=0; n<N; n++)
        {       tmp += theta[n];
        }
        tmp /= N;
        for (n=0; n<N; n++)
        {       theta[n] -= tmp;
        }
        /*******************************/

        coef = 2.0 * 3.141596/N;
        for (n=0; n<N; n++)
        {       theta[n] *= 0.5*(1-cos(coef*n));
                y[n] = 0;
        }

        c06ecf_(theta, y, &I, &ifail);

        coef = sqrt((double) N);
        for (n=0; n<N; n++)
        {       theta[n] *= coef;
                y[n] *= coef;
        }

        for (k=0; k<N; k++)
        {       theta[k] = theta[k]*theta[k]
                         + y[k]*y[k];
                theta[k] = sqrt(theta[k]);
        }
        /********       k_m1     **********/
        k_m1 = 2;
        b1 = theta[2];
        for (k=2; k<N/2; k++)
        {       if (theta[k] > b1)
                {       b1 = theta[k];
                        k_m1 = k;
                }
        }
        /********       b1      ***********/
```

```
        k = k_m1;
        b1 += theta[k -1] + theta[k -2]
              + theta[k +1] + theta[k +2];
        b1 /= sin( 2.0*3.141596*k_m1 /N );
        b1 *= 2.0/N;
        /*******************************/
        set_window(-0.1, 1.1, -0.1, 1.1);
        create_retained_segment(++seg);
                move_abs_3(0.25, 0.0, 0.8);
                sprintf(str,
                  "Original: a=%.3f, k_o=%.1f, b=%.3f, k_m=%.1f",
                  a, k_o, b, k_m);
                text(str);
                move_abs_3(0.25, 0.0, 0.4);
                sprintf(str,
                  "Extracted: a1=%.3f, k_o1=%.1f, b1=%.3f, k_m1=%.1f",
                  a1, k_o1, b1, k_m1);
                text(str);
        close_retained_segment();
        /*******************************/
}

void    results_for_chirp(file_name)
char    file_name[];
{
        FILE    *fp, *fopen();

        fp = fopen(file_name, "w");

        fprintf(fp, "\\caption{");
        fprintf(fp, "Original: $a=%.3f$, $\\alpha=\\frac{%.3f\\pi}{N}$, ",
                a, frac);
        fprintf(fp, "Extracted: $a=%.3f$, $\\alpha=\\frac{%.3f\\pi}{N}$. ",
                a1, frac1);
        fprintf(fp, "}");

        fclose(fp);
}

void    results_for_fm(file_name)
char    file_name[];
{
        FILE    *fp, *fopen();

        fp = fopen(file_name, "w");

        fprintf(fp, "\\caption{");

        fprintf(fp, "Original: ");
        fprintf(fp, "$a=%.3f$, ", a);
```



```
        fprintf(fp, "$\\theta_o=%.1f\\frac{2\\pi}{N}$, ", k_o);
        fprintf(fp, "$b=%.3f$, ", b);
        fprintf(fp, "$\\theta_m=%.1f\\frac{2\\pi}{N}$, ", k_m);

        fprintf(fp, "Extracted: ");
        fprintf(fp, "$a=%.3f$, ", a1);
        fprintf(fp, "$\\theta_o=%.1f\\frac{2\\pi}{N}$, ", k_o1);
        fprintf(fp, "$b=%.3f$, ", b1);
        fprintf(fp, "$\\theta_m=%.1f\\frac{2\\pi}{N}$, ", k_m1);

        fprintf(fp, "}");

        fclose(fp);
}
```

Extraction — suncore.c

```
/************************************************/
/*              suncore.c                       */
/************************************************/

#include        "Extraction.h"


extern  int     pixwindd();
struct  vwsurf
        vwsurf  = DEFAULT_VWSURF(pixwindd);

int     keyboard_number = 1;
char    input_string[80];
int     buffer_size = 80;
char    initial_string[80] = {"enter:"};
int     initial_cursor_position = 7;
double  echo_x, echo_y;
int     echo_type = 1;
int     length;

int     seg = 0;
/************************************************/

void    set_up()
{
        initialize_core(DYNAMICC,SYNCHRONOUS,THREED);
        initialize_view_surface(&vwsurf,FALSE);
        select_view_surface(&vwsurf);

        set_view_reference_point(0.0,0.0,0.0);
        set_view_plane_normal(0.0,1.0,0.0);
        set_projection(PARALLEL, -1.0,1.732,-1.0);
        set_view_up_3(0.0,0.0,1.0);

        initialize_device(KEYBOARD,keyboard_number);
        set_echo(KEYBOARD,keyboard_number, echo_type);
        set_echo_surface(KEYBOARD,keyboard_number, &vwsurf);
}

/************************************************/

void    clean_up()
{
        terminate_device(KEYBOARD,keyboard_number);
        deselect_view_surface(&vwsurf);
        terminate_core();
}

/************************************************/
```

Extraction — suncore.c

```
char*   io_by_keyboard(prompt, x, y)
char*   prompt;
double  x, y;
{
        int     MAXINT = 2147483647;
        char    str[80], *p;

        strcpy(initial_string, prompt);
        initial_cursor_position = strlen(initial_string)+ 5;
        echo_x = x;   echo_y = y;

        set_echo_position(KEYBOARD,keyboard_number,
                echo_x,echo_y);
        set_keyboard(keyboard_number,buffer_size,
                initial_string, initial_cursor_position);
        await_keyboard(MAXINT,keyboard_number,
                input_string, &length);

        input_string[ strlen(input_string)-1 ] = '\0';
        p = input_string;
        while( *p == ' ' || *p == '\t')
        {       p++;
        }
        strcpy(str, p);
        strcpy(input_string, str);

        return input_string;
}

/************************************************/

int     go_on_or_not(text)
char    text[];
{
        io_by_keyboard("", 0.2, 0.4);
        while( seg > 0 )
        {       delete_retained_segment(seg--);
        }

        io_by_keyboard(text, 0.2, 0.4);
        if (input_string[0] == 'n')
                return 1;
        else if (input_string[0] == 'N')
                return 1;
        else
                return 0;
}

/************************************************/
```

Extraction suncore.c

```
/*************************************************/
```

Extraction misce.c

```
#include        "Extraction.h"

void    store_sig_re(v, type_of_signal)
double  v[];
char    type_of_signal[];
{
        char    file_name[100];

        strcpy(file_name, "Data/");
        strcat(file_name, type_of_signal);
        strcat(file_name, ".sig.re");
        store_vector(v, N, file_name);
}

void    store_sig_im(v, type_of_signal)
double  v[];
char    type_of_signal[];
{
        char    file_name[100];

        strcpy(file_name, "Data/");
        strcat(file_name, type_of_signal);
        strcat(file_name, ".sig.im");
        store_vector(v, N, file_name);
}

void    store_ana_re(v, type_of_signal)
double  v[];
char    type_of_signal[];
{
        char    file_name[100];

        strcpy(file_name, "Data/");
        strcat(file_name, type_of_signal);
        strcat(file_name, ".ana.re");
        store_vector(v, N, file_name);
}

void    store_ana_im(v, type_of_signal)
double  v[];
char    type_of_signal[];
{
        char    file_name[100];

        strcpy(file_name, "Data/");
        strcat(file_name, type_of_signal);
        strcat(file_name, ".ana.im");
        store_vector(v, N, file_name);
}
```

Extraction misce.c

```
void    store_mom_p(v, type_of_signal)
double  v[];
char    type_of_signal[];
{
        char    file_name[100];

        strcpy(file_name, "Data/");
        strcat(file_name, type_of_signal);
        strcat(file_name, ".mom.p");
        store_vector(v, N, file_name);
}

void    store_mom_t(v, type_of_signal)
double  v[];
char    type_of_signal[];
{
        char    file_name[100];

        strcpy(file_name, "Data/");
        strcat(file_name, type_of_signal);
        strcat(file_name, ".mom.t");
        store_vector(v, N, file_name);
}


void    store_wd(w, type_of_signal)
double  w[N][N];
char    type_of_signal[];
{
        char    file_name[100];
        FILE    *fp, *fopen();
        int     n, k;

        strcpy(file_name, "Data/");
        strcat(file_name, type_of_signal);
        strcat(file_name, ".wd");

        fp = fopen(file_name, "w");

        for (k=N2; k < N+N2; k += 4)
        for (n=0; n < N; n += 4)
        {
                fprintf(fp, "%f\n", w[n][k%N]);
        }

        fclose(fp);
}
```

Extraction misce.c

```
void    store_vector(v, length, file_name)
double  v[];
int     length;
char    file_name[];
{

        FILE    *fp, *fopen();
        int     i;

        fp = fopen(file_name, "w");
        for (i=0;  i < length; i++)
        {       fprintf(fp, "%f\n", v[i]);
        }
        fclose(fp);
}


void    plot_vector(v, length, xlabel, ylabel)
double  v[];
int     length;
char    xlabel[], ylabel[];
{
        double  min, max;
        int     i;

        min = max = v[0];
        for (i=0; i<length; i++)
        {       if (min > v[i])
                {       min = v[i];
                }
                if (max < v[i])
                {       max = v[i];
                }
        }

        set_window(-0.1*length, 1.1*length,
                min-0.1*(max-min), max+0.1*(max-min) );
        create_retained_segment(++seg);
        {       move_abs_3(0.0, 0.0, 0.0);
                line_abs_3((double)length, 0.0, 0.0);
                move_abs_3(0.0, 0.0, min);
                line_abs_3(0.0, 0.0, max);

                move_abs_3(0.0, 0.0, v[0]);
                for (i=0; i<length; i++)
                {       line_abs_3( (double)i, 0.0, v[i]);
                }

                move_abs_3((double)length, 0.0, 0.0);
```

Extraction misce.c

```
                text(xlabel);

                move_abs_3(0.0, 0.0, max+0.05*(max-min));
                text(ylabel);
        }
        close_retained_segment();
}


void    plot_wd(w, xlabel, ylabel, zlabel)
double  w[N][N];
char    xlabel[], ylabel[], zlabel[];
{
        double  min, max, scale, shift;
        int     n, k;



        min = max = w[0][0];
        for (n=0; n<N; n++)
        {   for (k=0; k<N; k++)
            {   min = (w[n][k]<min) ? w[n][k] : min;
                max = (w[n][k]>max) ? w[n][k] : max;
            }
        }

        scale = 1.0 / (max - min);
        shift = (-min) * scale;
        /*******************************/
        set_window(-0.16, 1.7, -0.16, 1.7);
        create_retained_segment( ++seg );
                move_abs_3(0.0, 0.0,  shift);
                line_abs_3(1.0, 0.0,  shift);
                move_abs_3(0.0, 0.0,  shift);
                line_abs_3(0.0, 1.0,  shift);
                move_abs_3(0.0, 0.0,  shift);
                line_abs_3(0.0, 0.0,  shift+max*scale);
                for (n=0; n < N; n += 5)
                {   move_abs_3(n/((double)N), 0.0, w[n][0]*scale+shift );
                    for (k=0; k<N; k += 5)
                    {   line_abs_3(n/((double)N),k/((double)N),
                                w[n][k]*scale+shift);
                    }
                }
                move_abs_3(1.05, 0.0,  shift);
                text(xlabel);
                move_abs_3(0.0, 1.0,  shift+max*scale*0.2);
                text(ylabel);
                move_abs_3(0.0,0.0,  max*scale + shift);
                text(zlabel);
```

Extraction misce.c

```
        close_retained_segment();

        /*******************************/

}

void    error_message(text)
char    text[];
{
        void    exit();

        fprintf(stderr, "ERROR:   ");
        fprintf(stderr, "%s\n", text);
        exit(1);
}
```

Appendix F

Extraction of Vibration by the WD

This program extracts vibration information from roundess signature, it covers both simulation and real cases.

```
#
#       Makefile
#
#
OBJ =   turning.o choose.o \
        real_parameters.o real_roundness.o plot_roundness.o cut_it_out.o \
        simu_parameters.o simu_roundness.o \
        level_data.o hilbert.o wd.o moments.o extraction.o \
        suncore.o misce.o
FLAGS = -g
EXEC = turning

$(EXEC): $(OBJ)
        cc $(FLAGS) $(OBJ) -o $(EXEC) \
        -lnag -lF77 -lI77 -lU77 \
        -lcore -lsunwindow -lpixrect -lm

turning.o: turning.h Makefile
        cc $(FLAGS) -c turning.c -o turning.o
choose.o: turning.h Makefile
        cc $(FLAGS) -c choose.c -o choose.o
real_parameters.o: turning.h Makefile
        cc $(FLAGS) -c real_parameters.c -o real_parameters.o
real_roundness.o: turning.h Makefile
        cc $(FLAGS) -c real_roundness.c -o real_roundness.o
cut_it_out.o: turning.h Makefile
        cc $(FLAGS) -c cut_it_out.c -o cut_it_out.o
plot_roundness.o: turning.h Makefile
        cc $(FLAGS) -c plot_roundness.c -o plot_roundness.o
simu_parameters.o: turning.h Makefile
        cc $(FLAGS) -c simu_parameters.c -o simu_parameters.o
simu_roundness.o: turning.h Makefile
        cc $(FLAGS) -c simu_roundness.c -o simu_roundness.o
hilbert.o: turning.h Makefile
        cc $(FLAGS) -c hilbert.c -o hilbert.o
level_data.o: turning.h Makefile
        cc $(FLAGS) -c level_data.c -o level_data.o
wd.o: turning.h Makefile
        cc $(FLAGS) -c wd.c -o wd.o
moments.o: turning.h Makefile
        cc $(FLAGS) -c moments.c -o moments.o
extraction.o: turning.h Makefile
        cc $(FLAGS) -c extraction.c -o extraction.o
suncore.o: turning.h Makefile
        cc $(FLAGS) -c suncore.c -o suncore.o
misce.o: turning.h Makefile
        cc $(FLAGS) -c misce.c -o misce.o
```

Machining Makefile

```
/****************************************/
/*      turning.h                       */
/****************************************/

/*********************************/
#include        <stdio.h>
#include        <math.h>
#include        <strings.h>
#include        <usercore.h>

#define         L       2048
#define         N       256
#define         N2      128
#define         M       127
/*********************************/

/*********************************/
extern          double  feed;
extern          double  rpm;
extern          double  r_w;
extern          double  r_t;

extern          double  a_y, f_y, phi_y;
extern          double  a_z, f_z, phi_z;

extern          double  a, k_o, phi_o;
extern          double  b, k_m, phi_m;

extern          double  a1, k_o1;
extern          double  b1, k_m1;

extern          double  a_y1, f_y1;
extern          double  a_z1, f_z1;
/****************************************/
extern  void    choose();
extern  void    real_parameters();
extern  void    real_roundness();
extern  void    plot_roundness();
extern  void    cut_it_out();
extern  void    simu_parameters();
extern  void    simu_roundness();
extern  void    level_data();
extern  void    hilbert();
extern  void    wd();
extern  void    moments();
extern  void    extraction();

extern  void    store_wp();
extern  void    store_sig();
```



```
extern  void    store_ana_re();
extern  void    store_ana_im();
extern  void    store_mom_p();
extern  void    store_mom_t();
extern  void    store_wd();
extern  void    results();
extern  void    store_vector();
extern  void    plot_vector();
extern  void    plot_wd();
/*********************************/
extern  void    set_up();
extern  void    clean_up();
extern  char*   io_by_keyboard();
extern  int     go_on_or_not();
extern  char    input_string[];
extern  struct vwsurf   vwsurf;
extern  int     seg;
/*********************************/
extern  void    input();
extern  void    hilbert();
extern  void    wd();
extern  void    moment_p();
extern  void    moment_theta();
extern  void    extraction();

extern  void    set_up();
extern  void    clean_up();
extern  char*   io_by_keyboard();
extern  int     go_on_or_not();
/*********************************/
```

```
/************************************************/
/************************************************/

#include        "turning.h"

main()
{
        static  double  d[L];
        int     middle;

        static  double  f[2][N];
        static  double  w[2][N][N];
        static  double  p[N];
        static  double  theta[N];
        char    type_of_signal[100];

        int     finished=0;

        set_up();

        while( !finished )
        {
                set_viewport_2(0.0, 1.0, 0.0, 0.75);
                choose(type_of_signal);
                if (type_of_signal[0] == 'r')
                {       real_parameters();
                        real_roundness(type_of_signal, d);
                        plot_roundness(d);
                        cut_it_out(d, &middle, f);
                        finished = go_on_or_not("Go Ahead?");
                        if (finished) error_message("***Abort");
                        store_wp(d, middle, type_of_signal);
                }
                else if (type_of_signal[0] == 's')
                {       simu_parameters(type_of_signal);
                        simu_roundness(f, type_of_signal);
                }
                else
                {       error_message("***Wrong option!");
                }

                level_data(f[0], N);

                set_viewport_2(0.0, 1.0, 0.68, 0.75);
                plot_vector(f[0], N, "n", "f[n]");
                store_sig(f[0], type_of_signal);

                hilbert(f[0],f[1]);
```



```
                set_viewport_2(0.0, 1.0, 0.615, 0.68);
                plot_vector(f[0], N, "n", "Real part of f_a[n]");
                store_ana_re(f[0], type_of_signal);

                set_viewport_2(0.0, 1.0, 0.55, 0.615);
                plot_vector(f[1], N, "n", "Imaginary part of f_a[n]");
                store_ana_im(f[1], type_of_signal);

                wd(f[0], f[1], w[0], w[1]);

                set_viewport_2(0.0, 1.0, 0.2, 0.55);
                plot_wd(w[0], "n", "k", "W[n,k]");
                store_wd(w[0], type_of_signal);

                moments(w[0], p, theta);

                set_viewport_2(0.0, 1.0, 0.125, 0.2);
                plot_vector(p, N, "n", "P");
                store_mom_p(p, type_of_signal);

                set_viewport_2(0.0, 1.0, 0.05, 0.125);
                plot_vector(theta, N, "n", "theta");
                store_mom_t(theta, type_of_signal);

                set_viewport_2(0.0, 1.0, 0.0, 0.05);
                extraction(p, theta, type_of_signal);
                results(type_of_signal);

                finished = go_on_or_not("Go on ?");

        }

        clean_up();

}
```

Machining — choose.c

```
#include        "turning.h"

void    choose(type_of_signal)
char    type_of_signal[];
{
        set_viewport_2(0.0, 1.0, 0.0, 0.75);
        set_window(0.0, 1.0, 0.0, 1.0);
        create_retained_segment(++seg);
        {       move_abs_3(0.25, 0.0, 0.6);
                text("Choose from:");
                move_abs_3(0.25, 0.0, 0.5);
                text("    r----real cases");
                move_abs_3(0.25, 0.0, 0.45);
                text("    s----simulation");
        }
        close_retained_segment();

        io_by_keyboard("Enter:  ", 0.25, 0.25);
        strncpy(type_of_signal, input_string, 5);

        delete_retained_segment(seg--);
}
```

Machining — real_parameters.c

```
/***********************************************/
/*              real_parameters                */
/***********************************************/

#include        "turning.h"

double  feed, rpm, r_w, r_t;

double  f_z, a_z, phi_z;
double  f_y, a_y, phi_y;

double  a, k_o, phi_o;
double  b, k_m, phi_m;

void    real_parameters()
{
        FILE    *fp, *fopen();
        char    infofilename[250];

        io_by_keyboard("InfoFileName:", 0.2, 0.4);
        strcpy(infofilename, "/home/hawk/eng/es036/source/vib/");
/*      strcpy(infofilename, "/home/hawk/eng/es036/source/wear/"); */

        strcat(infofilename, input_string);

        fp = fopen(infofilename, "r");

        fscanf(fp, "%lf", &feed);
        fscanf(fp, "%lf", &rpm);
        rpm /= 60.0;

        fscanf(fp, "%lf", &r_w);
        fscanf(fp, "%lf", &r_t);

        fscanf(fp, "%lf %lf", &a_z, &f_z);
        fscanf(fp, "%lf %lf", &a_y, &f_y);

        a = feed * a_z /(2.0 * r_t);
        b = (f_z * a_y) /(rpm * r_w);
        k_o = (f_z /rpm) * 0.125;
        k_m = (f_y /rpm) * 0.125;

        fclose(fp);

}
```

Machining — real_roundness.c

```
#include        "turning.h"

void    real_roundness(type_of_signal, d)
char*   type_of_signal;
double  d[];
{
        FILE    *fp, *fopen();
        char    datafilename[200];

        int     n;

        char    str[200];

        io_by_keyboard("DataFileName:", 0.2, 0.4);
        strcpy(datafilename, "/home/hawk/eng/es036/source/vib/");
/*      strcpy(datafilename, "/home/hawk/eng/es036/source/wear/");*/
        strcat(datafilename, input_string);
        strcpy(type_of_signal, input_string);

        fp = fopen(datafilename, "r");
        fscanf(fp, "%s", str);
        for (n=0; n<L; n++)
        {       fscanf(fp, "%lf", d+n);
        }

        fclose(fp);
}
```

Machining — cut_it_out.c

```
/*********************************************/
/*              cutitout.c                   */
/*********************************************/

#include        "turning.h"

void    cut_it_out(d, p_middle, f)
double  d[];
int     *p_middle;
double  f[2][N];
{
        int     MAXINT = 2147483647;
        int     locator_number = 1;
        int     button_number = 1;
        int     echo_type = 1;
        float   x,y, x0, y0, x1, y1, arg;
        int     i0, i;
        char    str[20];

        initialize_device(LOCATOR,locator_number);
        initialize_device(BUTTON, button_number);
        set_echo_surface(LOCATOR,locator_number, &vwsurf);
        set_echo_surface(BUTTON, button_number, &vwsurf);
        set_echo(LOCATOR,locator_number, echo_type);

        set_window(0.0, 1.0, 0.0, 0.75);
        create_retained_segment(++seg);
                await_any_button_get_locator_2(MAXINT,
                        locator_number,
                        &button_number, &x, &y);
                move_abs_3(x, 0.0, y);
                text("A");
                x0 = x;
                y0 = y;

                await_any_button_get_locator_2(MAXINT,
                        locator_number,
                        &button_number, &x, &y);
                move_abs_3(x, 0.0, y);
                text("B");
                x1 = x;
                y1 = y;

                x = (x0+x1)/2;
                y = (y0+y1)/2;
                move_abs_3(x, 0.0, y);
                text("C");

                move_abs_3(x0, 0.0, y0);
```

Machining — cut_it_out.c

```
            line_abs_3(x, 0.0, y);
            line_abs_3(x1, 0.0, y1);
            line_abs_3(x0, 0.0, y0);

            x = (x0+x1)/2 - 0.5;
            y = (y0+y1)/2 - 0.375;
            if (x==0 && y==0)
                    arg = 0;
            else if (x==0 && y<0)
                    arg = -3.141596/2;
            else if (x==0 && y<0)
                    arg = 3.141596/2;
            else if (x>0)
                    arg = atan(y/x);
            else if (x<0 && y>= 0)
                    arg = atan(y/x) +3.141596;
            else if (x<0 && y< 0)
                    arg = atan(y/x) -3.141596;
            else
                    arg = 0.0;

            arg *= 180/3.141596;
            sprintf(str, "%.2f", arg);
            x = (x0+x1)/2;
            y = (y0+y1)/2;
            x = (x+0.5)/2;
            y = (y+0.375)/2;

            move_abs_3(x, 0.0, y);
            text(str);
            x = (x0+x1)/2;
            y = (y0+y1)/2;
            move_abs_3(x, 0.0, y);
            line_abs_3(0.5, 0.0, 0.375);

            i0 = (arg + 360.0)/(360.0/L);
            *p_middle = i0;
            for (i=0; i<256; i++)
            {       f[0][i] = d[(i-128+i0) % L];
                    f[1][i] = 0;
            }

    close_retained_segment();

    terminate_device(LOCATOR,locator_number);
    terminate_device(BUTTON, button_number);

}
```

Machining — plot_roundness.c

```
#include "turning.h"

void    plot_roundness(d)
double  d[];
{
        double  low, high;
        double  r, coef, x, y;
        int     i;

        low = high = 0.0;
        for (i=0; i<L; i++)
        {       low = (low < d[i]) ? low : d[i];
                high = (high > d[i]) ? high : d[i];
        }
        r = (high-low)*1.5;
        r = (r+low < 0.0) ? -low : r;

        set_viewport_2(0.125, 0.875, 0.0, 0.75);
        set_window(-1.125*(r+high), 1.125*(r+high),
                -1.125*(r+high), 1.125*(r+high) );
        create_retained_segment(++seg);
                coef = 2.0 * 3.141159 / L ;
                x = (r + d[0]) * cos(coef*0);
                y = (r + d[0]) * sin(coef*0);
                move_abs_3(x, 0.0,y);
                for (i=0; i<L; i++)
                {       x = (r + d[i]) * cos(coef*i);
                        y = (r + d[i]) * sin(coef*i);
                        line_abs_3( x, 0.0, y);
                }

                x = (r + low) * cos(coef*0);
                y = (r + low) * sin(coef*0);
                move_abs_3(x,0.0, y);
                for (i=0; i<L; i+=8)
                {       x = (r + low) * cos(coef*i);
                        y = (r + low)  * sin(coef*i);
                        line_abs_3( x, 0.0, y);
                }

                x = r * cos(coef*0);
                y = r * sin(coef*0);
                move_abs_3(x, 0.0,y);
                for (i=0; i<L; i+=8)
                {       x = r * cos(coef*i);
                        y = r  * sin(coef*i);
                        line_abs_3( x, 0.0, y);
                }
```

```
                x = (r + high) * cos(coef*0);
                y = (r + high) * sin(coef*0);
                move_abs_3(x,0.0, y);
                for (i=0; i<L; i+=8)
                {       x = (r + high) * cos(coef*i);
                        y = (r + high)  * sin(coef*i);
                        line_abs_3( x, 0.0, y);
                }

                move_abs_3(-0.1*r,0.0, 0.0);
                text(input_string);

        close_retained_segment();
}

/***************************************/
```



```
/***********************************************/
/*              simu_parameters                */
/***********************************************/

#include        "turning.h"

double  feed, rpm, r_w, r_t;

double  f_z, a_z, phi_z;
double  f_y, a_y, phi_y;

double  a, k_o, phi_o;
double  b, k_m, phi_m;

void    simu_parameters(type_of_vibration)
char    *type_of_vibration;
{
        io_by_keyboard("feed(um), rpm:", 0.2, 0.4);
        sscanf(input_string, "%lf %lf",&feed, &rpm);
        rpm /=  60.0;

        io_by_keyboard("r_w(um), r_t(um):", 0.2, 0.4);
        sscanf(input_string, "%lf %lf",&r_w, &r_t);

        io_by_keyboard("a_y(um), f_y(Hz), phi_y(Deg):", 0.20, 0.42);
        sscanf(input_string, "%lf %lf %lf", &a_y, &f_y, &phi_y);
        phi_y *= 3.141596/180.0;

        io_by_keyboard("a_z(um), f_z(Hz), phi_z(Deg):", 0.20, 0.38);
        sscanf(input_string, "%lf %lf %lf", &a_z, &f_z, &phi_z);
        phi_z *= 3.141596/180.0;

        sprintf(type_of_vibration, "simu_az%d_ay%d", (int)a_z, (int)a_y);
}
```

```
/************************************************/
/*              roundness                       */
/************************************************/

#include "turning.h"

void    simu_roundness(f, type_of_vibration)
double  f[2][N];
char*   type_of_vibration;
{
        double  lowFrequencyPart, highFrequencyPart, mainPart;
        double  theta, coef;
        int     n;

        a = (feed * a_z) / (2.0 * r_t);
        b = (f_z * a_y) / (rpm * r_w);
        k_o = (f_z * (double) N) / (rpm * (double) L);
        k_m = (f_y * (double) N) / (rpm * (double) L);
        phi_o = (f_y * 3.141596 / rpm) * ( (double)(L-N) /  (double)L)
                + phi_z;
        phi_m = (f_y * 3.141596 / rpm) * ( (double)(L-N) /  (double)L)
                + phi_y;

        coef = (2.0 * 3.141596) / (double)N;
        for (n=0; n<N; n++)
        {       theta = k_o * coef *n + phi_o
                        + b * sin(k_m * coef *n + phi_m);

                lowFrequencyPart = (feed * feed) / (8.0 * r_t);

                highFrequencyPart = (a_z * a_z) / (2 * r_t)
                        * cos(theta) * cos(theta);

                mainPart = a * cos(theta);

                f[0][n] = lowFrequencyPart + highFrequencyPart + mainPart;
                f[1][n] = 0.0;
        }

}
```

Machining simu_roundness.c

```
/************************************************/
/*              hilbert.c                       */
/************************************************/

#include        "turning.h"

void    hilbert(real, imag)
double  real[], imag[];
{
        double  f[N];
        int     I=N, ifail=0;

        double  peak;
        int     i,i_peak, i_low, i_high;

        /********       FFT     *********/
        c06ecf_(real, imag, &I, &ifail);
        /*********************************/

        for (i=0; i<I; i++)
        {       f[i]= sqrt(real[i]*real[i] + imag[i]*imag[i]);
        }

        i_peak = 2;
        peak = f[i_peak];
        for (i=0; i< N2; i++)
        {       if (f[i] > peak)
                {       peak = f[i];
                        i_peak = i;
                }
        }

        i_low = i_peak /2;
        i_high = i_peak + i_peak * 3 /2;
        i_high = i_high < N2 ? i_high : N2;
        for (i=0; i<I; i++)
        {       if ( i < i_low || i > i_high)
                {       real[i] = 0.0;
                        imag[i] = 0.0;
                }
                else
                {       real[i] *= 2.0;
                        imag[i] *= 2.0;
                }
        }

        /*********************************/
        /********       IFFT    *********/
```



```
        c06gcf_(imag, &I, &ifail);
        c06ecf_(real, imag, &I, &ifail);
        c06gcf_(imag, &I, &ifail);
        /*********************************/
        /*********************************/
}
```

Machining — level_data.c

```
#include "turning.h"

void    level_data(d, length)
double  d[];
int     length;
{
        double  slope, intercept, t[6];
        int     n;

        t[0] = t[1] = t[2] = t[3] = t[4] = t[5] = 0;
        for (n=0; n<length; n++)
        {       t[0] += n * n;
                t[1] += n;
                t[2] += d[n] * n;
                t[3] += n;
                t[4] += 1;
                t[5] += d[n];
        }
        slope = (t[2]*t[4] - t[1]*t[5])/(t[0]*t[4] - t[1]*t[3]);
        intercept = -(t[2]*t[3] - t[5]*t[0]) / (t[0]*t[4] - t[1]*t[3]);

        for (n=0; n<length; n++)
        {       d[n] -= slope *n + intercept;
        }
}
```

Machining — wd.c

```
/*************************************************/
/*              wd.c                             */
/*************************************************/

#include        "turning.h"


void    wd(freal, fimag, wdreal, wdimag)
double  freal[N], fimag[N];
double  wdreal[N][N], wdimag[N][N];
{
        int     n, m, m1, m2, k;
        int     I=N, ifail=0;
        double  treal, timag, arg, c, s;


        for (n=0; n<N; n++)
        for (m=0; m<N; m++)
        {       m1 = n + m -M;
                m2 = n - m +M;

                if (-1<m1 && m1<N && -1<m2 && m2<N)
                {       wdreal[n][m] = freal[m1] * freal[m2]
                                       + fimag[m1] * fimag[m2];
                        wdimag[n][m] = fimag[m1] * freal[m2]
                                       - freal[m1] * fimag[m2];
                        wdreal[n][m] *= 2.0;
                        wdimag[n][m] *= 2.0;
                }
                else
                {       wdreal[n][m] = 0;
                        wdimag[n][m] = 0;
                }
        }

        for (n=0; n<N; n++)
        {       c06ecf_(wdreal[n], wdimag[n], &I, &ifail);
        }

        for (k=0; k<N; k++)
        {       arg = 2.0 * M * 3.14159265358979323846;
                arg *= k;
                arg /= N;
                c = cos(arg);
                s = sin(arg);
                for (n=0; n<N; n++)
                {       treal = wdreal[n][k]*sqrt((double)N);  /* nag */
                        timag = wdimag[n][k]*sqrt((double)N);  /* nag */
                        wdreal[n][k] = treal * c - timag * s;
```

Machining wd.c

```
                wdimag[n][k] = treal * s + timag * c;

            }
        }
}
```

Machining moments.c

```
/*************************************************/
/*              moments.c                        */
/*************************************************/

#include        "turning.h"

void    moments(w, p, theta)
double  w[N][N];
double  p[N];
double  theta[N];
{
        double  x[N], y[N], coef;
        int     n, k;

        /********** p  *****************/
        for (n=0; n<N; n++)
        {       p[n] = 0;
                for (k=0; k<N; k++)
                {       p[n] += w[n][k];
                }
                p[n] /= 2.0*N;
        }
        p[0] = 0; /* for the sake of plot */

        /********** x ***************/
        coef = 2.0 * 3.141596 /N;
        for (n=0; n<N; n++)
        {       x[n] = y[n] = 0.0;
                for (k=0; k<N; k++)
                {       x[n] += w[n][k] * cos(coef*k);
                        y[n] += w[n][k] * sin(coef*k);
                }
        }
        for (n=0; n<N; n++)
        {
                if (y[n] == 0 && x[n] > 0)
                {       theta[n] = 0;
                }
                else if (y[n] == 0 && x[n] < 0)
                {       theta[n] = 3.141596;
                }
                else if (y[n] == 0 && x[n] == 0)
                {       theta[n] = 0;
                }
                else if (x[n] < 0 )
                {       theta[n] = atan(y[n]/x[n]) + 3.141596;
                }
                else if (x[n] == 0 )
                {       if (y[n] > 0)
```

```
                        theta[n] = 3.141596/2.0;
                else if (y[n] < 0)
                        theta[n] = 3.0*3.141596/2.0;
                else
                        theta[n] = 0;
        }
        else
        {       theta[n] = atan(y[n]/x[n]);
        }

        theta[n] /= 2.0;
    }
}
```



```
/*************************************************/
/*              extraction.c                     */
/*************************************************/
#include        "turning.h"

double  a1, k_o1;
double  b1, k_m1;

double  a_y1, f_y1;
double  a_z1, f_z1;

void    extraction(p, theta, type_of_vibration)
double  p[N];
double  theta[N];
char    type_of_vibration[];
{
        double  y[N];
        int     I=N, ifail = 0;
        int     n, k;


        double  coef;
        double  tmp;

        char    str[120];

        /********       a1     ***********/
        a1 = 0;
        for (n=0; n<N; n++)
        {       a1 += p[n];
        }
        a1 /= N;
        a1 = sqrt(a1);
        /********     k_o1     ***********/
        k_o1 = 0.0;
        for (n=0; n<N; n++)
        {       k_o1 += theta[n];
        }
        k_o1 /= (2.0 * 3.141596);
        k_o1 = (int)(k_o1 + 0.5);
        /*******************************/
        /*******************************/
        tmp = 0.0;
        for (n=0; n<N; n++)
        {       tmp += theta[n];
        }
        tmp /= N;
        for (n=0; n<N; n++)
```

```
        {       theta[n] -= tmp;
        }

        coef = 2.0 * 3.141596/N;
        for (n=0; n<N; n++)
        {       theta[n] *= 0.5*(1-cos(coef*n));
                y[n] = 0.0;
        }

        /*********************************/

        c06ecf_(theta, y, &I, &ifail);

        coef = sqrt(N+0.0);
        for (n=0; n<N; n++)
        {       theta[n] *= coef;
                y[n] *= coef;
        }

        for (k=0; k<N; k++)
        {       theta[k] = theta[k]*theta[k]
                        + y[k]*y[k];
                theta[k] = sqrt(theta[k]);
        }
        /********        k_m1    **********/
        k_m1 = 2;
        b1 = theta[2];
        for (k=2; k<N/2; k++)
        {       if (theta[k] > b1)
                {       b1 = theta[k];
                        k_m1 = k;
                }
        }
        /********        b1      ***********/
        k = k_m1;
        b1 += theta[k-1] + theta[k-2]
              + theta[k+1] + theta[k+2];
        b1 /= sin( 2.0*3.141596*(k_m1+0.0)/(N+0.0) );
        b1 *= 2.0/N;
        b1 *= 2.0;
        /*********************************/
        a_z1 = 2.0 * r_t * a1 / feed;
        f_z1 = k_o1 * rpm * (double) L / ( (double)N );
        a_y1 = b1 / ( f_z1 / (rpm * r_w));
        f_y1 = k_m1 / ( (double) N / (rpm * (double) L) );
        /*********************************/

        set_window(-0.1, 1.1, -0.1, 1.1);
        create_retained_segment(++seg);
                move_abs_3(0.25, 0.0, 0.9);
```



```
                sprintf(str,
                  "Original: a_z=%.1f, f_z=%.d, a_y=%.1f, f_y=%d",
                  a_z, (int)f_z, a_y, (int)f_y);
                text(str);

                move_abs_3(0.25, 0.0, 0.6);
                sprintf(str,
                  "Origianl:  a=%.3f, k_o=%.2f, b=%.3f, k_m=%.2f",
                  a, k_o, b, k_m);
                text(str);

                move_abs_3(0.25, 0.0, 0.3);
                sprintf(str,
                  "Extracted: a=%.3f, k_o=%.2f, b=%.3f, k_m=%.2f",
                  a1, k_o1, b1, k_m1);
                text(str);

                move_abs_3(0.25, 0.0, 0.0);
                sprintf(str,
                  "Extracted: a_z=%.1f, f_z=%d, a_y=%.1f, f_y=%d",
                  a_z1, (int)f_z1, a_y1, (int)f_y1);
                text(str);

        close_retained_segment();
        /*********************************/
}
```

```
/************************************************/
/*              suncore.c                       */
/************************************************/

#include        "turning.h"


extern  int     pixwindd();
struct  vwsurf
        vwsurf  = DEFAULT_VWSURF(pixwindd);

int     keyboard_number = 1;
char    input_string[80];
int     buffer_size = 80;
char    initial_string[80] = {"enter:"};
int     initial_cursor_position = 7;
double  echo_x, echo_y;
int     echo_type = 1;
int     length;

int     seg = 0;
/************************************************/

void    set_up()
{
        initialize_core(DYNAMICC,SYNCHRONOUS,THREED);
        initialize_view_surface(&vwsurf,FALSE);
        select_view_surface(&vwsurf);

        set_view_reference_point(0.0,0.0,0.0);
        set_view_plane_normal(0.0,1.0,0.0);
        set_projection(PARALLEL, -1.0,1.732,-1.0);
        set_view_up_3(0.0,0.0,1.0);

        initialize_device(KEYBOARD,keyboard_number);
        set_echo(KEYBOARD,keyboard_number, echo_type);
        set_echo_surface(KEYBOARD,keyboard_number, &vwsurf);
}

/************************************************/

void    clean_up()
{
        terminate_device(KEYBOARD,keyboard_number);
        deselect_view_surface(&vwsurf);
        terminate_core();
}

/************************************************/
```



```
char*   io_by_keyboard(prompt, x, y)
char*   prompt;
double  x, y;
{
        int     MAXINT = 2147483647;
        char    str[80], *p;

        strcpy(initial_string, prompt);
        initial_cursor_position = strlen(initial_string)+ 5;
        echo_x = x;   echo_y = y;

        set_echo_position(KEYBOARD,keyboard_number,
                echo_x,echo_y);
        set_keyboard(keyboard_number,buffer_size,
                initial_string, initial_cursor_position);
        await_keyboard(MAXINT,keyboard_number,
                input_string, &length);

        input_string[ strlen(input_string)-1 ] = '\0';
        p = input_string;
        while( *p == ' ' || *p == '\t')
        {       p++;
        }
        strcpy(str, p);
        strcpy(input_string, str);

        return input_string;
}

/************************************************/

int     go_on_or_not(text)
char    text[];
{
        io_by_keyboard("", 0.2, 0.4);
        while( seg > 0 )
        {       delete_retained_segment(seg--);
        }

        io_by_keyboard(text, 0.2, 0.4);
        if (input_string[0] == 'n')
                return 1;
        else if (input_string[0] == 'N')
                return 1;
        else
                return 0;
}

/************************************************/
```

Machining — suncore.c

```
/************************************************/
```

Machining — misce.c

```
#include        "turning.h"


void    results(type)
char    type[];
{
        FILE    *fp, *fopen();
        char    file_name[100];

        strcpy(file_name, "Data/");
        strcat(file_name, type);
        strcat(file_name, ".res");

        fp = fopen(file_name, "w");

        fprintf(fp, "\\caption{");

        fprintf(fp, "Original: ");
        fprintf(fp, "$a_z = %.1f$, $f_z = %.1f$, ", a_z, f_z);
        fprintf(fp, "$a_y = %.1f$, $f_y = %.1f$. ", a_y, f_y);
        fprintf(fp, "Extracted: ");
        fprintf(fp, "$a_z = %.1f$, $f_z = %.1f$, ", a_z1, f_z1);
        fprintf(fp, "$a_y = %.1f$, $f_y = %.1f$. ", a_y1, f_y1);
        fprintf(fp, "}");

        fclose(fp);
}

void    store_wp(d, middle, datafilename)
double  d[];
int     middle;
char    datafilename[];
{

        FILE    *fp, *fopen();
        char    workpiece_filename[100];
        int     n;

        strcpy(workpiece_filename, "Data/");
        strcat(workpiece_filename, datafilename);
        strcat(workpiece_filename, ".wp");

        fp = fopen(workpiece_filename, "w");

        fprintf(fp, "%12d\n", middle);
        for (n=0;  n<L; n++)
        {       fprintf(fp, "%12.4f\n", d[n]);
        }
```

```
        fclose(fp);
}

void    store_sig(v, type)
double  v[];
char    type[];
{
        char    file_name[100];

        strcpy(file_name, "Data/");
        strcat(file_name, type);
        strcat(file_name, ".sig");
        store_vector(v, N, file_name);
}

void    store_ana_re(v, type)
double  v[];
char    type[];
{
        char    file_name[100];

        strcpy(file_name, "Data/");
        strcat(file_name, type);
        strcat(file_name, ".ana.re");
        store_vector(v, N, file_name);
}

void    store_ana_im(v, type)
double  v[];
char    type[];
{
        char    file_name[100];

        strcpy(file_name, "Data/");
        strcat(file_name, type);
        strcat(file_name, ".ana.im");
        store_vector(v, N, file_name);
}
```



```
void    store_mom_p(v, type)
double  v[];
char    type[];
{
        char    file_name[100];

        strcpy(file_name, "Data/");
        strcat(file_name, type);
        strcat(file_name, ".mom.p");
        store_vector(v, N, file_name);
}

void    store_mom_t(v, type)
double  v[];
char    type[];
{
        char    file_name[100];

        strcpy(file_name, "Data/");
        strcat(file_name, type);
        strcat(file_name, ".mom.t");
        store_vector(v, N, file_name);
}


void    store_wd(w, type)
double  w[N][N];
char    type[];
{
        char    file_name[100];
        FILE    *fp, *fopen();
        int     n, k;

        strcpy(file_name, "Data/");
        strcat(file_name, type);
        strcat(file_name, ".wd");

        fp = fopen(file_name, "w");

        for (k=N2; k < N+N2; k += 4)
        for (n=0; n < N; n += 4)
        {
                fprintf(fp, "%f\n", w[n][k%N]);
        }

        fclose(fp);
}
```

```
void    store_vector(v, length, file_name)
double  v[];
int     length;
char    file_name[];
{

        FILE   *fp, *fopen();
        int    i;

        fp = fopen(file_name, "w");
        for (i=0;  i < length; i++)
        {       fprintf(fp, "%f\n", v[i]);
        }
        fclose(fp);
}


void    plot_vector(v, length, xlabel, ylabel)
double  v[];
int     length;
char    xlabel[], ylabel[];
{
        double  min, max;
        int     i;

        min = max = v[0];
        for (i=0; i<length; i++)
        {       if (min > v[i])
                {       min = v[i];
                }
                if (max < v[i])
                {       max = v[i];
                }
        }

        set_window(-0.1*length, 1.1*length,
                min-0.1*(max-min), max+0.1*(max-min) );
        create_retained_segment(++seg);
        {
                move_abs_3(0.0, 0.0, 0.0);
                line_abs_3((double)length, 0.0, 0.0);
                move_abs_3(0.0, 0.0, min);
                line_abs_3(0.0, 0.0, max);

                move_abs_3(0.0, 0.0, v[0]);
                for (i=0; i<length; i++)
                {       line_abs_3( (double)i, 0.0, v[i]);
                }
```



```
                move_abs_3((double)length, 0.0, 0.0);
                text(xlabel);

                move_abs_3(0.0, 0.0, max+0.05*(max-min));
                text(ylabel);
        }
        close_retained_segment();
}


void    plot_wd(w, xlabel, ylabel, zlabel)
double  w[N][N];
char    xlabel[], ylabel[], zlabel[];
{
        double  min, max, scale, shift;
        int     n, k;



        min = max = w[0][0];
        for (n=0; n<N; n++)
        {   for (k=0; k<N; k++)
            {   min = (w[n][k]<min) ? w[n][k] : min;
                max = (w[n][k]>max) ? w[n][k] : max;
            }
        }

        scale = 1.0 / (max - min);
        shift = (-min) * scale;
        /*******************************/
        set_window(-0.16, 1.7, -0.16, 1.7);
        create_retained_segment( ++seg );
                move_abs_3(0.0, 0.0,  shift);
                line_abs_3(1.0, 0.0,  shift);
                move_abs_3(0.0, 0.0,  shift);
                line_abs_3(0.0, 1.0,  shift);
                move_abs_3(0.0, 0.0,  shift);
                line_abs_3(0.0, 0.0,  shift+max*scale);
                for (n=0; n < N; n += 5)
                {   move_abs_3(n/((double)N), 0.0, w[n][0]*scale+shift );
                    for (k=0; k<N; k += 5)
                    {   line_abs_3(n/((double)N),k/((double)N),
                                w[n][k]*scale+shift);
                    }
                }
                move_abs_3(1.05, 0.0,  shift);
                text(xlabel);
                move_abs_3(0.0, 1.0,  shift+max*scale*0.2);
                text(ylabel);
                move_abs_3(0.0,0.0,  max*scale + shift);
```

```
                text(zlabel);
        close_retained_segment();

        /*******************************/

}

void    error_message(text)
char    text[];
{
        void    exit();

        fprintf(stderr, "ERROR:   ");
        fprintf(stderr, "%s\n", text);
        exit(1);
}
```